COMMUNICATIONS QUARTERLY

THE JOURNAL OF COMMUNICATIONS TECHNOLOGY

Winter 1991 $9.95

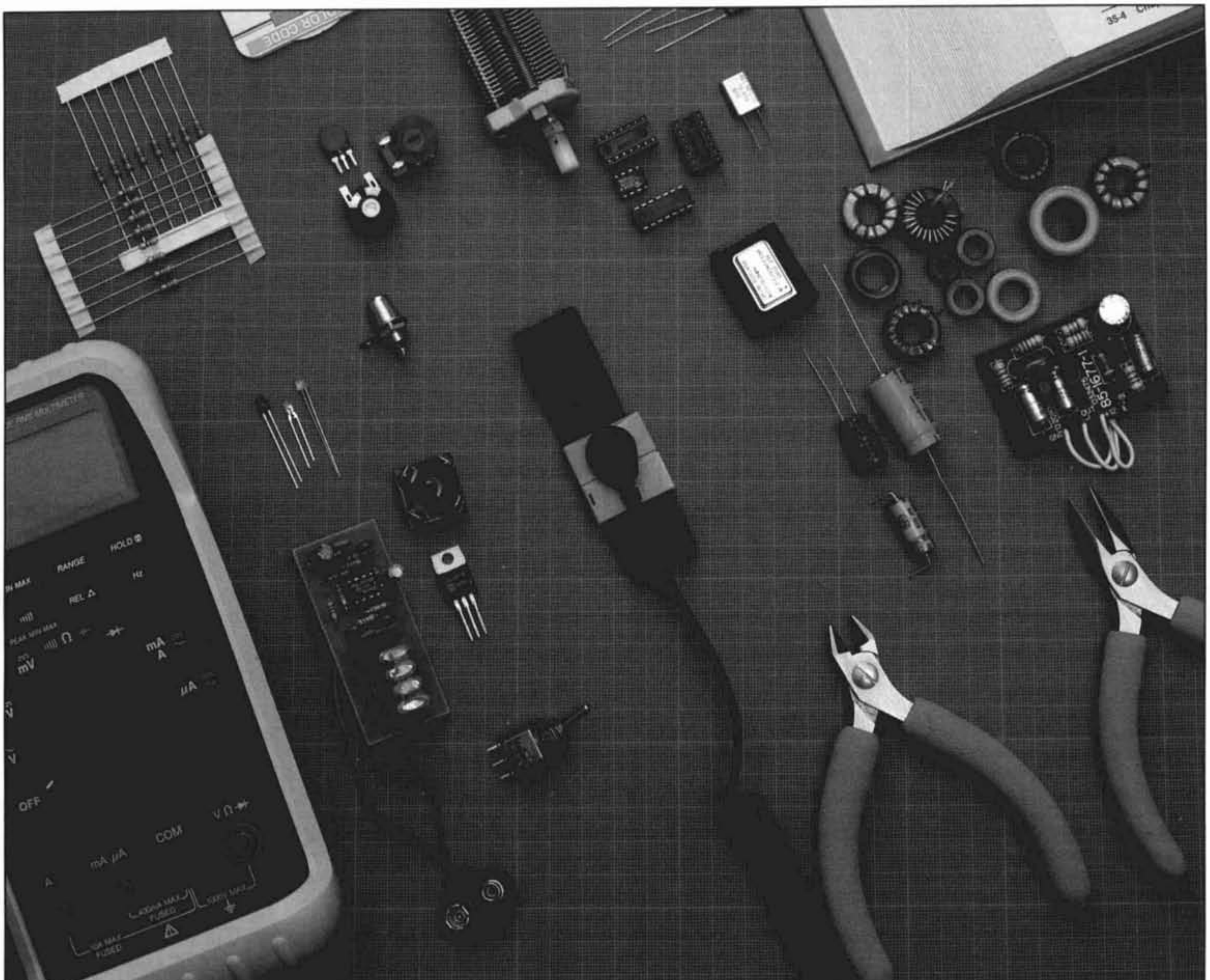

SSN 1053-9433

ICOM
IC-4KL
REMOTE-CONTROLLED LINEAR AMPLIFIER SYSTEM
REMOTE CONTROLLER IC-4KL
METER 1
METER 2
FUNCTION SWITCHES : METER 1
FUNCTION SWITCHES : METER 2

ICOM

COMMUNICATIONS QUARTERLY

THE JOURNAL OF COMMUNICATIONS TECHNOLOGY

CONTENTS

Volume 1, Number 1 Winter 1991

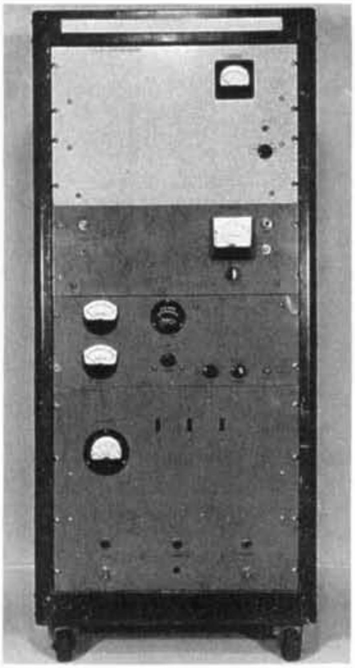

WA6EXV, page 9

WA7SXB, page 25

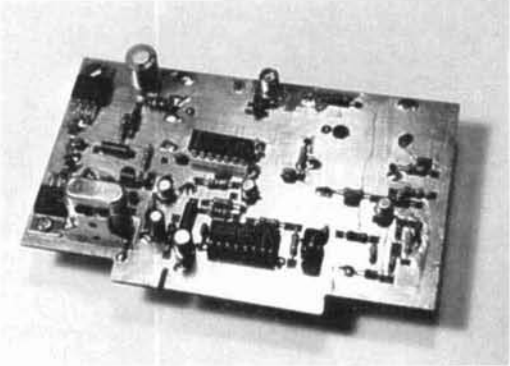

WA9HUV, page 93

Cover photo: Bryan Bergeron, NU1N

EDITORIAL

Whither the Weather: The Weather and Amateur Radio Operation

Weather. We often complain and grouse about it, but there's nothing we can do to change it.

However, there are ways in which we can use weather information to enhance our Amateur Radio challenges and increase our knowledge of propagation phenomena.

In this second issue of *COMMUNICATIONS QUARTERLY*, the articles by Jim Bacon, G3YLA, and Ron Ham will give you insights into tracking and using the weather as part of your VHF Amateur Radio activities.

Bacon's piece gives a good explanation of the atmospheric physics that make up our daily weather. He also explains how VHF and UHF radio waves can be propagated using different weather events. The discussion on how the jet stream can trigger sporadic E was of great interest to me. Ron Ham's article discusses one of the best tools you can use to predict tropospheric openings – the recording barometer, or barograph. By charting the trend in atmospheric pressure, you can learn when to expect tropospheric ducts. Ham includes examples of how this technology has proven to work for him.

In addition to newspaper weather maps and your local TV station, which really only give you a broad overview of the weather, there are a number of sources that you can tap into to examine weather patterns in much more depth.

There are two weather database services that I use regularly to get updates on current and forecasted weather information. Accu-Weather, located in State College, Pennsylvania, is familiar to many as a contract weather service on commercial radio stations. Their database includes all of the information you need to examine and predict the possibility of VHF and UHF radio openings – as well as a virtual treasure trove of other information. I also subscribe to the WeatherBank in Salt Lake City, Utah. They have a full range of maps, charts, and historical data to help you understand and predict how the weather can be used in Amateur operations.

During the 1930s, ARRL Staffer Ross Hull, (VK)3JU, pioneered a study of how weather effects radio communications. His first work appeared in June of 1935 in *QST* and was titled "Air Mass Bending of UHF Radio Waves." This report was also presented at a meeting of the IRE and URSI, two professional organizations, and was quite a feather in Hull's cap! K.B. Warner commented in a sidebar to the article: "It is not unreasonable to expect that this result of amateur radio activity will open up new avenues, not only in radio communications but also in meteorological studies related to weather forecasting." Remember, this work was done in the days before RADAR, satellites, and many of our other modern forecasting tools, so his words are even more true today. (There's a follow-up to the June 1935 article in the May 1937 issue of *QST*. Both articles make for fascinating reading and will help add to your understanding of tropospheric ducting.)

Enhancing and advancing the state-of-the-art in communications technology has always been the goal of the Radio Amateur service. Reviewing Hull's work in preparation for this editorial pointed out just how much we Amateurs have contributed to the science of radio communications. Reading through all those old magazines was an enlightening experience for me. Now, if I could only find the time to take advantage of what I've learned!

Craig Clark NX1G

P.S. There have been a number of articles run on how weather effects radio communication. We have put together a short bibliography that's available for a SASE.

A publication of
CQ Communications, Inc.
76 North Broadway
Hicksville, NY 11801-USA

Editorial Offices: Main Street, Greenville, NH 03048. Telephone: (603) 878-1441. FAX: (603) 878-1951.

Business Offices: 76 North Broadway, Hicksville, NY 11801. Telephone: (516) 681-2922. FAX: (516) 681-2926.

Communications Quarterly is published four times a year by *CQ Communications, Inc.* Subscription prices: Domestic – one year $29.95; Foreign – $39.95.

Allow six weeks for change of address.

Second-class postage paid pending at Hicksville, NY and additional mailing offices.

Postmaster: Please send change of address to Communications Quarterly, CQ Communications, Inc., 76 North Broadway, Hicksville, NY 11801.

ISSN 1053-9433

Kantronics**DataEngine**

If you'd like to run fast packet today, perhaps experiment with faster modes too, yet be compatible with today's 1200 baud system, then install a DataEngine at your station or node. The Kantronics DataEngine runs 1200, 2400, and 9600 baud packet with matched plug-in modems and appropriate transceivers now. For example, you can install a DE9600 modem in the DataEngine, attach a Kantronics DVR2-2 9600 baud data ready transceiver and run 9600 on 2-meters! Most off-the-shelf transceivers are not 9600 ready.

Better yet, you can add a free G8BPQ networking EPROM (download from our factory TELCO BBS) and run the 9600 combination as a node! Further, with the BPQ code, you can run the DataEngine in multi-drop KISS mode, attaching a KPC-2 or KPC-4 to the RS-232 port, creating a three or four port node!

Or, plug in a DE9600 or DE19200 modem and couple the DataEngine with the Kantronic's D4-10 data ready transceiver for 440 MHz high speed packet operation. (The D4-10 shall be released in early 1991).

Or, if you're interested in the DX spotting network or in transferring computer files to a buddy at 2400 baud, plug in the DE2400 modem and couple the DataEngine to any off-the-shelf transceiver. The 2400 baud QPSK modem is compatible with existing narrow band FM rigs and matches the industry standard Kantronics KPC-2400 modem.

Or, roll your own, attaching an experimental modem(s) via the disconnect headers! You might want to work satellites, play with a new form of modulation, or design your own HF modem. The disconnect headers on the DE pc board leave room for two internal or external modems. Experimenters already report interfacing the DataEngine with a PSK modem for working satellites. To aid in this fun process, you can order the DE Developer's Manual.

After all, the DataEngine is designed with an open architecture. It's a dual port, full duplex TNC with 16-bit V40 microprocessor running at 10 MHz, 85C30 communications controller, capable of speeds to 56KB per port. It comes with 64K of EPROM and 64K of RAM, and has socket space for up to .5 megabytes of EPROM and .5 megabytes of RAM!

Even better, the DataEngine comes factory stock with a DE1200 modem already plugged in and an end-user EPROM which supports terminal, KISS, HOST and BBS modes. It's ready to go on existing 1200 baud channels! The host mode enables use of sophisticated terminal programs, such as the DataEngineer, developed for the DataEngine, including windows/split screen etc. Or again, dial your own terminal program! In effect the DataEngine is "developer and user ready."

Specs: size 1-3/4"x6"x9", weight 2-1/2 lbs, power requirements nominally 12VDC at 150 ma. Input sensitivity 20 mvpp, Audio output drive jumper selectable from 10mvpp to 2vpp.

Options include: DE19200, DE9600, DE2400 and DE1200 modems, plus a developer's manual for modem and protocol experimenters. Plus more modems from Kantronics on the way!

For detailed specifications contact Kantronics. The Kantronics DataEngine, the TNC that can run fast today, and the platform to develop the next generation of advanced TNC applications.

Kantronics 1202 E. 23rd St., Lawrence, KS 66046, 913.842.7745 TELCO BBS 913.842.4678

ASTRON CORPORATION
9 Autry
Irvine, CA 92718
(714) 458-7277

MODEL VS-50M

ASTRON POWER SUPPLIES

• HEAVY DUTY • HIGH QUALITY • RUGGED • RELIABLE •

SPECIAL FEATURES

- SOLID STATE ELECTRONICALLY REGULATED
- FOLD-BACK CURRENT LIMITING Protects Power Supply from excessive current & continuous shorted output
- CROWBAR OVER VOLTAGE PROTECTION on all Models except RS-3A, RS-4A, RS-5A, RS-4L, RS-5L
- MAINTAIN REGULATION & LOW RIPPLE at low line input Voltage
- HEAVY DUTY HEAT SINK • CHASSIS MOUNT FUSE
- THREE CONDUCTOR POWER CORD except for RS-3A
- ONE YEAR WARRANTY • MADE IN U.S.A.

PERFORMANCE SPECIFICATIONS

- INPUT VOLTAGE: 105-125 VAC
- OUTPUT VOLTAGE: 13.8 VDC ± 0.05 volts (Internally Adjustable: 11-15 VDC)
- RIPPLE Less than 5mv peak to peak (full load & low line)
- All units available in 220 VAC input voltage (except for SL-11A)

SL SERIES

• LOW PROFILE POWER SUPPLY

MODEL	Colors Gray	Colors Black	Continuous Duty (Amps)	ICS* (Amps)	Size (IN) H × W × D	Shipping Wt. (lbs.)
SL-11A	•	•	7	11	2¾ x 7⅝ x 9¾	11

RS-L SERIES

• POWER SUPPLIES WITH BUILT IN CIGARETTE LIGHTER RECEPTACLE

MODEL	Continuous Duty (Amps)	ICS* (Amps)	Size (IN) H × W × D	Shipping Wt. (lbs.)
RS-4L	3	4	3½ x 6⅛ x 7¼	6
RS-5L	4	5	3½ x 6⅛ x 7¼	7

RM SERIES

MODEL RM-35M

• 19" RACK MOUNT POWER SUPPLIES

MODEL	Continuous Duty (Amps)	ICS* (Amps)	Size (IN) H × W × D	Shipping Wt. (lbs.)
RM-12A	9	12	5¼ × 19 × 8¼	16
RM-35A	25	35	5¼ × 19 × 12½	38
RM-50A	37	50	5¼ × 19 × 12½	50
RM-60A	50	55	7 × 19 × 12½	60
• Separate Volt and Amp Meters				
RM-12M	9	12	5¼ × 19 × 8¼	16
RM-35M	25	35	5¼ × 19 × 12½	38
RM-50M	37	50	5¼ × 19 × 12½	50
RM-60M	50	55	7 × 19 × 12½	60

RS-A SERIES

MODEL RS-7A

MODEL	Colors Gray	Colors Black	Continuous Duty (Amps)	ICS* (Amps)	Size (IN) H × W × D	Shipping Wt. (lbs.)
RS-3A		•	2.5	3	3 × 4¾ × 5¾	4
RS-4A	•	•	3	4	3¾ × 6½ × 9	5
RS-5A		•	4	5	3½ × 6⅛ × 7¼	7
RS-7A	•	•	5	7	3¾ × 6½ × 9	9
RS-7B	•	•	5	7	4 × 7½ × 10¾	10
RS-10A	•	•	7.5	10	4 × 7½ × 10¾	11
RS-12A	•	•	9	12	4½ × 8 × 9	13
RS-12B		•	9	12	4 × 7½ × 10¾	13
RS-20A	•	•	16	20	5 × 9 × 10½	18
RS-35A	•	•	25	35	5 × 11 × 11	27
RS-50A	•		37	50	6 × 13¾ × 11	46

RS-M SERIES

MODEL RS-35M

MODEL	Continuous Duty (Amps)	ICS* (Amps)	Size (IN) H × W × D	Shipping Wt. (lbs.)
• Switchable volt and Amp meter				
RS-12M	9	12	4½ × 8 × 9	13
• Separate volt and Amp meters				
RS-20M	16	20	5 × 9 × 10½	18
RS-35M	25	35	5 × 11 × 11	27
RS-50M	37	50	6 × 13¾ × 11	46

VS-M AND VRM-M SERIES

MODEL VS-35M

• Separate Volt and Amp Meters • Output Voltage adjustable from 2-15 volts • Current limit adjustable from 1.5 amps to Full Load

MODEL	Continuous Duty (Amps) @13.8VDC	Continuous Duty (Amps) @10VDC	Continuous Duty (Amps) @5VDC	ICS* (Amps) @13.8V	Size (IN) H × W × D	Shipping Wt. (lbs.)
VS-12M	9	5	2	12	4½ × 8 × 9	13
VS-20M	16	9	4	20	5 × 9 × 10½	20
VS-35M	25	15	7	35	5 × 11 × 11	29
VS-50M	37	22	10	50	6 × 13¾ × 11	46
• Variable rack mount power supplies						
VRM-35M	25	15	7	35	5¼ × 19 × 12½	38
VRM-50M	37	22	10	50	5¼ × 19 × 12½	50

RS-S SERIES

MODEL RS-12S

• Built in speaker

MODEL	Colors Gray	Colors Black	Continuous Duty (Amps)	ICS* Amps	Size (IN) H × W × D	Shipping Wt. (lbs.)
RS-7S	•	•	5	7	4 × 7½ × 10¾	10
RS-10S	•	•	7.5	10	4 × 7½ × 10¾	12
RS-12S	•	•	9	12	4½ × 8 × 9	13
RS-20S	•	•	16	20	5 × 9 × 10½	18

*ICS — Intermittent Communication Service (50% Duty Cycle 5min. on 5 min. off)

PUT THE PC10 IN YOUR PC FOR MORE COUNTER POWER.

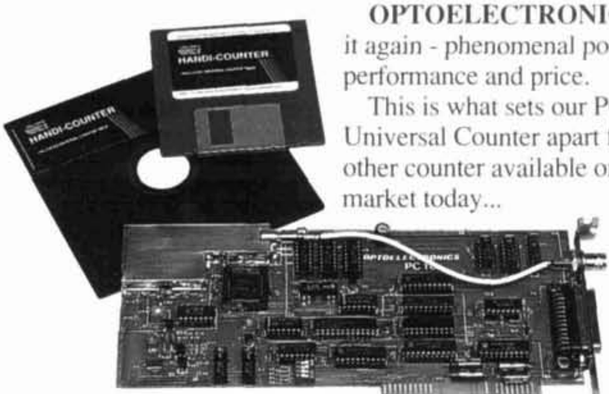

OPTOELECTRONICS does it again - phenomenal power, performance and price.

This is what sets our PC Based Universal Counter apart from any other counter available on the market today...

Model PC10 Universal Counter Timer Board for the PC. Introductory Price $339.

The PC10 has on board 50 ohm RF input with amplifiers and prescalers to operate as a stand alone 1MHz to 2.4GHz RF counter. TTL level input signals can be connected directly to the miniature 25 pin D connector on the mounting bracket. For low frequency, high impedance inputs, the Model AP10H companion amplifier must be used.

Model AP10H Dual High Impedance Amplifier Head Unit (Not Shown). Introductory price $299.

The AP10H is the companion head unit that supports all PC10 Universal Counter functions from 10Hz to 100MHz with 1 megohm inputs. Input attenuators, low pass filters and trigger levels are software selectable.

Options: TCXO 10 Precision Temperature Compensated Time Base $195. *± 0.2ppm 20°-40°C, 1ppm - year aging.*

- Instant Direct Tune - Set a communications receiver such as ICOM R7000 to frequency detected by counter. Patent pending.
- Data logging and data file creation to keep records or measure frequency drift.
- Menu selection for Units includes CPM/RPM, Hz, KHz, MHz, GHz, Sec, mS, uS and nS.
- Software timebase calibration of 1ppm TCXO timebase.
- Windows 3.0 operating environment with fully developed operating and signal conditioning controls accessible through pull down menus.

In addition to these unique features, PC10 is a down right high performance counter...

- 10 digit 10Hz to 2.4GHz frequency range.
- Measurement Period (Gate Time) continuously variable from 1 milli-second to 28 seconds.
- Reciprocal Counting for high resolution measurement.
- Input sensitivity is less than 10mV from 10Hz to over 1.6GHz.
- Direct count frequencies over 200MHz with 1Hz resolution in 1 sec.

OPTOELECTRONICS

Toll Free Order Line: 1-800-327-5912
FL(305)771-2050 • FAX(305)771-2052
5821 NE 14th Avenue • Fort Lauderdale, Florida 33334

Wide Dynamic Range and Low Distortion — The Key to Superior HF Data Communications

- Dynamic Range > 75 dB
- 400 to 4000 Hz
- BW Matched to Baud Rate
- BER $< 1 \times 10^{-5}$ for S/N = 0 dB
- 10 to 1200 Baud
- Linear Phase Filters

ST-8000 HF Modem

Real HF radio teleprinter signals exhibit heavy fading and distortion, requirements that cannot be measured by standard constant amplitude BER and distortion test procedures. In designing the ST-8000, HAL has gone the extra step beyond traditional test and design. Our noise floor is at -65 dBm, not at -30 dBm as on other units, an extra 35 dB gain margin to handle fading. Filters in the ST-8000 are all of linear-phase design to give minimum pulse distortion, not sharp-skirted filters with high phase distortion. All signal processing is done at the input tone frequency; heterodyning is NOT used. This avoids distortion due to frequency conversion or introduced by abnormally high or low filter Q's. Bandwidths of the input, Mark/Space channels, and post-detection filters are all computed and set for the baud rate you select, from 10 to 1200 baud. Other standard features of the ST-8000 include:

- 8 Programmable Memories
- Set frequencies in 1 Hz steps
- Adjustable Print Squelch
- Phase-continuous TX Tones
- Split or Transceive TX/RX
- CRT Tuning Indicator
- RS-232C, MIL-188C, or TTL Data
- 8, 600, or 10K Audio Input
- Signal Regeneration
- Variable Threshold Diversity
- RS-232 Remote Control I/O
- 100-130/200-250 VAC, 44-440 Hz
- AM or FM Signal Processing
- 32 steps of M/S filter BW
- Mark or Space-Only Detection
- Digital Multipath Correction
- FDX or HDX with Echo
- Spectra-Tune and X-Y Display
- Transmitter PTT Relay
- 8 or 600 Ohm Audio Output
- Code and Speed Conversion
- Signal Amplitude Squelch
- Receive Clock Recovery
- 3.5" High Rack Mounting

Write or call for complete ST-8000 specifications.

HAL Communications Corp.
Government Products Division
Post Office Box 365
Urbana, Illinois 61801
(217) 367-7373

By Chuck Swedblom, *WA6EXV*
P.O. Box 605
Ridgecrest, California 93556

A HIGH-POWER, 13-CM MAGNETRON TRANSMITTER

Here's a new use for your microwave oven's magnetron

The greatest obstacle to overcome in working moon bounce (EME) or tropospheric scatter (tropo) in the 13-cm band lies in generating the RF power required. Very few devices are available to the radio Amateur which can be used to build a high power transmitter. But I've found one that's capable of delivering high power (500 to 1000 watts of RF output) and is inexpensive ($50 to $75). Some of these devices even operate at the upper end of the 13-cm ham band. I'm referring to the microwave-oven magnetron.

I wanted to investigate the feasibility of designing a low-cost, high-power transmitter for the 13-cm band using a microwave oven magnetron in the injection-locked configuration. After some investigation, I designed and built the 1-kW, 13-cm oven-magnetron transmitter described here.

Magnetron characteristics

A magnetron is a single port device to which the load is connected. Any change in the reactance component of the load changes the frequency of the free-running magnetron. **Figure 1** is a typical load diagram showing how the frequency varies with changes in magnetron loading. The center of the diagram corresponds to the matched condition, where no reflection occurs. As the reactive component of the load changes, the frequency changes accordingly. Because

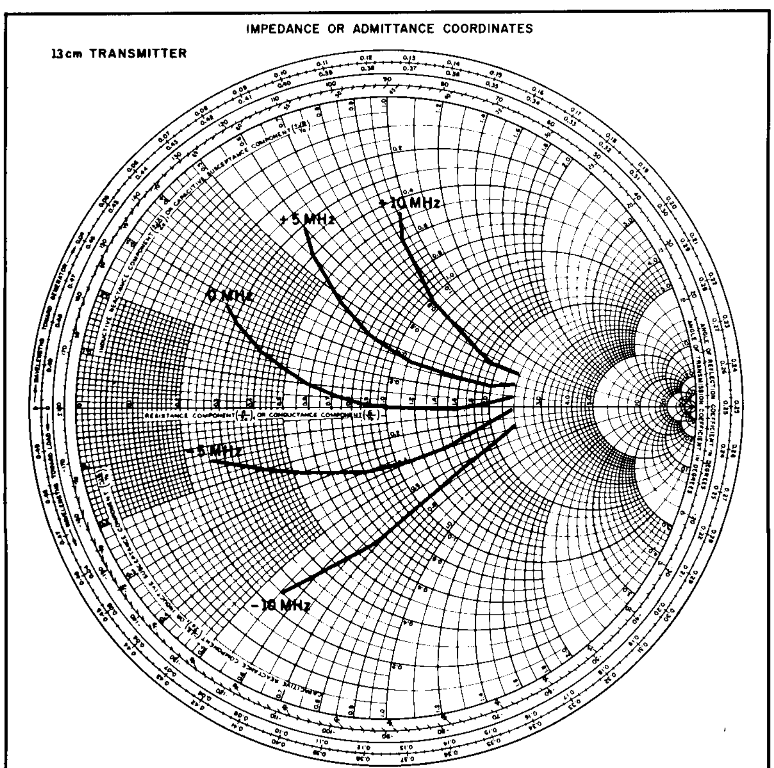

Figure 1. Magnetron load diagram.

the magnetron can't distinguish between reflected power from a passive load and power injected into it from some other source, it's possible to lock the free-running magnetron to a stable source.

To inject an external signal source into the magnetron, it's necessary to connect a circulator between the magnetron and the load, as shown in **Figure 2**. The amount of power required to lock the magnetron is derived from:[1]

$$\sqrt{Pl/P} > Qe\,|\Delta fo/fo| \qquad (1)$$

where Pl is the injection power, P is the magnetron output power, Qe is the loaded Q of the magnetron, Fo and ΔFo are the frequency and frequency deviation in MHz.

The amount of power required to injection lock a typical oven magnetron at Fo = 2448 MHz, Qe = 20, P = 750 watts, and a locking range of 20 MHz, so Fo = 10 MHz, is:

$$\sqrt{Pl/750} > 20 \times 10/2448 = 0.082$$

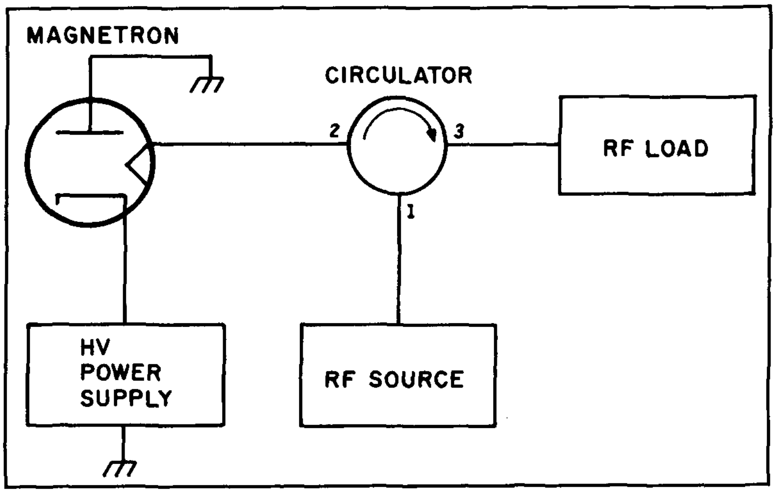

Figure 2. Injection-locked magnetron, block diagram.

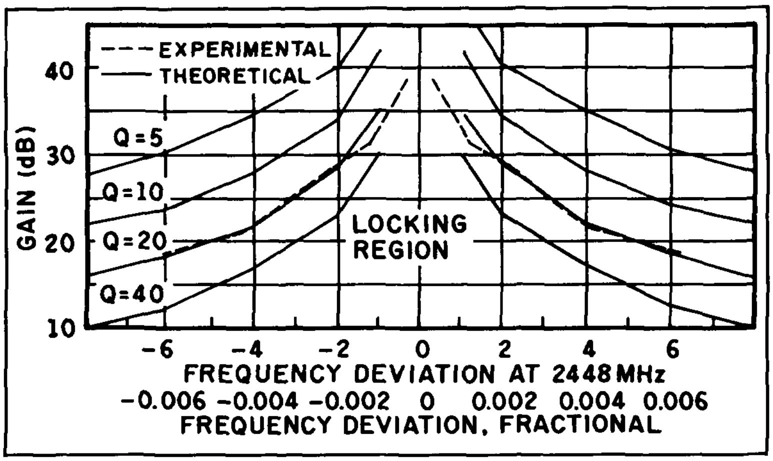

Figure 3. Theoretical locking range of magnetron and experimental data.

or

$$Pl = 5.0 \text{ watts}$$

In practice, approximately 10 watts would be used to overcome circuit losses, giving a gain of almost 19 dB.

Plots of **Equation 1** are shown in **Figure 3** for four values of Qe, along with an actual plot of an oven magnetron. As you can see, the experimental data are close to theoretical.

Frequency response

For complete information, it's necessary to determine how fast the magnetron will respond to variations in the injection frequency. The data in **Figure 3** are based on static conditions of the magnetron and do not indicate its ability to follow high-frequency modulation. The pull-in is complete when:

$$t = Qe/Fo\,\sqrt{P/Pl} \qquad (2)$$

where t is in μsec, if Fo is in MHz.[2] For the previous example, the pull-in time is about 0.07 μsec. This is the time required to swing across the lock-in range. It represents one-half Hz of the modulation. Thus, the maximum modulation frequency is about 7 MHz. The modulation will normally be restricted to less than the full lock-in range, so **Equation 2** becomes

$$F = Fo/2Qe\,\sqrt{Pl/P} \qquad (3)$$

where F in MHz is the maximum modulation frequency and Fo is in MHz.

This means the injection-locked magnetron can be used at any modulation frequency desired, including ATV.

Automatic frequency control

The magnetron will remain locked to the injection source frequency as long as the phase difference doesn't vary more than 90 degrees. This limit may be exceeded if there's power-supply drift and/or thermal drift of the magnets on the magnetron. To prevent the magnetron from dropping out of lock, you could use a phase-sensitive detector to monitor injection signal versus output signal. The phase detector output could then control the magnetron cathode current and maintain lock to within a few degrees.

Safety first

Before discussing the transmitter, I'd like to take note of some safety precautions.

High Voltage

The high voltages used in this transmitter are in the *lethal* range. Great care must be taken when testing, troubleshooting, and operating this type of transmitter. The voltages used are somewhat higher than those in common Amateur high-power amplifiers. Because the magnetron anode is operated at ground potential, the filament circuit is at a very high negative potential. Most high-power Amateur amplifiers have the anode at high voltage and the filament at near ground potential. It's very important not to forget this fact. *Negative voltage will kill just as quickly as positive voltage.*

High RF radiation

The RF power output of this transmitter is at the same level as that developed in the usual Amateur high-power amplifier. However, the chance for exposure to dangerous RF radiation is much greater at 13 cm. A 2-1/2 × 1/64-inch gap in the side panel of an HF power amplifier will let little radiation escape. But this same size gap in a 13-cm transmitter forms a 1/2-wavelength slot antenna, which has the potential to radiate the full power of the transmitter. This could be 250 watts/per square centimeter, or 250,000 times the radiation level I consider safe at this frequency.

The 13-cm transmitter design

The 13-cm transmitter **(Photo A)** consists of four major sections: the RF deck, 13-cm transverter, constant-current regulator, and magnetron HV power supply.

Figure 4 shows the block diagram of the transmitter. The RF output of the magnetron is fed to the transmit port of a three-

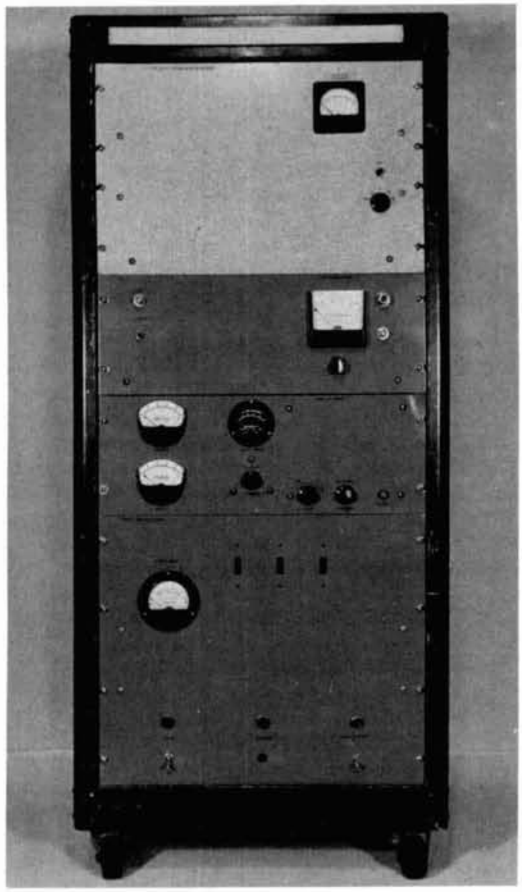

Photo A. 13-cm oven-magnetron transmitter. Top to bottom: RF deck, 13-cm transverter, constant-current regulator, and HV power supply.

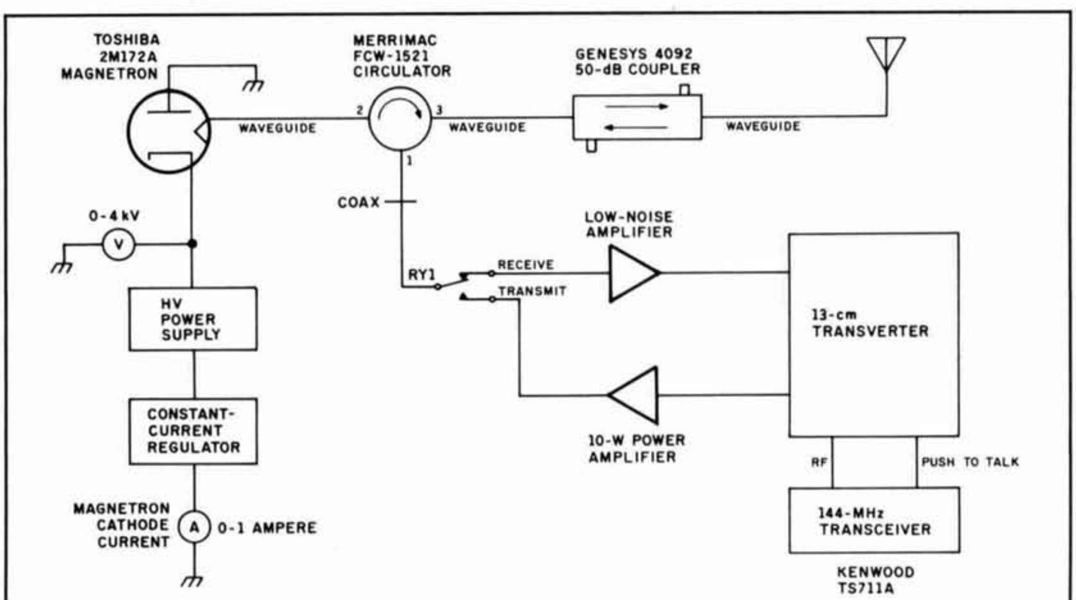

Figure 4. 13-cm magnetron transmitter, block diagram.

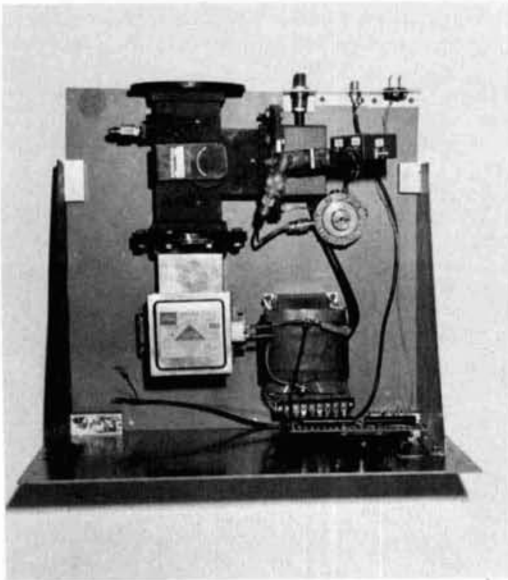

Photo B. RF deck, top view.

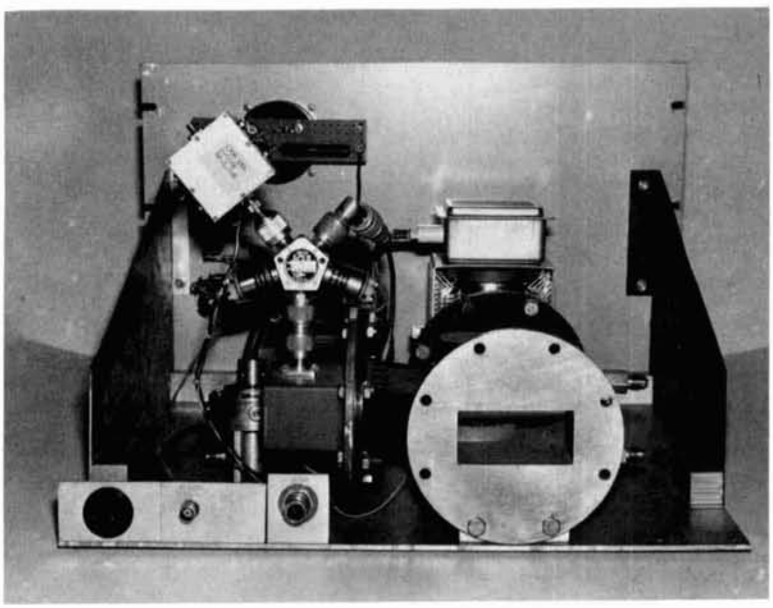

Photo C. RF deck, rear view.

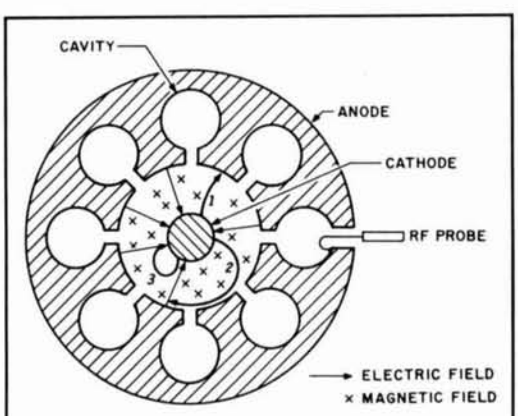

Figure 5. Action of an electron in a non-oscillating magnetron.

port circulator. The circulator load port feeds a dual-directional coupler used for testing, and then the antenna or load. The third port of the circulator, which I call the injection port, is fed from the 10-watt power amplifier through transmit/receive relay RY1, when in the transmit position. Input power for the 10-watt power amplifier comes from the transmit port of the 13-cm transverter, which up-converts the 144-MHz transceiver.

When in receive mode, the signal from the antenna is fed through the dual-directional coupler to the circulator load port. It then goes to the injection port, and through RY1 to the 13-cm transverter receive port, which down-converts the signal to the 144-MHz transceiver.

The DC power for the magnetron is supplied by the magnetron HV power supply. There must be a constant-current regulator in the power-supply circuit to maintain proper magentron operation. This constant-current regulator will allow control of the free-running magnetron power output and frequency. The transmitter has various meters and indicators to aid in system operation and maintenance.

The 13-cm transverter converts the 144-MHz signals from the transceiver up and down. It contains the transmit/receive (T/R) sequencer for proper power control timing.

RF deck

The RF deck, shown in **Photos B** and **C**, contains the major high-power RF components. These are: the oven magnetron, filament transformer, circulator, 10-watt power amplifier, RF transfer relay, and low-noise amplifier (LNA). A dual-directional coupler and high-power load for testing is required, and is included in this section, but it is not a physical part of the RF deck.

Magnetron

The heart of the transmitter is the microwave oven magnetron. The magnetron is basically a diode vacuum tube operating in a magnetic field.[3] The magnetron anode consists of a circular group of cavities surrounding the cathode. Each cavity has a narrow slot connecting it to the space around the cathode. The magnetic field is concentrated in the same plane as the cathode.

Magnetic and electric fields

When a weak magnetic field and a strong electric field exists between the cathode and anode (see **Figure 5**), an electron emitted from the cathode will be attracted almost directly to the anode, and no RF energy will be generated (path 1). As the magnetic field is increased, the direction of the electron traveling toward the anode will be altered into a curve (path 2). If the magnetic field is increased far enough, the electron will fall back to the cathode, never reaching the anode (path 3).

At some critical value of magnetic and electric field, the electron will just graze the gap of the anode cavity and generate an RF field at the cavity's resonant frequency. The interaction of the RF field and the magnetic field at the gaps of the cavities will cause the electrons emitted from the cathode to form bunches that will rotate like the spokes of a wheel past all of the gaps in synchronism with the RF field (**Figure 6**), creating a very large amount of RF energy in each of the cavities.

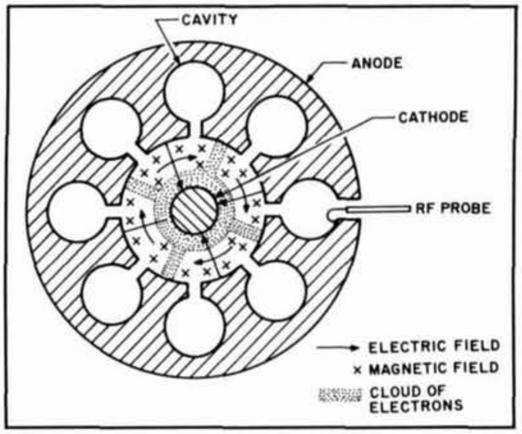

Figure 6. Cloud of electrons rotating in the interaction space of a magnetron oscillator.

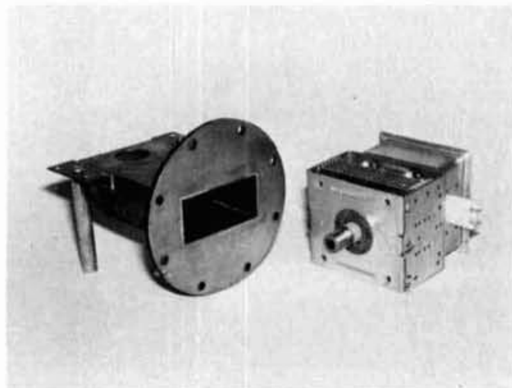
Photo D. Typical oven magnetron and waveguide-mounting section.

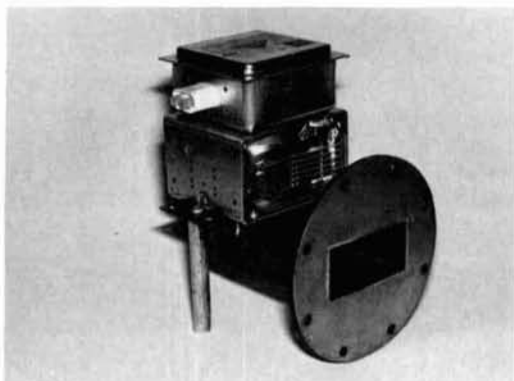
Photo E. Oven magnetron mounted on waveguide section.

Mode skipping

A probe inserted into one of the cavities extracts RF energy from the cavity to an external load. If the magnetic field is held constant, and the anode voltage is increased, a point will be reached where electron clouds form another spoke which will not be an even multiple of the number of cavities. When this occurs, there's no longer synchronism with the cavities, and an uneven distribution of energy is supplied to the output cavity. This action is called mode skipping and, if allowed to continue, will damage the magnetron. It is *imperative* that the power supply be designed to prevent mode skipping in the magnetron.

Waveguide choices

RF energy from an oven magnetron is provided by a quarter-wave probe inserted into a length of waveguide. **Photo D** shows a typical oven magnetron and a section of WR-284 waveguide which has been prepared for mounting. **Photo E** shows the magnetron mounted on the waveguide section.

The location of the probe along the waveguide depends on the size of waveguide. The WR-284 or RG-48/U series are the most readily available waveguide components on the surplus market. This waveguide is marginal for the 13-cm band because it's rated for 2.60 to 3.95 GHz. This means that attenuation will start to increase. However, I haven't experienced any difficulty with this size waveguide because I'm not running long sections of it. A better choice of waveguide would be the WR-340 or RG-112/U, which is rated from 2.2 to 3.3 GHz. When the WR-284 waveguide is used, the magnetron RF probe is mounted 1.0 inch from the shorted end. If WR-340 waveguide is used, the magnetron RF probe is mounted 0.8 inch from the shorted end.

Magnetron noise and operating modes

When I say that I use a magnetron for a transmitter, I often hear: "The output spec-

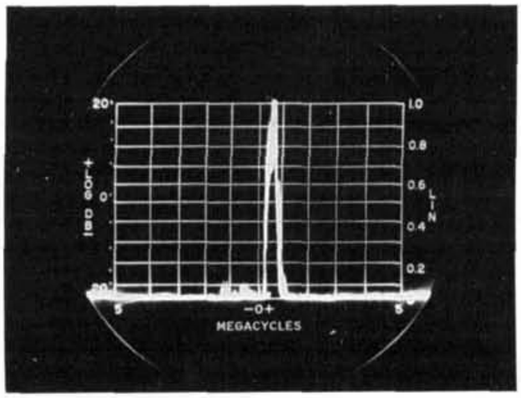

Photo F. Oven-magnetron output with filament voltage on.

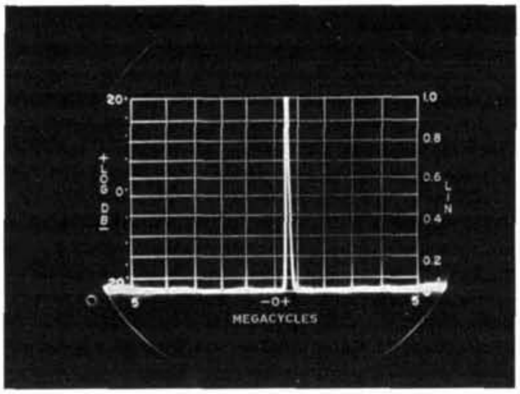

Photo G. Oven-magnetron output with filament voltage off.

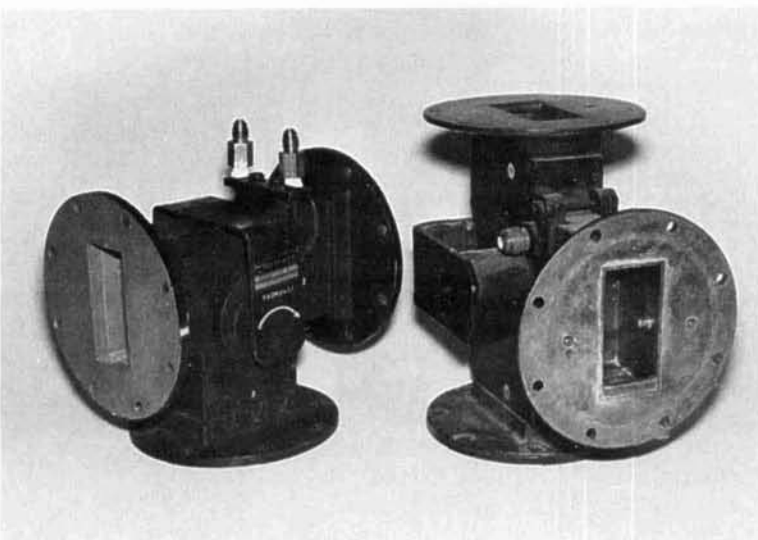
Photo H. Two typical high-power circulators.

trum of a magnetron is very noisy. How can it be used for communications?" I've found that by turning off the filament voltage after the magnetron reaches the rated power output, the spectrum is very clean. **Photos F** and **G** show the spectrum with the filament voltage on and off, respectively.

As long as the high voltage is applied to the magnetron, the back bombardment of the cathode will continue to keep the cathode hot enough to supply the electrons required to maintain RF power output. Once the high voltage is removed, the magnetron won't oscillate, and the filament voltage must be turned on to restart the magnetron.

Because the magnetron is an oscillator and not an amplifier, it isn't possible to operate the transmitter in SSB, CW, or AM modes. FM and FSK are the only modes available for communication. I've been using the FSK mode to generate a CW-type signal by producing a 10-kHz shift in frequency between key down and key up. As long as I give the other station the correct frequency, we have no trouble working each other.

The frequency allocation for microwave-oven service is from 2440 to 2460 MHz, so it's possible that not all oven magnetrons can be operated within the Amateur 13-cm band. I've only tested two, and in each case I was able to tune them to 2448 MHz at nearly full power output. More testing is required to find out which tubes are best suited for Amateur service.

The tubes I used came from discarded microwave ovens with defective power supplies or timers. I tested several other tubes whose filaments were in good shape, but there was no longer any cathode emission. New tubes can be purchased from service dealers or distributors for less than $100.

Circulator

The circulator is the key to injecting a locking signal into the magnetron at the same time that the magnetron is supplying RF output power to the load or antenna.

A circulator can be constructed as either a three or four-port device. I use a three-port circulator. The adjacent ports of the circulator are effectively connected together in one direction but isolated from each other in the opposite direction. Therefore, the signals can pass easily from the transmit port to the load port, and from the load port to the injection port; but, they will be attenuated in opposite directions.

The waveguide circulator is made by joining three waveguide arms, 120 degrees apart, at a common junction containing a slab of ferromagnetic material. The ferromagnetic material rotates the standing wave pattern so RF coupling can only accomplished in one direction. When circulators are designed to handle high power, they are generally water cooled by wrapping copper tubing around the central part containing the ferrite material. **Photo H** shows two typical high-power circulators. The one on the left is a model FCW-1521 built by Merrimac Microwave Co.; the one on the right is a model 4095 built by Genesys Systems, Inc.

Because the circulators are built from ferromagnetic material, caution must taken when handling them. They should be mounted away from any magnetic material and protected from jarring due to sharp blows.

Circulators operate efficiently only over a narrow bandwidth, typically less than that of the the waveguide.

Dual-Directional Coupler

The dual-directional coupler measures the forward power of the transmitter and the return loss, or VSWR, of the antenna or load.

The directional coupler is designed to couple power from the transmission line at some designated attenuation level in one direction, and at a much greater attenuation level in the opposite direction. The value of coupling attenuation should be such that the maximum power level at the coupled port is close to the input power rating of the power meter, or other measuring device.

10-watt power amplifier

I found that approximately 10 watts of injection power was sufficient to ensure that the oven magnetron locks on frequency while operating at full power. I built an amplifier using a 7289 tube in a quarter-wave cavity and operate it with 300-volts Eb with 0-volt bias. Some solid-state power amplifiers which operate near this power level are available at flea markets.

Low-noise amplifier

The low-noise amplifier (LNA) is a two-stage, GaAsFET amplifier which uses Dexcel D432 devices that produce about 20 dB of gain with a noise figure of under 2 dB.

Waveguide load

A load for testing transmitters should be designed with low VSWR and the capability to absorb the transmitter's total power without overheating.

A typical waveguide load is made by mounting a large piece of tapered carbon rod at the closed end of the waveguide. The angle and length of the taper determines how well the load is matched. In the case of a high-power load, there must be a good

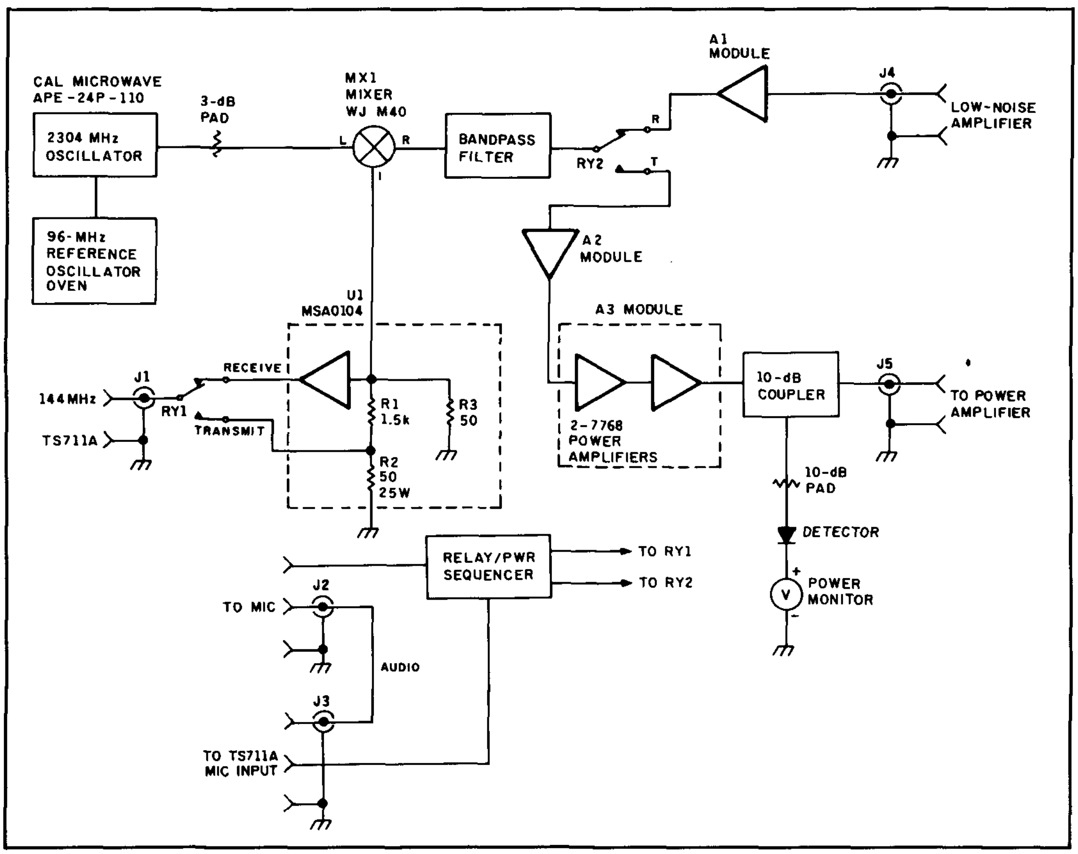

Figure 7. 13-cm transverter, block diagram.

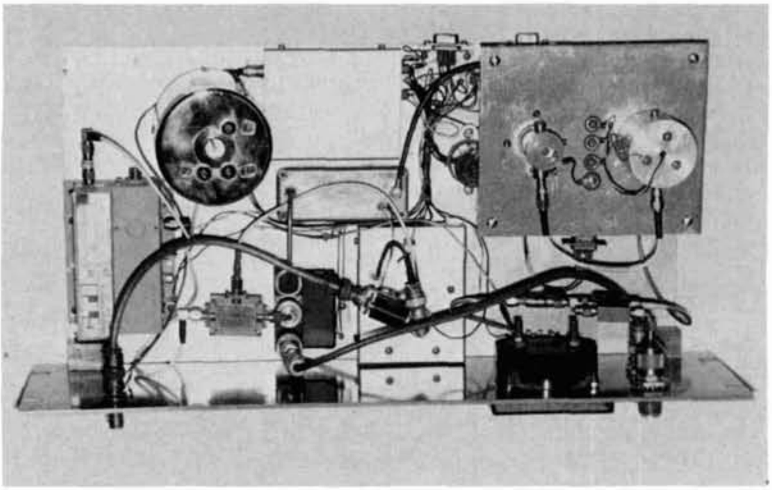

Photo I. 13-cm transverter, top view.

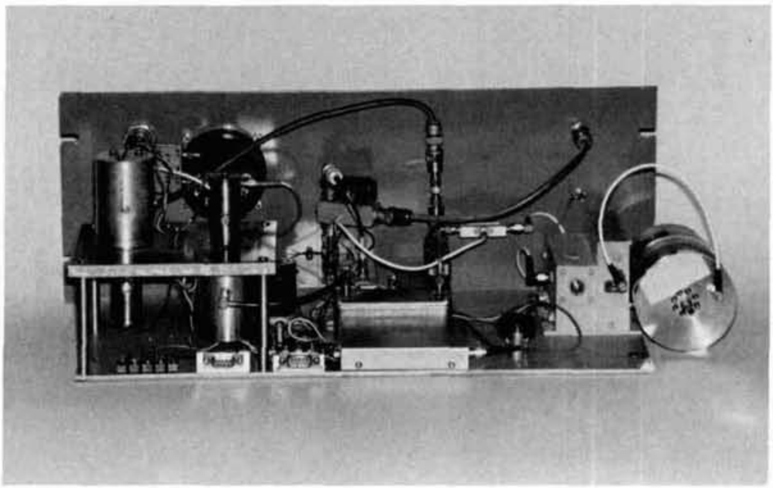

Photo J. 13-cm transverter, rear view.

thermal bond between the carbon absorber and the heat sink.

Water absorbs RF energy well. Many high-power loads are made by creating a section of the waveguide through which water can be pumped in and out. These loads are small and light, but require a great amount of pressurized water to dissipate large amounts of RF power.

13-cm transverter

The 13-cm transverter block diagram, shown in **Figure 7**, will convert RF signals up and down from a 144-MHz transceiver into the 13-cm band. The power output of the 13-cm transverter is about 1 watt on transmit. The noise figure is about 4 dB on receive. **Photos I** and **J** show the top and rear views of the 13-cm transverter, respectively.

Local oscillator

A 2304-MHz local oscillator (LO) in the 13-cm transverter generates a signal at 2448 MHz when using the microwave oven magnetron. If the 13-cm transverter is to be used for Phase III satellite work, or at the bottom of the 13-cm band, the LO to 2256 or 2160 MHz can be changed easily by replacing the oscillator and reference generator. The oscillators I use are from California Microwave Corporation; Communications Technology, Inc.; or Frequency Source West. They are available at flea markets, or through ads in various ham magazines.*

Mixer

The mixer is a surplus Watkins-Johnson M-40 which covers a 1 to 5-GHz frequency range (**Figure 7**). The maximum LO power for the mixer is 23 dBm. The mixer will easily provide 0 dBm output at the RF port when 10 dBm is supplied at the IF port.[4]

A four-pole, interdigital filter is used at the output port of the mixer to suppress image frequencies during transmit and receive. A good match must be provided at the filter input.

Modules A1 and A2 (**Figure 7**) are two-stage, 20-dB gain, transistor amplifiers which use Dexcel D-432 GaAsFET devices. Module A3 is a two-stage, coaxial-type power amplifier, using GE 7768 vacuum tubes in a grounded-grid configuration. Each stage has a power gain of about 12 dB at 1 watt RF output. The input and output cavities are 3/4-wavelength long with tuning slugs that cover the entire 13-cm band.

It has been my experience when trying to operate the Kenwood TS711A or TS811A transceivers at reduced power, that the RF-power output rises to full power (25 watts) for a few microseconds before it settles to lower power. When driving mixer diodes, this short spike of high power can sometimes damage the diodes. I now use a high-power power divider when building transverters, and run the transceiver at full power output. This requires another properly sequenced RF relay, but it's the only way I've found to prevent the loss of valuable mixers.

Push-to-talk line

When going from receive to transmit, or vice versa, it's imperative that the transfer relays be properly sequenced. When going

*One source of local oscillators is: Alan Dickinson, N5BHX, 154 Basswood, San Antonio, Texas 78213.

to transmit, the T/R relays must be in the transmit position before the 144-MHz transceiver goes into the transmit mode. Likewise, when going from transmit to receive, the 144-MHz transceiver power output must drop to zero before the T/R relays return to the receive position. This is accomplished by a delayed push-to-talk line to the 144-MHz transceiver.

Constant-current regulator section

Once the magnetron starts to draw current, it will continue to do so unless some form of limiting is provided. Microwave oven manufacturers use current-limiting power transformers designed to supply the rated voltage and current. Because the current level supplied by these transformers may not be at the value Amateurs need to operate the magnetron, some external means of controlling the current to the magnetron is needed.

There are several ways to build constant-current regulators that will do the job, but most are not easily adjustable under load at the current values required for the oven magnetron. Because high voltages are present, I felt it was necessary to use vacuum tubes.

After considering the many types of tubes that could be used as current regulators for this rig, I selected the 4CX250B power tetrode. It has one of the flattest Eb/Ib curves of any tube available.[5] At a maximum current of 250 mA per tube, I needed four of them operating in parallel to provide the proper constant-current regulator for the oven magnetron.

The schematic diagram of the constant-current regulator is shown in **Figure 8**. The positive terminal of the magnetron HV power supply is tied to the plates of the 4CX250Bs through 18-ohm limiting resistors and a 1-A full-scale meter to measure magnetron cathode current. The screen voltage for the 4CX250Bs is supplied from a 250-volt, 100-mA regulated power supply. The adjustable bias for the tubes is supplied from a negative 68-volt regulated bias-power supply.

To balance the slight tube differences, there are individual bias adjustments for each. The cathode, control grid, and screen grid of each tube is bypassed with 0.01-μF, 500-volt ceramic capacitors. The anodes are bypassed collectively with a 1200-pF, 2500-volt feedthrough capacitor. The current of each regulator tube can be monitored on the multimeter so it can be adjusted for a balanced condition. The total cathode current of the regulators can also be read from this meter. This provides a means of determining the 4CX250B total screen current. **Photos K** and **L** show the top and rear views, respectively, of the constant-current regulator.

Magnetron HV power supply section

The typical microwave oven magnetron operates at an anode-to-cathode potential of about 3.2 kV with an anode current of 300 to 800 mA – depending on the magnetron power output. Filament requirements

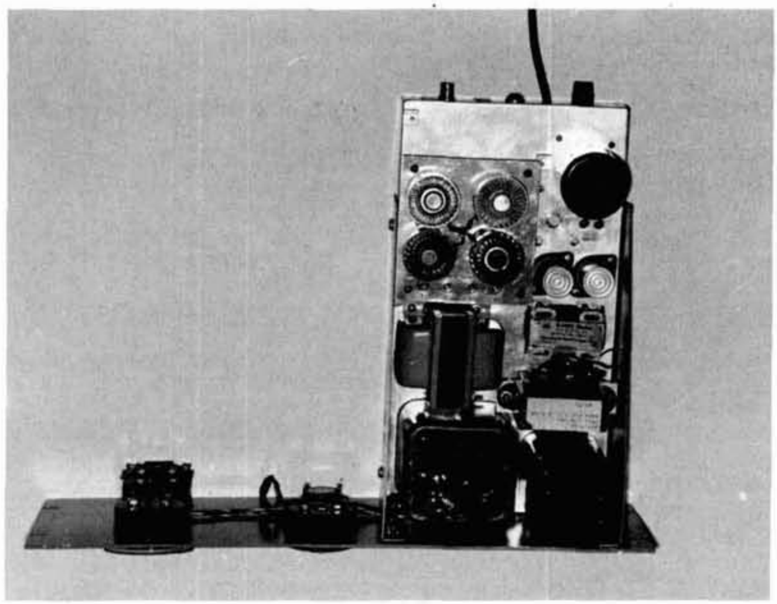

Photo K. Constant-current regulator, top view.

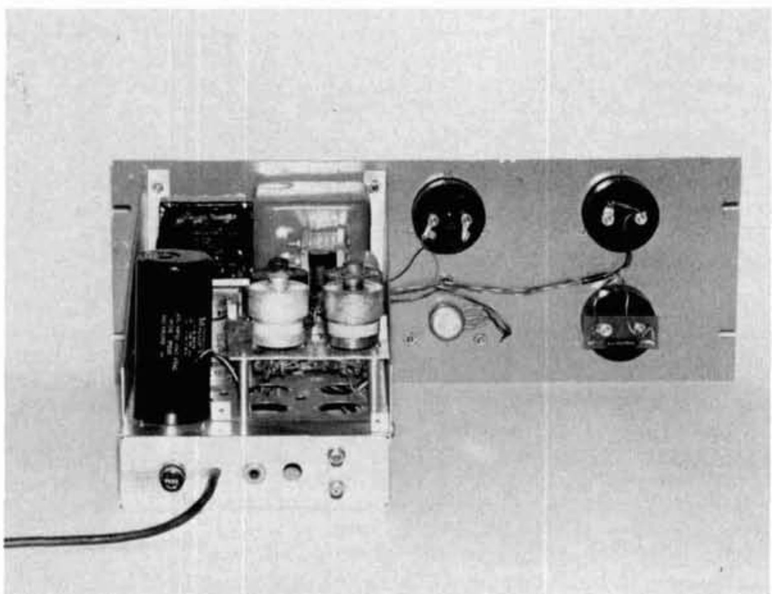

Photo L. Constant-current regulator, rear view.

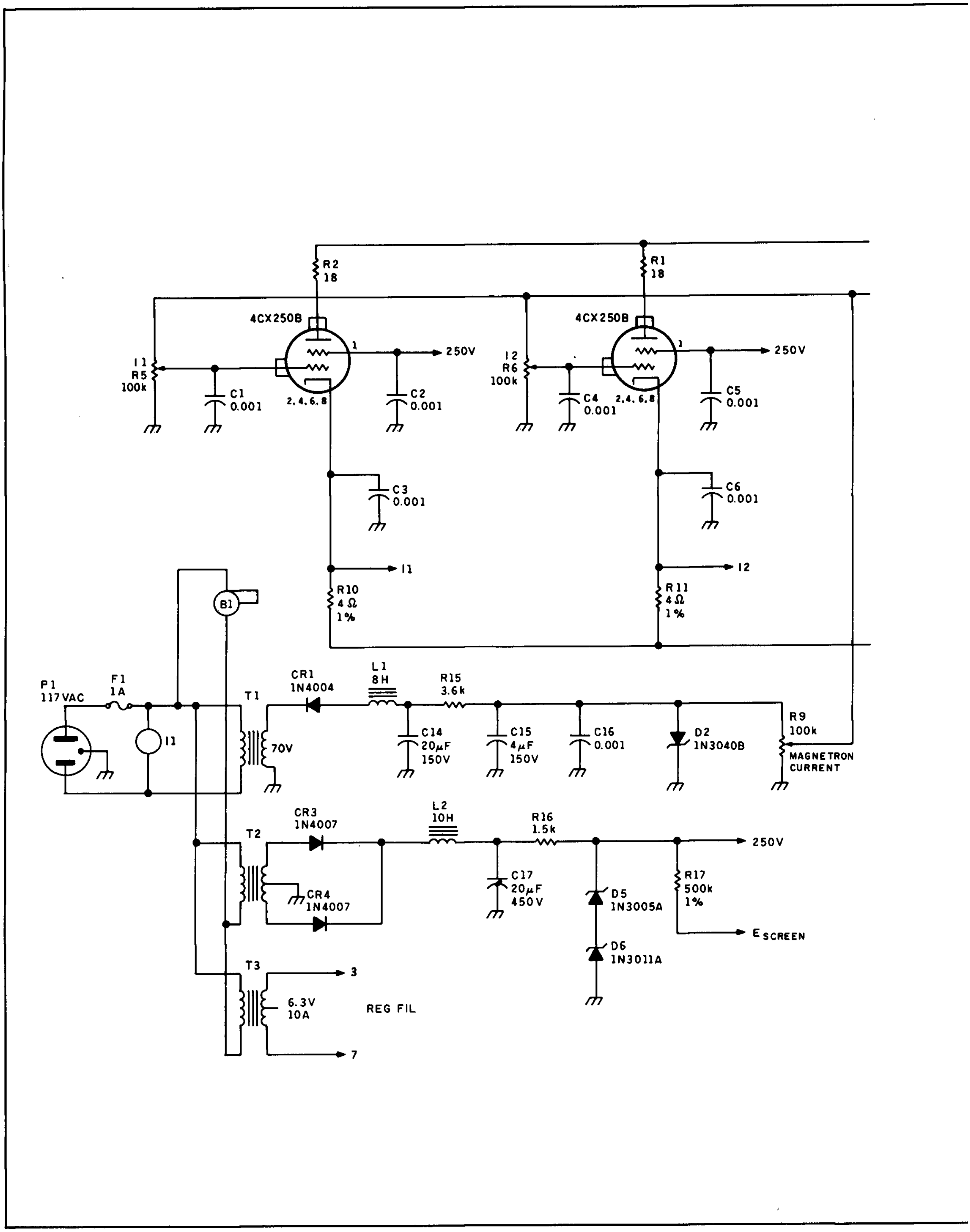

Figure 8. Constant-current regulator, schematic diagram.

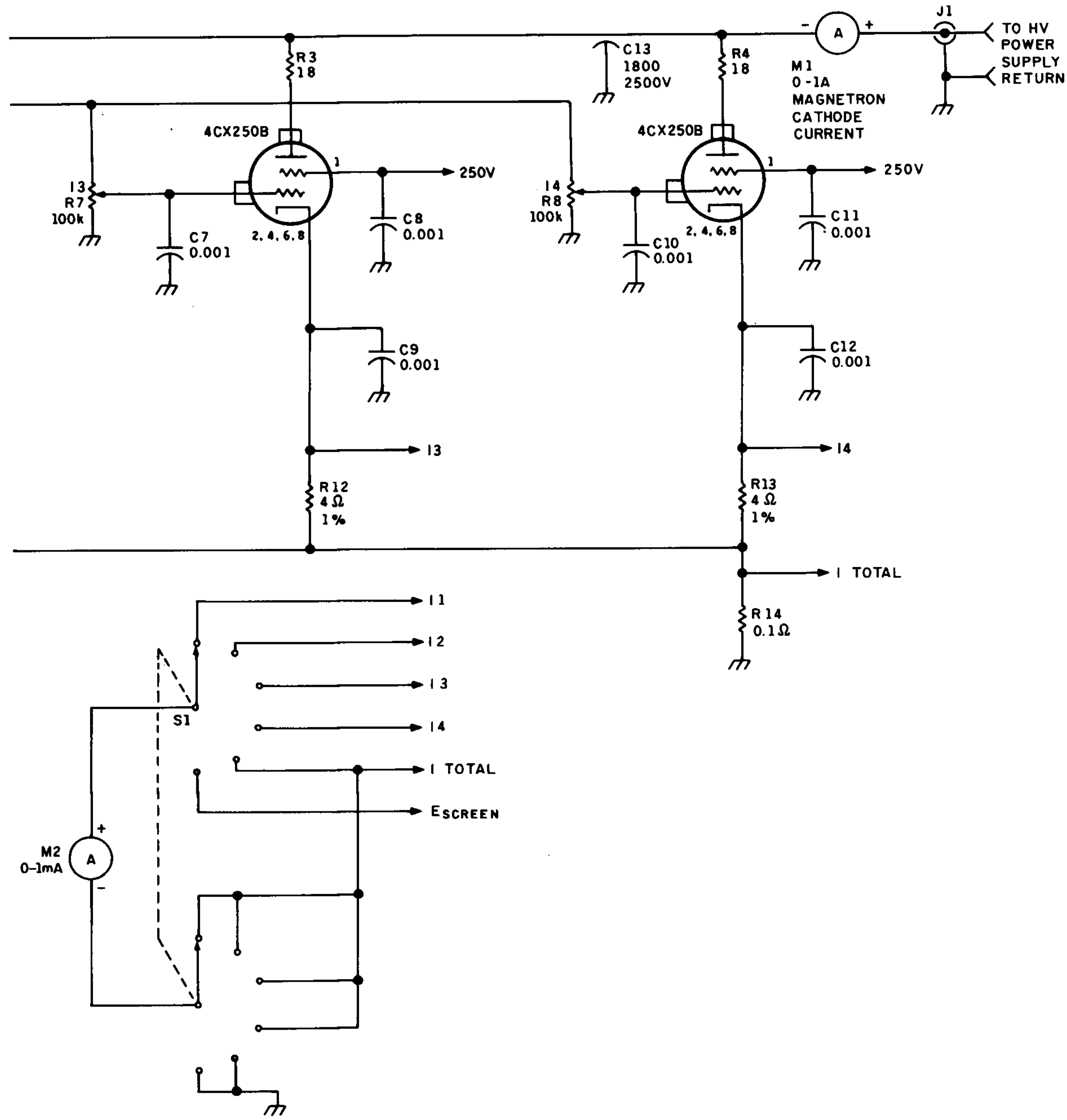

R3
18
R4
18
C13
1800
2500V
M1
0-1A
MAGNETRON
CATHODE
CURRENT
J1
TO HV
POWER
SUPPLY
RETURN
4CX250B
4CX250B
250V
250V
I3
R7
100k
I4
R8
100k
C7
0.001
C8
0.001
C9
0.001
C10
0.001
C11
0.001
C12
0.001
2, 4, 6, 8
2, 4, 6, 8
I3
I4
R12
4 Ω
1%
R13
4 Ω
1%
I TOTAL
R14
0.1 Ω
I1
I2
I3
I4
I TOTAL
ESCREEN
S1
M2
0-1mA

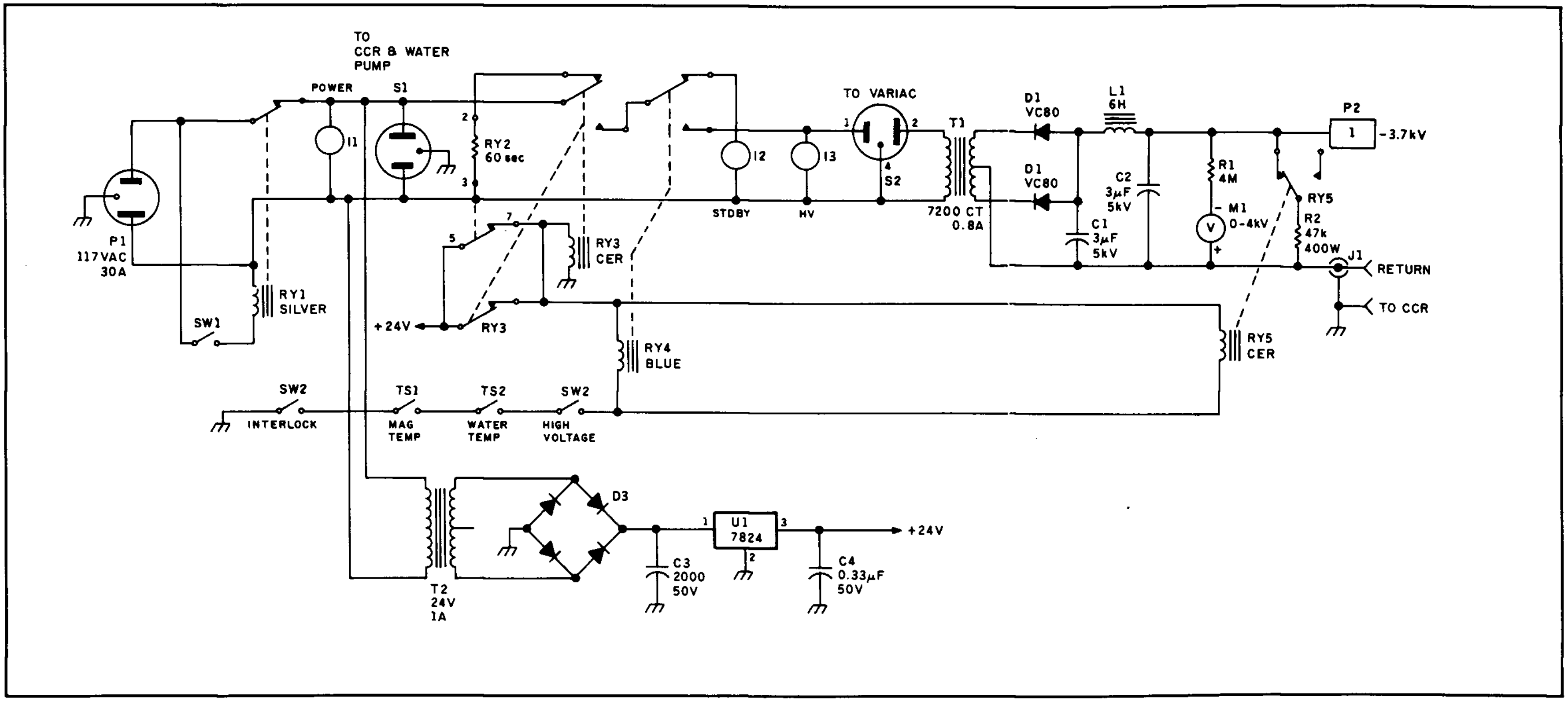

Figure 9. Magnetron HV power supply, schematic diagram.

will be in the 3 to 5-volt range at current ratings of 20 to 40 A. There's a large current in-rush when power is turned on, so some means of current limiting must be provided for both filament and anode supplies. A means of protecting the magnetron from damage due to overheating must also be provided, either by forced air or water cooling.

The magnetron in a typical microwave oven is operated from a power supply that has a current-regulated, high-voltage power transformer and uses full-wave rectifiers with unfiltered output voltage. Consequently, the tube is operated in the pulse mode with a duty cycle of about 50 percent. This is done to prevent mode skipping. In Amateur operation, the tube must operate at 100 percent duty cycle from a well-filtered power supply because the magnetron frequency is sensitive to supply voltage changes. Due to the microwave oven's 50 percent duty cycle, I've found that the power transformer from the the oven isn't "husky" enough to be used in an Amateur transmitter. The magnetron filament is supplied from a winding on the high-voltage transformer. Thus, the transformer can be used for this purpose without surge protection for the filament (required if a separate filament transformer is used). It is necessary to protect oneself, and the circuit, from the transformer's unused high-voltage terminal.

I built the magnetron HV power supply using a 7200-volt center-tapped transformer with full-wave rectifiers into a pi-network filter, as shown in **Figure 9**. The output voltage is controlled by a 30-A Variac®. A time-delay relay in the primary allows the filament to reach temperature before high voltage can be applied. The high-voltage switch is in series with the temperature-sensing thermostats installed on the magnetron and on the water-cooling system, so high voltage can't be applied to the magnetron if the temperature is too high.

To discharge the filter capacitors, a large bleeder resistor is placed across the power-supply output when the high voltage is turned off. The bleeder resistor is removed from the circuit when high voltage is on, because there's no reason to waste power during transmit. A 5-kV voltmeter reads the power supply output voltage. Indicator lights are provided for main power, standby, and high-voltage ON. The power supply weighs over 200 pounds, so it rests in the lowest position of the transmitter rack.

Testing the transmitter

The following pieces of test equipment are required to evaluate the performance of the 13-cm transmitter:

- A frequency meter capable of measuring the transmit frequency to within 1 MHz.
- A power meter and attenuator pads to measure the transmitter power output.
- Directional coupler.
- Spectrum analyzer.

It's also necessary to have some means of observing the spectrum to ensure the magnetron isn't mode skipping. A receiver covering the frequency of interest, with a panadapter that has a minimum of 1-MHz sweep width, can be substituted for a spectrum analyzer. Panoramic Radio, Inc. panadapters with 5-MHz sweep widths, used in the telemetry industry, are available at most flea markets.

Free-running mode

The first tests on the 13-cm transmitter are done in free-run mode; that is, not locked to a stable source. A suitable load is connected to the transmitter output, and the spectrum analyzer is connected to the forward port of the dual-directional coupler (see **Figure 10**). If required, an attenuator pad should be used to prevent damage to the spectrum analyzer. The frequency meter should be connected in a manner appropriate for the type used.

With the power to the transmitter turned on, the magnetron cathode voltage and current is adjusted to the recommended values, and the spectrum is observed. A single line should appear on the screen. If not, the cathode current is readjusted to a value that produces a single line. The line should look similar to that in **Photo F**. Next, the filament voltage to the magnetron is turned off. The line should now look like **Photo G**. The magnetron cathode current is adjusted to lower values and the power output observed. At some lower value of cathode current, the magnetron will fail to operate. These magnetron cathode current and frequency values are recorded for future reference.

Magnetron pushing characteristics

With the filament voltage turned back on, and the magnetron cathode current

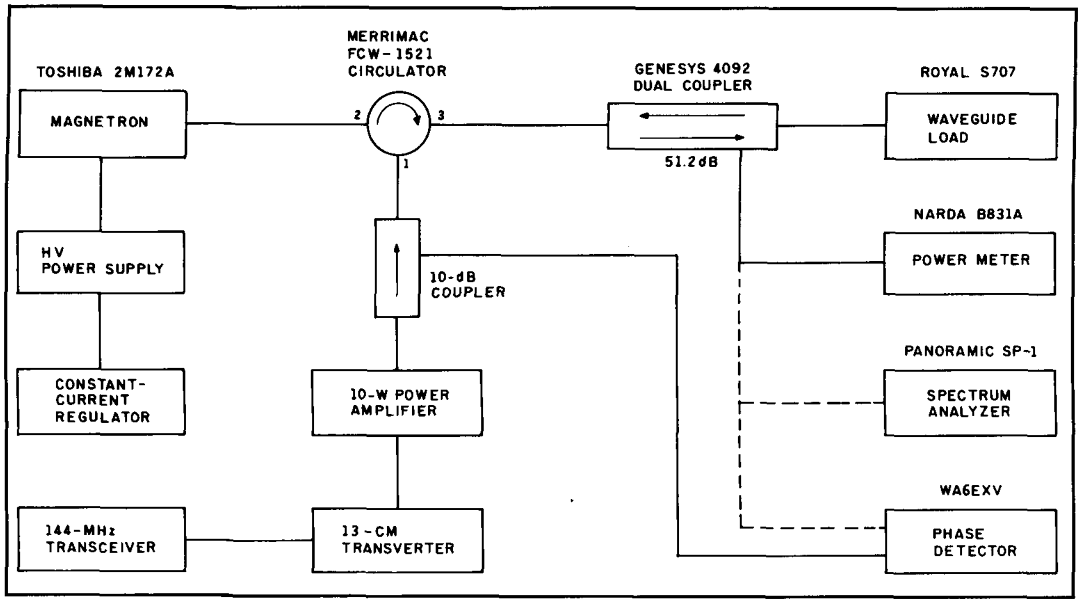

Figure 10. 13-cm transmitter test setup, block diagram.

readjusted for full-power operation, the frequency is measured. This is the magnetron's maximum frequency. As the magnetron cathode current is reduced, frequency and power output decreases. These values are recorded and plotted on a graph of magnetron-cathode current versus frequency similar to the one in **Figure 11**. This curve shows the magnetron pushing characteristics. From this graph, the frequency at which the 13-cm transmitter will be operated is determined and the magnetron cathode current is adjusted to that value.

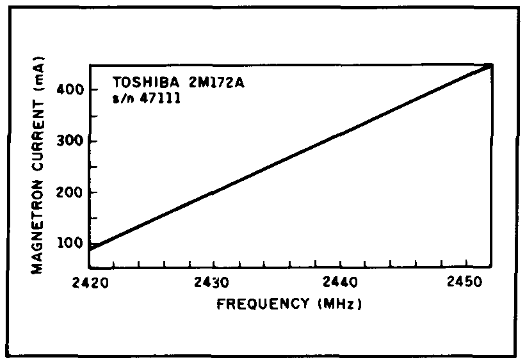

Figure 11. Typical oven magnetron frequency-pushing characteristics.

Magnetron pulling characteristics

The output from the 10-watt power amplifier is connected to the transmit port of the T/R relay on the RF deck. The transmit port of the 13-cm transverter is connected through a suitable variable attenuator to the 10-watt power amplifier input. The attenuator is adjusted for 10-watts output of the amplifier. The 13-cm transmitter is brought up in the transmit mode to the predetermined frequency, and the magnetron-cathode current is adjusted up and down until the magnetron drops out of lock. These two values are recorded.

These steps are repeated with lower and lower power output, and another graph similar to the one in **Figure 12** is generated by plotting magnetron cathode current versus locking power. This curve shows the pulling characteristics of the magnetron. By using the pushing characteristics graph,

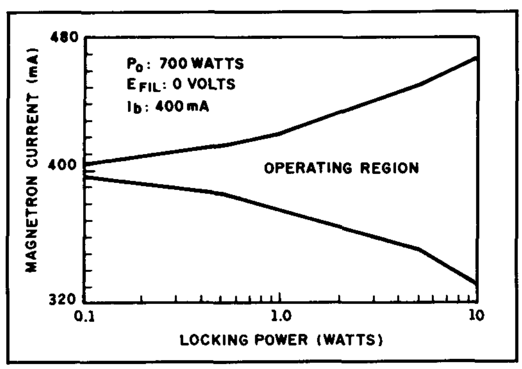

Figure 12. Typical oven magnetron frequency-pulling characteristics.

pulling characteristics graph, and the power levels recorded, it's possible to determine the injection locking power required to operate at a particular output power level and frequency. **Figure 13** is a graph of frequency-locking range versus locking power.

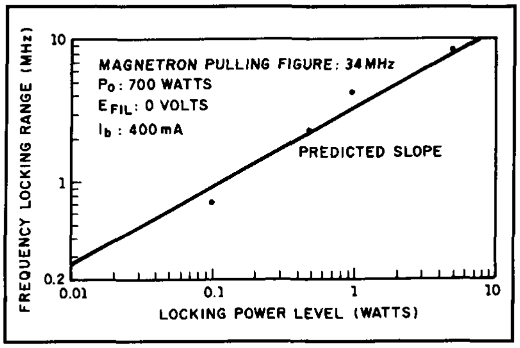

Figure 13. Frequency range for locked operation.

Conclusions

I hope my suggestions for using inexpensive oven magnetrons operating in the injection mode for Amateur transmitters will generate more interest in 13-cm EME.

Although this isn't a construction article, and some of the parts may be difficult to locate, I feel this information will give the serious experimenter some new ideas on how to go about building a high-power 13-cm transmitter.

I wish to thank Ed Nyswander, Senior Design Engineer, Naval Weapons Center, China Lake, California, for suggestions which helped me start this project; Dick Kolbly, K6HIJ, for his help in designing the constant-current regulator; my daughter, Sharon Scoles, for editing my work; and my wife, Jean, for her continuous support. ■

REFERENCES

1. R. Adler, "A Study of Locking Phenomena in Oscillators," *Proceedings*, IRE, 34, June 1946, pages 351-357.
2. R.C. Mackey, "Injection Locking of Klystron Oscillators," *Space Technology Laboratories Report AFBMD-TN-61-15* for Air Force Ballistic Missile Division, ASTIA #AD257622.
3. J. Francis Reintjes and Godfrey T. Coate, *Principles of Radar*, McGraw-Hill Book Company, 1952, pages 763-805.
4. *RF Signal-Processing Components*, Watkins-Johnson Company, 1983/84.
5. "RCA Transmitting Tubes," *Technical Manual TT-5*, pages 212-216.

By Steven M. O'Kelley, *WA7SXB*
P.O. Box 46785
Seattle, Washington 98146

BUILD A REMOTE DISPLAY FOR YOUR ICOM HF RADIO

This digital readout is handy for mobile or home use

Thanks to today's compact, solid-state transceivers, many Amateurs are enjoying mobile operation. The newer equipment is easier to use and will fit into almost any vehicle. However, the most common method of installation requires that the user look down and away from the road to tune around the band. A readout on the dashboard will let you watch your frequency and still keep your eye on the road.

You'll also find this display is handy indoors when operating. The completed unit is small and lightweight, and an experienced builder can put it together in a few evenings. Parts are readily available and will cost you about $50. Best of all, you don't need to modify your rig. The display was designed around the IC-735, but has also been used with the 725, 751A, 765, and 781. It will work with any ICOM radio equipped with a CI-V port.

Newer radios have a data port

Before discussing how the display works, let's take a look at what the radio does. Most newer radios come with a data port for interfacing to computers or other devices. ICOM radios come with an interface called a CI-V (computer interface five), which allows control over many of the radio's functions.

Whenever you change the radio's frequency using the main dial, a memory button, the VFO A-B button, or the mic up-down buttons, it automatically sends a ten-byte data message (see **Figure 1**). Each byte contains eight information bits representing two hexadecimal values. The first two bytes are a preamble alerting other devices that data is on the way. Bytes 3 and 4 contain the addresses of the devices receiving and sending the data, respectively. Byte 5 is a control code that specifies the function to be executed; that is, set mode or set band. The next four bytes contain the frequency information. Byte 10 holds the hex value of FD, and marks the end of the message.

Note that, in the examples given, the frequency information is sent in reverse order. The information for 10 and 1 MHz is sent last. Also note that in the data message for

TEN BYTES (8-BIT WORDS)

FE	FE	00	04	00	00	41	05	07	FD
PREAMBLE		RX ADR	TX ADR	CTL CODE	FREQUENCY DATA				EOM

FREQUENCY IS 7.0541 MHz

FE	FE	00	04	00	00	31	02	28	FD
PREAMBLE		RX ADR	TX ADR	CTL CODE	FREQUENCY DATA				EOM

FREQUENCY IS 28.0231 MHz

FE	FE	00	04	00	50	49	23	14	FD
PREAMBLE		RX ADR	TX ADR	CTL CODE	FREQUENCY DATA				EOM

FREQUENCY IS 14.23495 MHz

Figure 1. Examples of the serial data message sent by the radio. Note that the frequency information is contained in bytes 6-9 and is sent in reverse.

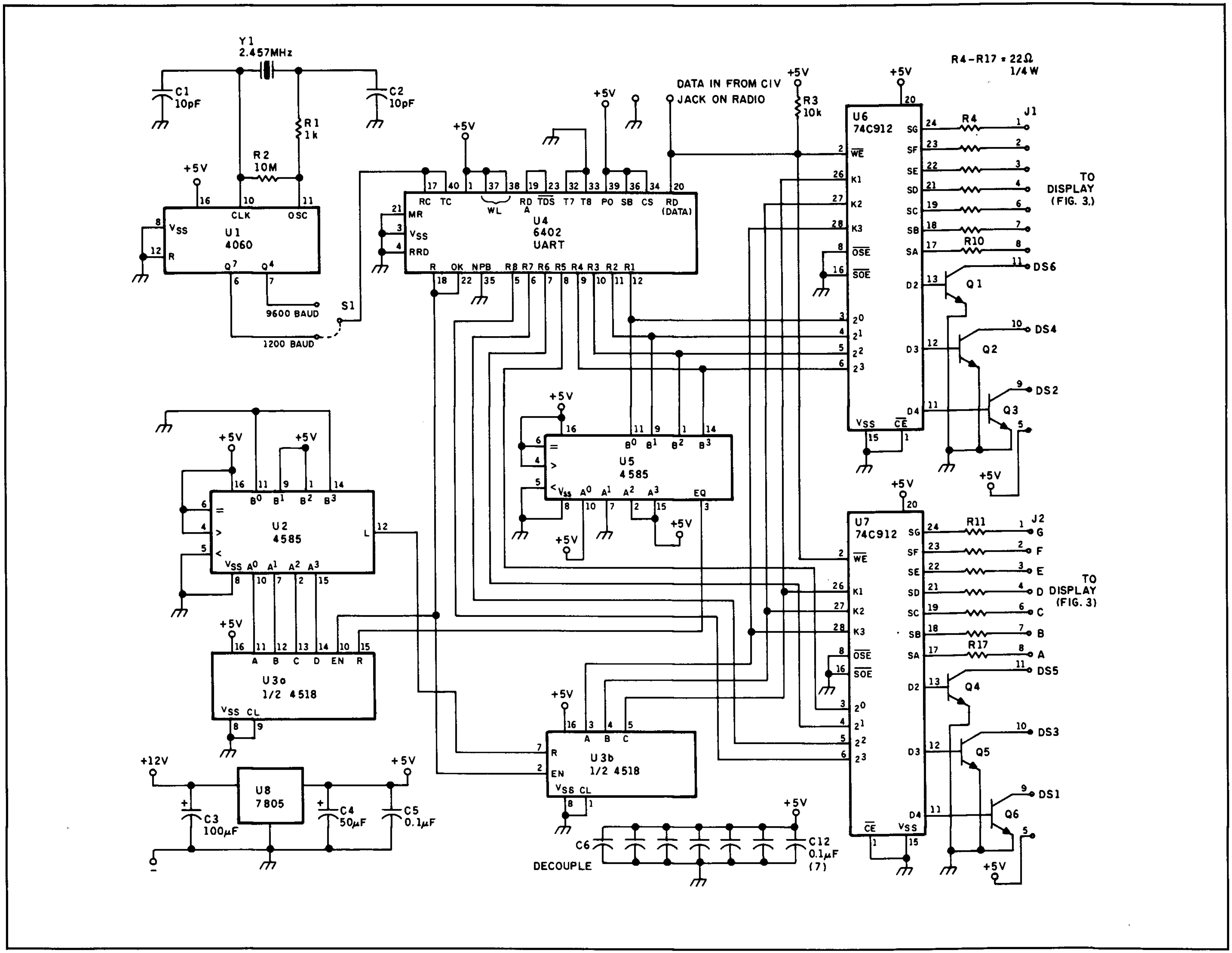

Figure 2. Logic-board schematic.

14 MHz, byte 6 (see **Figure 1**) represents 50 Hz. Information for the 10-Hz digit is always sent, but isn't displayed. The 1-Hz information is a dummy message and is always zero.

This CI-V message is sent to a miniature phone jack on the back of the radio and relays the radio's frequency to the remote display.

How it works

Figure 2 shows the display's logic schematic. The design centers around U4, a UART (universal asynchronous receiver transmitter), which receives serial data from the radio and presents it in parallel form. Two binary values are present on pins 5 through 12 for each byte of data the radio sends. When the end-of-message (FD) byte is received in the preceding example, an F (binary 15) appears on pins 5 through 8 and a D (binary 13) on 9 through 12.

Transmit data

Data from the radio goes directly into the UART on pin 20. When a valid word is received, pin 19 goes high. This signal is applied to pin 23 and tells the UART to load its transmitter register with whatever data is present on the transmit inputs. The transmit data isn't used, but as it's loaded, pin 22 supplies a low to pin 18, which resets pin 19 to a low. Pin 22 is normally high. Thus for every byte of data sent, there will be a falling-edge clock pulse which allows the circuit to count the number of incoming data bytes.

Counter and comparator

U3 is a dual BCD counter. Pulses from the UART are sent to the enable inputs of each counter. The reset input of U3A is a logic low. This counter increments as data is sent. U2, a magnitude comparator, compares the BCD value from U3A against a preset value of 6. Remember that the frequency information starts with the 6th byte. When the count reaches 6, U3A's count is no longer less than 6, and U2 pin 12 goes low. This enables U3B to begin counting on byte 7.

Display drivers

U6 and U7 are six-digit display controller-drivers. Data from the UART is fed into these devices as U3B counts up. Information for bytes 6 through 9 is stored in the display drivers. As the CI-V message is sent, the data is clocked into the UART. The data is also connected to the not-write enable lines of the display drivers. As the data line goes low, the display drivers read the parallel data from the UART. Bytes 6 through 9 are stored in registers for digits 1 through 4, respectively. The display drivers decode the information and will drive any common-cathode seven-segment LED display. Segment and digit information are applied to the display board through two ribbon cables which connect to J1 and J2.

Byte 10 contains a value of FD – the end-of-message signal. U5 is another magnitude comparator preset to a D (binary 13). It compares this data against the data from U4 pins 9 through 12. When byte 10 is sent, these two values are equal. U5 pin 3 goes high, resetting U3A. U2 pin 12 then goes high and resets U3B. The circuit remains in this state until a new message is sent.

Ripple counter

U1 is a 14-bit binary ripple counter. This IC has an internal oscillator whose frequency is determined by crystal Y1. A frequency of 2.457 MHz is divided by U1 to obtain one 16 times the baud rate of the serial data from the radio. ICOM radios are set for 1200 baud at the factory. For this data rate, the UART gets its clock from U1 pin 6. The data can be sent at 9600 baud by changing a plug-in jumper in the radio. If you've made this modification, or plan to do so, make sure to connect the UART clock to U1 pin 7. The display won't function unless the clock frequency is correct.

Display board

The display board, shown in **Figure 3**, consists of six common-cathode seven-segment LED displays, DS1 through DS6. DS1, 3, and 5 are driven by U7. U6 drives DS2, 4, and 6. Display information is multiplexed. To minimize power consumption, the display controllers turn on just one digit at a time. Notice that DS1 is wired to digit 4 on the controller. Because frequency data from the radio is sent in reverse, it can be displayed in the proper sequence by driving the displays in reverse. Resistors R1 and R2 provide current limiting for the decimal points on DS2 and DS5. If you use displays with left-hand decimal points, connect these resistors to DS3 and DS6. Although they aren't necessary for the operation of the remote display, the decimal points will make it easier to read.

All power is supplied by U8, a 5-volt regulator **(Figure 2)**. The circuit shown uses

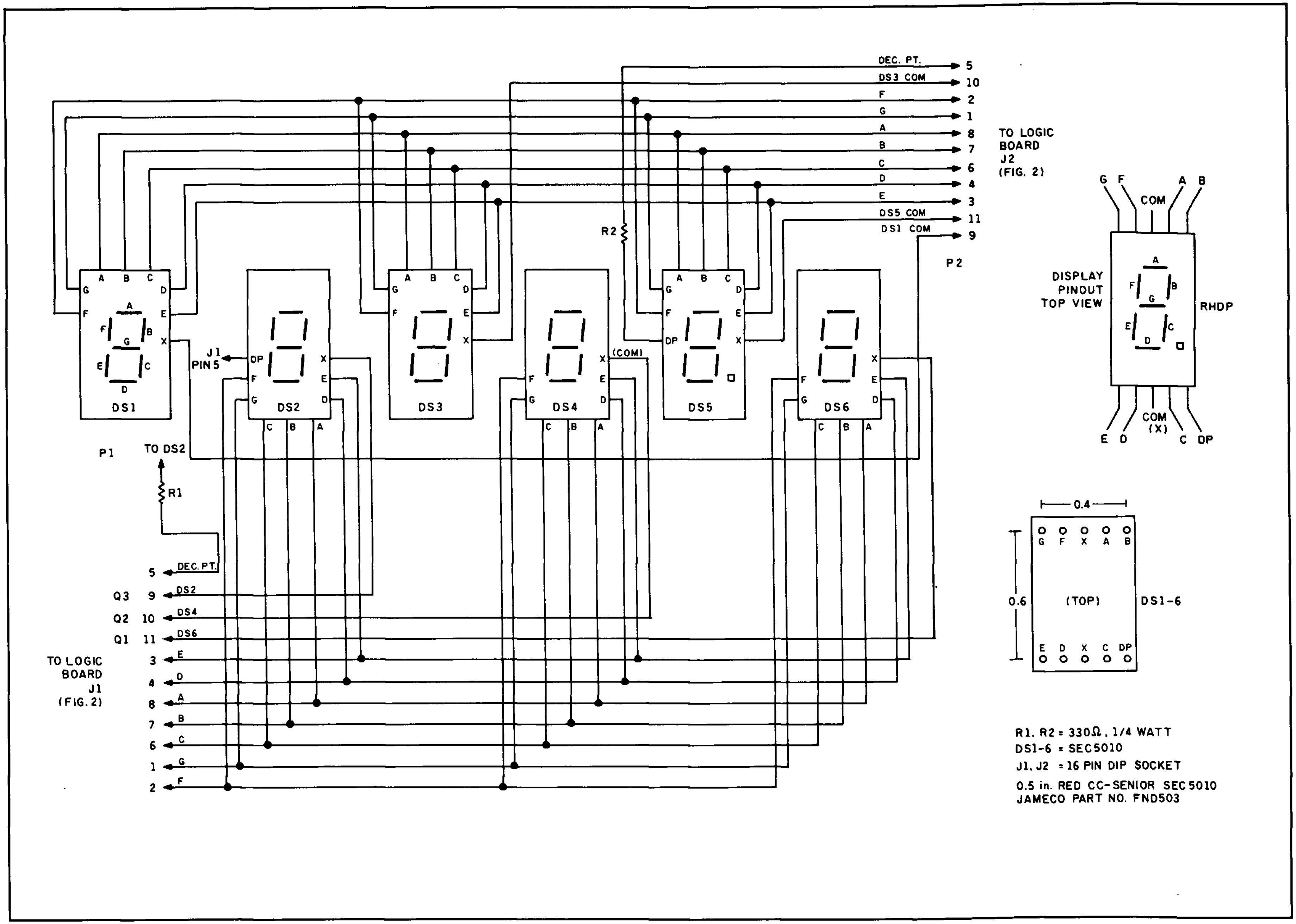

Figure 3. Display-board schematic. The display is built on a Radio Shack 276-170 circuit board.

a 7805 which supplies about 1 A. During operation, the display requires 450 to 500 mA.

Building the logic board

I built the logic board on perfboard using point-to-point wiring. You can also wire wrap the connections. A board cut to approximately 6 by 4-1/2 inches will accommodate all parts and wiring. **Photo A** shows a breadboard version of the display. **Photos B** and **C** are views of the remote display made using the construction techniques described here.

Use IC sockets for U1 through U7, J1, and J2. This will make it easy to unplug the display board or replace any ICs that fail. **Figure 4** shows a suggested parts placement. Align J1 pin 1 with U6 pin 24 and J2 pin 1 with U7 pin 24 so resistors R4 through R17 can be wired pin for pin between the display drivers and the display board sockets. Use ordinary 16-pin IC sockets for J1 and J2.

Make sure to mount U8 on an outside edge of the logic board, with the metal tab facing out. This IC must have an adequate heatsink. A piece of medium-gauge aluminum around the back and sides of the board will provide both the heatsink and the framework for attaching a housing.

Y1, R1, R2, C1, and C2 (**Figure 2**) should be mounted close to U1. Make the lead lengths as short as possible.

Before wiring the board, make a couple of extra copies of the schematic. As you make each connection, trace it on a copy in red pencil. This will help you keep track of the connnections you've made. Wire the regulator circuit first and test it. The output should be 5 volts.

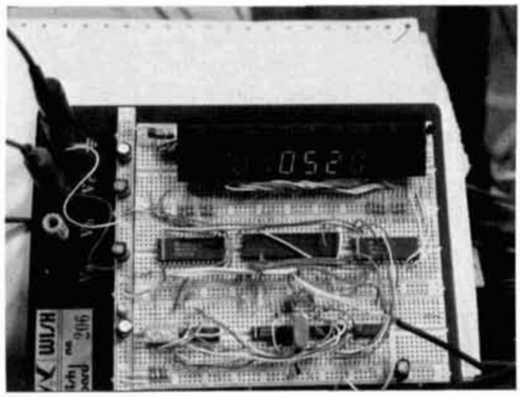

Photo A. Breadboard version of the remote frequency display.

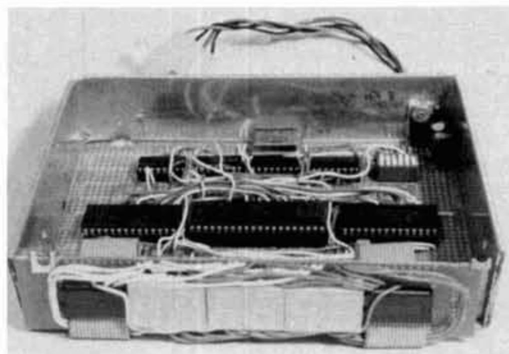

Photo B. Completed unit showing display board.

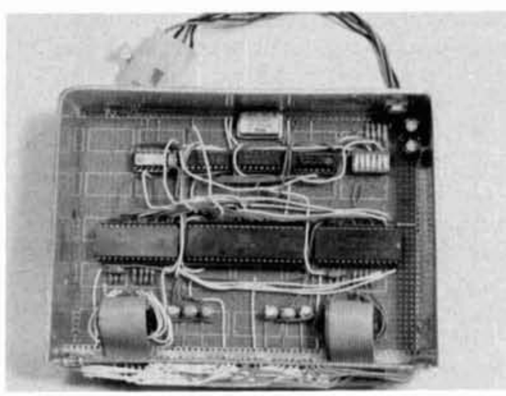

Photo C. Top view of a completed remote display.

Building the display board

I built the display board on a Radio Shack 276-170 circuit board. Using a bandsaw, trim each edge of the board lengthwise until you have only the 47 rows of foil patterns. The board should measure 6 by 1-1/4 inches. When the displays are centered, there will be two holes available for wiring to each pin. Use these to wire the displays and ribbon-cable connectors.

Solder the ribbon-cable connectors directly to the display board. Make the connectors from 4-inch lengths of 16-conductor ribbon and DIP plug connectors similar to Jameco part no. 609-16. You can attach connectors by inserting them into a socket on a breadboard. With the cable properly oriented in the connector, use a small piece of wood and a hammer to gently compress the connector until it's locked.

You can use any common-cathode seven-segment display of any size or color. Placing a piece of colored Plexiglas™ in front of the digits will make them easier to read and also hide your wiring. Make sure that the Plexiglas is the color of the LEDs. Most commercial plastics dealers have large enough scrap pieces for sale.

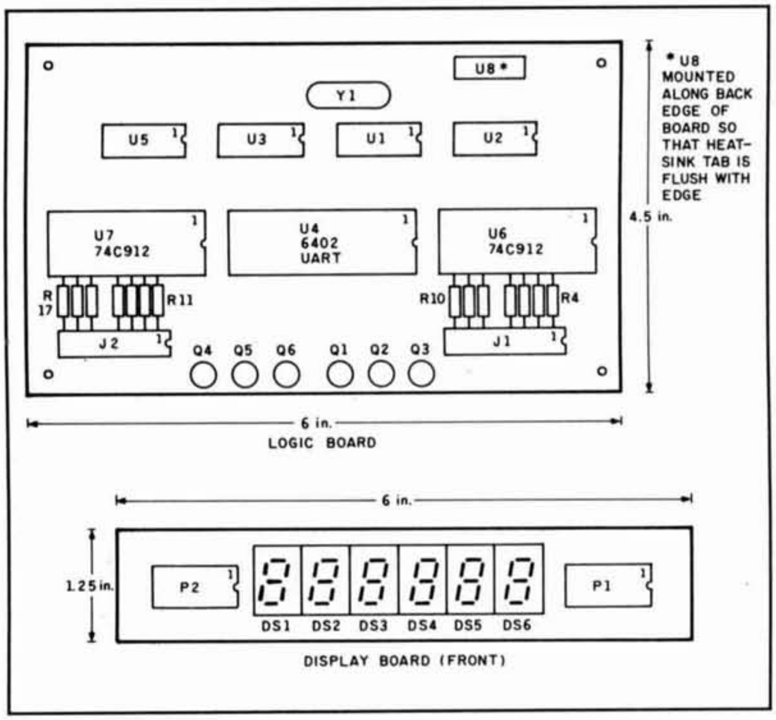

Figure 4. Suggested parts placement for ICs; logic and display boards.

Photo D. Remote display connected to ICOM 735. Case was made from surplus pc board by K7YLM.

Whether your remote display is for mobile or home use, you'll find it a handy accessory and a fun construction project. ■

Mount the completed unit in the enclosure of your choice. If you wish, you can make a homemade cable to go between the radio and the remote display. Use shielded wire for the line to the CI-V data jack. You can obtain power from the radio's accessory jack. But if you do, make certain to fuse it at 1A to protect the radio.

Operation

With the unit completed and wired to the radio, turn the power on. The remote display shows the same frequency as the radio. As you rotate the VFO, or press the memory buttons, the display changes accordingly.

For mobile use, you can fasten the unit to the dashboard with a couple of pieces of Velcro™. This makes the display easy to remove. You might also like to place a small mirror in front of the unit. Light from the display is reflected forward, and you can read the frequency in the windshield.

In my shack, I've wired my radio's frequency up-down functions to a switch near the computer. Because the rig is several feet away, it makes RTTY and AMTOR modes a bit easier to operate. The large LEDs are easy to see from across the room **(Photo D)**.

PARTS LIST

CAPACITORS

C1,C2	*10 pF, 500 volts, silver mica*
C3	*100 μF, 50 volts, electrolytic*
C4	*50 μF, 50 volts, electrolytic*
C5-C12	*0.1 μF, 50 volts, monolythic ceramic*

DIODES

DS1-DS6	*FND503 (SEC5010), seven-segment display*

TRANSISTORS

Q1-Q6	*2N2222 NPN silicon*

RESISTORS

R1	*1 k, 1/4 watt*
R2	*10 meg, 1/4 watt*
R3	*10 k, 1/4 watt*
R4-R17	*22 ohms, 1/4 watt*

INTEGRATED CIRCUITS

U1	*4060 14-bit binary ripple counter*
U2,U5	*4585 4-bit magnitude comparator*
U3	*4518 Dual-binary up counter*
U4	*6402 CMOS UART*
U6,U7	*74C912 Display controller-driver*
U8	*7805 5-volt positive voltage regulator*

MISCELLANEOUS

Y1	*2.457-MHz crystal*

IC sockets
Ribbon cable
Dip connectors
Proto board

All parts are available from:

Jameco Electronics
1355 Shoreway Road
Belmont, California 94002

By Jim Bacon, *G3YLA*
Reprinted from Practical Wireless
October 1990

AMATEUR RADIO AND METEOROLOGY GO HAND-IN-HAND

Professional meteorologist and Anglia ITV "weatherman" Jim Bacon, G3YLA, provides an introduction to weather and its effects on radio propagation

The idea behind this article is to discuss the benefits of weather study to operation on the VHF/UHF amateur bands. It will cover the two main weather-related propagation events, "tropo" and sporadic-E. Each depends on different characteristics of the weather patterns, and a basic knowledge of the physics behind these features will greatly improve your chances of working the DX.

On a superficial glance, "weather" seems to consist of two fundamental chart features: the **high** and **low** pressure areas which can be seen on TV weather maps and some newspaper weather pages. While it's true that these are only one part of the complex series of factors which go to produce the actual weather we observe, they do establish many of the ground rules for the day's weather, and largely determine the chance of any propagation benefits.

Highs and inversions

Most of you will be familiar with the idea that areas of high pressure are often times of DX on VHF and UHF. This is a direct result of the air motion within a large high and the effect this has on the refractive index of the air.

Developing highs are characterized by a large-scale descent of air within the region of the high (see **Figure 1**). This vertical motion (typically 1 cm/s downwards) is much more gentle (100 times less) than the horizontal motion of air around the high (the wind, 5 to 10 m/s).

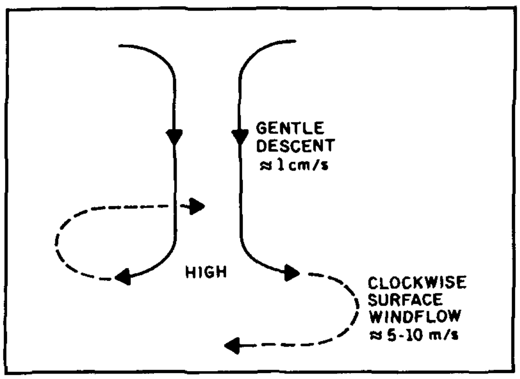

Figure 1. Developing highs are characterized by a large scale descent of air within the region of the high.

It's important to realize that much of our weather is due to the vertical rather than horizontal motion of the air. In this case it is downwards but, as we will see later, upwards motion is important in areas of low pressure.

Let's go back to the high and consider what happens to the air as it descends in this pressure system. Pressure is greatest at the surface and decreases as you go upwards. Therefore, air that travels downwards (subsides) is moving into a region of greater pressure.

Increasing pressure

You are probably aware of one example of increasing pressure. When pumping up a bicycle tire, the end of the pump gets hot. This is not due to friction, but is a direct result of increasing the pressure of the air inside the pump. This same principle is at work inside the area of high pressure; as the air descends, it warms.

Meanwhile, the air near the surface has not been warmed by this subsidence, and we notice that a temperature **inversion** is established. Let me explain: Normally, temperature decreases with height because the air is warmed by contact with the ground (see **Figure 2A**). This is not surprising – as you move away from the heat source, it gets cooler.

Near the surface in the lowest 0.5-km (1500 feet) region of a large high, you will find air which has not been modified by subsidence. It probably shows the expected temperature decrease with height. Above this you will find air which has subsided in the high and become warmer relative to the surface air below. This subsided air also becomes drier; that is, its relative humidity decreases.

Subsidence inversion

The contrast between these two air masses forms a temperature inversion. Strictly, it should be referred to as a **subsidence inversion** to identify its cause. The term inversion states that the temperature trend (normally a decrease in height) is reversed or "inverted," and you now see a temperature increase over a small height interval (see **Figure 2B**).

The first signs of a useful subsidence inversion often do not appear until it has come below 1.5 km (4500 feet). It may then intensify further as it descends. Many inversions end up around 0.5 to 1 km (1500 to 3000 feet) and some may eventually reach the surface in the middle of large highs.

This whole physical process takes place over vast areas of the weather chart. Highs are among the largest of the weather systems when it comes to horizontal dimensions. This, in turn, determines the geographical scale of any radio path enhancements produced by highs.

On still, clear nights the ground can lose its heat quite rapidly. This cooling affects the air near the surface and forms a **surface inversion**. This may be in addition to the subsidence inversion at a greater height (see **Figure 2C**).

The surface inversion rarely extends higher than about 0.3 km (1000 feet) and will be destroyed by daytime heating of the ground the next day. They are essentially late evening, overnight, and early morning phenomena.

Very effective

This horizontal layering of the atmosphere is very effective at limiting vertical motion from the surface. In fact smoke,

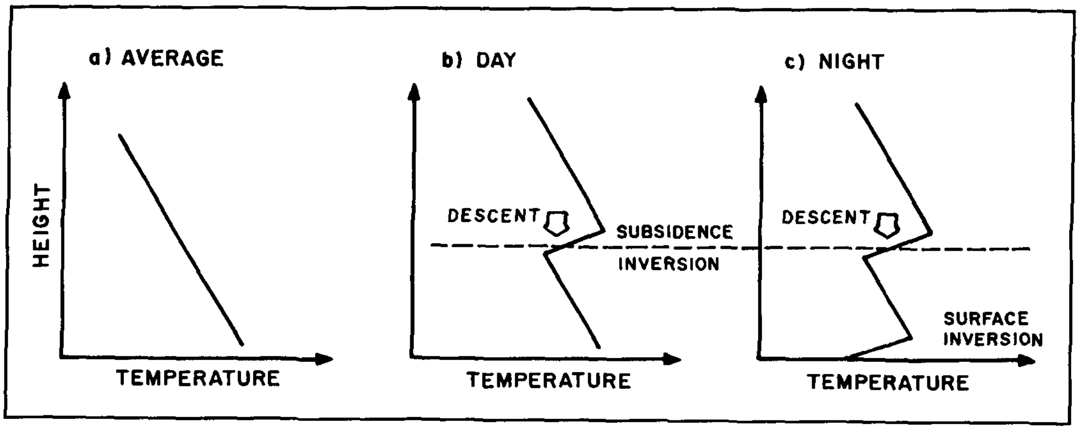

Figure 2. Subsidence inversion: (A) normal variation of temperature with height, (B) subsidence inversion taking place above the Earth's surface, (C) subsidence inversion and a surface inversion due to the loss of surface heat on a clear night.

dust, pollution, and cloud will be trapped underneath any inversion, often producing an obvious haze layer. Although invisible, water vapor (a gas) is also trapped and becomes noticeable when this moisture condenses to form low cloud or fog (**Figure 3**).

The characteristic movement of highs is a slow drift (about 5 m/s or 10 kt). They can even become semipermanent features like the Azores High or Siberian High. Usually, the slower they move, the better they are for radio amateurs. Typically highs last for 1 to 2 weeks, but sometimes they last just for a day or two, serving as separators between successive lows.

The important point to remember about highs and the inversions they produce is that the lower atmosphere becomes horizontally layered over large distances with cool, sometimes moist air near the surface and dry, warm air above the inversion. This makes quite an abrupt boundary between these two different air masses.

Lows and fronts

Lows and fronts are the disturbed parts of the weather chart. It's often lows that bring the strong winds which are the bane of large antenna arrays! If you look at a sequence of Atlantic weather charts, you will notice that lows usually move quite fast compared with highs and that their movement is often anything but straight.

The speed of movement can be up to 25 m/s (50 kt) at a low's early stages of development. The speed will drop to as little as 10 m/s (20 kt) as it gets older and larger. In fact, some lows may become quasi-stationary for several days.

As a general rule, small lows (sometimes called "wave depressions" because of the shape of the fronts) move the quickest. As the low gets larger, it will often turn to the left of its original track and slow down, finally occupying much of the Atlantic with a diameter in excess of 1500 km.

Weather fronts

Weather **fronts** are really the birth place of lows and, in general, the greater the contrast of temperature across a front, the greater the potential for development of lows.

At our latitudes, the main front on the charts is usually the Polar Front which separates cold polar air over the Northern Atlantic from warm tropical air further south. The "spikes" and "bowler hats" on illustrations of fronts point in their direction of movement. The former represents a cold front and the latter a warm front.

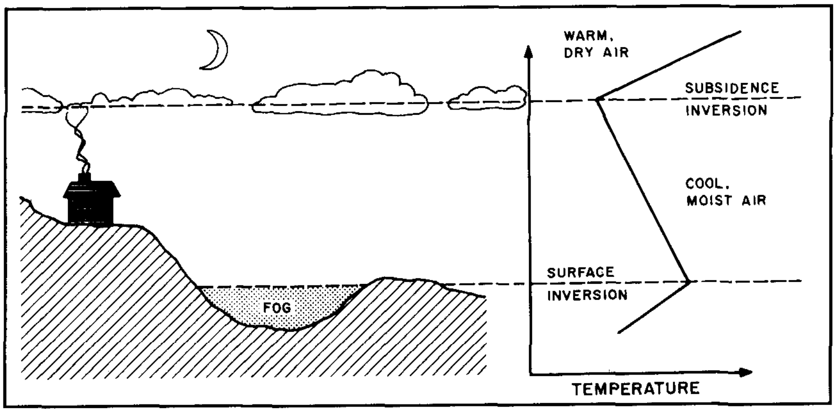

Figure 3. Water vapor is trapped underneath a temperature inversion, becoming noticeable when it condenses to form low cloud or fog.

As you will no doubt be aware, a cold front will bring colder air behind it and vice-versa for a warm front (see **Figure 4**). The best way to picture the chain of events is to think of the whole Atlantic Front as a long "skipping rope." The lows behave as if they have been given a flick at one end, and the resultant "ripple" has moved along the rope. In the atmosphere, the "ripples" may also grow in size as they move along.

Typical sequence

The typical sequence of events is shown in **Figure 5**. Starting on the left, the Atlantic Front has three different lows along its length in order of increasing maturity. The left-most low is probably a day old, the middle low is about 2 days old, and the right-hand low may be 3 days old. These are, of course, very much approximations, but they serve to give a feeling for the time scales involved. Often the low will be deepening most rapidly at the middle stage of the sequence, and probably will be at its most intense in terms of the wind speed in its circulation.

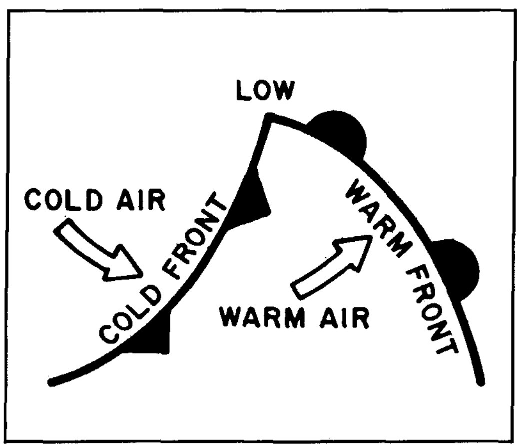

Figure 4. A cold front brings colder air behind it. A warm front brings warmer air in its wake.

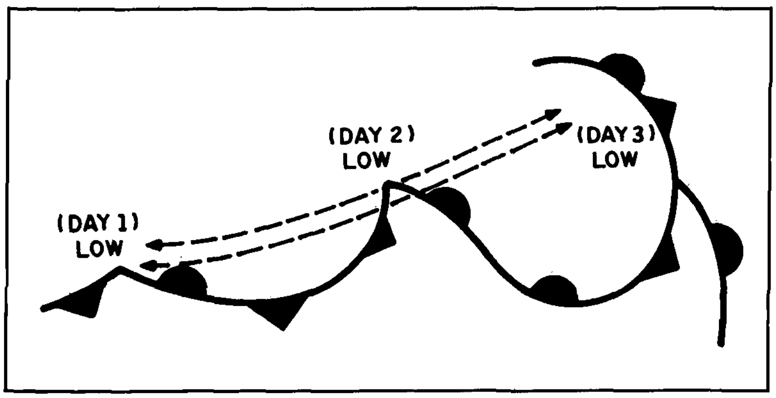

Figure 5. Typical sequence of events which occur as part of frontal movement.

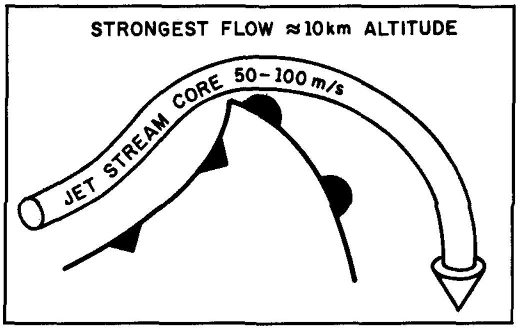

Figure 6. The connection between fronts and jet streams.

Jet Stream

The remaining feature to mention is the jet stream. This is a core of strong winds in the upper atmosphere, about 10 km (3000 ft) above ground, and is directly related to the strength of the weather front with which it is associated.

The connection between fronts and jet streams is shown in **Figure 6**. As a general rule, the jet stream blows parallel to the front, just to the rear of a cold front and ahead of a warm front.

Jet streams are usually strongest in winter, up to 100 m/s (200 kt), and about half that in summer, 50 m/s (100 kt). This is reflected in the relative strength of the weather systems in the two seasons.

Often the location of the jet stream is marked by a long smooth edge to frontal cirrus cloud behind a cold front, or by fast moving streaks of cirrus cloud ahead of a warm front.

A final point of meteorological interest lies in the pattern of a weather chart at jet stream heights. If you strip away the surface features and look at the high altitude flow at 10 km, you will notice that the flow is much smoother.

Troughs and ridges

There is a series of troughs and ridges which move across the chart like a sine wave on an oscilloscope out of synchronization. The analogy may be used further; the low amplitude, high frequency sine waves move quicker than the high amplitude, low frequency waves.

Jet streams mark the strongest flow through the pattern, which is itself moving bodily across the chart. The axis of a ridge/trough is worth noting (see **Figure 7**), as it may play a role in Es development. A typical ridge/trough movement may be as much as 25 m/s (50 kt), but it is usually less – around 10 to 15 m/s (20 to 30 kt). Upper ridges which are growing in amplitude can provide good displays of "mares tails" cirrus cloud, and may be a useful visual clue to Es.

Tropo

You have waded through a lot of meteorology to get to this, but I hope it will be easier to grasp as a result. The development of an inversion is the crucial factor for tropo because this forms the required contrast of temperature and moisture over a relatively small height interval.

The radio refractive index of the air is a function of temperature, pressure, and moisture; the last factor being the most important. As a first approximation, it is necessary to consider only the changes of moisture under an inversion to get a feel for the likely changes in the tropo conditions.

The formula used to calculate the refractive index is:

$$N = \frac{77.6 \times P}{T} + \frac{3.733 \times e \times 10^5}{T^2} \qquad (1)$$

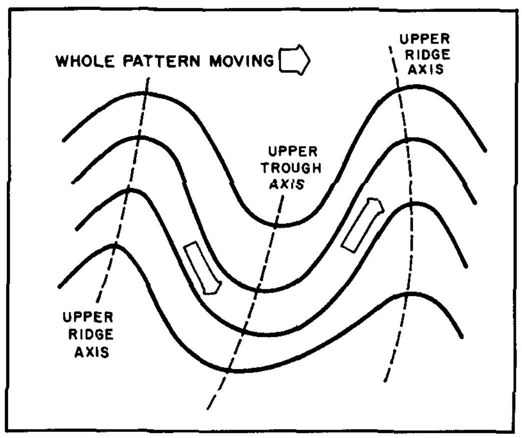

Figure 7. The axis of a ridge/trough.

where P = pressure(mb), e = vapor pressure(mb), T = degrees Kelvin, and N is a modified refractive index. The relationship of N to n (the real index) is $N = (n-1)\times10^6$. This has the effect of making the numbers easier to deal with, as a real index of 1.000350 becomes 350.

This modified index gives figures of the order 350 at ground level, decreasing upwards. A change of 40 units per km height is "normal"; a decrease of more than 157 units is cause for VHF excitement. This is because it will produce sufficient bending of the signal path to bring the signal back to earth at some greater distance than would usually occur.

As you will appreciate from earlier notes, inversions typically form too low (1.5 km or less) to support a single skip HF type of path for some of the extreme ranges reported (1500 to 3000 km). To explain this we need to rely upon some sort of ducting mechanism, where the signal is trapped in an "atmospheric waveguide" formed by the inversion. It can then travel for large distances with little loss in strength.

Good reading

The chapter on propagation in the *VHF/UHF Manual** published by the RSGB covers this subject in greater detail, as will the soon to be published *VHF/UHF PW Handbook*. I highly recommend both.

I aim to finish this section with some tips on how to find out when conditions will be right for DX. First, I will refer you to **Figure 8**, which shows some of the locations where tropo can occur. It is a symbolic chart, and I don't suppose that all these features will be present at once.

- Past tropo openings suggest the best distances are achieved around the sides of large, slow-moving highs.
- Occasionally, a short-lived path may exist parallel to, and just behind, a cold front.
- Paths across the center of a high may be shortened by the inversion lowering to ground level.
- I know it may seem obvious, but don't go above the inversion. Climbing hills may put you above the cloud/haze layer into the sunshine, but you will then be above the inversion!
- As a large high moves away, the surface flow of air below the inversion is drawn up from the southwest. This brings it across the nearby Atlantic/Biscay and, hence, picks up moisture. Remember, we need moist air below the inversion. (This is the reason why falling pressure after a long spell of high pressure is taken to be good for DX.)
- Conditions often improve in the evening and overnight as the surface inversion develops, providing a shallow entry angle to the main subsidence inversion above where ducting may be possible.
- Onshore sea breezes, which develop around our coast in the summer, can bring moist sea air well inland and provide good conditions at the end of a hot sunny day. This is the reason why inland stations suddenly hear DX as the sea breeze front arrives.

  There's no need to feel left out if you live well inland. A strong sea breeze has been known to reach as far as Birmingham in the late evening!
- Sea paths in the summer can provide very long-haul contacts; for example, G to EA8 or EA1, East Coast G to GM/LA, etc.
- VHF/UHF contests can be won or lost on the behavior of the weather. A slow-moving weather front along the English Channel can cut off the continental signals from G stations.
- Tropo works best at higher frequencies. If 144 MHz is open, try 432 MHz or 1.3 GHz. (This is the reverse of Es.)

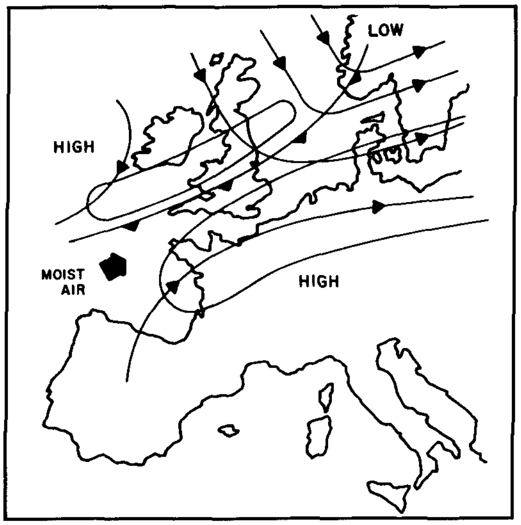

Figure 8. Locations where tropo can occur.

Sporadic-E

Sporadic-E, or Es, is largely a summer phenomenon (at least on 144 MHz). Although events can take place at other times of the year, they are rare. On lower frequencies, the picture is very different. On 28 MHz there is evidence of Es on many days throughout the year (usually referred to "short skip"), while on 50 MHz it occurs somewhere on most days in summer and on quite a few days in winter.

*Available from the CQ bookstore for $29.95 plus $3.75 shipping and handling.

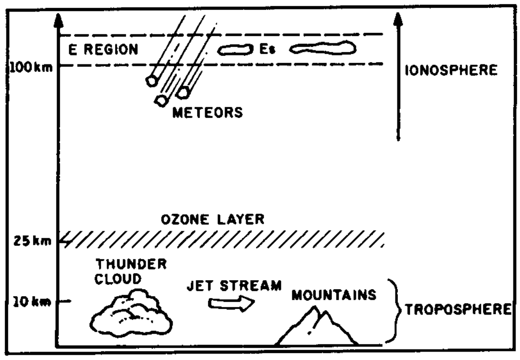

Figure 9. The height of the various layers of interest.

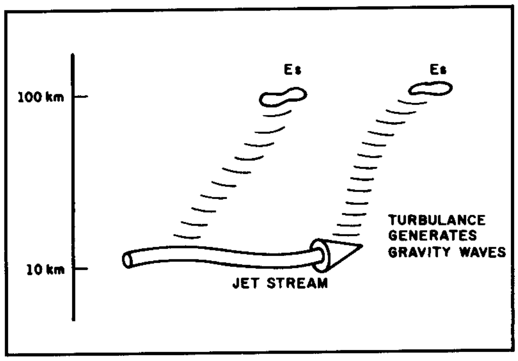

Figure 10. The trigger for Es is believed to be due to gravity waves, or a wave motion in the flow of air above some disturbing obstacle.

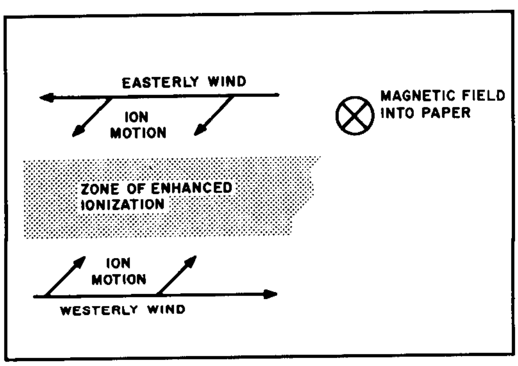

Figure 11. Charged particles are deflected when the wave moves through the Earth's magnetic field.

The cause of Es and a possible link with the weather are both being hotly debated by the scientific community. However, some features of Es can be explained by the current literature. I will deal with these next.

The present understanding is that Es is caused by **wind shear** in the lower ionosphere. First, I should explain that wind shear is the term given to a change of wind speed or direction with height or distance. On the edge of jet streams, for example, there is a large amount of wind shear.

It's important to get a basic grasp of where all this is happening, because confusion abounds on this point. The heights of the various layers of interest are shown in **Figure 9**. Es is found at about 100 to 120 km in the E region, and this is where the wind shear is located. The original cause of the wind shear is, however, much lower down in the troposphere where the "weather" is found.

Sporadic-E trigger

The trigger for Es may well be some weather feature which can be followed on the charts, in the same way as highs are followed for tropo. The mechanism by which the weather provides the trigger is interesting.

It's believed to be due to gravity waves, or a wave motion in the flow of air above some disturbing obstacle (see **Figure 10**). The gravity reference simply states that gravity is the restoring force for the wave motion. There's nothing unusual in this as it is how waves on the sea work.

The current favorites for possible Es triggers are jet streams, thunderstorms, and ridge patterns in the upper atmosphere. Once this wave motion is generated, it can spread upwards to the E region, even growing in amplitude so that it may be 10 to 20 km pk-pk by 110 km.

The next stage in the theory is that this gravity wave activity causes the wind shear mentioned earlier. The wind shear manifests itself as a reversal of wind direction with height in the ideal case.

The next bit which occurs is a result of the deflection of charged particles when the wave is moving through the Earth's magnetic field (see **Figure 11**). If you move the particles one way at one height and the opposite way at some nearby height, it's possible to gather the charge into a thinner layer.

The opposite combination of wind directions will cause the charges to spread out into a thicker layer. The thin layer produces a greater density of charge; a high charge density means higher frequency reflected by the Es patch. This is the physical background to a weather event in the troposphere affecting the appearance of Es.

Other factors

Two other factors stem from this wind shear effect. One is that changes in the Earth's magnetic field may influence whether Es takes place. It has been found that the K index (a measure of the disturbance of the magnetic field) should be 3 or less.

The other factor is the supply of charged particles for deflection. This is most likely to be contributed by meteors burning up in the upper atmosphere.

A further influence on the appearance of Es is the tidal effect on the atmosphere of the Sun's heating. This would normally be expected to happen once per day, but the harmonic (twice per day) seems to be more important.

This leads to certain preferred times in the day when Es are most likely to be found. These times are mid-morning and late afternoon.

As in the section on tropo, I'll finish with a list of operating tips:

- Is the K index 3 or less?
- Are there any weather triggers present (jet streams, thunderstorms, or upper air-ridge patterns)?
- Is there any meteor activity? (Check shower dates.)
- Is there any short skip on 28 MHz? If the answer is yes, try 50 MHz.
- Is there any short skip on 50 MHz? If the answer is yes, try 144 MHz.
- Use 28-MHz beacons to select the direction of a possible VHF opening.
- Because of the tidal effects, look for an afternoon opening about 5 to 6 hours after any morning event.
- Evening openings are possible from 20 to 21 UTC, especially when K index is high.

Helping research

I hope this article will encourage you to use weather information to make DXing less of a "black art" and more of a skill. I'm sure you will gain from learning about a new subject, and from the DX in the log.

As a final note, may I request copies of your Es logs. It is only by a full analysis of past events that we can begin to make some sense of the real mechanisms at work. This is still an area where Amateurs can contribute to scientific research. ■

By Ron Ham
Reprinted from Practical Wireless
October 1990

INSTRUMENTS FOR WEATHER OBSERVATION

To obtain the best results in Amateur Radio meteorology, you need the right equipment. Ron Ham tells us about the basic "tools for the job" and how to use them.

We must accept the fact that VHF and UHF signals have a relatively short range under normal atmospheric conditions. This has already been taken into consideration by the international frequency planners when they allow broadcast transmitters, with a reasonable distance between them, to operate on the same frequency (co-channel working).

Frequency sharing is essential if thousands of transmitters are to provide broadcasting on a limited part of the radio-frequency spectrum. The techniques work well until some form of atmospheric disturbance increases the range of the co-channel signals and makes reception chaotic!

The march of time

Prior to the advent of the Independent Television Authority (now IBA) in the mid-1950s, the only service available in the United Kingdom (UK) was that provided by the BBC. Their 405-line programs were transmitted on five channels in Band I (41 to 69 MHz).

Unfortunately, during the midsummer months, the Band I pictures were often affected by outbreaks of sporadic-E. The ITA was allocated 13 channels in Band III (175 to 213 MHz) and, although outside the influence of sporadic-E, their transmissions were sometimes upset by natural changes within the troposphere.

Sporadic-E can occur at any time during the year and usually coincides with a spell of fine weather and high atmospheric pressure. However, TV broadcasting in the UK is now done only on UHF Bands IV and V, away from the effects of sporadic-E.

Co-channel interference

There is no doubt that UHF television is a great success with its sharper 625-line pictures and lower susceptibility to manmade interference. But despite this, there is still occasional co-channel interference due to tropospheric disturbances.

Natural disturbances to radio propagation have interested me since my early days in TV and radio servicing. I soon found that a fascinating DX "hunting ground" for Amateur Radio operators occurred at the same time as these disturbances. While radio amateurs would be busily using 144 to 432 MHz, TV DXers would be looking for continental transmissions in Bands III, IV, and V.

Scientific literature told me that a close relationship existed between tropospheric openings and the Earth's weather, so I began to look for a set of rules by noting the atmospheric pressure and general weather conditions accompanying abnormal reception. If you have a household barometer, you can join in by taking the pressure readings two or three times per day and plotting the results on graph paper.

Tools for the job

For about eight years prior to 1962, I kept a watchful eye on a standard aneroid barometer. It was calibrated between 28.0 and 31.0 inches and had an outer dial scribed with the words "Stormy," "Rain," "Change," "Fair," and "Very Dry," respectively.

Experience proved that it would be better for my work if I could record the atmospheric pressure continually. So, in January 1962, I installed a Short & Mason barograph.

The barograph explained

Briefly speaking, a barograph is a recording barometer. It's basically a large meter movement with a mechanical structure strong enough to carry a pen across a paper chart, instead of just moving a short pointer over a scale.

For example, where the standard household barometer has one aneroid device and a simple mechanical linkage to operate its indicator, a barograph has a "pile" of aneroid chambers. This mechanism enables the indicating arm to overcome the friction of its pen nib rubbing against the paper chart on the clockwork-powered recording drum.

Long term recording

During its 28 years of operation this instrument has shown me, in a practical way, the type of weather to expect as the pressure changes and, what's more, when to expect good DX conditions on the VHF and UHF bands.

High pressure

There would have been real cause for alarm had the atmospheric pressure ever exceeded the scale limits! My barograph did almost reach 31.0 inches at midday on March 3, 1990, and recorded lows of 28.9 inches as a hurricane passed over Southern England on October 17, 1987.

The lowest pressure reading I recorded, 28.3 inches, occurred at 2200 on February 25, 1989. This pressure drop accompanied a period of very heavy rain and squalls. In a period of three days, my rain gauge collected 1.53 inches of water!

Watch that barometer!

By comparing the barometer readings with VHF conditions during the past 30 years, I have learned to expect some form of tropospheric opening when a period of high atmospheric pressure, above about 30.2 inches, begins to fall.

There have been times when Band II (87.5 to 106 MHz) has opened up shortly before the fall begins, thus offering a warning that the weather is about to change and a more extensive opening is imminent.

Let's take, for example, several warm and clear sunny days accompanied by steady high pressure. Watch out for "wispy clouds" leading a weather front, the pressure starting to fall, extra stations popping up in Band II, and co-channel interference appearing on television pictures in the UHF bands.

I witnessed a typical example of this on July 12 and 13, 1990, following a pressure climb from 29.7 inches on the 5th to 30.5 inches on the 11th, when a really hot sunny spell began. However, at noon on the 12th, the barograph began a slow decline to reach 30.2 inches at midday on the 14th.

It's not often that I leave home without a portable television receiver in the car. During the afternoon of the 12th, while parked at Chiddingstone in Kent, I saw the first signs of a tropo opening when French pictures were beginning to show themselves in Band III.

Later that evening, from home, I noted co-channel interference on TV pictures in the UHF band. Early next morning, a path to the northeast was wide open. It was very interesting for three hours, until it all faded away around 1030 a.m.

During that time I counted 25 predominantly German broadcast stations in Band II, and received a strong steady test card, in color, from Holland on Channel E4 (62.25 MHz). I also received programs from four German television stations in Band III.

I checked the same frequencies several times during the day on my journey to and from Polsden Lacey in Surrey. It pays to carry a portable TV for monitoring purposes!

Unfortunately, there were no further signs of the disturbance. The peak had obviously occurred early on the 13th, in the middle of this pressure fall.

Notable events

I ran a special project between May 1 and September 30, 1969 to see how the signal strength of the 144-MHz beacon in Wales (GB3GW) received at my home in Sussex was influenced by the changes in atmospheric pressure.

During this five month observation period there was positive evidence that when the high pressure began to fall, the signal from this tiny transmitter increased.

The final result of the experiment occupies six sheets of A4 graph paper, from which I have selected a couple of examples covering the periods June 1 to 15 (**Figure 1**) and June 25 to July 9 (**Figure 2**).

The dotted line on each graph represents the atmospheric pressure and the hard trace indicates the variations in strength of the received beacon signal. The "Y" axis combines the signal strength (0 to 8) and the atmospheric pressure (30.0 to 30.5 inches).

An experiment such as this must have a consistent signal to be of any value; the beacons are very useful. This is one of the many areas where the RSGB's VHF and UHF beacon service has made a valuable contribution to tropospheric propagation research.

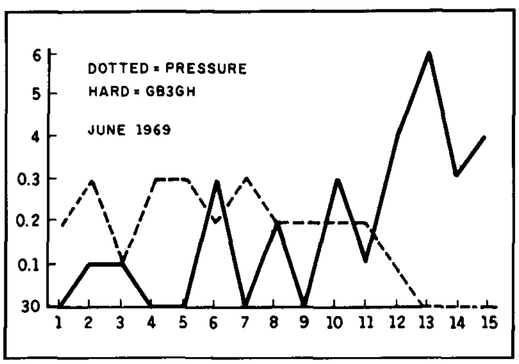

Figure 1. Example of atmospheric pressure change and accompanying VHF signal strength variation observed during the period June 1 to 15, 1969.

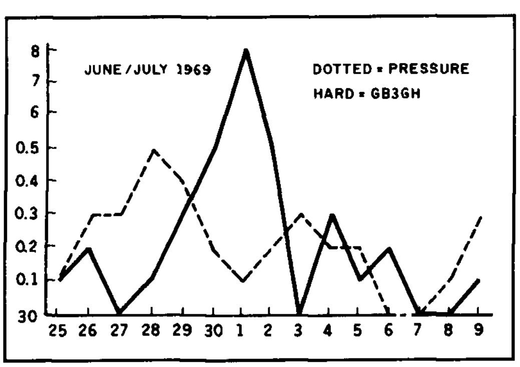

Figure 2. Example of atmospheric pressure change and accompanying VHF signal strength variation observed during the period June 25 to July 9, 1969.

Remarkable openings

One of the most remarkable tropospheric openings that I have ever witnessed occurred between January 18 and 21, 1974. It's difficult to say when such an event began but, like some others, the event followed a sudden pressure drop.

The barometric pressure fell to 29.6 inches on the 16th as severe weather passed over. This was followed by a sharp rise to 30.4 inches by 1400 on the 17th. The pressure peaked at 30.5 inches around noon on the 19th, and then slowly declined.

This fall speeded up during the afternoon of the 20th. The first signs of a VHF disturbance came when I heard a few French broadcast stations between 97 and 100 MHz during the afternoon and evening of the 18th.

It soon became obvious on the 19th that the disturbance was spreading, as more continental stations appeared between 93 and 100 MHz. The range of European VHF radio signals increased dramatically on the 20th, reaching a peak at midday and lasting until the early hours of the 21st.

Throughout the 20th, I received strong pictures from the Midlands IBA transmitter on Channel 8 with only a dipole feeding my television receiver. (The IBA was still transmitting ITV on Band III at that time.)

During the event a dozen continental broadcast stations were "dug-in" between 90 and 100 MHz, and their strength frequently equalled that of the established BBC stations transmitting in the UK.

By 2300 the signal path to Germany was really open and, for a few hours, the signals from Nord Deutscher Rundfunk dominated the band. At that time there were approximately 50 transmitters listed for NDR and at 0220 on the 21st, after the BBC stations had closed down, I counted 20 of these between 88 and 100 MHz (then the extent of Band II).

"Quickies"

Over the years, I have seen short periods of "extra" high pressure rise and fall produce an opening from a steady high pressure trace. One of these occurred in March 1977 (**Figure 3**), when the pressure jumped up from a steady 30.0 inches at midnight on the 23rd to midnight on the 27th.

An approximate 24-hour VHF opening took place between midmorning on the 25th

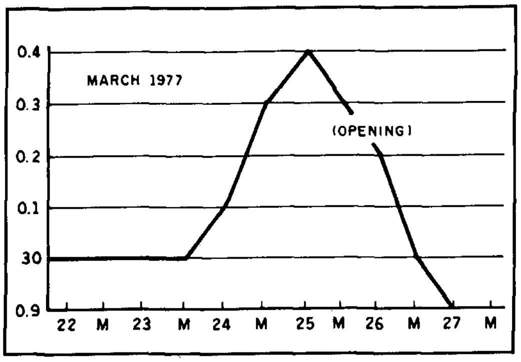

Figure 3. Short period of "extra" high pressure followed by a tropo opening.

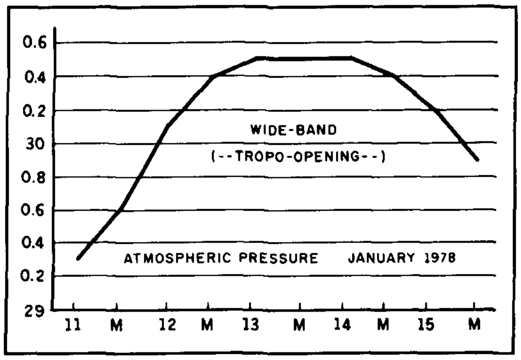

Figure 4. Period of high pressure followed by an extended tropo opening.

and noon on the 26th. This was a case of being in the right place at the right time, because these short-lived openings are usually very directional and can produce some unexpected DX.

A typical event

Another interesting event began between midday on January 10, 1978 and noon on the 12th, when the atmospheric pressure plunged from 30.1 inches to 29.3 inches and back to 30.1 inches.

During this period gale force winds, rain, and snow prevailed. The sharp rise continued, and by noon on the 13th, the barograph was showing almost 30.5 inches. It remained at this level until about 1400 on the 14th, when it commenced a rapid decline to 29.7 on the 16th.

The graph in **Figure 4** begins at 1200 on the 11th, when the pressure began its sharp rise, and continues to show the readings at noon and again at midnight, through to the 15th. An extensive tropospheric opening began around 0800 on the 13th, reached its peak overnight on the 14th and 15th, and died away later on the 15th.

Setting up

If you start your own observations, don't forget that a new instrument has to be adjusted for its height above sea level. Barometers usually have an adjustment screw at the rear. A barograph — certainly my favorite instrument — like mine has an adjuster which looks like a large terminal, on a plate directly above the aneroid "pile" and the pen-arm linkage mechanism.

The manufacturer's instructions should indicate these points clearly, and once you've set your barometer, you're ready to explore and experiment! ■

By John A. Cowan, *W4ZPS*
962 Harris Parkway
Cartersville, Georgia 30120

THE POWER INDUCTOR

The technology behind and many uses for power inductors

I've long been interested in power inductors. I'd like to discuss the theory and design of power inductors, their construction and testing, and how to build a high-efficiency switching power supply using inductive components.

The inductive effect

When current flows through a conductor, some of the energy driving the current is stored in a magnetic field which surrounds the wire. When the driving forces change, the intensity of current flow doesn't vary immediately, because the magnetic field reacts in a manner that opposes the change. If the wire is wound into the shape of a coil, the magnetic field of one part of the wire sums with the field from adjacent parts, and the interaction is enhanced. Coils fashioned in this manner are called inductors. The magnitude of their effect is called inductance, and is measured in henries.

In general, the value of an inductor is given by:

$$L = A_L N^2 \qquad \textbf{(1)}$$

where L is the inductance in henries, N is the number of turns, and A_L is a constant derived from the magnetic property of the core material (μ_o), its volume (V_e), its magnetic length (ℓ_e), and whether the core is gapped or continuous.

When a voltage is placed across an inductor, the current begins to change according to:

$$Rate = \frac{V}{L} \textit{ (amps per second)} \qquad \textbf{(2)}$$

where L is the inductance in henries and V is the voltage.

If there's zero current at time zero, and V is constant, then the current at any later time is:

$$I = \frac{V}{L} T \textit{ (amps)} \qquad \textbf{(3)}$$

where T is in μs.

The amount of energy contained within the inductor is given by:

$$E = \frac{1}{2} L I^2 \textit{ (in joules)} \qquad \textbf{(4)}$$

Consider the implications of **Equations 2, 3,** and **4** with the help of **Figure 1.** At time zero (point A), 10 volts is placed across an inductance. Initially, there's no current flow. However, the rate of current change is established, and after 2 μs, a current of 2 amps flows. The rate of current change has been 2 amps in 2 μs or 1 volt per μs.

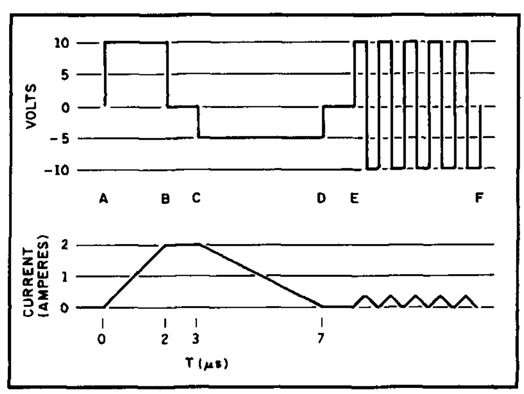

Figure 1. Current response to voltage across inductor.

You can calculate the inductance by rearranging **Equation 3** to obtain **Equation 5**.

$$L = \frac{V \times T}{I} = \frac{10 \text{ volts} \times 2 \mu s}{2 \text{ amps}} = 10 \mu H \quad (5)$$

During this time, energy has been stored in the inductor's magnetic field. Plugging values into **Equation 4**, the energy is:

$$\frac{1}{2} \times (10 \times 10^{-6}) \times (2)^2 = 20 \text{ microjoules}$$

At point B in **Figure 1**, the voltage across the inductor is reduced to zero. Note again, that there's no sudden current change. Rather, the rate of change drops to zero (V = 0 in **Equation 2**), and the current is held constant at 2 amps. At point C, the voltage is reversed to −5 volts. From **Equation 2**, the rate of current change will be −0.5 volt per μs. Energy now leaves the inductor and is returned to the voltage source. It will take twice as long for the current to decline to zero because the discharge rate is one-half the charging rate. (This ability to store and release energy is put to good use in switching power supplies).

At point E, a square-wave voltage of 20 volts p-p is placed across the inductor. As long as the value of L is large and the frequency is high, the current changes only slightly. (Power output filters and RF filters all take advantage of this property.)

The core

The magnetic property of a material is called its *permeability* (μ_O) and is expressed as a ratio compared to air (μ_O = 1). Increasing the core's permeability increases the value of A_L and greatly decreases the number of turns for a given inductance. In almost every case, power inductors will use a core made of ferromagnetic materials, many with permeabilities in the thousands.

This property is most easily explained if you think of the core as containing trillions of molecular "springs," which under the effect of an applied magnetic field, come under tension and store energy. When the driving force changes, the springs store and release their energy in opposition to the voltage applied, decreasing the driving force's effect on current flow.

Unfortunately, the storage capacity of these materials has a molecular limit. At this point, the core is said to be *saturated.* The magnetic springs suddenly become rigid and the current, which has been slowly changing, rises precipitously — usually taking adjacent components for a fatal ride! **The major challenge of inductor design is to avoid this calamity.**

Core geometry

A core material will exhibit maximum inductive effect if it's formed into a continuous structure. If a gap is introduced, the *effective permeability* (μ_e) of the material decreases, but its saturation characteristics improve significantly.

Consider **Figure 2**. An inductor is constructed using a ferrite 77 core (μ_O = 2000) with no gap and 3 turns around the core. Ten volts are applied across the inductor, and the current is measured over time. Line segment ABC shows the result. Initially, the current rises in a controlled manner, but at point B the core saturates and the current rises sharply. Using **Equations 4** and **5**, your calculations will show that this is a 10μH inductor, usable at up to 2 amps, and that the core is capable of storing 20 microjoules of energy before saturation.

If the core is modified by placing a 3-mil (0.003-inch) gap in its path, the effective permeability drops to 231 and the inductance decreases to 1.1 μH. If the number of turns is increased to 9, this effect is counteracted and the inductance is brought back to 10 μH. Note the improved performance in segment ADE. Now the inductor tolerates 8 amps before saturation, and the core stores 80 microjoules. Increasing the gap and the number of turns will continue to improve performance until the gap approaches 15 percent of the magnetic length — or until so many turns are required that resistance losses or winding space become limiting. At this point, you must choose a larger core.

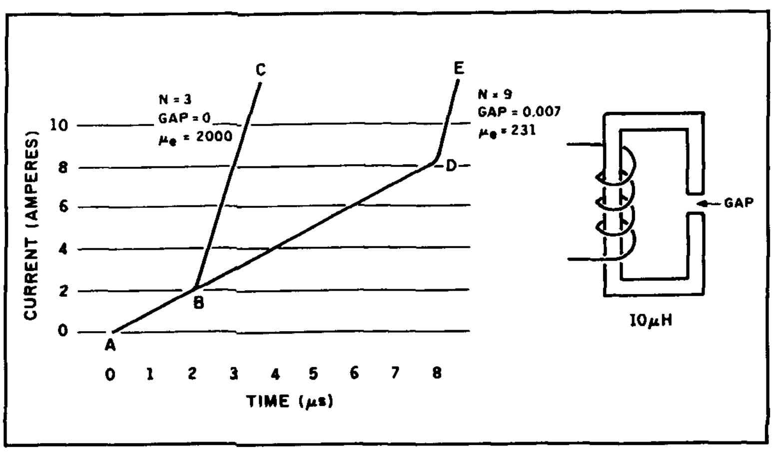

Figure 2. Improved performance with gapping.

The Hanna curve

In 1927, C.F. Hanna presented a graphical method which greatly simplified inductor design.* He showed that if the energy density were plotted against the magnetizing force per unit length, inductor parameters could be easily computed. Energy density is given by:

$$ED = \frac{L \times I^2}{V_e} \quad \frac{(\mu H) \times (amps)^2}{(cm)^3} \tag{6}$$

and the magnetizing force is:

$$MF = \frac{N \times I}{\ell_e} \quad \frac{(turns) \times (amps)}{(cm)} \tag{7}$$

where V_e = the core volume in cm^3 and ℓ_e = the magnetic length in cm.

The gap is displayed as a ratio along the curve and can be calculated from:

$$GAP = ratio \times \ell_e \tag{8}$$

A modified Hanna curve for ferrite 77 is shown in **Figure 3**. As an example, I'll design a 100-μH inductor that will handle 3 amps of current. I'll use a PC-2213-77 pot core,** with a V_e of 1.99 cm^3 and an ℓ_e of 3.16 cm.

First calculate the energy density:

$$ED = \frac{LI^2}{V_e} = \frac{100\ \mu H \times (3\ amps)^2}{1.99\ cm^3} = 452$$

The value 452 is located on the Y axis. Moving horizontally to the curve and then vertically to the X axis, shows a magnetizing force of 17.

Now rearrange **Equation 7** to obtain **Equation 9**:

$$N = \frac{MF \times \ell_e}{I} = \frac{17 \times 3.16\ cm}{3\ amps} = 18\ turns \tag{9}$$

Note where these lines intersect the curve. Interpolate between 0.005 and 0.01, and you'll read about 0.007. Using **Equation 8**, the gap is given by:

$$GAP = 0.007 \times 3.16\ cm = 0.022\ cm = 0.0087\ inches$$

*Should you want a larger copy of the Hanna curve, as well as the listing of a BASIC program to aid in inductor design, just send me a self-addressed stamped envelope.

**Iron-powder and ferrite coil forms are available from Amidon Associates, 12033 Otsego Street, North Hollywood, California, 91607

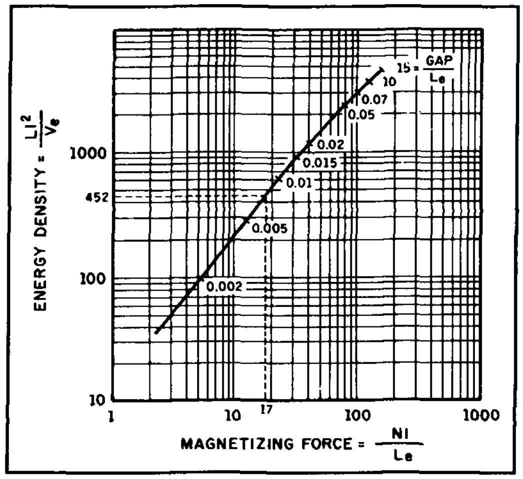

Figure 3. The Hanna curve for ferrite-77.

Eighteen turns around this core, gapped to 0.0087 inch (8.7 mils), will produce a 100-μH inductor that will carry 3 amps. If the core can't hold this number of turns in a suitable wire size, choose a larger core and repeat the process.

Often in output filter design, you really want to know the maximum inductance obtainable from a particular core at a specified current. In this case, you choose a wire size appropriate for the current and see how many turns the core can hold. Because you know N and I, you can calculate the magnetizing force using **Equation 7**. Take the energy density from the graph in **Figure 3**, and rearrange **Equation 6** to solve for inductance.

As it turns out, this core holds 18 turns of 18-gauge wire. If you want to design a maximum inductance that need only carry 2 amps, calculate:

$$MF = \frac{N \times I}{\ell_e} = \frac{18 \times 2\ amps}{3.16\ cm} \approx 11$$

Locate 11 along the X axis in **Figure 3**, and go up to the curve. The gap ratio is 0.004, so the gap will be:

$$GAP = 0.004 \times 3.16\ cm = 0.012\ cm = 0.005\ inches$$

Following left to the Y axis, you'll see an energy density of 250. Rearranging **Equation 6**:

$$L = \frac{ED \times V_e}{I^2} = \frac{250 \times 1.99\ cm^3}{(2\ amps)^2} = 124\ \mu H \tag{10}$$

Therefore, with 18 turns and a gap of 5 mils, you have an inductor of 124 μH that carries 2 amps without saturating.

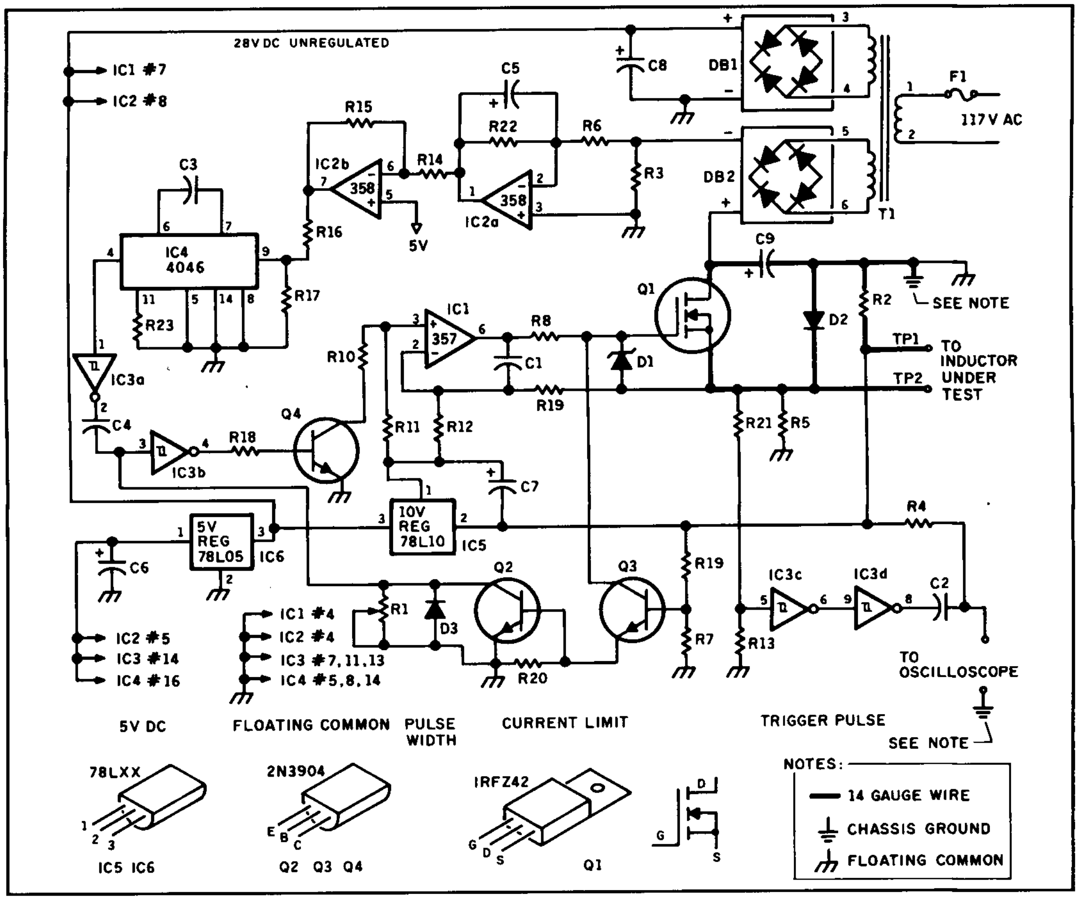

Figure 4. Schematic of the inductor tester.

An inductor tester

Unfortunately, theory doesn't always match practice. At best, it's hard to gap an inductor exactly. I'll continue by giving the details of how to build a test instrument that, with the aid of an oscilloscope, will let you wind, gap, and test homebrew inductors and transformers precisely.

Method

As I said before, if you apply a fixed voltage across an unknown inductor and measure the current flow over time, you can compute the inductance. You determine the point of saturation by finding the "break point" in an otherwise linear curve. The schematic diagram of such a device is shown in **Figure 4**.

Circuit description

The circuit is a pulse generator which places a constant 10-volt pulse across a test inductor. The current is determined by measuring the voltage drop across R2, a 0.1-ohm resistor, which produces 1 volt for every 10 amps of current. The energy is furnished by C9 using a power op-amp circuit formed by IC5, IC1, and Q1. The reference common is referenced from TP1, so the feedback loop holds a constant 10 volts across the test inductor as the current rises. The voltage reference is normally pulled to zero by Q4.

Under the control of IC3A, IC3B, and the time constant R1-C4, Q4 is turned off and the 10-volt pulse is applied until the interval set by R1 times out, or until the current limit is reached. The one shot (IC2) is triggered by IC4, which functions as a voltage-controlled oscillator.

The frequency-control voltage is derived by the inverse integration of the current flowing to charge C9. This is accomplished by R3 and IC2. The effect is to decrease the cycle freqency as the energy per pulse increases, keeping the total power consumption nearly constant.

The current-limiting function uses Q2, Q3, and the voltage divider R19-R7. The output voltage (proportional to the current) is divided by R19 and R7. This voltage is applied to Q3's base. When this value

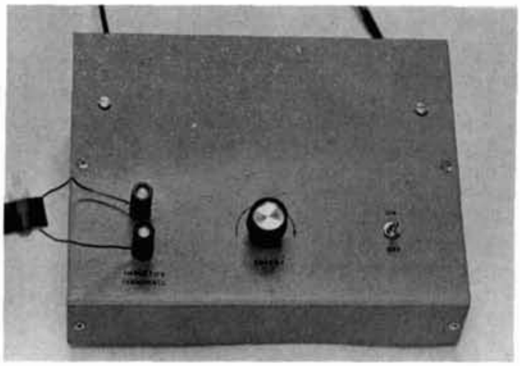

Photo A. Front view of tester.

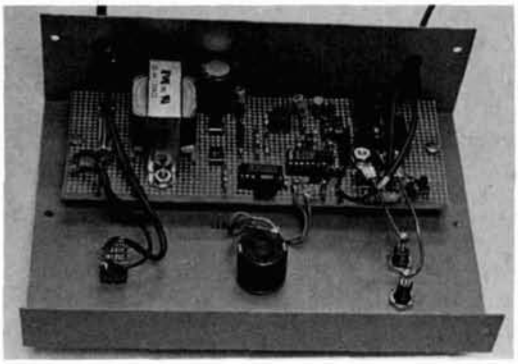

Photo B. Underside view of tester.

aproaches 1 volt, Q3 pulls the gate of Q1 low to limit the current instantly. Q2 resets the one shot to terminate the cycle. With the values listed, the current limit is 45 amps. If you want higher currents, reduce the value of R7 or make it variable. I wouldn't suggest pushing much above 80 amps!

The voltage at TP2 is divided by R11 and R12 and fed through two Schmitt triggers. This pulse is coupled through C2 to the output, and superimposes a 2-volt trigger pulse on it. This pulse starts the scope trace at time zero. D1 protects Q1's gate from overvoltage; D2 provides a discharge path for the inductor.

Construction

You may use perfboard for the board material, but because of the high currents involved, you must take some care in layout (see **Photos A** and **B**). Keep the leads around IC2, IC5, and Q1 short **(Figure 4)**. The bold lines of wiring in the schematic carry high current, so use 14 gauge or larger wire. Note the chassis ground at the cold end of R2 and C9. The ground return for the oscilloscope (chassis ground) must come directly from this point to avoid ground loop errors. The other grounds can be connected to this point by smaller wire. This grounding technique is called a "floating common" because these grounds return to the chassis ground at this one point only.

It's handy to use a ten-turn pot at R1 and banana jacks at TP1 and TP2. Handle the FET gate with care. It's a good idea to leave the foam protection on until you've completed construction. Remember, the tab of the FET is connected to the drain. Although dissipation is low, you should place a small heat sink over the tab on the FET for added protection.

Initial testing

Apply power with R1 set to zero ohms. Attach the oscilloscope to TP2. As R1 is increased, verify that a 10-volt square wave is present, and that its duty cycle is varied by R1. If all is well, attach the scope to the output, and look for the 2-volt trigger pulse as R1 is increased.

At this point, you can place an inductor across the terminals. The current should read 10 amps/volt. Initially the frequency will be high (about 1000 Hz), but as the pulse width is increased, the frequency will decrease. At very high energy levels, it may reduce to a few Hz.

Building the inductor

Remember the 100-μH, 3-amp inductor mentioned earlier? The graph suggested you use 18 turns wound on a PC-2213-77 core gapped to 8 mils. First, wind the inductor using the data in **Figure 3**.

Using a wooden dowel or a screwdriver shimmed with tape, wind 18 turns of 18-gauge wire tightly around the nylon bobbin supplied with the core **(Photo C)**. Loop sewing thread or dental floss around the terminal end of the wire and continue it a few more turns to hold the winding in place **(Photo D)**. It's important that the winding be tight and that the core clears the bobbin easily.

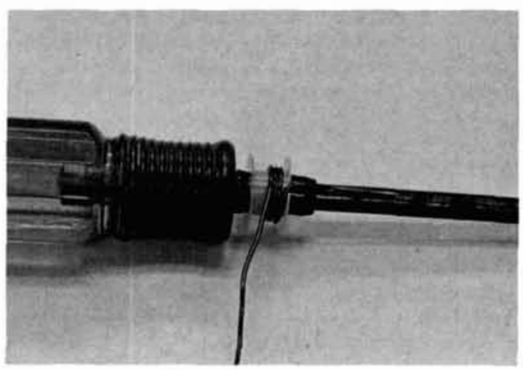

Photo C. Starting the winding using shimmed screwdriver.

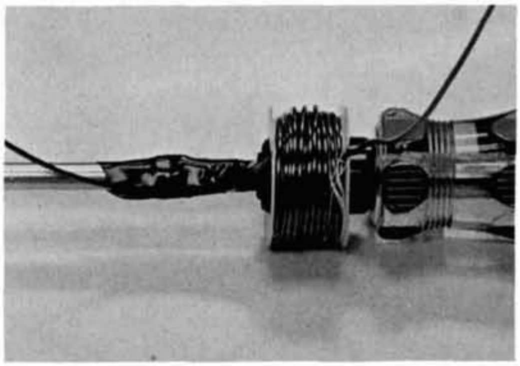

Photo D. Finished winding tied with sewing thread.

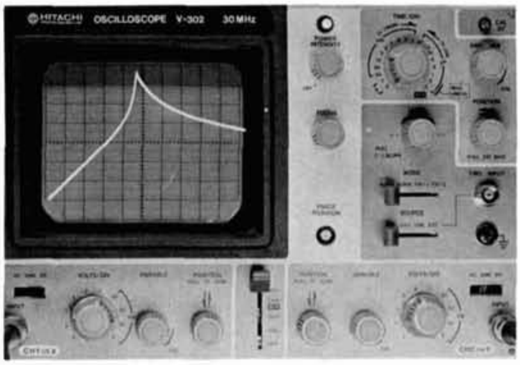

Photo E. Oscilloscope trace of 100-μH, 3-amp inductor under test.

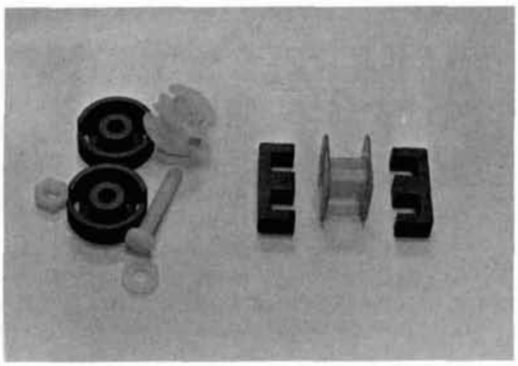

Photo F. Pot and E-core forms with winding bobbins.

To use this tester, you must first calculate a target point based on the desired inductance. Rearrange **Equation 3** to obtain **Equation 11**, and insert the desired values:

$$T = \frac{L \times I}{V} = \frac{100\ \mu H \times 3\ amps}{10\ volts} = 30\ \mu sec \qquad \textbf{(11)}$$

When the inductor under test is set to exactly 100 μH, the trace on the scope should cross the 3-amp point (0.3 volt) in 30 μs. The saturation break point should also be *beyond* this limit.

Place the core over the bobbin and attach the inductor to the tester. Set the voltage and sweep so the target point can be displayed conveniently. Then, observe the trace while varying the core gap, until it passes through the target point. Normally, the saturation point will be approximately 20 percent higher than calculated.

Photo E shows this inductor under test (1 cm vertical = 1 amp and 1 cm horizontal = 10 μs). The current rises linearly and then breaks at $\approx$ 4 amps. It rises rapidly until the one-shot times out (see the peak at the upper middle of the screen in **Photo D**). The right half shows the current decreasing during discharge.

If the inductor performs as expected, remove the core and apply thinned enamel generously to the bobbin. The winding must be well secured or vibration might wear away the insulation. After the enamel has dried thoroughly, apply 5-minute epoxy between the core halves as a "gap gasket." Reconnect the inductor and squeeze on the core, holding the proper gap by watching the scope until the epoxy hardens. The magnetic field tends to draw the core together, so some care must be taken until the epoxy has cured completely. The inductor is now finished and ready for use.

Choosing the right core

Ferrite cores are generally available as pot cores and E cores (see **Photo F**). Pot cores offer better shielding and are a little easier to wind. The E cores have more winding space and offer better air circulation for cooling. For most power applications, 14 through 18 gauge wire is used. So when you're doing hand winding, the larger cores make life easier because they require fewer turns and offer more space.

If the value of the inductance isn't critical (as is true in many output filter applications), choose a core of a physically reasonable size, and see what inductance it can deliver at the required current. If the inductance isn't high enough, choose the next larger size and try again. If you need a

Model No.	Core Volume V_e (cm^3)	Magnetic Length ℓ_e (cm)
PC-2213-77	1.99	3.16
PC-2616-77	3.46	3.72
PC-3019-77	6.10	4.50
PC-3622-77	10.6	5.20
EA-77-188	0.90	4.01
EA-77-250	1.93	4.80
EA-77-375	6.24	6.88
EA-77-500	12.3	7.67
EA-77-625	18.0	9.80

Table 1. Core magnetic data.

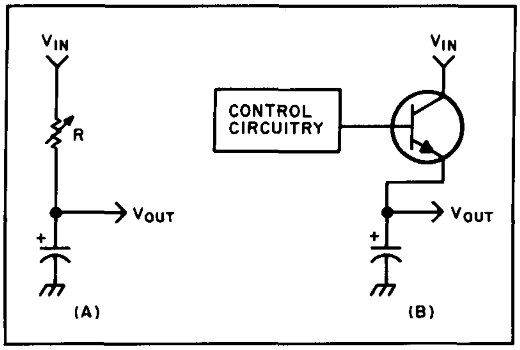

Figure 5. Linear voltage regulation.

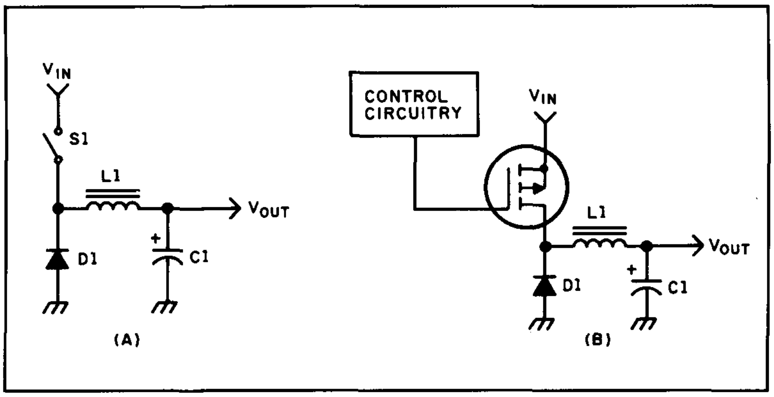

Figure 6. Switching voltage regulation.

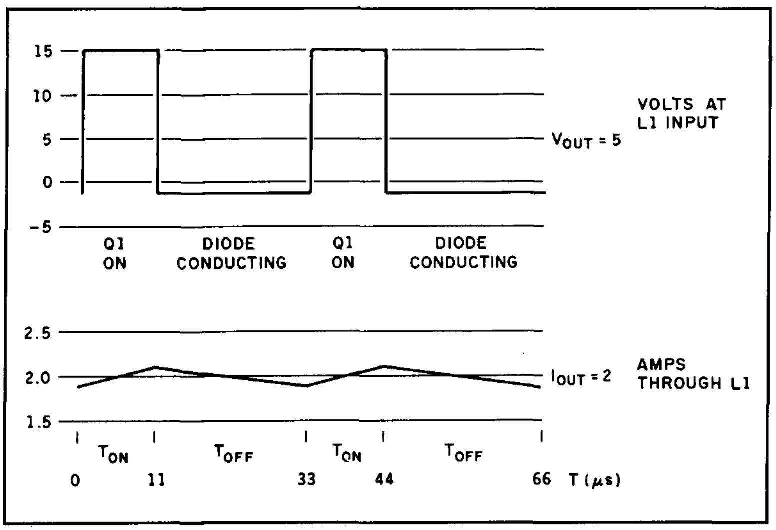

Figure 7. Voltage and current waveforms through L1.

specific value, choose a core whose V_e gives an energy density of around 1000. With a little practice, this approach will allow you to do a surprisingly fast and accurate job.

I've included some core information in **Table 1**. The units have been converted to cm to make the math easier. V_e has been calculated for the pot cores from the area and length obtained from coil form sources. Be careful of the units if you use other sources. You can calculate the core volume if it's not given.

Building a switching power supply

Next, I'll show you how to build a 5-volt, 2-amp switching power supply. You'll need two 100-µH, 3-amp inductors and one 500-µH, 3-amp inductor. But before I go into the details of this project, I'd like to discuss the advantages of switching power supplies over their linear counterparts and present a practical application of power inductors.

Linear regulators

Most Amateurs are familiar with linear voltage regulators. In these circuits, the voltage is reduced to the desired value using a resistance equivalent. The power section of this type of regulator is shown in **Figure 5**. The value of R **(Figure 5A)** is varied so that, for any current, its voltage drop will result in the desired V_{out}. Electrically, this is accomplished by using a pass transistor and varying the base drive **(Figure 5B)**. This approach gives excellent regulation and has the advantage of simplicity, though at the expense of efficiency. The voltage drop across the resistor (or transistor) is converted to heat and therefore wasted. If, for example, V_{in} = 15 volts and V_{out} = 5 volts, then for every watt of output, 2 watts of heat are wasted. This yields a conversion efficiency of 33 percent.

Switching solution

You can improve the efficiency of conversion greatly using a switching power supply. Assume a V_{in} of 15 volts and a V_{out} of 5 volts and consider **Figures 6A** and **7**. If S1 is closed, current I flowing from V_{in} through L1 into C1 and V_{out} will rise according to:

$$\frac{dI}{dT} = \frac{(V_{in} - V_{out})}{L\ (\mu H)} \frac{amps}{\mu s} \qquad \textbf{(12)}$$

where dI and dT represent the *change* in I and T, respectively.

As this occurs, a portion of the energy — $I \times V_{out}$ — flows immediately into the output as useful power. The remainder, $V_{in} - V_{out} \times I$, is stored in the magnetic field of L1. When S1 is open, the inductor tries to keep the current constant by "flying back" until D1 is forced into conduction. At this point, the stored energy flows as current through D1 and L1 into the output circuit. The energy that was lost in the linear circuit has been salvaged. Some loss is incurred in the switching transistor and across the diode, but in a properly designed circuit, this can be kept surprisingly low.

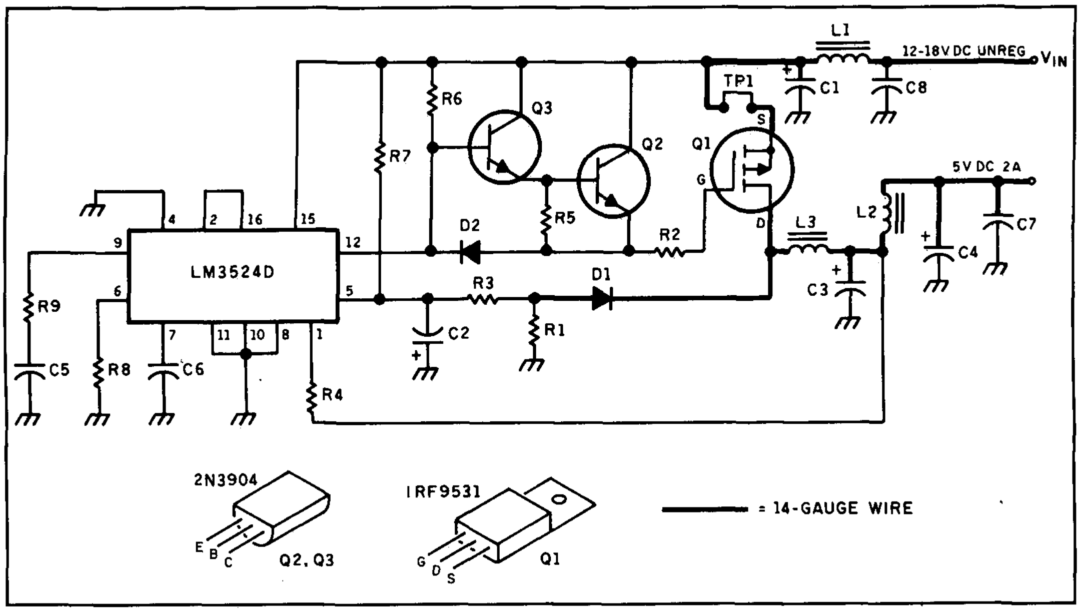

Figure 8. Schematic of switching regulator.

A little math

In a practical circuit, a transistor switch is used **(Figure 6B)**, and an oscillator with a variable duty cycle drives the transistor. Control circuitry varies the duty cycle so the appropriate output voltage is maintained.

Assume a fixed oscillator frequency, F. The period is:

$$T = \frac{1}{F} = T_{on} + T_{off} \qquad (13)$$

When the circuit has stabilized into a fixed load, the current increase during T_{on} will equal the current decrease during T_{off}. The average current over the entire cycle will be I_{out} (see **Figure 7**). Rearranging **Equation 12** to obtain **Equation 14**:

$$dI = \frac{V_L}{L} \times dT \qquad (14)$$

where V_L is the voltage across the inductor and dI is the current change after time dT. During T_{on}, the voltage across the inductor is $V_{in} - V_{out}$. During T_{off}, it's $-V_{out}$. Because $dI_{on} = -dI_{off}$, you can write:

$$\frac{V_{in} - V_{out}}{L} \times T_{on} = \frac{V_{out}}{L} \times T_{off} \qquad (15)$$

Solving for V_{out}, you have:

$$V_{out} = \frac{V_{in} \times T_{on}}{T_{on} + T_{off}} = V_{in} \times T_{on} \times F \qquad (16)$$

In a step-down configuration, the frequency and inductance are chosen so the inductor current variation is small ($dI_{on} << I_{out}$). This reduces output ripple and improves overall performance. For example, with $V_{in} = 15$, $V_{out} = 5$, and a frequency of 30 kHz, you can rearrange **Equation 16**:

$$T_{on} = \frac{V_{out}}{V_{in} \times F} = \frac{5}{15 \times 30000} = 11\ \mu s \qquad (17)$$

If L = 500 µH, you can use **Equation 14**:

$$dI = \frac{10}{500\ \mu H} \times 11\ \mu s = 0.22\ amps$$

Therefore, the switch would be on 11 µs, off 22 µs ($T - T_{on}$), and the output current would vary just 0.22 amps. The output capacitor smoothes this ripple current.

Circuit description

Figure 8 shows a 5-volt, 2-amp switching regulator. A LM3524D switching regulator generates the oscillator frequency, the voltage reference, and varies the output duty cycle using a ramp generator. Unregulated DC voltage is applied to the regulator through L1. L1-C8 filters the high-frequency pulses that might feed back into the power source and cause radio frequency interference (RFI). The current is switched on by Q1. This allows current to flow through L3 into C3 and into the output. During the off cycle, current flows through R1, D1, and L3, and into the output as before.

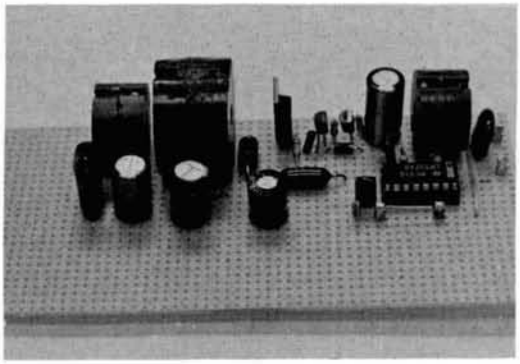

Photo G. Top view of switching regulator.

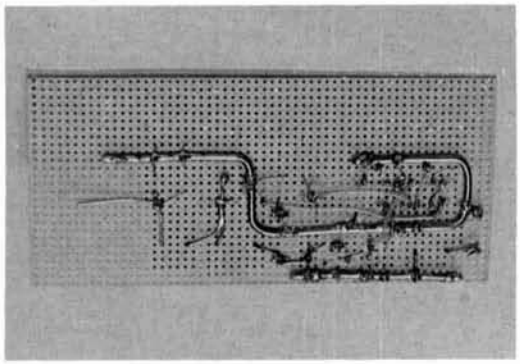

Photo H. Bottom view of switching regulator.

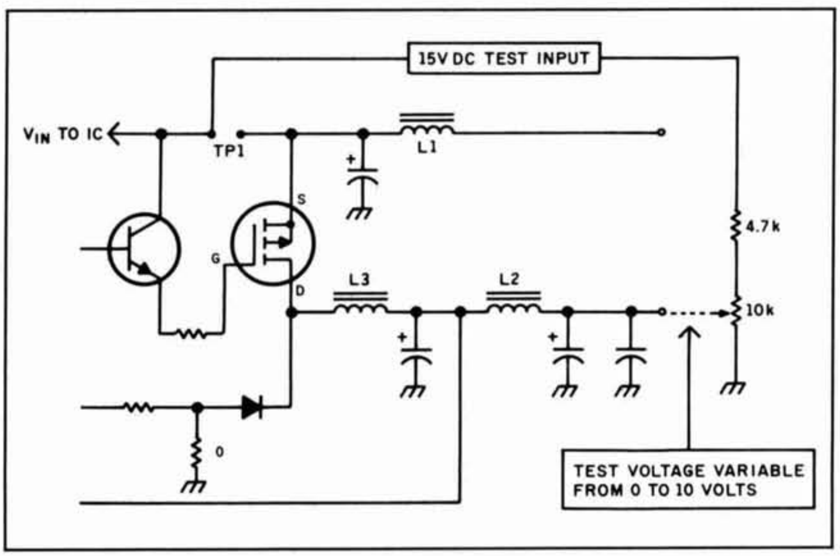

Figure 9. Initial setup.

R1 generates a voltage proportional to the output current. Because current flows through R1 only during T_{off}, R7 adds a correction so that the voltage presented to pin 5 of the IC closely follows the actual output current. C2 acts as a low-pass filter in the current feedback loop.

The switching transistor needs special attention. It must conduct 2 amps at low voltage drop, and the transition time must be fast, because heat is dissipated during these times. Q2 and Q3 form a Darlington driver, which speeds up turn on by overcoming the gate capacitance. The IC contains an adequate current sink, so no boost is needed. The sink current flows through D1 into the IC.

The oscillator frequency is determined by R8-C6. R9-C5 form a low-pass filter for the error amplifier in the IC. Fast switching speeds produce lots of RF energy, so shielding and power-line filtering are important. L1, L2, C4, C7, and C8 serve as filters — both for the 30-kHz ripple and for RFI.

Construction

The regulator shown in **Photos G** and **H** was built on perfboard. I used 14-gauge wire (from 14-2 service wire) to form a ground bus, and to carry V_{in} through L1 and C1 to Q1. This same wire can be used for the output through D1, R1, L3, C3, L2, C4, and C7 (note the bold lines on the schematic). The remainder of the wiring is noncritical, although close wiring techniques should be used.

I mounted the FET upright and used a small clip-on heat sink. Actually, the FET runs quite cool, but this adds some extra protection. As always, handling the FET gate requires static protection. I leave the foam on the leads until wiring is completed.

L1 and L2 are designed for 100 μH at 3 amps. They are wound using 18 turns of 18-gauge wire on a PC-2213-77 Amidon core, gapped to 10 mils. L3 is 500 μH at 3 amps, and is wound similarly using 40 turns of no. 18 wire on a PC-3019-77 Amidon core, gapped to 22 mils. You must use the techniques presented earlier to assure the proper inductance and a saturation current greater than 3 amps.

Initial testing

After construction and a thorough wiring check, break the power lead at TP1 (**Figure 9**) and apply 12 to 18 volts to the IC side of the power bus. There should be 5 volts on IC pins 2 and 16 (this is the internal reference) and a 30 to 40-kHz square wave on the gate of Q1. If all's well, raise the voltage at V_{out} to above 5 volts using a voltage divider. Observe that the duty cycle varies as the voltage is varied above and below 5 volts.

At this point, reconnect TP1 and apply the 12 to 18 volts to V_{in}. At low-current output levels the supply functions in a discontinuous mode, so the switching waveform is chaotic. The supply functions well enough, although the ripple is higher and more RFI is generated. Above $\approx$ 0.22 amps the waveform becomes a smooth, variable duty-cycle square wave according to **Equation 17**.

Practical uses

Although more complex, the switching regulator offers many advantages over the linear version. One of these is efficiency. This particular unit runs at approximately 85 percent. Another advantage is size. The capacitors are smaller, and because less heat is generated, less space is needed for cooling. **Figure 10** shows a useful summary of the input possibilities for this supply. You can use a 12-volts AC, 1.5-amp transformer. You need only a 10,000-μF capacitor because there's a 12 to 18-volt ripple range. Note the battery backup option. If the AC power fails, the battery voltage conducts through the diode. Rc is used to trickle charge the battery. The 12-volt battery can be used alone, leaving out the diode and resistor. I would, of course, keep the fuse!

Summary

In this article, I've covered the technology and many uses of the power inductor. I've discussed power inductor theory and design, construction and testing, and given information on how to build a high-efficiency switching power supply using inductive components. I hope the ability to design and construct power inductors will add to your enjoyment of our hobby. ■

BIBLIOGRAPHY

1. *Linear/Switchmode Voltage Regulator Handbook*, Motorola Inc., Box 20912, Phoenix, Arizona 85036.
2. *General-Purpose Linear Devices*, National Semiconductor Inc., Box 58090, Santa Clara, California 95952-8090.

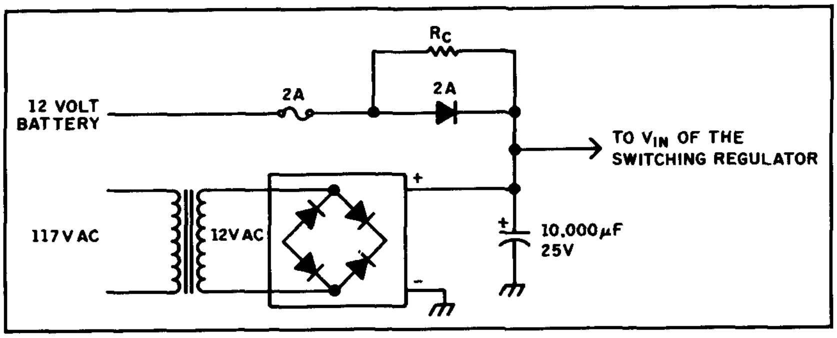

Figure 10. Backed-up power supply.

PARTS LIST

INDUCTOR TESTER

PART NO.	DESCRIPTION	DIGI-KEY* NO.
R1	*50-k ten-turn pot*	*73JA503-ND*
R2	*0.1 ohm, 3 watt*	*VC3D0.1*
R3	*1.0 ohm, 1/2 watt*	*1.0H*
R4	*100 ohm, 1/4 watt*	*100Q*
R5	*100 ohm, 1 watt*	*100W-1*
R6,R7	*470 ohm, 1/4 watt*	*470 Q*
R8	*1000 ohm, 1/4 watt*	*1.0 KQ*
R9	*1800 ohm, 1/4 watt*	*1.8 KQ*
R10-R12	*4.7 k, 1/4 watt*	*4.7 KQ*
R13-R21	*10 k, 1/4 watt*	*10 KQ*
R22,R23	*10 k, 1/4 watt*	*100 KQ*
C1	*47 pF*	*P4020*
C2	*100 pF*	*P4024*
C3,C4	*0.01 µF*	*P4513*
C5-C7	*22 µF @ 16 volts*	*P1218*
C8	*330 µF @ 35 volts*	*P6254*
C9	*3300 µF @ 35 volts*	*P6258*
D1	*15-volt Zener diode*	*1N4744A*
D2	*5-A Schottky diode*	*SR504*
D3	*1N4148 diode*	*1N4148*
D4,D5	*1-A diode bridge*	*DB102-ND*
Q1	*46-A 50-volt IG-FET*	*IRFZ42-ND*

INDUCTOR TESTER (cont.)

Q2-Q4	*2N3904 NPN transistor*	*2N3904*
IC1	*LF357 op amp*	*LF357N*
IC2	*LM358 dual op amp*	*LM358N*
IC3	*74HC14 hex Schmitt*	*MM74HC14N*
IC4	*4046 PLL*	*CD4046BCN*
IC5	*10-volt regulator*	*AN78L10*
IC6	*5-volt regulator*	*AN78L05*
F1	*1/2-A Slo-Blo*	*F314-ND*
T1	*17-volt transformer*	*T106-ND*

Banana jacks for TP1 and TP2

*Digi-Key Corporation, P.O. Box 677
Thief River Falls, Minnesota 56701-0677.

PARTS LIST

SWITCHING POWER SUPPLY

PART NO.	DESCRIPTION	DIGI-KEY NO.
R1	*0.25 ohm, 3 watt*	*VCD0.25*
R2	*22 ohm, 1/4 watt*	*22Q*
R3,R4	*100 ohm, 1/4 watt*	*100Q*
R5,R6	*4.7 k, 1/4 watt*	*4.7KQ*
R7,R8	*10 k, 1/4 watt*	*10KQ*
R9	*39 k, 1/4 watt*	*39KQ*
C1	*470 µF @ 25 volts*	*P1223*
C2,C3,C4	*470 µF @ 10 volts*	*P1204*
C5	*0.01 µF @ 50 volts*	*P4513*
C6	*0.0015 µF @ 50 volts*	*P4515*
C7,C8	*0.1 µF @ 50 volts*	*P4525*
D1	*3-A Schottky diode*	*SR304*
D2	*1-A Schottky diode*	*SR102*
Q1	*12-A, 60-volt P-FET*	*IRF9531-ND*
Q2,Q3	*2N3904 NPN transistor*	*2N3904*
IC1	*LM3524D switching regulator*	*LM3524N*
L1,L2	*100 µH, 3-A inductor*	*(see text)*
L3	*500 µH, 3-A inductor*	*(see text)*

**Note: L1,L2 = 18 turns on a PC-2213-77 gapped 10 mils
L3 = 40 turns on a PC-3019-77 gapped 22 mils**

By Aaron J. Fishman, *K1BAF*
40 Cross Street
Ashland, Massachusetts 01721

DO SUNSPOTS EVER END?

Can you imagine 80 to 200 years without sunspots?

If ancient civilizations worshipped the sun for its role in supporting life and providing food and fuel, then surely Hams worship the sun for giving life to HF via sunspots. But if Hams ride an 11-year rollercoaster with the sunspots, what would they do if the solar flares ended?

Although recent history has shown the sunspot cycle to be fairly regular at about 11 years, ancient history points to periods of 80 to 200 years when the sunspots were gone or, at best, so infrequent that a 10-meter enthusiast would cry. These periods of solar inactivity have been documented by carbon 14 dating techniques and data collected by Chinese astronomers long ago.

The surface of the sun is about 5800 degrees Kelvin. A sunspot's temperature runs about 2000 degrees below this level, thus it appears dark relative to the surrounding photosphere (the sun's visible surface). Typically, a solar flare is larger in diameter than the Earth and some flares are many Earth diameters wide. Because of their great size, sunspots can be seen from Earth through telescopes. (Of course, it's necessary to use filtered telescopes to prevent damage to the optic nerve or blindness which can occur if you stare straight at the Sun.) In the early 17th century, Galileo, the father of the telescope, projected images of the Sun which allowed him to view the sunspots safely. In 1843, after 17 years of observation, a German amateur astronomer named Heinrich Schwabe noted that sunspots seemed to follow a cyclical pattern of approximately 11 years. It's a strange quirk of history that an amateur astronomer discovered the cycle, even though sunspots had been observed and studied for over 100 years by generations of professsional astronomers.

Modern reconstruction of the sunspot cycles show that the periods they cover can extend anywhere from eight to 15 years (see **Table 1** and **Figure 1**). The average cycle runs 11 years. There seems to be no information on sunspot rates before the year 1700. That's not because 17th century astronomers were unaware of solar flares, but because there weren't many to observe. Royal Astronomer John Flamsteed, after observing a sunspot in 1684, wrote: "These appearances, however frequent in the days of Sheiner and Galileo, have been so rare of late that this is the only one I have seen in his (the Sun's) face since December 1676."

In 1889 German astronomer Gustav Sporer drew attention to a very unusual period of low sunspot activity which lasted from the mid-17th to the early 18th century. Walter Maunder, the superintendent of the Solar Department of the Royal Observatory Greenwich, followed up on this observation. In 1890 he reported to the Royal Astronomical Society that: "For a period of about seventy years, ending in 1716, there seems to have been a remarkable interruption of the ordinary course of the spot cycle. In several years no spots appear to have been seen at all, and in 1705 it was recorded as a most remarkable event that two spots were seen on the sun at the same time, for a similar circumstance had scarcely ever been seen during the 60 years previous."

For 30 years, Maunder's ideas that solar flares had periods where they were dormant drew no following. It was thought that if the sunspot cycles were cyclical in recent times, they must have been that way forever. In more recent history, American solar astronomer Jack Eddy verifed that the sunspot activity was very low between 1645 and

Year	Sunspot Number	Year	Sunspot Number	Year	Sunspot Number	Year	Sunspot Number	Year	Sunspot Number	Year	Sunspot Number
1700	5										
1701	11	1756	10.2	1811	1.4	1866	16.3	1921	26.1	1976	2.6 m
1702	16	1757	32.4	1812	5.0	1867	7.3 m	1922	14.2	1977	27.5
1703	23	1758	47.6	1813	12.2	1868	37.6	1923	5.8 m	1978	92.5
1704	36	1759	54.0	1814	13.9	1869	74.0	1924	16.7	1979	155.4 M
1705	58 M	1760	62.9	1815	35.4	1870	139.0 M	1925	44.3	1980	154.6
1706	29	1761	85.9 M	1816	45.8 M	1871	111.2	1926	63.9	1981	140.4
1707	20	1762	61.2	1817	41.1	1872	101.6	1927	69.0	1982	115.9
1708	10	1763	45.1	1818	30.1	1873	66.2	1928	77.8 M	1983	66.6
1709	8	1764	36.4	1819	23.9	1874	44.7	1929	64.9	1984	45.9
1710	3	1765	20.9	1820	15.6	1875	17.0	1930	35.7	1985	17.9
1711	0	1766	11.4 m	1821	6.6	1876	11.3	1931	21.2	1986	13.4 m
1712	0 m	1767	37.8	1822	4.0	1877	12.4	1932	11.1	1987	29.4
1713	2	1768	69.8	1823	1.8 m	1878	3.4 m	1933	5.7 m	1988	100.2
1714	11	1769	106.1 M	1824	8.5	1879	6.0	1934	8.7	1989	157.6 M?
1715	27	1770	100.8	1825	16.6	1880	32.3	1935	36.1	1990	144.2*
1716	47	1771	81.6	1826	36.3	1881	54.3	1936	79.7		
1717	63 M	1772	66.5	1827	49.6	1882	59.7	1937	114.4 M		
1718	60	1773	34.8	1828	64.2	1883	63.7 M	1938	109.6		
1719	39	1774	30.6	1829	67.0	1884	63.5	1939	88.8		
1720	28	1775	7.0 m	1830	70.9 M	1885	52.2	1940	67.8		
1721	26	1776	19.8	1831	47.8	1886	25.4	1941	47.5		
1722	22	1777	92.5	1832	27.5	1887	13.1	1942	30.6		
1723	11 m	1778	154.4 M	1833	8.5 m	1888	6.8	1943	16.3		
1724	21	1779	125.9	1834	13.2	1889	6.3 m	1944	9.6 m		
1725	40	1780	84.8	1835	56.9	1890	7.1	1945	33.2		
1726	78	1781	68.1	1836	121.5	1891	35.6	1946	92.6		
1727	122 M	1782	38.5	1837	138.3 M	1892	73.0	1947	151.6 M		
1728	103	1783	22.8	1838	103.2	1893	85.1 M	1948	136.3		
1729	73	1784	10.2 m	1839	85.7	1894	78.0	1949	134.7		
1730	47	1785	24.1	1840	64.6	1895	64.0	1950	83.9		
1731	35	1786	82.9	1841	36.7	1896	41.8	1951	69.4		
1732	11	1787	132.0 M	1842	24.2	1897	26.2	1952	31.5		
1733	5 m	1788	130.9	1843	10.7 m	1898	26.7	1953	13.9		
1734	16	1789	118.1	1844	15.0	1899	12.1	1954	4.4 m		
1735	34	1790	89.9	1845	40.1	1900	9.5	1955	38.0		
1736	70	1791	66.6	1846	61.5	1901	2.7 m	1956	141.7		
1737	81	1792	60.0	1847	98.5	1902	5.0	1957	190.2 M		
1738	111 M	1793	46.9	1848	124.7 M	1903	24.4	1958	184.8		
1739	101	1794	41.0	1849	96.3	1904	42.0	1959	159.0		
1740	73	1795	21.3	1850	66.6	1905	63.5 M	1960	112.3		
1741	40	1796	16.0	1851	64.5	1906	53.8	1961	53.9		
1742	20	1797	6.4	1852	54.1	1907	62.0	1962	37.6		
1743	16	1798	4.1 m	1853	39.0	1908	48.5	1963	27.9		
1744	5 m	1799	6.8	1854	20.6	1909	43.9	1964	10.2 m		
1745	11	1800	14.5	1855	6.7	1910	18.6	1965	15.1		
1746	22	1801	34.0	1856	4.3 m	1911	5.7	1966	47.0		
1747	40	1802	45.0	1857	22.7	1912	3.6	1967	93.8		
1748	60	1803	43.1	1858	54.8	1913	1.4 m	1968	105.9 M		
1749	80.9	1804	47.5 M	1859	93.8	1914	9.6	1969	105.5		
1750	83.4 M	1805	42.2	1860	95.8 M	1915	47.4	1970	104.5		
1751	47.7	1806	28.1	1861	77.2	1916	57.1	1971	66.6		
1752	47.8	1807	10.1	1862	59.1	1917	103.9 M	1972	68.9		
1753	30.7	1808	8.1	1863	44.0	1918	80.6	1973	38.0		
1754	12.2	1809	2.5	1864	47.0	1919	63.6	1974	34.5		
1755	9.6 m	1810	0.0 m	1865	30.5	1920	37.6	1975	15.5		

Each M marks a sunspot cycle maximum and each m a minimum. Through 1944, yearly means were calculated as the average of the 12 monthly means; since 1945, yearly means have been calculated as the average of the daily means.

*Provisional through October 1990.

This data has been provided by Peter O. Taylor, Solar Division Chairman, AAVSO—Solar Division, Athens, Georgia.

Table 1. Yearly mean sunspot numbers.

1715. In fact, there may have been no cycle at all during those years. In recognition of Maunder's effort, this extended period of solar inactivity is known as the Maunder minimum.

If one Maunder minimum has occurred, could there be others in the past or future? Needless to say it seems fruitless to try and piece together accurate records of sunspot activity before the 1600s. There are, however, certain historical findings, which when combined with modern dating methods based upon radioisotopes like carbon 14, can give some fairly accurate clues as to what happened to the sunspots in ancient history.

Carbon 14 is produced in the upper atmosphere as a result of cosmic ray bombardment. The cosmic ray flux is shielded by the intensity of the extended solar magnetic flux which, in turn, varies with sunspot activity. Carbon 14 is preserved in the wood of dead trees for periods of up to 700 years as a byproduct of photosynthesis. Although measuring carbon 14 in tree rings doesn't indicate the existance of an 11-year cycle per se, it does point to long periods of sunspot inactivity. Carbon 14 production shows a marked increase during the Maunder minimum (increased carbon 14 means less sunspots to block the cosmic rays). Other periods which point to the existence of few or no sunspots (increased carbon 14) are the years from 1420 to 1520 (the Sporer minimum), 1300 to 1350, and 600 to 810 (the Dark Ages minimum). Although these periods are pretelescope eras, historical data from the Ming dynasty indicates sunspots were regularly recorded during the first few decades of that dynasty. However, a gap does appear in the records even though all other astronomical recordings of the period continue throughout. The Ming dynasty coincides with the Sporer minimum of 1420 to 1520.

So there you have it, a fairly safe assumption that sunspot occurences aren't guaranteed. But with our current vigorous cycle in progress, I wouldn't worry about the sunspots disappearing for at least another 100 years!

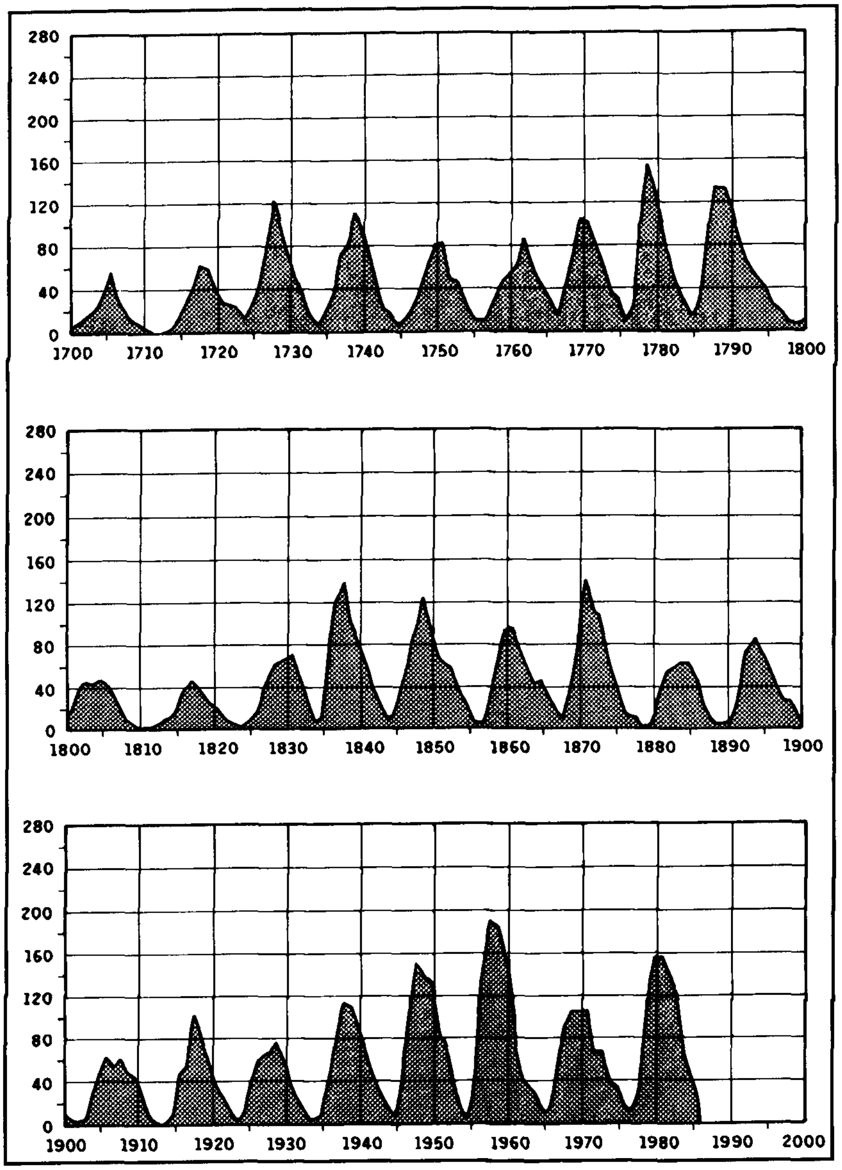

Figure 1. Yearly mean sunspot numbers from 1700 to 1985. Sunspot counts rise and fall approximately every 11.1 years. The cycle, though, isn't symmetrical, for the spot count takes on the average about 4.8 years to rise from a minimum to a maximum and another 6.2 years to fall to a minimum once again. The largest annual mean number (190.2) occurred in 1957. (Data provided by Peter O. Taylor, Solar Division Chairman, AAVSO Solar Division, Athens, Georgia.)

Editor's note

The collection of sunspot data is done by experienced amateur astronomers. Anyone interested in becoming involved in this activity may contact: Mr. Peter O. Taylor, Solar Division Chairman, AAVSO—Solar Division, P.O. Box 5685, Athens, Georgia 30604-5685.

AAVSO not only analyzes relative sunspot numbers, they also operate a program whereby observers monitor very low frequency radio signals through SES techniques and detect solar flares through their effects on the ionosphere (SIDs). This work began in 1956 as part of the International Geophysical Year, and is of interest to Amateur Radio enthusiasts, astronomers, and those researching the solar-terrestrial relationship. ■

BIBLIOGRAPHY

1. Dr. David Clark, "Our Inconstant Sun," *New Scientist*, January 18, 1979.

By Eric P. Nichols, *KL7AJ*
P.O. Box 0
North Pole, Alaska 99705

THE BROADCASTER'S T

A competitive antenna transmatch

There's an ongoing debate about the relative merits of various transmatch configurations like the pi network, L network, SPC, differential C, the Ultimate Transmatch, and so on. But the Broadcaster's T, the most thoroughly tested transmatch in radio history, has gone unnoticed.

The Broadcaster's T network is a simple circuit which has been used almost universally in the standard AM broadcast industry for at least 50 years. I believe this circuit could be used in most Amateur stations with remarkable results. **Figure 1** shows the entire circuit.

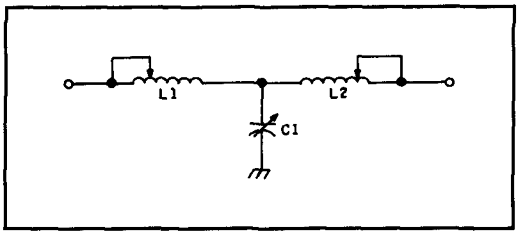

Figure 1. Broadcaster's T network.

Background

Before the advent of directional AM antennas, most standard broadcast stations used a self-supporting grounded tower fed with a slant wire. This was a very effective and simple system. Coax hadn't been invented and the voltage standing wave ratio (VSWR) on the feed line was unimportant. It was also unlikely that there would have been anyone around at that time who would have known how to measure VSWR.

During the 1930s, it became obvious that it would be necessary to have directional antennas at most AM stations to prevent interference on the increasingly congested AM band. The advent of multiple towers made it logistically impossible, or at least extremely difficult, to feed them all from a single transmitter with sloping wires. It was apparent that genuine transmission lines were needed to get the RF to all the towers.

Phasing was a problem, too. Even if it were possible to place the transmitter at a central location in the antenna array, and feed the towers with slant wires, there wasn't much that could be done to adjust the relative RF phasing to each tower.

The only practical way to adjust the phasing was to run a *matched* and properly trimmed transmission line to each tower in the array. With a properly matched (flat) transmission line, the phasing problem became a relatively simple one. The line was cut to the proper length and the propagation delay was allowed to go to work.

However, impedance matching continued to be a problem. Contrary to popular opinion, few, if any, broadcast Marconi antennas are truly self resonant. Depending on their vintage, towers come in standard sections of 20 or 60 feet, and the broadcaster must round off his tower height to the nearest sectional length. I don't know of any broadcaster who has his antenna trimmed to be truly self resonant! Even if he were to cut his antenna to the theoretically correct length, unknowns like tower lighting and guy wires would change the resonant frequency *significantly.* In the industry, it goes without saying that *all* towers are considered to be reactive as well as resistive.

Broadcasters needed a universal network which would match any series-fed tower of any impedance to a standard transmission line. The Broadcaster's T was their answer.

The T also helps fulfill one additional requirement — good harmonic suppression. Second and third harmonic radiation from a standard AM station must be −80 dB down from the fundamental signal. Obviously, any matching network which degenerated into a high-pass filter under certain matching conditions would be absolutely unacceptable. The Broadcaster's T is *always* a low-pass network. That's certainly not something that can be said for the Ultimate Transmatch. And, although the standard pi network used in most low-cost antenna tuners is good for harmonic attenuation, it performs poorly when the antenna is highly reactive.

Performance examples

Here are some examples of how the T does its job under different circumstances. For the time being, assume that the transmitter has a low-impedance output.

High-impedance multiband antenna

For starters, take a very high-impedance resonant antenna of the type that might be found in a multiband situation. A one-wavelength wire will exhibit about 2000 ohms at its feed point. This condition lets you tap all of L2 out of the circuit, creating the standard low input, high output impedance L network depicted in **Figure 2**. L1,C1 form a series-resonant circuit, as far as the transmitter is concerned. This presents a very low impedance to the transmitter.

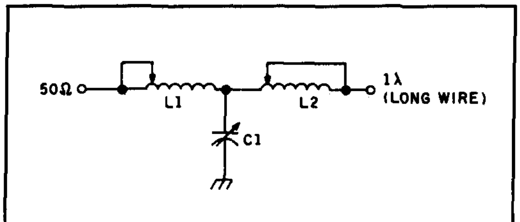

Figure 2. Example of a low-input, high-output impedance L network. L1,C1 form a series-resonant circuit. The load is high impedance (resistive).

Assuming L1 has infinite Q, the impedance at the input will be zero, even without an antenna connected. The junction of L1,C1 will have infinite impedance and infinite voltage. Looking back into the network, a parallel-resonant circuit will be presented to the antenna. But, when you attach your antenna to the load end of the network, you'll find that it's as if you had shunted a 2000-ohm resistor across the resonant circuit, lowering the Q. Because a resonant network looks like a typical quarter-wave transmission line, the network input will show an increase in impedance from its theoretical zero value. By changing the ratio of L1 and C1, you can change the loading while maintaining the resonance.

You can look at this situation in another way. Think of L1 and C1 as a voltage divider. Assume that resonance is always maintained. When the value of C1 is high, its reactance is low because

$$X_C = \frac{1}{2\pi fC}.$$

This also means that the voltage across C1 must be low because $E = IZ$. Because the antenna impedance (in this case equivalent to a 2000-ohm resistance) appears across C1, the voltage across the load must be the same as the voltage across C1. Owing to the fact that power dissipated in a resistance equals $\frac{E^2}{R}$, the power delivered to the antenna must also be small. Thus, you have light loading. If, however, C1 is very small, all the previous conditions are reversed, and you have heavy loading.

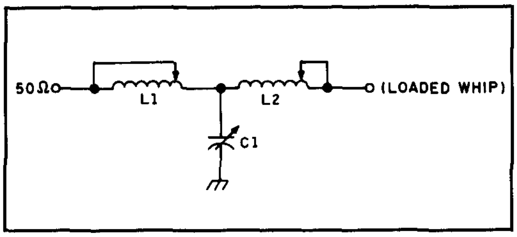

Figure 3. Same as *Figure 2*, but with a low-impedance resistive load presented to the L network.

Loaded mobile whip antenna

Now, look at **Figure 3**. A loaded mobile whip may have an impedance of only a few ohms. Once again, assume that the load is purely resistive. You need to transform your fractional ohm impedance up to 50 ohms, or so. In this case, you can tap out L1 and reverse the L network of the previous example. Because you're not tuning out any reactances, L2 and C1 must have equal reactances. Think of C2 as an extra loading capacitor across the transmitter output. This lets you decrease the loading of the system greatly. To use another analogy, if the resistance of your antenna is extremely low, you can think of it as a short circuit between the right-hand side of L2 and ground. This converts the network to a parallel resonant circuit from the transmitter. The input impedance is very high, limited only by the overall circuit Q. Lowering the Q by decreasing the value of C1 or L2 will increase the loading.

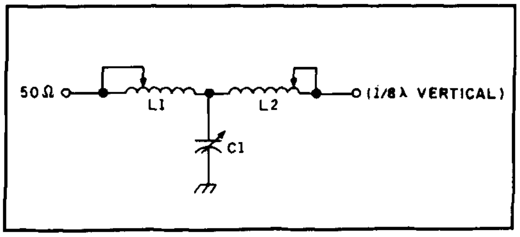

Figure 4. The L network with a low-impedance, capacitive-reactive load.

1/8-wave vertical antenna

Things get interesting when reactances are involved. With an 1/8-wave vertical (**Figure 4**), you'll not only have a low radiation resistance, but a capacitive reactance as well. You can assume that, because you are going from a 50-ohm transmitter impedance to a somewhat lower antenna impedance, the network will more closely resemble that of **Figure 3** than that of **Figure 2**. You can also reason that L2 should have more inductance than L1. In addition, it would be logical to suppose that L1 must contain *some* inductance.

Using the analogy of the second circuit, you can adjust the ratio of L2 and C1 to bring the impedance to 50 ohms from whatever low value was present at the antenna side. But, you'll also find that, although there is a 50-ohm resistive component at the input, there's capacitive reactance as well. You simply need to add a little series inductance with L1 and you'll have a 50-ohm resistive load to present to your transmitter.

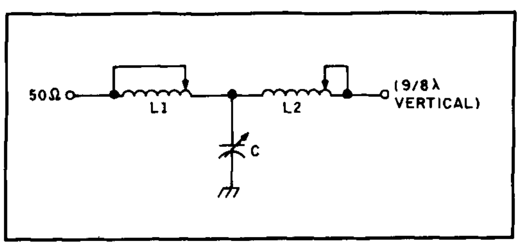

Figure 5. Load presented to the L network is high impedance, inductive reactive.

9/8-wave vertical antenna

Here's how to handle a 9/8-wave vertical (**Figure 5**). While I realize that nobody in his right mind would intentionally build a 9/8-wave vertical, I know of a case where a broadcaster temporarily found himself dealing with this situation after acquiring a frequency change.

This antenna has a moderately high impedance of around 400 ohms and a lot of inductive reactance. Because the output impedance is high, the circuit should be a "case 1" type. But, a problem exists because there's already too much inductance, or so it would seem. For starters, retain all of L2 because it's on the antenna side.

Next, tune C1 and L1 for resonance, with the antenna disconnected. An L network acts like a quarter-wave transmission-line transformer whether you're dealing with reactances or resistances.

You may recall that a capacitor at the end of a transmission line acts like an inductor a quarter wave away, and vice versa. The L network does the same thing. So, if you add a bit of inductive reactance to the output of the resonant L network, it will act like a capacitor at the input side. What you do in this case, is add even more inductance on the output side of the network with L2. This will make the input look capacitive. Compensate by adding more series inductance with L1. It really works!

I hope these four examples have given you an idea of the versatility of the Broadcaster's T. My prototype uses a roller inductor at both L1 and L2. Admittedly, a two-roller transmatch would be rather expensive for many Amateurs, but a pair of tapped inductors does a good job.

One thing I haven't mentioned is that the T is very useful for shifting phase independently of resonance. You do this by ganging the inductors together in a differential fashion — a common approach in broadcast stations at the transmission lines' input.

Try the Broadcaster's T. I can all but guarantee that it will be the last transmatch you'll ever use. ■

By Lloyd Butler, *VK5BR*
Reprinted from *Amateur Radio*
December 1989

A VLF-LF RECEIVER

10 to 500 kHz with resistance tuning

Few communications receivers tune to frequencies below 500 kHz. Because of this, many radio enthusiasts are unfamiliar with this section of the radio frequency spectrum which supports numerous radio services.

I did not have a receiver which could tune these frequencies and set out to design a simple one for just that purpose. The superheterodyne receiver described here is the result. I call it a VLF-LF receiver because it tunes the VLF-LF range from 10 to 300 kHz, and also tunes part of the MF spectrum from 300 to 500 kHz. The VLF and LF bands have their own unique useful characteristics and these will be discussed further on.

The receiver design is a little different from the usual form. It has no variable capacitors or inductors, except for one preset trimmer in a trap circuit. Tuning is carried out by a potentiometer, the resistance of which sets the frequency of the heterodyne oscillator. The RF end is untuned and the receiver bandwidth is set by two inexpensive ceramic filters in the IF channel. All inductive elements are provided by stock lines of miniature RF chokes.

Because of the low frequencies involved, it has been possible to use a number of excellent integrated circuit packages which would be unsuitable on the HF bands. The circuit diagram of the receiver is shown in **Figure 1** and the following discussion refers to elements in that diagram.

The mixer stage

Mixing is carried out by an operational multiplier package type XR2208. This device is suitable for use at frequencies up to 8 MHz, and its performance is outstanding as a mixer at low frequencies. Performance tests at an input frequency of 200 kHz and an intermediate frequency (IF) of 455 kHz have produced the following results:

Conversion gain (ratio of output level at 455 kHz to input level at 200 kHz): minus 6 dB.

Equivalent noise level at input: 10 microvolts in a 1-kHz band.

Third-order intermodulation products: At input levels below 70 microvolts, products are below the noise floor. Even at 1-volt input, the third-order products are 55 dB below signal level at 455 kHz.

Level of signal at the output, equal in frequency to the input signal: 33 dB below the level at the input.

Level of signal at the output, equal in frequency to the local oscillator frequency: 53 dB below the level of the oscillator at the mixer input.

The low level of third-order intermodulation products adds up to a low order of nuisance intermodulation beats or "birdies." The low level of local oscillator signal in the output assists in achieving operation with the oscillator frequency close to the intermediate frequency, as is needed when tuning at signal frequencies down to 10 kHz.

The tunable local oscillator

For a tunable oscillator, I selected precision oscillator package type XR2209 so variable resistance tuning could be applied. This device can be operated at frequencies up to 1 MHz, and for an R-C tuned oscillator, has the excellent temperature stability of 20 parts per million per degree Celsius. For the maximum oscillator frequency of 955 kHz required, frequency drift over a 20-degree change is only 360 Hz.

The XR2209 can be connected for either square-wave or triangular-wave output. The latter is fed to the mixer via a sine-shaping filter. The filter is used to reduce the possibility of oscillator harmonics mixing with high level high frequency signals which manage to get through the RF filter at the receiver input and produce unwanted IF beats.

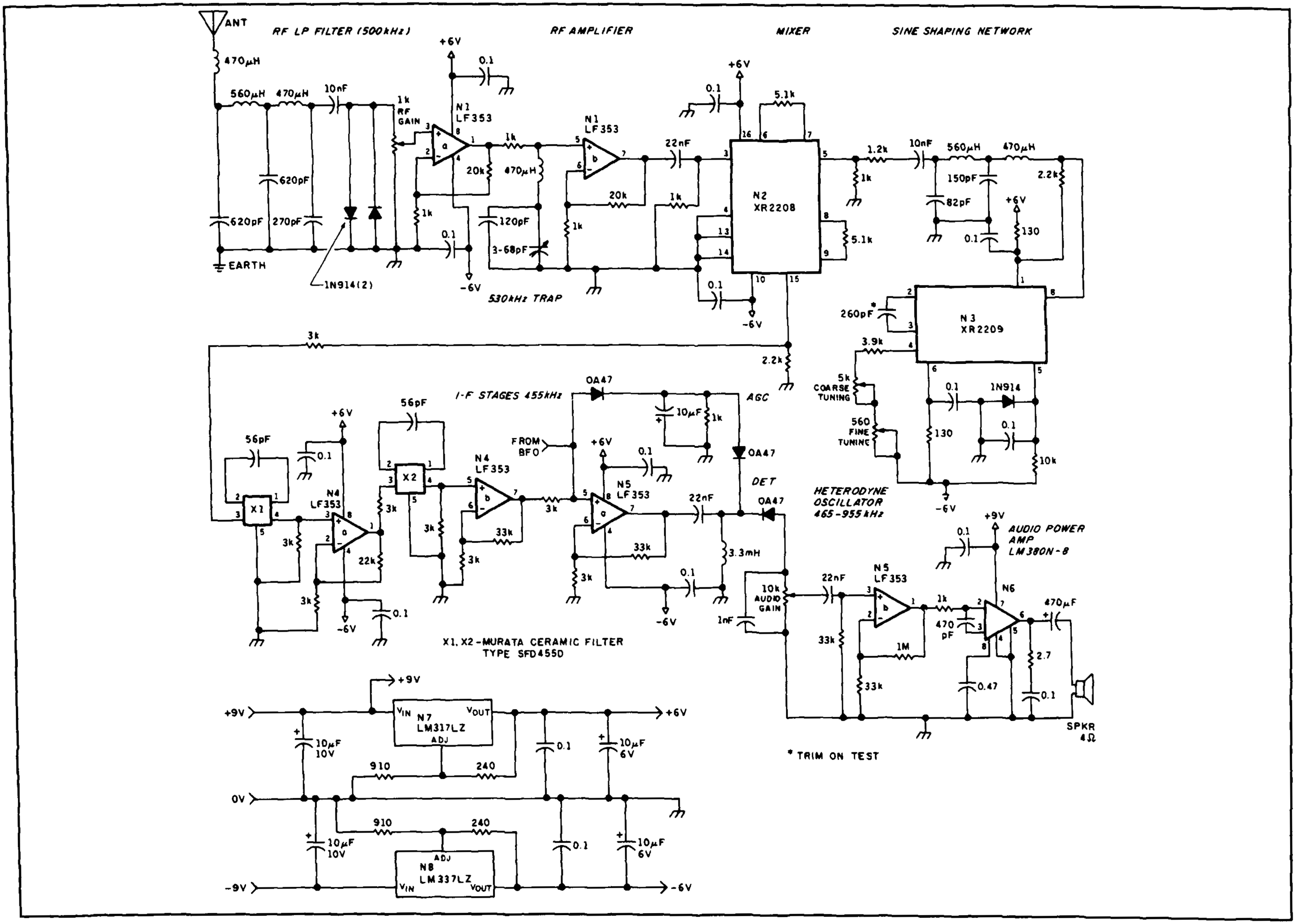

Figure 1. VLF-LF receiver circuit diagram. (Refer also to *Figure 4* for BFO).

The tuning is carried out by two potentiometers, one for coarse tuning and one for fine tuning. The fixed tuning capacitance and the limiting resistance in series with the two potentiometers are trimmed to obtain an oscillator frequency range of 465 to 955 kHz — 455 kHz higher than the tuning range of 10 to 500 kHz. The coarse-tuning potentiometer is connected to a dial which is calibrated in coarse frequency. The values of resistance and capacitance have been selected to suit the full resistance range of the coarse potentiometer. If a vernier dial is used with a shaft rotation of only 180 degrees, the value of limiting resistance can be decreased and the value of fixed capacitance increased to correct for this condition.

RF and IF amplification

To provide RF and IF gain, I used JFET operational amplifier packages type LF353. These are eight-pin DIL packages containing two amplifiers with a 4-MHz gain-bandwidth product. At the frequencies involved, there is a gain of 100 for each package. The RF amplifiers are actually set to realize a gain of 20 per unit at low frequencies, giving a total gain of 400. Of course, this gain decreases at the high frequency end of the tuning range.

One LF353 package is used for RF amplification and one and a half LF353 for IF amplification. The remaining odd half is used as an audio driver following detection.

The RF circuit

The front end of the receiver is broadbanded up to a frequency of around 500 kHz above which higher frequencies are attenuated by a low-pass filter. The function of the low-pass filter is to reject signals at image frequency which, as it happens, fall within the broadcast band. It also rejects higher frequency signals which could mix with harmonics of the local oscillator to produce a 455-kHz IF beat. The 3-dB cutoff point of the filter is set at 500 kHz and its response is 55 dB down at the second harmonic of the cutoff frequency.

A trap circuit is included in the coupling circuit between the two RF amplifier stages. In the first instance, the receiver was made to reject signals above 420 kHz and the trap was fitted to reject direct signal pick up at the intermediate frequency. Direct pick up at 455 kHz proved to be no problem. I attribute this to the properties of the XR2208 which balance out the input signals. The receiver could also be tuned across 455 kHz with no undesirable effects. Consequently, I changed the input filter for a cutoff frequency of 500 kHz to extend the range of the receiver. The only problem with this change was that it opened up the RF end to signal entry at the extreme end of the broadcast band. Strong local station 5UV on 530 kHz mixed with the second harmonic of the heterodyne oscillator to produce a signal when the receiver was tuned to receive 37.5 kHz. Furthermore, if the RF gain was set too high, 5UV would cross modulate other signals. To eliminate this problem, I set the trap to the 5UV frequency just above 500 kHz.

The IF circuit

The selectivity of the receiver is achieved with two Murata-type SFD455D ceramic filters in the IF channel. These are low-price units essentially made to replace 455-kHz IF transformers in transistor receivers. Using the two of these filters, the 3-dB bandwidth is 3.7 kHz. Adjacent channel rejection is 47 dB at 10 kHz from center frequency, and 65 dB at 20 kHz from center frequency. The response of the IF channel is shown in **Figures 2A** and **B**. **Figure 2B** is an expanded version of **2A**. The steep slope of the IF

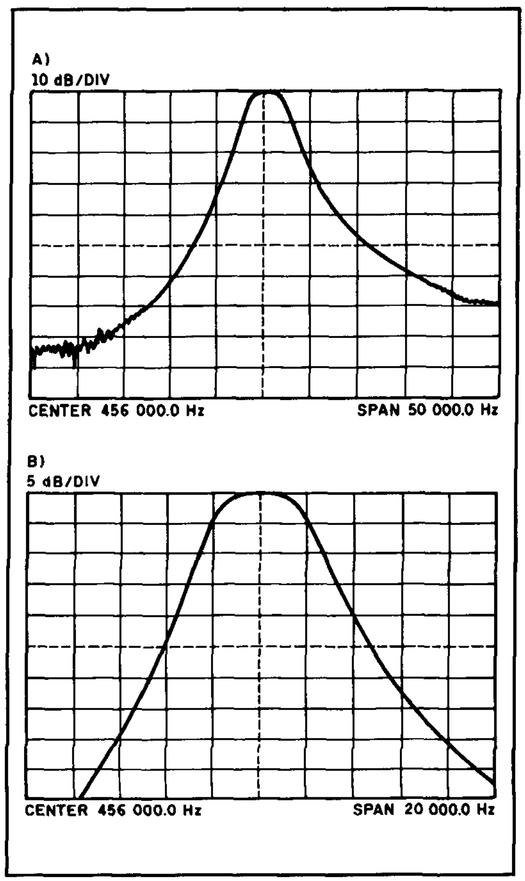

Figure 2. Intermediate frequency (IF) response.

response enables signal reception down to 10 kHz. For this tuned condition, the heterodyne oscillator runs at 465 kHz and this must be rejected by the IF channel.

The values of components connected around the filters are as suggested in the manufacturer's brochure. If a wider bandwidth is desired, it can be achieved by a change in these values. I experimented with one of these filters and found that its bandwidth could be expanded to around 7 kHz by operating with the circuit constants shown in **Figure 3**.

Audio stages

The IF signal is detected by a diode and following R-C filter. The audio output is fed via the half LF353 preamplifier to an eight-pin version of the LM380 power amplifier. The LM380 has internal thermal limiting, and using heat sinking only via the circuit board pins, it can deliver an audio power of up to 1 watt into a 4-ohm load with a power supply of 9 volts.

Beat frequency oscillator (BFO)

Most of the signals heard within the frequency range transmit in the AM or MCW mode, so the receiver was initially wired up for only that type of reception. However, there are also CW signals on the bands, like those transmitted by the marine coastal radio, for which a BFO is needed. A BFO is also useful for detecting the presence of some of the navigational signals like Omega. Eventually, I added a BFO. This is shown in **Figure 4**.

Because the 455-kHz ceramic filters used in the IF stages are quite inexpensive, this provided an impetus to use a third filter for crystal control of a stable BFO. Tests on the filter showed that a crystal element could be accessed between pin 5 and any of the other pins on the filter, and each element gave a parallel resonance around 456.85 kHz. Pins 1 and 2 elements were found to produce a higher Q than pins 3 or 4 elements.

Another half LF353 was pressed into service to form the oscillator, in conjunction with the ceramic element across pins 1 and 5 and other components as shown in **Figure 4**. I measured the frequency of oscillation to be 456.36 kHz. This was a satisfactory offset to 455 kHz to operate the incoming signal within the 3.7 kHz IF passband and give a suitable audio frequency beat. The series inductor and shunt capacitor at the amplifier output form a sine-shaping filter fitted as a precaution in case harmonics of the BFO caused any problems. The second buffer amplifier is really unnecessary, but I gave it a job to do because it was available as a spare in the LF353 package and required no extra components.

The component values shown to make the circuit oscillate were determined experimentally on a single LF353 and a single ceramic filter. I point this out because, in duplicating the circuit, you may find that constants in these devices (particularly the filter) might well vary in different samples, possibly resulting in the need for a change of component values in the feedback path.

Power rails

Split power rails of plus and minus 6 volts are used for all stages except the audio power amplifier. The split rails enable precise centering of amplifier operating points making it easy to couple directly, without capacitors, many of the amplifier stages.

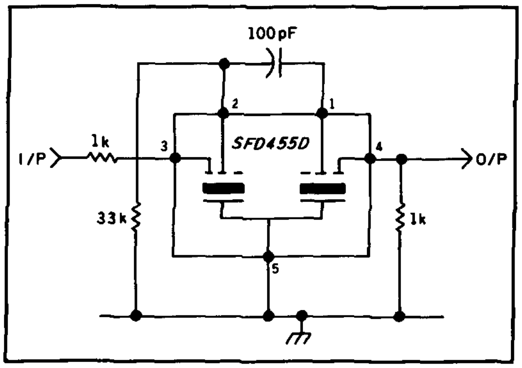

Figure 3. Ceramic filter — connection for wider bandwidth.

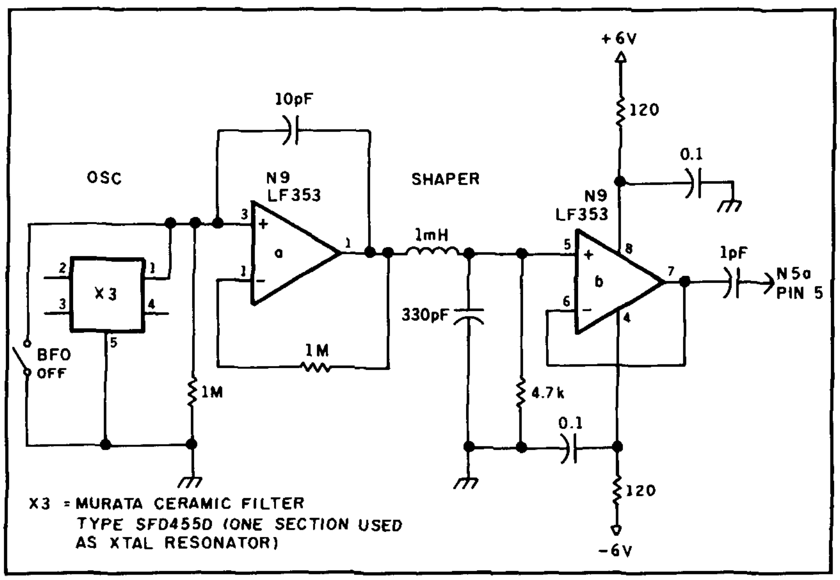

Figure 4. Beat frequency oscillator (BFO) circuit diagram.

The 6-volt rails are derived by voltage regulators type LM317LZ and LM337LZ from a nominal source of plus and minus 9 volts. These very compact regulators are packaged in standard TO-92 transistor cases. The regulators are needed to stabilize the voltage, in particular the voltage to the XR2208 oscillator, as its high frequency stability can only be achieved if its power rail voltages are held constant.

Decoupling of the 6-volt rails is used in feeding both oscillator circuits. These are running at a high signal level, and the decoupling is necessary to prevent coupling into other circuits via the power rails.

The audio power amplifier is powered directly from the positive 9-volt source and does not load the regulator.

The regulated load current is approximately 30 mA per 6-volt rail and is well within the 100-mA capacity of the regulators. The additional load current from the LM380 increases the current on the 9-volt positive supply to 37 mA in the quiescent state and to 134 mA when the power amplifier is driven to its maximum output with continuous sine-wave signal. Under signal conditions, average current is on the order of 50 mA.

The 9-volt power sources can be two small flashlight batteries or twin unregulated DC supplies rectified from a transformed AC supply. If batteries are used, the positive supply must be shunted with a 2200-μF electrolytic capacitor to prevent the swinging load current of the LM380 from developing a corresponding voltage drop across the battery internal resistance. If the voltage is allowed to swing below 7.7 volts, the regulators cannot do their job and instability occurs. This also puts a limit on how far the batteries can be discharged before the regulated voltage fails. The possibility of instability is eliminated if a separate (third) battery is used for the LM380, so supply to the regulators is unaffected by the LM380 varying load.

Overall sensitivity

For satisfactory performance, receiver generated noise level, referred to the receiver input, must be lower than the noise from the antenna. At low radio frequencies, the atmospheric noise is very high and receiver sensitivity does not have to be as good as that normally sought for receivers operating in the HF or VHF bands. In this receiver, the minimum discernible signal level is around 3 μV for frequencies below 100 kHz. Above 100 kHz, sensitivity falls because of the shaped response caused by the RF filter and the 530-kHz trap and, to a lesser extent, by the failing response of the RF amplifiers at high frequencies. **Figure 5** plots the minimum discernible signal level as a function of frequency together with a plot of atmospheric noise against frequency. The noise is that anticipated from a 10 to 30 meter antenna in a bandwidth equal to that of the receiver, or 3.7 kHz. The figures have been derived from information published in the *ITT Reference Data for Radio Engineers* and based on a noise level for Australia of around 45 dB above KTB at 1 MHz. Based on **Figure 5**, and using the range of antenna lengths specified, the receiver has adequate sensitivity for frequencies up to 350 kHz. The receiver still operates up to 500 kHz, but owing to the shaped RF response, it has a considerable reduction in sensitivity as 500 kHz is approached.

I have not provided full automatic gain control (AGC) in the RF and IF circuits, partly because the LF353 amplifiers did not quite lend themselves to control of gain and partly because ionospheric fading was not anticipated on this band. Had I contemplated AGC, gain controlled amplifiers like the Motorola MC1590 or the Plessey SL6120 might have been a better choice for RF amplification. Because RF gain is manually controlled, some care must be taken in setting the RF gain control to prevent receiver overload when tuning to a very strong signal, such as the local airport beacon. The

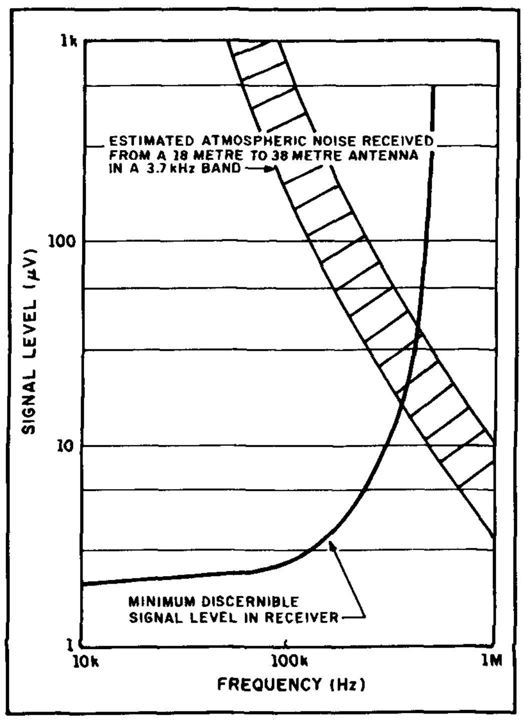

Figure 5. Minimum discernible signal level and estimated atmospheric noise level.

placing of the gain control at the RF amplifier input might appear open to question, as attenuation at its input effectively degrades the receiver noise figure. On the other hand, it is the best place to control the input signal level to prevent cross modulation in the amplifier. Furthermore, at the frequencies concerned, incoming noise is generally predominant over receiver noise, and the noise figure is not so important.

I found the main nuisance of not having an AGC was the audio overload which occurred when shifting the tuning from a weak signal to a very strong signal. This effect was reduced by applying a form of AGC which lowered the gain of the last IF stage on very strong signals. To achieve this, DC voltage is rectified from the IF output of the stage and applied to a germanium diode connected at the stage input. The variable resistance of the diode acts as the shunt element of an inverted L network. The higher the signal voltage, the higher the diode current, the lower the resistance of the shunt element and, hence, the greater the loss in the network.

One might well ask why I did not apply this AGC system at the RF input as is usually done. I did, in fact, experiment with this idea, but found it encouraged cross modulation from strong stations within the passband of the RF filter. This is a problem with broadband RF stages. There is no selective tuning to attenuate the level of the strong signal, and the variable slope gain characteristic needed for AGC control is also a good mixing medium for the strong signal to cross modulate any other signal.

Alignment

The only tuned circuit is the trap. This can be aligned by feeding a modulated signal at a fairly high level into the receiver input at a frequency just above 500 kHz and adjusting the series trimmer for minimum audio output. You might choose to select the frequency of the lowest frequency local broadcast station, as I did. In my case, the receiver was tuned to 37.5 kHz and the trap was set for minimum signal from 5UV (refer to the previous discussion in the section on the RF circuit).

The only other possible adjustment is the setting of the heterodyne oscillator frequency to cover the frequency range of 465 to 955 kHz, over the tuning range of the coarse potentiometer control. This is done with the fine potentiometer control set to center position. Trimming of the capacitance across pins 2 and 3 of N3 and the fixed resistor at the pin of N3 may be necessary to suit individual samples of the XR2209 package. Its frequency range can be checked using a frequency counter connected across its output, or by feeding the receiver input with a signal generator set to the extremities of the input frequency range; that is, 10 kHz and 500 kHz.

Notes on assembly and components

There is nothing particularly critical about the receiver layout except that the circuit wiring should flow from input to output in order, as is normal practice, and outputs should be kept away from inputs. It is not an arduous task to hardwire the whole unit (except for controls) on a small piece of Vero board. My experimental receiver fit on a card space of 12 by 10 cm.

All the inductors used are the miniature ferrite-cored types, like the Siemens range of RF chokes type 878 108-S. These are about the size of a small resistor, are color coded like a resistor, and can easily be mistaken for one. There are a few precautions to observe in mounting these chokes. Unlike toroidal-cored inductors, the field around them is not confined. They should be mounted with extended leads, at least 1 cm off any metal on the circuit board, to prevent change of inductance and a lowering of Q. If two of them are mounted close together, they should be mounted at right angles to reduce interaction between their fields.

As a general rule, capacitors with a low resistive component should be selected for filters and tuned circuits. This also applies to the filters and trap circuit in this receiver. Most people choose ceramic capacitors for use in their projects because of their small size, but their resistive component varies from sample to sample in a batch, and it is often quite high. Unless they can be carefully selected for low resistive component using an impedance bridge or Q meter, ceramic capacitors should be avoided if possible. Mica capacitors are good, but are usually much larger. There are some high quality ceramic capacitors, such as the Vitramon VP31 range, but they might be difficult to obtain at the local electronics store.

The only other components which require particular mention are the capacitor and variable resistances used to control the frequency of the heterodyne oscillator. The capacitor across pins 2 and 3 of N3 should be a good stable type (perhaps a mica) and the potentiometers should be noninductive with good resolution. Good quality 1-watt carbon or cermet-type potentiometers will give nice smooth tuning. I emphasize this because there are some very poor potentiometers on the market today – particularly in the miniature variety. One of their faults is the high degree of mechanical backlash which seems to be caused by the elasticity of the bush sealing the shaft. Fortunately, this backlash is steadied when the shaft is loaded down by the reduction gear on a tuning dial.

What can be heard

The VLF and LF bands have their own unique and useful characteristics. Transmission is by ground wave. It is virtually unaffected by reflection from the ionosphere and, because of this, transmission is highly predictable and very useful for direction finding and other forms of radio navigation. Atmospheric attenuation falls as frequency is lowered, and given sufficient radiated power, signals at VLF travel large distances around the Earth's surface. A difficulty is the massive aerial system needed to achieve some order of antenna efficiency and, hence, radiated power.

Another limitation is the restricted amount of channel space not suitable for wideband systems. For example, one television channel of around 6-MHz bandwidth, on its own, takes up 20 times more band space than the whole of the VLF and LF spectrums put together.

Radio waves are highly attenuated when passing through water, but waves in the VLF region are attenuated the least. (I discussed this in an article in the April 1987 issue of *Amateur Radio.*) Because of the comparatively low attenuation, the VLF band is used for communication to submarines.

Within the Australian region, there are many strong signals transmitted in the VLF and LF band and the part of the MF band tuned by the receiver. Included in these are the following:

The Omega navigation system can be heard in a frequency band of 10 to 13 kHz. There are actually five different frequencies transmitted which are switched in a certain order of eight segments in a 10-second time frame. One of the Omega stations is located in Victoria, Australia.

The North West Cape VLF station can be heard with a frequency shift of 100 Hz between 23.25 and 23.35 kHz.

A proliferation of aeronautical homing beacons (known as nondirectional beacons or NDBs) within the spectrum of 200 to 420 kHz, transmit continuous carrier with Morse ident code. Some also transmit with voice aerodrome traffic or information.

Australian maritime coastal radio stations operate with CW on a range of fixed frequencies between 420 and 490 kHz and listen for merchant ships on 425, 468, 480, and 512 kHz. The maritime distress frequency is 500 kHz.

Throughout the world, there are several stations in the VLF-LF spectrum which transmit standard time and frequency. GBR (Rugby UK) is well known for its time services on 16 kHz. MSF (Rugby) transmits on 60 kHz. At low frequencies, these typical signals are ducted around the Earth in a type of wave guide formed by the D layer and the Earth. With a bit of luck, one might pick up some of these.

There are various teletype services which can be heard from time to time. Of course it is difficult to identify who they are unless you can decode their signals.

In Europe, frequencies between 150 and 300 kHz are used for long-wave broadcasting but, at these frequencies, distances are too great for reception within Australia.

For those enthusiasts who are interested in short-wave listening and identifying various stations, there is another field of endeavor in long-wave listening.

Other options

Though I have discussed the design of a complete VLF-LF receiver, there are a few other simple options which might be attractive to others interested in these bands. If you have an existing receiver with a 455-kHz IF channel, you could build just the RF end of the receiver described and feed the XR2008 mixer output into the second receiver IF stage via a switch which selects either the VLF-LF front end, or the existing receiver RF end.

Another option is to use the VLF-LF RF end as a converter and feed the mixer output into the second receiver tuned at the low frequency end of the broadcast band. A frequency would have to selected clear of strong broadcast carriers, and the connecting lead would have to be carefully shielded. The capacitor across pins 2 and 3 of the XR2209 oscillator would also have to be decreased to shift the oscillator frequencies up a little. Do not try to shift it up too far as the frequency limit of the XR2209 is specified as 1 MHz, although you might get it to operate a little higher than that.

In the receiver described, the IF channel was specifically designed with a narrow bandwidth and a steep out-of-band slope so

10 kHz could be tuned. If an attached receiver option is used, tuning quite as low as 10 kHz might be restricted if the receiver bandwidth happens to be too wide.

A different type of RF amplifier could easily be used, perhaps with better performance at the MF end of the tuning range. I strongly recommend that you stay with the XR2208 as a mixer because of its balanced mixing type of performance and its low order of intermodulation products.

Bandwidth control

As has been discussed, bandwidth was set at 3.7 kHz by two Murata 455-kHz type SFD455D ceramic filters. This bandwidth is ideal for medium bandwidth type modes, like AM speech, but is wider than necessary for narrow-band mode signals which exist at frequencies below 100 kHz. These signals are received in the presence of very high noise levels inherent to the LF spectrum and the low end of the VLF spectrum. For these signals, an improvement in signal-to-noise ratio can be achieved by reducing the bandwidth of the receiver. As it turns out, the bandwidth can be narrowed quite simply by switching in a minor circuit change around one of the two ceramic filters.

Curve A of **Figure 6** plots the spectral response of the original ceramic filter circuit shown in **Figure 7**. The bandwidth of the circuit can be narrowed to less than 1 kHz by decreasing the 56-pF inter-filter coupling capacitor to 4.7 pF and terminating the filter in a high impedance. The resulting spectral response is shown by curve B in **Figure 6**. The high impedance can be achieved by increasing the value of the terminating resistor. However, in the receiver circuit, this resistor is also an input return for the following operational amplifier. Increasing its value without a corresponding change at the amplifier inverting input would affect the DC offset of the amplifier. To avoid changing the inverting input components, I achieved the high impedance by inserting a 4.7-mH choke in series with the original 3-k terminating resistor. The modified circuit for narrow bandwidth is shown in **Figure 8**.

Examining again the narrow bandwidth curve B of **Figure 6**, you will see that it peaks at 457.6 kHz. This works out quite well for centering a frequency to give an audio beat with the beat frequency oscillator (BFO) which is locked at 456.85 kHz. As you will remember, the BFO was locked by an element in the same type of ceramic filter unit used to control the IF bandwidth.

I found that switching between wide and narrow band, could be achieved easily by switching the inter-filter coupling capacitor between 56 and 4.7 pF and leaving the 4.7-mH choke in place for both conditions. **Figure 9** shows the effect of the choke when leaving it in circuit for the wideband condition. Curve A is the spectral response of the original circuit of **Figure 7**; curve B is the response with the choke in circuit. It can be seen that the latter condition gives an actual 6-dB gain at the expense of around 3 dB of asymmetrical ripple in the response curve.

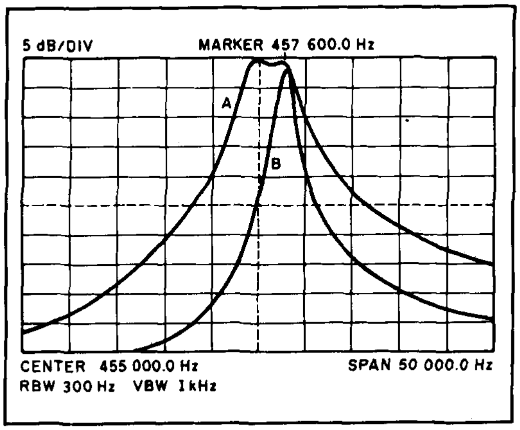

Figure 6. (A) Response of the original wideband filter circuit. (B) Response of the narrow-band filter circuit.

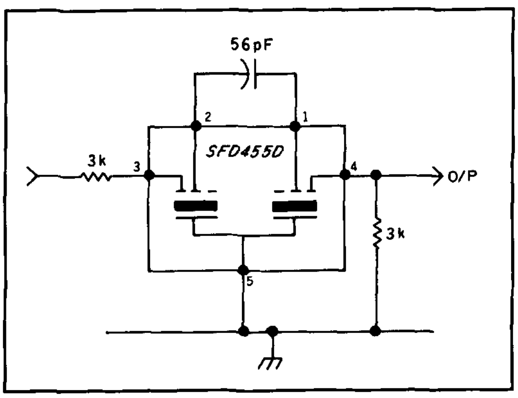

Figure 7. Original wideband filter circuit.

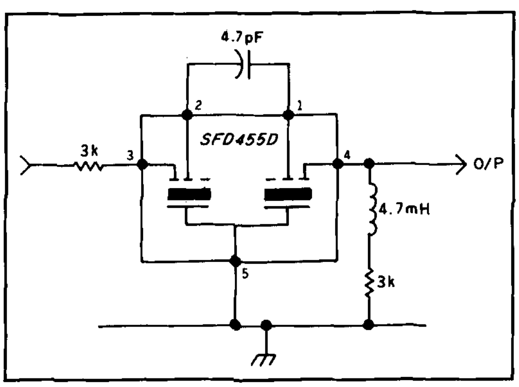

Figure 8. Narrow bandwidth filter circuit.

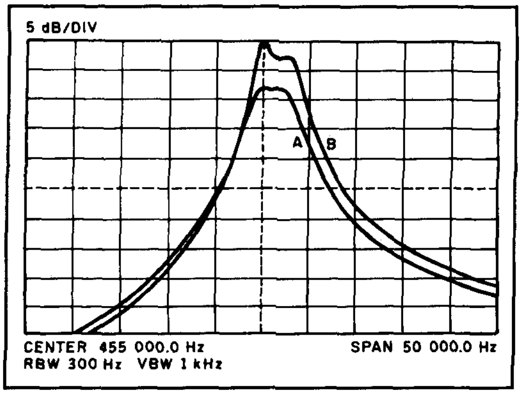

Figure 9. (A) Response of original wideband filter. (B) Response of wideband filter with 4.7 μH choke left in circuit.

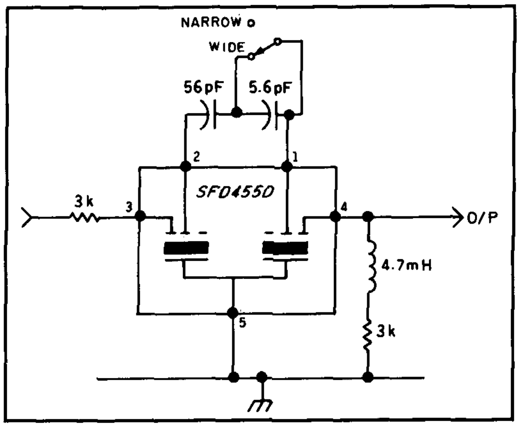

Figure 10. Filter circuit with wide/narrow bandwidth switching.

While the ripple looks untidy on paper, its effect on the practical performance of the receiver is unnoticeable. Furthermore, the 6 dB of gain improvement is also a 6-dB improvement in overall receiver sensitivity, which assists reception at the 500-kHz end of the tuning range where the sensitivity falls away.

The switchable bandwidth control circuit is shown in **Figure 10**. This was applied to the first ceramic filter in the IF chain because it was the easiest one to access on the already wired up board. (The modification could actually be performed without even removing the card from the receiver box.) Of course, there is no reason why the modification could not have been carried out on the second filter, had it been more convenient to achieve. The bandwidth switch was mounted on the receiver front panel and connected into the circuit board via a twisted wire pair. In the circuit shown, the 4.7-pF coupling capacitance for narrowband operation is formed from the series connection of 5.6 and 56 pF. Part of the 5.6-pF capacitance is made up of capacitance in the twisted wire pair to the switch. For wideband operation, the 5.6-pF section is shorted out so the coupling capacitance becomes 56 pF.

Other applications

The bandwidth control circuit was intended specifically for the VLF-LF receiver, but it could well be fitted to any receiver with a 455-kHz IF channel to improve the reception of narrow-band mode signals. Considering its cost and size, the Murata ceramic filter is a very versatile little unit. It can be purchased for but a few dollars. Its dimensions are just 7 × 6 × 7 mm. I have found that by altering the values of source resistance, load resistance, and interfilter coupling capacitance, bandwidth can be set at a range of values between 1 and 7 kHz. Not to be overlooked is the additional application of the filter for crystal control of the beat frequency oscillator.

A front end tuner

As originally designed, this VLF-LF receiver used a broadband front end. A problem with this type of front end is that it is prone to cross modulation from very strong signals or noise outside the tuning bandwidth, but within the broadband range of the front end. When this occurs, it is necessary to reduce the RF input level sufficiently to prevent the problem. However, this also reduces the wanted signal level, possibly well into the noise floor of the receiver. To overcome the problem, I added a front-end tuner.

A further advantage of front-end tuning is that selectivity at VLF can be greatly enhanced. For example, if a Q factor of 200 can be achieved in the front-end tuned circuit, the bandwidth at 10 kHz is only 10,000/200 = 50 Hz. One of the biggest problems in receiving signals at VLF is the high level of noise, both manmade and atmospheric. The VLF signals, of necessity, are transmitted in narrow-band modes and restriction of bandwidth received is the most effective way to reduce the noise. Furthermore, the narrow bandwidth is also needed to separate some of the signals closely spaced in frequency. All in all, front-end tuning improves the performance of the receiver immensely.

The tuning system

According to Norm Burton of NSW, who has been experimenting with VLF reception for at least 25 years, it is very important to tune the aerial at VLF. There is certainly nothing wrong in doing just that. However, I have aimed at a tuned-circuit system which is not resonated with the aerial. The reasons for this are as follows:

- Various wire aerials at the home installation, at low frequencies, appear much like a large capacitor in the vicinity of, say, 400 pF against ground. If made part of the tuning system, this residual capacity would have made it difficult to cover the tuning range of 10 to 500 kHz in four bands, as has been done using an ordinary receiver tuning gang.
- An aim in designing the tuner was to make a high Q circuit using a high Q inductor, and it was thought that loss resistance in the Earth system might restrict the maximum Q.
- It was also an aim to make the tuning independent of aerial reactance constants, so any aerial could be used.

Generally speaking, I have found that, at low frequencies, the long untuned length of wire gives highest output voltage when loaded into a fairly high resistance. A value of 1000 ohms works quite well, and the original receiver was designed to load the aerial with 1000 ohms. My initial design approach for the tuner was to couple the aerial via a voltage follower stage which presented a high resistance load to the aerial, but drive the tuned circuit in a series mode from its low output resistance to maintain high Q in the tuned circuit. This was unsatisfactory, as the follower stage introduced cross modulation – the very thing which the circuit was supposed to reduce.

The follower stage was ultimately replaced by a low value resistor, which shunts the aerial, but maintains the high Q. This results in voltage loss from the aerial, but this loss is more than made up for by voltage magnification in the tuned circuit. (The voltage gain of a tuned circuit is, of course, equal to the value of Q.)

One characteristic of the high Q circuit is that, in the presence of atmospheric static or other transient natured noise, the circuit tends to ring or oscillate on being shocked by the transient impulse. For a given Q, the decay time of oscillation is inversely proportional to frequency. At very low frequencies, this oscillation is detected as an audio ring when using the BFO. Because of this effect, a Q control switch is provided which controls the value of resistance in series with the tuned circuit and hence its Q. The idea

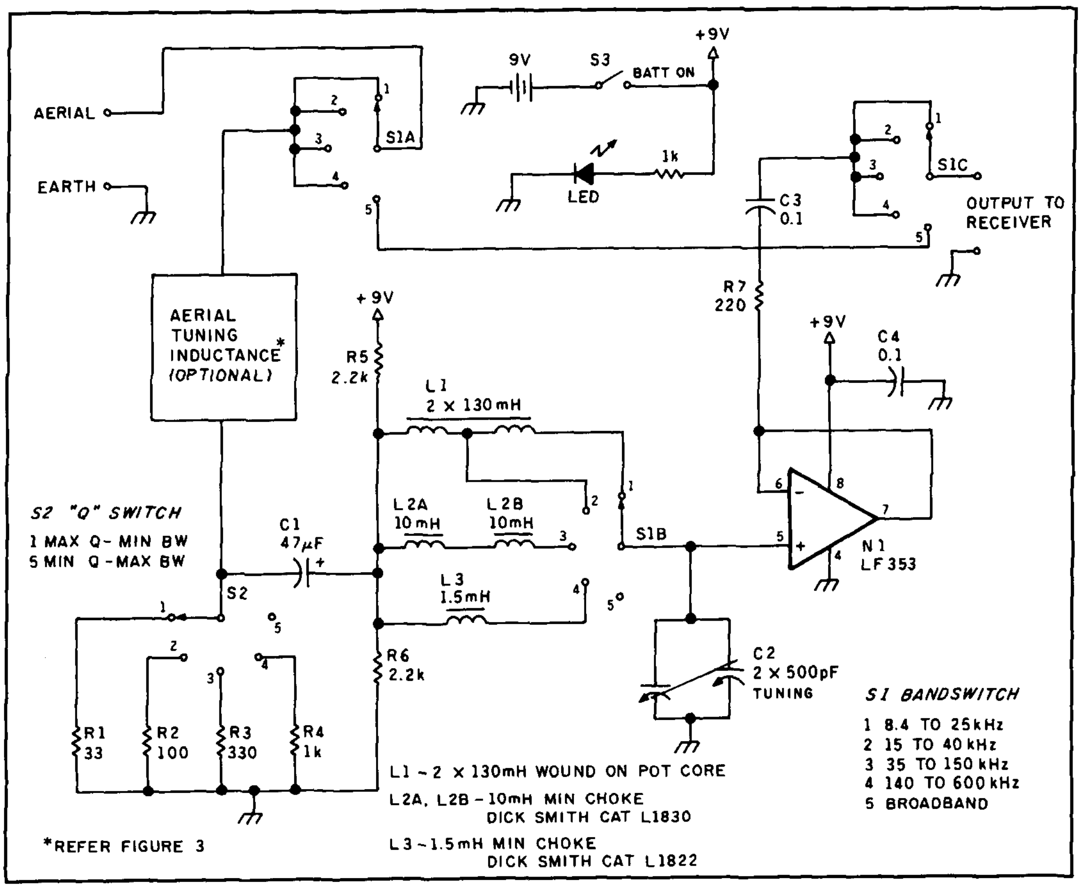

Figure 11. VLF-LF front-end tuner.

is to set the switch for the narrowest bandwidth possible, consistent with a tolerable amount of ringing in the presence of noise.

While the circuit design has been based on an untuned aerial, it does not inhibit additional tuning of the aerial circuit to further improve performance. The option of doing this is dealt with in the section headed "aerials."

The circuit

The circuit of the front end tuner is shown in **Figure 11**. The circuit provides a tunable frequency range of 8 to 600 kHz in four bands switched by SW1B. Other sections of the band switch, SW1A and SW1C, provide direct coupling of the aerial to the receiver for broadband operation when the switch is set to the fifth position.

The tuning system is formed by inductors L1, L2, or L3, which are resonated with variable capacitor C4. This is a two-section receiver tuning gang with a maximum capacity approaching 500 pF per section. Inductor L1 is a pot core assembly with two windings, each 130 mH. The windings are connected in series for band 1 to tune between 8 and 25 kHz. One single winding is used for band 2, which tunes between 15 and 40 kHz. Two 10-mH miniature chokes connected in series are used for band 3, which tunes between 35 and 150 kHz. A single 1.5-mH miniature choke is used for band 4, which tunes 140 to 600 kHz.

The ready-wound pot-core inductor was donated by Norm Burton. The 10 and 1.5-mH chokes are a miniature type supplied by Dick Smith Electronics.

Resistors R1 to R4, switched by SW2, terminate the aerial and determine the loss resistance added to the tuned circuit and the circuit Q.

The high input impedance of voltage follower stage N1 provides coupling to the receiver input with minimal loading of the tuned circuit. This is necessary to maintain the high value of Q in the tuned circuit. For the voltage follower, one half of a JFET operational amplifier package type LF353 is used. This has good high frequency performance and was also used in the VLF-LF receiver for RF and IF amplification. (The other half of N1 package is not used. It was originally intended as an interface for the aerial but, as explained earlier, its use proved to be unsatisfactory.) An emitter follower stage could be used as an alternative to the amplifier package. For this application, a Darlington-connected transistor pair might be advisable to achieve sufficiently high input resistance.

For anyone interested in duplicating the circuit, two components specified in the circuit might not be readily available at the local electronics store. The first is the tuning gang, an item not in good supply these days. The best bet is to recover one from a discarded broadcast receiver. Some gangs only have about 350-pF maximum capacity per section but a three-section gang in one of these would do the job.

The second item is the pot-cored inductor. This is an ideal type of inductor for the low frequency bands if one can obtain the pot-core parts assembly to wind one, or otherwise obtain one ready wound with a suitable inductance. I tried another idea and used eleven of the Dick Smith 10-mH chokes connected in series to make up 110 mH. This tuned band 2 from 15.7 to 67 kHz. To lower the frequency for band 1, an 820-pF fixed capacitor was switched across the tuning gang with a fourth switch bank of SW1. This gave a tuning range for band 1 of 11.3 to 15.9 kHz. The maximum circuit Q achievable with the 10-mH chokes was around 50 to 100 — not as good as the pot-cored inductor, but still quite good.

Changes to receiver

The front-end tuner was built as a stand alone unit which is simply inserted in the aerial feeder cable to the receiver. After I added it, the 530-kHz trap in the receiver was no longer required and disconnection of the trap provided some improvement to the low receiver sensitivity at frequencies approaching 500 kHz.

Another change is the addition of a selective audio filter. According to Norm Burton, a good audio filter is essential for receiving VLF signals. He suggests a filter bandwidth of 100 Hz or less. Encouraged by this, I added a simple resonant filter to the audio stages of the receiver as shown in **Figure 12**. The tuned circuit is formed by another of Norm's pot-core inductors (130 mH) which is resonated with a 0.12 μF capacitor. The circuit is driven in a series mode (much like the front-end tuner) from the low output resistance of amplifier N5B. As there is voltage gain (equal to Q) in the tuned circuit, the resistive output divider is used to prevent a steep rise in signal level when the filter is switched in.

The frequency of the filter is 1200 Hz, worked out as follows: In the narrow IF mode, the center frequency is 457.6 kHz. The BFO is needed to receive the narrowband modes. This runs at 456.4 kHz, 1200 Hz lower than the intermediate center frequency. Hence, maximum signal beat occurs

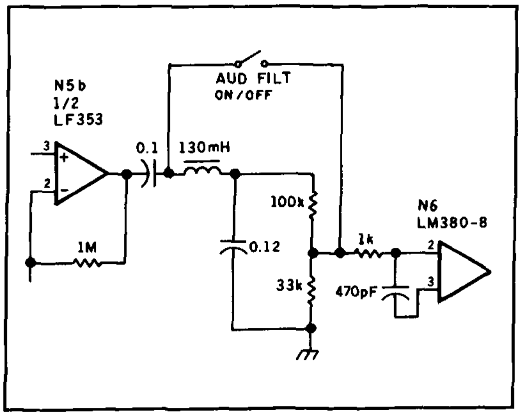

Figure 12. Addition of 1200-Hz audio filter to the receiver.

at a frequency of 1200 Hz, and this is the tuned frequency of the filter. The bandwidth of the filter is 100 Hz, and it is very effective in reducing much of the low frequency hash which gets through in spite of the narrow RF bandwidth.

Operation

Operation of the front-end tuner in conjunction with the receiver can be a little tricky, as the front end is not ganged to the receiver tuning. One method of tuning is to set the band switch to the broadband position and first locate the station with the receiver tuning dial. The band switch is then set to the appropriate band and the tuning gang is set for maximum signal level. Care must be taken not to tune in to the frequency of a strong signal which would simply enhance cross modulation by that signal. Tuning on the lowest frequency bands is very sharp, and on the unit constructed, a 2.5:1 reduction gear was fitted to the tuning knob to assist in adjustment. A calibrated scale marked in frequency for each band was also added to simplify setting of the front-end tuning near the frequency marked on the receiver tuning dial. With this aid, the front-end tuning is then simply trimmed for peak signal level with little chance of false tuning.

A problem at VLF-LF is noise from mains-operated equipment in the local vicinity, particularly in one's own house. I find it necessary to turn off fluorescent lamps, triac controlled light dimmer switches, and TV sets. The TV line time base at 15625 Hz, in the middle of the VLF band, is a particular nuisance. This type of noise tends to disappear after midnight, when everyone has switched things off and gone to bed.

Measured performance

Table 1 lists measurements taken of bandwidth and Q for various frequencies in each band of the tuner and with Q set maximum. It is interesting to observe the high Q factors obtained, particularly for bands 1 and 2 which use the pot core. This is something which could not be achieved in the early days, before ferrite cores, unless regeneration was applied.

Table 2 lists measurements taken of bandwidth and Q at 15 kHz on band 1 for different settings of the Q switch. This shows that a 6:1 range of bandwidth and Q can be selected.

Band	Frequency (kHz)	Bandwidth (Hz)	Q
1	10	48	208
1	15	60	250
1	20	84	238
1	25	132	189
2	16	85	188
2	25	121	207
2	35	234	150
3	40	610	66
3	70	802	87
3	120	1140	105
3	150	1360	110
4	150	1830	82
4	200	3480	57
4	300	2910	103
4	400	2300	174

Table 1. Bandwidth "Q" position 1.

Switch Pos	Bandwidth (Hz)	Q
1	60	250
2	83	181
3	145	103
4	226	66
5	360	42

Table 2. Bandwidth for different "Q" switch positions. At 15 kHz on band 1.

Aerials

At low frequencies the usual wire aerial is but a fraction of a wavelength long and, as a general rule, the more wire put up in the air, the greater the signal level captured. As one would expect, at the home location the longest of three wire aerials available gives the highest signal level. The signal level is also improved by about 6 dB when all three wires are paralleled together.

Earlier mention was made of tuning the aerial. This is an optional addition which can be made to the front-end circuitry. By resonating the inherent capacitance of the aerial with series inductance and loading the output into the terminal resistance set by the Q switch, a further gain in signal level of at least 10 dB is achieved. The three paralleled wires at the home location measure a capacitance of around 1000 pF and resonance with this, over most of the VLF band, was made possible by tapping along the bank of series connected 10-mH chokes used in a test previously discussed. Resonance was found to be fairly broad and the 10-mH increments proved to be small enough to allow peaking of the signal.

The front-end unit was ultimately fitted with a further switch, connected to ten of the 10-mH chokes and two other chokes, for tuning the aerial. The circuit diagram of this is shown in **Figure 13** and as an optional block in **Figure 11**. The 10-mH chokes provide aerial tuning adjustment in fine steps between 13 and 50 kHz. As there were only two spare positions on the 12-position rotary switch for the higher frequencies, I had to be satisfied with 1.15 mH to resonate around 150 kHz and 150 μH to resonate around 400 kHz. As stated before, tuning is quite broad, and even with this compromise, some gain is achieved over the whole of the higher frequency range by the addition of the inductors.

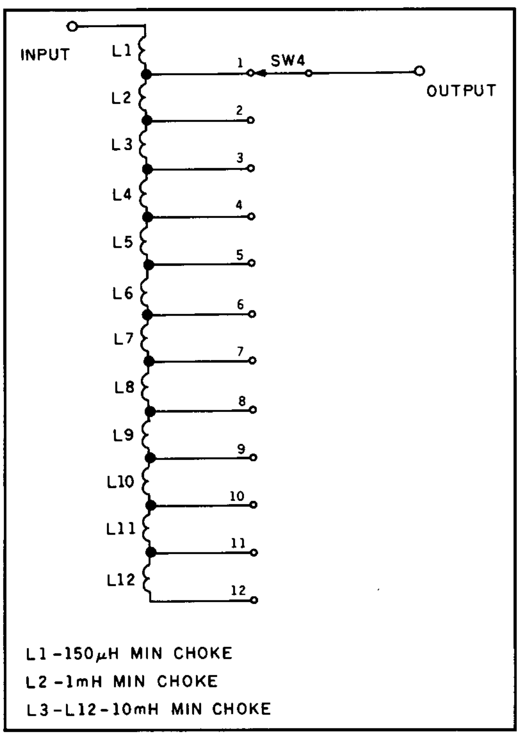

Figure 13. Aerial tuning circuit.

As is well known, the radiation resistance of an electrically very short aerial is but a fraction of an ohm. At resonance we see a low resistance, essentially that of the Earth, in series with the loss resistance of the inductor. This works out quite well to match into the low terminal resistance set by the Q switch. It must be pointed out, if not obvious, that the inductance values used in **Figure 13** are selected for a particular aerial capacitance and might have to be varied to suit another aerial.

At this stage, a brief mention of Norm Burton's aerial system might also be of interest. He uses a 33-foot 6-wire cage with 42 feet of 4-wire cage down lead. The cage at the top increases the capacitance to ground, raising its effective length and, therefore, its radiation resistance and aerial efficiency. He also uses a frame aerial, which gives lower signal level, but enables him to phase out some of the interference he gets from localized power lines. Norm tunes all his aerials and considers it essential for good reception at these low frequencies.

Some final remarks

It seems very clear that a highly selective front end is essential for good reception at VLF. A narrow bandwidth is needed to restrict the noise and this is more easily controlled in the IF stages of a superheterodyne, although some form of front-end tuning is clearly desirable to prevent cross modulation from strong local stations. What might seem less apparent is the fact that the noise level on this band is so high that the noise itself can cross-modulate the desired signal. It seems essential to restrict the noise bandwidth as much as possible before amplification takes place, and herein lies the need for the highly selective front end.

All this ties in with much of what Norm Burton has told me. He has two superheterodyne receivers and a Marconi CR200 TRF receiver which tune the VLF band. The CR200, which has two tuned RF stages before detection, outperforms the other receivers both in minimizing noise and separating one station from another, not to mention the odd spurious responses the superhets happen to generate. He has also pointed out how single-valve regenerative receivers were successfully used on these low frequency bands in the early years. By using regeneration, effective Q would have to be high with resultant narrow bandwidth and good selectivity. I am almost tempted to build one up to see how well it works.

Dick Hope, VK4DLJ, informs me that

there is quite a lot of interest in ELF-VLF-LF in the United States and that there is an organization called the Longwave Club of America. This club also distributes a magazine called, "Lowdown." Perhaps, in Australia, we should be pressing for an Amateur Radio section of the bands at these low frequencies. Judging by the lack of signals around 40 to 100 kHz, this spectrum does not appear to be greatly utilized.

To finalize the discussion, I have described a VLF-HF receiver, a bandwidth control, and a front-end tuner. The addition of the front end tuner improves the performance of the VLF-LF receiver immensely. In fact, it would be a useful addition to any receiver which happens to tune these bands. With separate sharp RF tuning, Q switch, and possibly aerial tuning, the receiver is a little complicated to adjust but, once mastered, the results are certainly worthwhile. One further control to be watched is the receiver RF gain. With all the extra gain in the front-end tuned circuits, it is very easy to lock up the receiver with too much signal level.

One might ask why the tuning could not be simplified by ganging the front-end tuned circuits with the receiver oscillator tuning. To make a highly selective tuned circuit at 10 to 30 kHz track accurately at 455 kHz difference, with the oscillator circuit at around 465 to 485 kHz, seems a highly difficult, if not impossible, task. It seems that with the superheterodyne, we must either trim the front end manually or tolerate the inferior performance of broader tuning. ■

CORRECTIONS

In NU1N's article "Digital Signal Processing: Working in the Frequency Domain," which appeared in the Fall 1990 issue, the following changes should be made to the equations on the Fourier Transform, Fast Hartley Transform, and the Hanning Function:

$$x(t) = \frac{1}{2\pi} \int_{-\infty}^{\infty} X(j\omega)e^{j\omega t}d\omega \qquad (1)$$

$$X(\omega) = \int_{-\infty}^{\infty} x(t)e^{-j\omega t}dt \qquad (2)$$

$$X(t) = \sum_{i=0}^{N-1} H(f)\, cas \left[\frac{\omega_i}{N}\right] \qquad (5)$$

$$H(f) = \frac{1}{N} \sum_{t=0}^{N-1} F(t) cas \left[\frac{2\pi ft}{N}\right] \qquad (6)$$

$$e^{-j\omega t} = \cos \omega t \pm j \sin \omega t$$

$$w\{i\} = 0.5\,(1-\cos\left(\frac{2\pi i}{N}\right))$$

In the article "Basic Concepts of Scattering Parameters," by WA1SPI, which appeared in the Fall 1990 issue, the "floating" 2 should be deleted from **Equation 2a** on Y-Parameters in **Figure 1**. In **Figure 2**, the equations for h_{11} and h_{12} should read as follows:

$$h_{11} = \frac{V1 - h_{12}V2}{I1} = \frac{1 - h_{12}\,(0)}{0.064} = 15.57$$

$$h_{12} = \frac{V1 - h_{11}I1}{V2} = \frac{0.946 - h_{11}\,(0)}{1} = 0.946$$

By John Pivnichny, *N2DCH*
3824 Pembrooke Lane
Vestal, New York 13850

A DIFFERENT APPROACH TO LADDER FILTERS

Another way to make crystal filters

The majority of ladder crystal filter articles appearing in Amateur Radio magazines have used identical frequency crystals in the series arms of a ladder network (see **Figure 1**). Hayward[1] and Hardcastle[2] have published excellent papers showing how to design these ladder filters. But what some Amateurs may not realize is that it's possible to construct crystal filters with crystals in the shunt arms.[3] I'll show simplified design equations that will let you select and build quality filters of this type. I've included a CW filter which uses inexpensive color-burst crystals as an example. This filter has excellent skirt selectivity for use in homebrew receivers with IFs in the 3.5 MHz range, like those designed by DeMaw.[4,5]

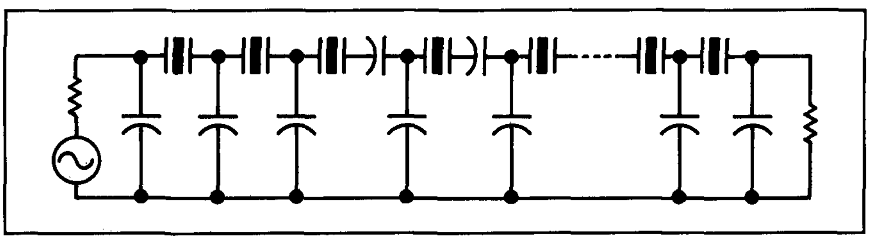

Figure 1. Conventional ladder filter design using crystals in series-arm configuration.

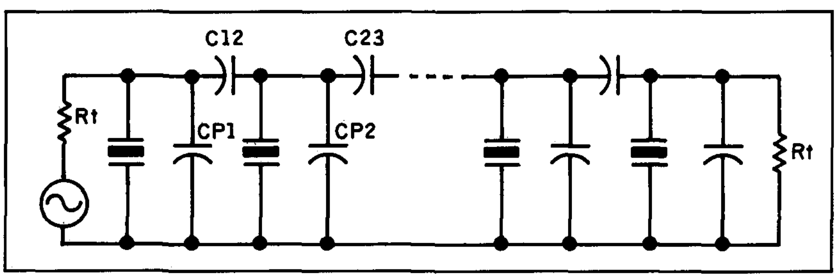

Figure 2. Using crystals in the shunt-arm configuration in a ladder filter.

A schematic of a shunt-arm filter is shown in **Figure 2**. Like the series-arm filter, only crystals and capacitors are used. As usual, it's necessary to terminate the filter at both ends with a specified resistance. The equivalent circuit for each crystal is shown in **Figure 3**. Element values are determined by measurements; these are described later. The values shown in **Figure 3** were determined by averaging readings on many color-burst crystals.

A shunt-arm ladder filter will have the passband and attenuation characteristics shown in **Figure 4**. There will be either a flat, rounded, or rippled passband depending on whether a maximally flat Butterworth, rounded Gaussian, or equi-ripple Chebyshev design is used when selecting the coupling capacitors C_{ij}. On the low frequency side, there's a cutoff which drops sharply from the 3-dB down point to a null, or nearly infinite attenuation at the series-resonant frequency of the crystals. On the high frequency side, the attenuation is more gradual and typically takes the shape shown. The steepness of both sides depends primarily on the number of crystals used in the filter. It also depends somewhat on the amount of ripple allowed in the passband and another design variable — 1/rov3.[3]

This somewhat mysterious variable is a measure of the "steepness" of the sharp cutoff side of the filter. As 1/rov3 increases, the steepness of the sharp side decreases, but the gradual cutoff side becomes steeper and deeper. Two curves are shown in **Figure 4** which illustrate this effect.

Dishal[3] states that "the parameter 1/rov3 sets directly the ratio of the bandwidth between the infinite attenuation frequency

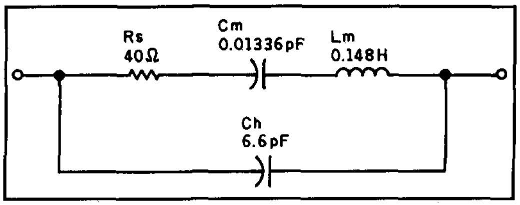

Figure 3. Electrical equivalent circuit of a standard 3.578-MHz color-burst crystal. Note that C_m and L_m are also referred to as C_x and L_x.

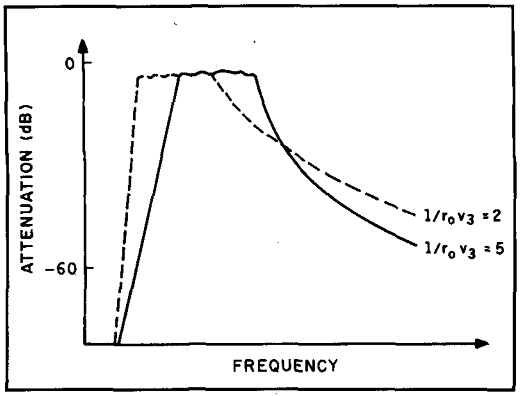

Figure 4. Plotted attenuation characteristics of a shunt-arm filter. Note that the sharp roll off on the low end of the frequency sweep suggests an ideal filter for upper sideband use (low-side BFO injection).

and the center of the passband, to the 3-dB down half-bandwidth." By selecting a value for 1/rov3, you can control how asymmetrical the filter you're designing will be. Values from 2 to 5 are a good starting point for Amateur use.

Design procedure

First pick an operating frequency f_0 for the filter. You can choose the series-resonant frequency of the crystals you intend to use as a starting point for f_0. Then select the 3-dB down bandwidth (BW3) that you desire. You also need to select a value for 1/rov3, and determine the number of crystals (poles) you'll be using.

Decide whether you wish to allow ripple in the passband. The greater the ripple, the steeper the cutoffs. Hayward[1] cautions against using Chebyshev (ripple) designs for CW filters. **Table 1** gives the design coefficients for maximally flat and 0.1-dB ripple filters using four, six, and eight crystals. These numbers are used in calculating the values for the coupling capacitors and terminator resistors of **Figure 2.** You can find tables like these for other filters (1-dB ripple filters, for example) in many references. The d's and k's are commonly called normalized decrements and normalized coefficients of coupling.

	Flat			0.1 dB	Ripple
Number Cystals	4	6	8	6	8
d	1.31	1.93	2.56	0.788	0.796
k12	0.841	1.17	1.52	0.716	0.727
k23	0.541	0.606	0.734	0.539	0.545
k34	0.841	0.518	0.551	0.518	0.516
k45		0.606	0.510	0.539	0.510
k56		1.17	0.551	0.716	0.516
k67			0.734		0.545
k78			1.52		0.727

Table 1. Normalized coefficients.

Note that the exact center frequency of the filter passband (f_m) will be higher than the series resonant frequency of the crystals as given by:

$$f_m = f_0 + (BW3/2)(1/rov3) \qquad (1)$$

The termination resistance is calculated from:

$$R = ((1/rov3)^2 - 1)BW3/2pi\, f_0\, C_x f_0\, d \qquad (2)$$

Coupling capacitors are then calculated from:

$$C_{ij} = C_x\, k_{ij} f_0/BW3\ ((1/rov3)^2 - 1) \qquad (3)$$

Finally, it's necessary to calculate values for the shunt capacitors across the crystals. These capacitors make the parallel-resonant frequency the same at every node, with all others short circuited. This means that the total capacitance C_t connected to each node — the shunt capacitor, plus the one or two coupling capacitors — must be given by:

$$C_t = C_x f_0/BW3\ ((1/rov3) - rov3) \qquad (4)$$

For example, the shunt capacitor at node 2, C_{p2}, is:

$$C_{p2} = C_t - C_{12} - C_{23} \qquad (5)$$

To arrive at the final value for each shunt capacitor, subtract the value of the crystal holder capacitance, C_h.

While **Equations 2** through **5** are somewhat complicated, the calculations are straightforward and give the correct results. I'll prove this by showing the design of a CW filter using low cost color-burst crystals available from Radio Shack.

Crystal measurements

Wes Hayward[1] showed how to measure the series resistance (R_s), center frequency (f_0), and 3-dB bandwidth (ΔF or BW3) of a

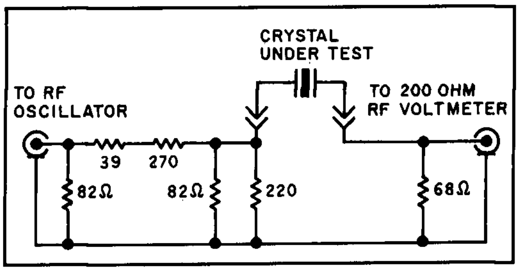

Figure 5. Test fixture used for determining crystal frequency (f_0) for selecting matched pairs. The test fixture is also used to determine the series-resistance (R_s) of each crystal.

crystal using a 50-ohm test fixture (see **Figure 5**). Tune the oscillator for a peak response and record the frequency as f_0. Substitute small value fixed resistors (4.7 to 82 ohm) until you get the same voltmeter reading. This resistor value will be the crystal series resistance, R_s. Replace the crystal and record the two frequencies at the point where the RF voltmeter reads 3-dB down from the peak. Subtract these two readings to get the 3-dB down bandwidth BW3. From f_0 and BW3, you can use Hayward's equations to calculate the motional capacitance and motional inductance.

$$C_x = 1.326 \times 10^{-15} (BW3/f_0^2)$$

$$L_x = 19.1/BW3$$

You can also locate the parallel-resonant frequency (f_p) with the crystal in the fixture by tuning the oscillator up in frequency until a null is reached on the RF voltmeter. This will be about 4 to 5 kHz higher than the series-resonant frequency (f_0) for a color-burst crystal in an HC-18 holder. The holder capacitance is given by:

$$C_h = C_x f_0^2/(f_p^2 - f_0^2)$$

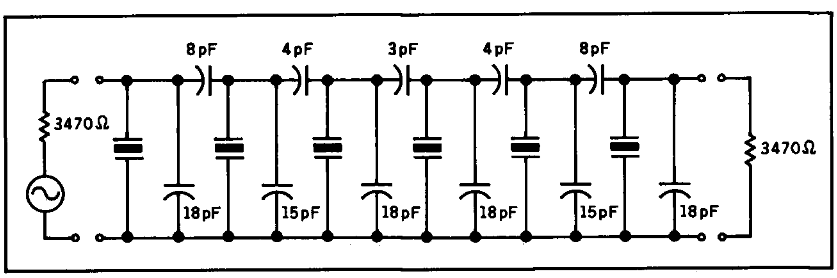

Figure 6. Schematic of the CW filter designed for a 3470-ohm termination. Capacitor values are in pF.

For example, one color-burst crystal measured f_0 = 3578619 Hz, f_p = 3582300 Hz. With a C_x = 0.01336 pF, the holder capacitance calculates out to C_h = 6.5 pF. This is the approximate value used in designing the CW filter.

Example

Let's design a 300-Hz bandwidth CW filter with a Butterworth response, six poles, and 1/rov3 = 5. Color-burst crystals are used and their characteristics are given in **Figure 3** as C_x = 0.01336 pF, C_h = 6.6 pF, R_s = 40 ohms, and L_x 0.1480497H. The series-resonant frequency is 3578.6 kHz. Using **Equation 1**, the center of the passband will actually be:

$$f_m = 3578600 + (300/2)(5) = 3579350 \text{ Hz}$$

The termination resistance is:

$$R = (24)300/2 pi \times 3.579 \times 10^6 \times 0.01336 \times 10^{-12} \times 3.579 \times 10^6 \times 1.93$$

$$R = 7200/2.075 = 3470 \text{ ohms}$$

The coupling capacitors are:

$$C_{ij} = (0.01336 \text{ pF})\, k_{ij} \times 3.579/0.3 \times (24)$$

$$C_{ij} = k_{ij} \times (6.64) \text{ pF}$$

$$C12 = 7.77 \text{ pF}$$
$$C23 = 4.02$$
$$C34 = 3.44$$
$$C45 = 4.02$$
$$C56 = 7.77$$

The total capacitance at each node must be:

$$C_t = 0.01336 \times 3579/0.3 (5/24) = 33.2 \text{ pF}$$

Therefore:

$$C_{p1} = C_t - C_{12} = 25.44 \text{ pF}$$
$$C_{p2} = C_t - C_{12} - C_{23} = 21.41$$
$$C_{p3} = C_t - C_{23} - C_{34} = 25.75$$
$$C_{p4} = C_{p3} \text{ by symmetry} = 25.75$$
$$C_{p5} = C_{p2} \text{ by symmetry} = 21.41$$
$$C_{p6} = C_{p1} \text{ by symmetry} = 25.44$$

Subtract the holder capacitance, C_h = 6.6 pF, from these values to determine the shunt capacitors required.

Use the nearest standard value capacitor for the accuracy you need. This will result in the final design shown in **Figure 6**.

Calculated response

Up until now, I've ignored the series resistance of the crystal R_s. This resistance will add some insertion loss to the design and reduce the ultimate attenuation slightly. For this design, with its high 3470-ohm termination resistance, the effect of 40 ohms in each crystal is small.

Amateurs with circuit simulator programs and personal computers may want to verify the calculations by entering the element values into their programs. These calculations will give your computer a good workout. They require several minutes of calculation time at each frequency point.

Figure 7 shows the calculated response. If you want the response to come out exactly on frequency, use the precise value of L_m = 0.1480497H in your calculations.

Construction

The filter is built on a 3/4 × 2-inch piece of single-sided circuit board with the copper side up. **Figure 8** shows a hole pattern for drilling the board. Component leads not connected directly to ground pass through a countersunk hole and are joined to the other component leads on the reverse side. It's easiest to solder in the capacitors first, then the crystals.

All six crystals must be matched in frequency to within 200 Hz, and preferably within 100 Hz. That is, the difference between the highest and lowest frequency crystal should be no greater than 200 Hz. You can verify this with a test oscillator and frequency counter. The crystals, as supplied by Radio Shack, are specified as ± 300 Hz, but I have found most of them fall within a ± 100 Hz range.

If the crystals aren't matched, the one or two highest ones will cause a narrowing of the passband and a step in the low frequency cutoff, as shown in **Figure 9**. If you find your filter has this step, replace the highest frequency crystal with a lower one. Overall, it's easier to ensure success by starting with matched units.

The capacitors, however, don't need to be matched. Ordinary ceramic capacitors are quite satisfactory because they aren't critical for setting the exact frequencies. The crystals do that. I used NTE 50-volt ceramic disc capacitors which I found at a local electronics store.

The measured response points are found in **Figure 7**. There's very good agreement with the calculated response.

Discussion

What differences will you find when using shunt-crystal ladder filters as opposed to series-arm crystals? The main difference is that the steep cutoff is on the low frequency side with shunt crystals, while the opposite is true for series crystals. These two approaches produce what are called, respectively, upper-sideband filters and lower-sideband filters. You might prefer one or the other, depending on which sideband you want to remove. This is especially true for SSB generation in a transmitter.

For a particular crystal characteristic, you'll find that the coupling capacitor values get larger and the termination resistance gets smaller as you reduce the desired bandwidth. This tends to increase the effect of crystal series loss (R_S) in CW filters, resulting in more insertion loss. Overall, the upper-sideband filter has a higher termination resistance, making it a better choice for

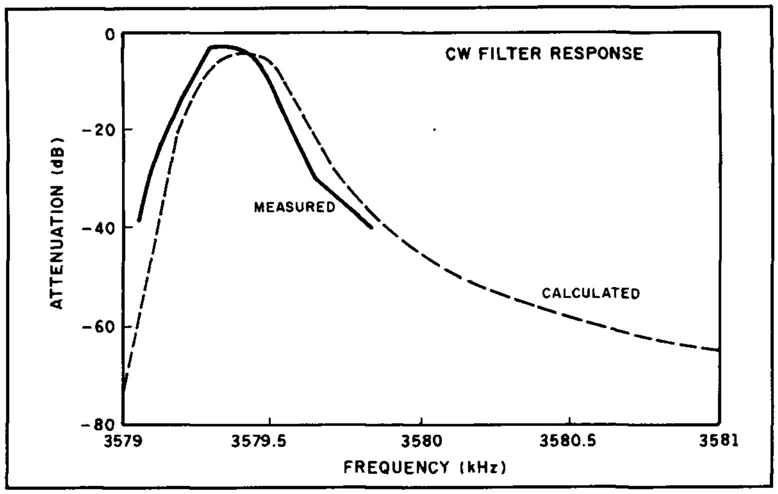

Figure 7. The calculated and measured response curves for the CW filter show little deviation from the desired results.

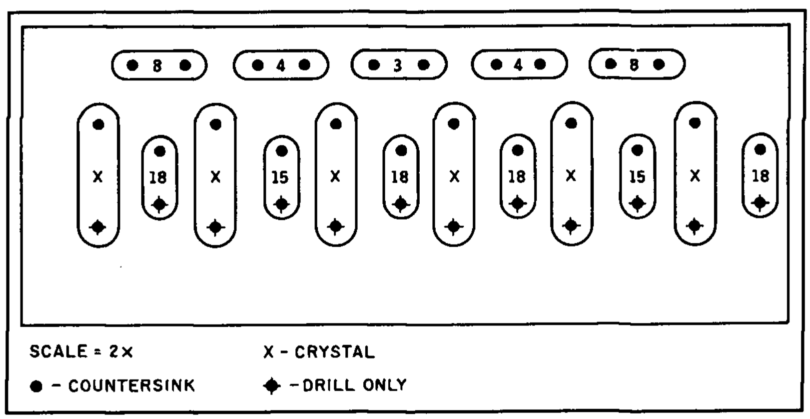

Figure 8. Hole patterns for pc board layout.

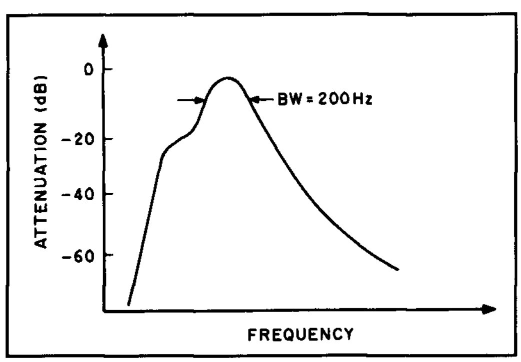

Figure 9. Filter response resulting from using unmatched crystals.

CW filters. This is more important with low-Q crystals like those in HC-18 holders.

When going to wider bandwidths for SSB, *it's possible for the upper-sideband designs to* wind up with very large resistances and impractically small coupling capacitors. A lower-sideband design with series crystals is often a better choice for SSB.

This design procedure takes into account the holder capacitance. Consequently, you can use all types of crystals. It may even be possible to use the well-known FT-243, with its high holder capacitance. In any case, the maximum possible bandwidth of a filter needs to be less than the difference between the series and parallel-resonant frequencies of the crystals. Otherwise, the required parallel capacitance will be lower than the holder capacitance. Hardcastle's data[2] indicates that the FT-243 crystals are limited to use only in CW filters because the frequency difference is only 1.6 kHz. Plated crystals, like the HC-6/U, have about 15 kHz difference at 9 MHz and are ideal for SSB filters.

Other ideas

A clever designer can use these upper-sideband design equations along with previously published lower-sideband (series-arm crystals) designs to create a pair of filters which use the same BFO frequency. Others may want to use these equations to design filters from the widely available microprocessor crystals. Using inexpensive components, the homebrew builder can afford to put several filters of a variety of bandwidths in his equipment. Or, he may want to try switching the bandwidth using ideas from **Reference 6**. Perhaps someone will find a way to adjust the bandwidth smoothly by adjusting the capacitor values simultaneously. This could be done with ganged-variable capacitors, or by using voltage-variable capacitors and adjusted voltage sources.

Conclusion

This set of design equations for shunt-arm ladder filters opens up another set of possibilities for Amateurs to explore. I hope to see more filter articles based on their use. ■

REFERENCES

1. Wes Hayward, W7ZOI, "A Unified Approach to the Design of Crystal Ladder Filters," *QST*, May 1982, page 21 and July 1987, page 41.
2. J. A. Hardcastle, G3JIR, "Some Experiments with High-Frequency Ladder Crystal Filters," *QST*, December 1978, page 22.
3. M. Dishal, "Modern Network Theory Design of Single-Sideband Crystal Ladder Filters," Proc. IEEE, September 1965, page 1205.
4. Doug DeMaw, W1FB, "The Mini-Miser's Dream Receiver," *QST*, September 1976, page 20 and November 1976, page 22.
5. Doug DeMaw, W1FB, "Build a Bare-Bones CW Superhet," *QST*, June 1982, page 29.
6. John Pivnichny, N2DCH, "Switchable Bandwidth Crystal Filter," *Ham Radio*, February 1990, page 22.

By Bryan Bergeron, *NU1N*
30 Gardner Road, #1G
Brookline, Massachusetts 02146

DIGITAL SIGNAL PROCESSING

Artificial intelligence techniques

Artificial intelligence, or AI, is a branch of computer science devoted to investigating such varied concepts as robotics, vision, speech recognition, and machine intelligence.[1] Much of this investigation deals with how to best represent data and knowledge, how to search vast amounts of data rapidly and efficiently, how to work with incomplete data, and how to provide for rapid pattern matching. I'd like to examine artificial intelligence techniques that have been applied to DSP in both the time and frequency domains.[2,3] I'll also discuss expert systems[4] and neural networks in order to highlight the general characteristics of DSP systems which rely on AI techniques.

Expert systems

Expert systems, computer programs that possess the same problem-solving abilities as human experts, rely on efficient pattern matching and search algorithms, as well as effective knowledge representation schemes, for their operation.[5] As **Figure 1** shows, an Expert System can be considered a program composed of two major, interdependent modules. The first is an *inference engine,* for interpreting rules specific to a problem area; the second is a *knowledge base*, which usually takes the form of "IF...THEN" rules. These rules are constructed by interviewing human experts and determining what heuristics ("rules of thumb") they use in solving specific problems. In most practical expert systems, there are usually additional modules concerned with input and output from the inference engine. Depending on the nature of the system, these modules may be connected to other programs (in an automated system) or to a work-station console (if human interaction is warranted by the design).

The programming of an expert system differs from the programming of a conventional application in that you must specify *what* is to be done (what problem is to be solved), but not *how* a solution is to be found.[6] In conventional programming, you specify a detailed procedure or algorithm which tells the program how to solve a problem. Given the nature of their design, expert systems are commonly constructed with nonprocedural languages like LISP (from LISt Processing), PROLOG (from PROgramming LOGic), and SmallTalk (a precursor to the Apple Macintosh Interface), as opposed to procedural languages like BASIC, C, PASCAL, or FORTRAN. AI techniques are generally easier to implement in nonprocedural languages. For example, pattern matching is built into the PROLOG language.[7]

Search strategies

Inference engines rely on a variety of AI inferencing techniques. These techniques include *forward chaining* (drawing conclusions from the available data), *backward*

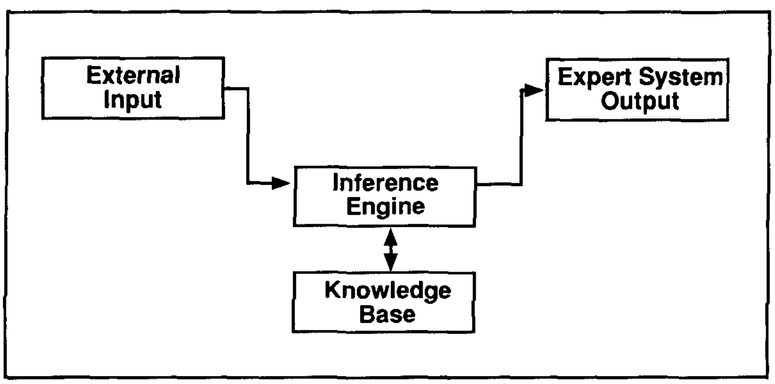

Figure 1. The basic building blocks of an expert system.

chaining (reasoning from observations to conclusions), and *induction* (creating general rules from specific examples). Regardless of the inferencing technique used, there's a need for rapid searching and pattern matching.

The three simplest search strategies are: *depth-first*, *breadth-first*, and *best-first*.[8] Depth and breadth-first searches are known as blind searches because their operation is independent of the problem at hand. In contrast, best-first searches use specific knowledge of the problem to conduct the search in the most efficient manner possible. Depending on the nature of the problem, the breadth-first or depth-first method may be more efficient. Efficiency issues aside, there may be other reasons for choosing one search method over the other. For instance, breadth-first searches require more memory for operation than do depth-first searches.

The best-search approach makes use of knowledge about a particular problem area. It uses rules to determine which node to select and when to follow a depth or breadth-first search. With proper rules, the best-first search will examine a knowledge base and find a match more efficiently than either breadth or depth-first search.[8]

Knowledge bases

Knowledge bases, which must effectively represent the domain-specific knowledge, commonly rely on *rules* (IF...THEN pairs of English-like statements) and/or *frames* (formats with a place for frequency, power, and type of modulation, and so on) for their operation. The format ultimately used for representing the knowledge in a knowledge base depends on the nature of the problem. Some problems are easily specified in terms of rules, while others are not. For example, the rule:

IF *there was a voltage transient*
THEN *check the power supply fuse*

may be the most intuitive way to represent a rule dealing with the troubleshooting of a piece of electronic equipment. Representing the above relationship as a frame wouldn't be as intuitive. For a good introduction to the use of frames in knowledge base design, see the text by Goldberg.[9]

A great deal of work in knowledge base development is concerned with verifying that a set of rules (or frames) comprehensively and precisely describes the knowledge of a particular problem.[10] Complex expert systems can have so many possible states that exhaustive testing may be either impossible or unfeasible — especially when one is operating with incomplete data.[11]

Neural networks

Neural networks are hardware/software systems that are loosely modeled on the structure of the brain. Like expert systems, neural networks rely on search strategies, pattern matching, and knowledge representation for their operation. And, like expert systems, neural networks do not rely on conventional algorithmic programming techniques. The great power of neural networks stems from the fact that, unlike the knowledge-based expert system just described, they generate their own internal rules which are refined with experience or training.[12] Neural networks are also highly resistant to noise, able to generalize, plastic, robust, simple, and can work a large number of different types of problems.[13] Even the simplest neural networks are error correcting in that noisy patterns tend to recall complete patterns.[14]

Neural networks are varied in their design, operation, abilities, and target application.[12] There are currently about 50 different types, some which have been in commercial use for over 20 years, designed for such varied applications as pattern recognition for radar and sonar images, speech recognition, speech synthesis, extraction of knowledge from data bases, robotic control, image compression, character recognition, and adaptive nulling of radar jammers.

Most inexpensive neural networks are available as software emulations which run on personal computers. (For listings of simple neural network emulators, see the articles by Reece[15] and Brown[16].) More powerful and expensive board-level emulators use special coprocessor chips. There are currently no commercial stand-alone "neural computers," mainly because neural networks don't handle input/output processing and traditional computers are better suited for this function.[12]

Knowledge representation

Knowledge representation in a neural network is highly structure dependent. For example, consider the neural network shown in **Figure 2**. This simple linear network consists of three input (I) and two output (O) nodes, with each input node connected to all of the output nodes. The numerical values associated with each connection (connection strengths) change with the number of test cases presented to the input nodes![17] The collection of connection strength values form the knowledge base of the neural network.

A linear neural network

In the neural network shown in **Figure 2**, *training* would be accomplished by repeatedly presenting the input and output nodes with a pattern (for example, 1,0,1 for I_1, I_2, and I_3, respectively and 0,1 for O_1, and O_2, respectively). With each presentation, the network automatically adjusts its connection strengths until the proper input-output transformation is learned. That is (following the above example) until presenting the input nodes I_1, I_2, and I_3 with 1,0,1 results in 0,1 at the output nodes O_1 and O_2.

The nature of the input-output transformation determines the types of problems a given network can solve. For example, the simple network in **Figure 2** (called a *linear* network because the transformations between input and output nodes are a *linear* function) can't learn to differentiate between some input transformations. The simple linear network can't differentiate between 1,1,0 and 0,0,0 because the connection strengths associated with the second pattern are always 0. Note that the linear nature of the input-output transformations supported by the network in **Figure 2** can't be determined by simply examining the schematic of the network. You need to examine the nature of the input-output transform function.

Because the only way to truly appreciate how a neural network functions is to work with one, I've included listings of two example systems. **Listing 1** implements a simple linear network, similar to the one described above, in BASIC for the IBM-PC. Lines 30 to 80 initialize the program variables and define the size of the network. In this implementation, there are eight input nodes (NIN) and five output nodes (NOUT). The connection strengths (CONM) are initialized to random values between 0 and 1 (lines 70 to 80) in preparation for the learning sessions.

Lines 110 to 260 are concerned with setting up the main user interface. Menu selections include exiting the program, entering teaching cases, teaching the network, and testing the network (asking the network to classify a case or pattern). Lines 300 to 410 collect user input in both training and testing modes of the network. Lines 500 to 590 are used for identifying a pattern in both training and testing modes.

Lines 610 to 700 are called repeatedly to teach an input-output pattern to the network. In lines 640 to 660, the target values

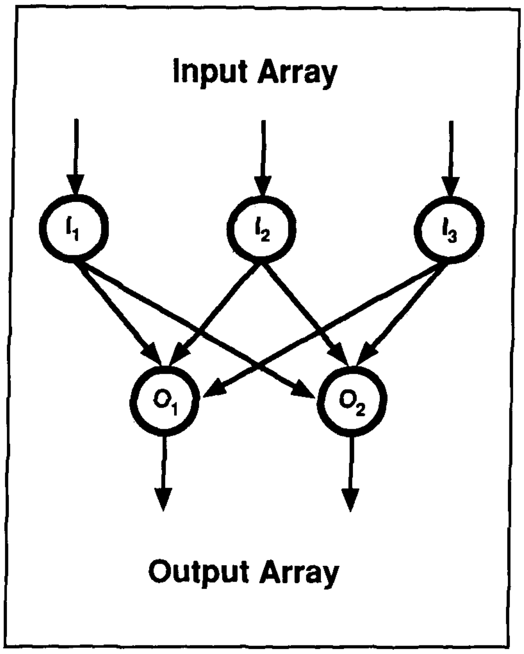

Figure 2. The structure of a simple five-node linear neural network.

(TARGA) for the output nodes (OUTPT) are defined as either 0 or 1. Notice that this represents a computationally intensive routine because, for each call to this subroutine, there are multiple calls to other subroutines. Through calls to other subroutines, lines 730 to 820 first request input node values from the user, then calculate output node values based on the current input-output transformation values stored in the connection matrix (CONM). The pattern consistent with the input node values is then printed.

Lines 900 through 1010 function to associate a particular collection of input values, like 00011001, with a given pattern, say, PATTERN A. Lines 1100 to 1140 calculate the output node values (OUTPT), based on the input node values (INPT) and the connection strength values stored in the connection matrix (CONM). Lines 1200 through 1240 update the connection matrix values based on the input node (INPT), output node (OUTPT), and target activation (TARGA) values. The larger the difference between the current output value (OUTPT) and the target value for a given node (TARGA), the larger the change in the connection matrix value with each training session. When the target and actual values are equal (for instance, when both are 0 or 1) there's no change in the connection matrix values. That is, there's no new learning.

Note that the learning rate (LRATE) influences both the speed of learning and the stability of the system. While a higher

```
10  REM ***** LINEAR NEURAL NET *****
12  REM         BRYAN BERGERON, NU1N
14  REM TCASE = TEST CASE ARRAY
16  REM LRATE = LEARNING RATE
18  REM INPT = INPUT ARRAY
20  REM OUTPT = OUTPUT ARRAY
22  REM CONM = CONNECTION MATRIX
24  REM TARGA = TARGET ACTOVATION ARRAY
26  REM
30  REM ***** LINEAR INITIALIZE *****
40  NIN=8: NOUT=5: NCASE=20: LRATE =.5
50  DIM INPT(NIN),OUTPT(NOUT),CONM(NOUT,NIN)
60  DIM TCASE(NCASE, 1 + NIN),TARGA(NOUT)
70  FOR J = 1 TO NOUT: FOR I= 1 TO NIN
80  CONM(J,I)=RND: NEXT I: NEXT J
90  REM
110 REM *** MAIN MENU ***
120 CLS: PRINT
130 PRINT "0. EXIT"
150 PRINT "1. ENTER CASES"
160 PRINT "2. TEACH THE NETWORK"
170 PRINT "3. ASK THE NETWORK"
180 PRINT: INPUT "YOUR CHOICE (0 - 3)";C
185 IF (C<0) OR (C>3) THEN GOTO 120
190 ON C+1 GOTO 200,220,240,260
200 CLS: END
220 GOSUB 900: GOTO 120
240 PRINT: INPUT "ROUNDS OF TEACHING (E.G., 10)"; C
250 FOR I= 1 TO C: GOSUB 610: NEXT I: GOTO 120
260 GOSUB 720: GOTO 120
270 REM
300 REM *****  INPUT PATTERNS ******
310 CLS: PRINT
320 PRINT "INPUT PATTERNS (0 OR 1)."
330 INPUT " INPUT 1"; INPT(1)
340 INPUT " INPUT 2"; INPT(2)
350 INPUT " INPUT 3"; INPT(3)
360 INPUT " INPUT 4"; INPT(3)
370 INPUT " INPUT 5"; INPT(3)
380 INPUT " INPUT 6"; INPT(3)
390 INPUT " INPUT 7"; INPT(3)
400 INPUT " INPUT 8"; INPT(3)
410 RETURN
420 REM
500 REM *****  LIST OF PATTERNS ****
510 IF PAT= 1 THEN PRINT "PATTERN A";
520 IF PAT= 2 THEN PRINT "PATTERN B";
530 IF PAT= 3 THEN PRINT "PATTERN C";
540 IF PAT= 4 THEN PRINT "PATTERN D";
550 IF PAT= 5 THEN PRINT "PATTERN E";
560 IF PAT= 6 THEN PRINT "PATTERN F";
570 IF PAT= 7 THEN PRINT "PATTERN G";
580 IF PAT= 8 THEN PRINT "PATTERN H";
590 RETURN
600 REM
610 REM **** TEACH CASES TO THE MATRIX ****
```

Listing 1. A BASIC listing which implements a linear neural network similar to the one described in *Figure 3*.

```
620  K=1
630  IF TCASE(K,1)=0 THEN 700
640  FOR J= 1 TO NOUT
650  IF J=TCASE(K,1)THEN TARGA(J)=1 ELSE TARGA(J)=0
660  NEXT J
670  FOR I = 1 TO NIN: INPT(I) = TCASE(K,I + 1): NEXT I
680  GOSUB 1200
690  K=K+1: IF K<=NCASE THEN GOTO 630
700  RETURN
710  REM
720  REM **** NAME THE PATTERN ***
730  GOSUB 310: GOSUB 1100: PAT = 1: MAX=OUTPT(1)
740  FOR J = 2 TO NOUT
750  IF OUTPT(J)<= MAX THEN GOTO 770
760  PAT=J: MAX = OUTPT(J)
770  NEXT J
780  PRINT: PRINT "THE PATTERN IS CONSISTENT WITH ";
790  GOSUB 500: PRINT".": PRINT
800  INPUT "ANOTHER CASE (O TO EXIT TO MAIN MENU)"; C
810  IF C<> 0 THEN GOTO 730
820  RETURN
830  REM
900  REM ***** ENTER TRAINING PATTERNS ******
910  K=1
920  PRINT: PRINT " 0 - NO MORE PATTERNS"
930  FOR J= 1 TO NOUT
940  PRINT J;" - ";: PAT=J: GOSUB 500: PRINT
950  NEXT J
960  PRINT: INPUT "WHICH PATTERN"; TCASE(K, 1)
970  IF TCASE(K,1)=0 THEN 920
980  GOSUB 310
990  FOR I=1 TO NIN:  TCASE(K,I + 1) = INPT(I): NEXT I
1000 K=K+1: IF K<= NCASE THEN GOTO 920
1010 RETURN
1020 REM
1100 REM **** LINEAR SIGNAL OUTPUT ***
1110 FOR J = 1 TO NOUT: OUTPT(J)=0: FOR I= 1 TO NIN
1120 OUTPT(J) = OUTPT(J) + CONM(J,I)*INPT(I)
1130 NEXT I: NEXT J
1140 RETURN
1150 REM
1200 REM ***** LINEAR MATRIX UPDATE   *****
1210 GOSUB 1100: FOR J= 1 TO NOUT: FOR I=1 TO NIN
1220 CONM(J,I)=CONM(J,I) + LRATE * (TARGA(J) - OUTPT(J)) * INPT(I)
1230 NEXT I: NEXT J
1240 RETURN
```

Listing 1, continued

learning rate increases the amount of learning which takes place, it may diminish the overall efficiency of the learning trials as a result of the introduction of a source instability into the system. That is, the output node values may swing wildly from teaching session to teaching session. The default value of 0.5 for LRATE is usually a good compromise for most problems.

Note also that the matrix update function:

CONM = CONM + LRATE * (TARGA − OUTPUT) * INPT

is a *linear* function. That is, the update value computed for the connection matrix is a product of a constant (LRATE), the input node value (INPT), and the difference between the target (TARGA) and current output (OUTPT) values.

A nonlinear neural network

More complex neural networks, like the nonlinear network shown in **Figure 3**, have more powerful learning and pattern matching abilities than single layer linear networks. In multi-level networks such as this, each input node (I) is connected to a layer of hidden nodes (H). Each node in the hidden layer is connected, in turn, to each of the output (O) nodes. Like the network in **Figure 2**, the nonlinear network is trained by forcing the input (I) and output (O) nodes to 0 or 1. The hidden (H) nodes are free to attain any value.

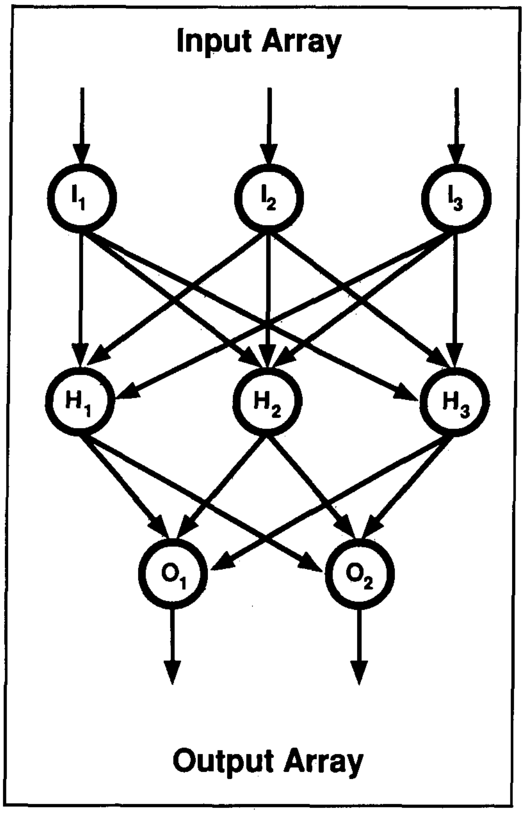

Figure 3. A five-node, nonlinear, multi-layered neural network.

Listing 2 shows source code modules required to convert the two-layer, linear network in **Listing 1** to a three-layered, nonlinear network. Substitute the nonlinear versions of the initialization, signal output, and matrix update subroutines for the subroutines of the same name in **Listing 1**. The other code segments – for example, the main menu, input patterns, teaching cases, name the pattern, and list of patterns – remain unchanged.

The nonlinear initialization routine in lines 30 through 80 defines a network with eight input and hidden nodes, and five output nodes. Two connection matrix arrays are also defined – one for the input-hidden node connections (CONIN) and one for the hidden-output node connections (CONOUT). As in the linear model, these connections are assigned random values before the learning runs (lines 60 to 75).

Lines 1100 to 1135 compute the output node values based on the input (INPT) and hidden node (HIDA) values, as well as the connection strengths between the node layers (CONIN and CONOUT). The nonlinear matrix update routine in lines 1200 through 1224 handles the updating of connection strength values maintained in CONIN and CONOUT. Note that, unlike the update function in the simple linear network, the update function in this network is *nonlinear* (hence the name). That is, the connection strength values between the hidden nodes and the output node are calculated as:

CONOUT = CONOUT + LRATE * DOUT * HIDA

where DOUT is represented by the nonlinear relationship:

(TARGA – OUTPT) * EXP(OUTNET)/((1 + EXP(OUTNET))^2)

The nonlinear nature of the connections, while considerably more computationally demanding than simple linear connections, is largely responsible for the increased power and capabilities of this network design. Unlike the linear network, this network can, with sufficient training, easily distinguish between all possible combinations of input patterns.

Operation

From a user perspective, the operation of both of these neural networks is identical. You first start a session by entering cases (1–ENTER CASE) from the main menu. For instance, you might enter Pattern A = 01010101, Pattern B = 11011011, and so on. You then teach the network (2–TEACH THE NETWORK) and determine how well the network has learned to recognize a test pattern (3–ASK THE NETWORK).

While the simple linear network may require only a few teaching cycles to learn a given pattern, the nonlinear network may require a thousand or more. Consequently, training can be time consuming, and several

```
10     REM ***** NON-LINEAR NEURAL NET *****
12     REM         BRYAN BERGERON, NU1N
14     REM TCASE = TEST CASE ARRAY
16     REM LRATE = LEARNING RATE
18     REM INPT = INPUT ARRAY
20     REM OUTPT = OUTPUT ARRAY
22     REM HIDA = HIDDEN ARRAY
24     REM CONIN = CONNECTION MATRIX INPUT
26     REM CONOUT = CONNECTION MATRIX OUTPUT
28     REM TARGA = TARGET ACTIVATION ARRAY



30     REM ***** NON-LINEAR INITIALIZE *****
40     NIN=8: NHID =8: NOUT=5: NCASE=20: LRATE =.5
45     DIM INPT(NIN),OUTPT(NOUT),HIDA(NHID),TCASE(NCASE, 1 + NIN)
50     DIM TARGA(NOUT), CONIN(NHID,NIN), CONOUT(NOUT,NHID)
55     DIM DOUT(NOUT), HIDNET(NHID),OUTNET(NOUT)
60     FOR I= 1 TO NHID: FOR J=1 TO NIN: CONIN(I,J)=RND
65     NEXT I: NEXT J
70     FOR I = 1 TO NOUT: FOR J= 1 TO NHID: CONOUT(I,J)=RND
75     NEXT I: NEXT J
80     REM



1100   REM **** NON-LINEAR SIGNAL OUTPUT ****
1105   FOR I= 1 TO NHID: HIDNET(I)=0: FOR J=1 TO NIN
1110   HIDNET(I) = HIDNET(I) + CONIN(I,J)*INPT(J): NEXT J
1115   HIDA(I) = 1/(1 + EXP( -HIDNET(I))): NEXT I
1120   FOR I = 1 TO NOUT: OUTNET(I)=0: FOR J= 1 TO NHID
1125   OUTNET(I) = OUTNET(I) + CONOUT(I,J)*HIDA(J): NEXT J
1130   OUTPT(I) = 1/(1 + EXP(-OUTNET(I))): NEXT I
1135   RETURN



1200   REM ***** NON-LINEAR MATRIX UPDATE *****
1202   GOSUB 1100: FOR I= 1 TO NOUT: E=EXP(OUTNET(I))
1204   DOUT(I) = (TARGA(I) - OUTPT(I))*E/((1 + E) ^2)
1206   FOR J= 1 TO NHID
1208   CONOUT(I,J) =CONOUT(I,J) + LRATE*DOUT(I)*HIDA(J)
1210   NEXT J: NEXT I
1212   FOR H = 1 TO NHID: TEMP=0: FOR J = 1 TO NOUT
1214   TEMP = TEMP + DOUT(J)*CONOUT(J,H): NEXT J
1216   E=EXP(HIDNET(H)): DHID = (E/((1 + E) ^2))*TEMP
1218   FOR I=1 TO NIN
1220   CONIN(H,I) = CONIN(H,I) + LRATE*DHID*INPT(I)
1222   NEXT I: NEXT H
1224   RETURN
```

Listing 2. Modifications to *Listing 1* required to implement a nonlinear neural network similar to the one described in *Figure 4*.

thousand cycles may be needed for the nonlinear neural network to accurately distinguish the differences between a few patterns. On my PC clone, a Toshiba T1000 running at 4.7 MHz, the linear network takes about 2 seconds to process each teaching presentation. About 20 seconds are required for a round of ten teaching presentations. In comparison, the nonlinear network requires about 5 seconds per presentation, or about an hour for 1000 teaching cycles.

You can minimize the learning time by compiling the source code listing (**Listings 1** and **2** are compatible with Borland's Turbo Basic Compiler); changing the initialize routine to specify fewer input, hidden, and output nodes (for example, three input and two output nodes for the linear network, and three input, three hidden, and two output nodes for the nonlinear network); or converting the BASIC code to a more computationally efficient language, like C or ASSEMBLER. Faster learning times and increased levels of operation are also available through the use of special add-on cards that implement the functioning of *thousands* of nodes in high-speed hardware.

The application areas of these simple networks are limited mainly by your imagination. Any input signal that can be represented in a binary (yes-no, true-false, 0-1, hot-cold) form can be mapped automatically onto a binary output, which can in turn be linked automatically to a text string. A base converter (a tool for converting numbers from base 10 to base 8, or base 3 to base 4) is easily implemented with these networks.

Linear and nonlinear neural networks can also perform tasks as complex as equipment diagnosis. For example, the input nodes can correspond to the presence (1) or absence (0) of a finding, and the output patterns can be mapped to text descriptions (by modifying the List of Patterns routine) of the diagnosis. In such a system, you might substitute "Line Voltage Normal," "Fuse Intact," "Output Power Low," and so on, for "INPUT 1," "INPUT 2," "INPUT 3," etc. The List of Patterns routine could likewise be modified to substitute "Power Supply Failure," "Final Amplifier Failure," and so on, for "Pattern A," "Pattern B," etc.

Remember that, even with only three input and two output nodes, there are 2^3, or eight, possible input patterns that can be associated with 2^2, or four, possible output states (the possible output set = {00, 01, 10, 11}), with each different output state linked to a different text string. If you have eight input and five output nodes, there are 2^8, or 256, possible input patterns which the system can learn to distinguish, and 2^5, or 32, different output states. However, even this processing capacity is limited for some practical applications. In the next section, you'll see how both high-end expert system and neural networks are used in real-world applications.

Applied AI techniques

Given a basic understanding of both expert systems and neural networks, the next step is to examine a few real-world applications of these technologies in the realm of digital signal processing (DSP). In general, the pattern matching capabilities of both expert systems and neural networks form the basis for their utility in DSP applications. Some of the more notable DSP applications in which expert systems and neural networks have been used successfully include: adaptive filtering, signal detection, DSP circuit design, and image recognition. These areas are described in more detail in the sections which follow.

Adaptive filters

Adaptive filters are filters which cancel noise and interference by dynamically updating their filter coefficients to adapt to the characteristics of the interference.[18] Although they can be constructed with conventional analog components, adaptive filters are commonly implemented digitally because of the inherent stability and mathematical tractability of the algorithms used for the computation of the filter coefficients.

Like expert systems, adaptive filter algorithms must often work with imperfect knowledge in a noisy environment. Since their inception, the challenge has been to determine the optimum filter coefficients in the shortest possible time, and to accurately determine filter coefficients with rapidly varying signal channels.[19] Adaptive filter algorithms are, therefore, primarily concerned with efficient searching strategies – techniques for guiding a program through all possible filter coefficient combinations in an effort to find the values best suited to a particular problem.

Conventional methods for determining optimum adaptive filter coefficients, like the popular Widrow-Hoff Least Mean Square (LMS) algorithm,[20] may be insufficient for some complex problems. Expert systems containing rules specific to the particular signal processing, like RADAR, can be used to reduce the search space to manageable size. That means that instead of having to consider 10,000 possible filter coefficient combinations, an expert-system directed adaptive filter algorithm might have to consider just 100 possible combinations – realizing significant time and computational savings.

Signal detection

Although efficient pattern matching is commonly considered to belong to the realm of AI, signal detection based on conventional pattern matching techniques isn't new. In the mid-1960s, medical researchers developed a DSP scheme based on pattern matching for the detection of bioelectric data – like EKGs.[21] In this system, signals were considered to be one of a class of possible, predefined signals.

Although the solutions to the majority of current DSP signal detection problems are based on the statistical analysis of signal detectors,[22] there are systems under development which rely heavily on expert system technology. **Figure 4** shows the simplified schematic of a real-time DSP system under development at Plymouth Polytechnic and Derriford Hospital, Plymouth, England.[23] This EEG (brain wave) system uses a knowledge-based expert system to recognize and distinguish between artifacts and physiological signals, so the adaptive filter can be adjusted to remove the artifacts. The inference engine directs the selection of the most appropriate coefficients for the adaptive filter based on information derived from both the knowledge base and the temporal and spectral features of the signal. In this system, the knowledge base consists of IF...THEN rules derived from human experts.

During operation, the input signal (EEG signal + instrumentation noise + other artifacts) is applied to a preprocessor. Output from the preprocessor is routed to an adaptive filter, a rule interpreter, and a feature classification program. After the pertinent temporal and spectral features of the input signal have been extracted by the feature classification program, the signal is classified and labeled. The signal classification and label are then communicated to both the knowledge base and the inference engine, or rule interpreter. Based on the characteristics of the input signal and the rules in the knowledge base, the inference engine modifies the coefficients of the adaptive filter to minimize the effects of any artifacts in the EEG signal.

In addition to the work being done with knowledge-based DSP systems in biomedicine, there is considerable activity in the military arena. The Admiralty Research Establishment in the United Kingdom is supporting the development of a knowledge-based, real-time DSP system for the automatic detection, surveillance, and identification of RADAR signals.[23] This DSP system, which operates on signals with a pulse density of about 1 million/second, relies on its knowledge base as an aid in the separation of multiple signals (deinterleaving) into distinct, continuous signals (merge processing). The knowledge base contains rules about generic RADAR signals, as well as rules describing specific failure patterns of the deinterleaving process. The developers have found that merge processing under the control of a rule-based expert system is clearly superior to a conventional algorithmic approach.

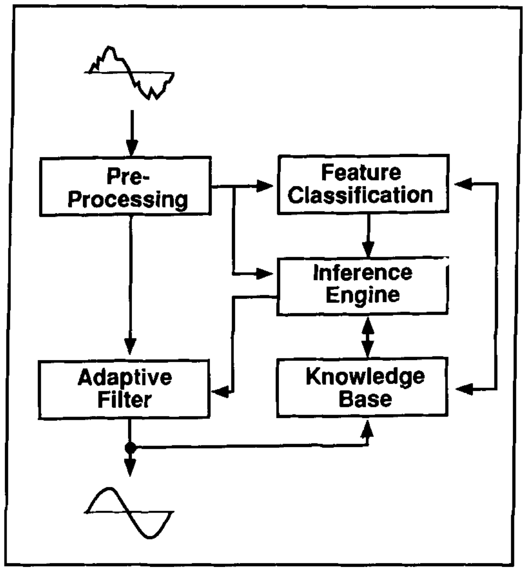

Figure 4. Schematic of an EEG monitoring system under development at Plymouth Polytechnic and Derriford Hospital, Plymouth, England, illustrates how expert system technology can be coupled with conventional DSP techniques to remove artifacts from a signal.

DSP circuit design

Expert systems have been used to facilitate DSP circuit design and operation – from component value selection to managing the spectrum of transmitter systems that use DSP techniques.[24] In general, expert system technology can help facilitate DSP circuit design in three areas: *simulation* (predicting circuit behavior as a function of the structural description of a device or group of devices and some initial conditions), *diagnosis* (identifying the abnormal device or devices in a system responsible for abnormal behavior), and *verification* (determining which particular circuit design will produce results consistent with the functional specifications of the system)?[25]

Expert system technology is of value in the simulation, diagnosis, and verification of DSP systems because it offers a great potential for time savings. For example, to use a particular DSP chip in an expert system-based simulation, the chip's characteristics need only be defined in a simple rule base. The operation of the chip is defined in terms of *what* it has to do, not in terms of *how* it is to be done. Typically, the nonalgorithmic approach is much easier to code than traditional algorithmic relationships.

This argument holds true for verification and diagnostic programs designed around a rule-based description of a given DSP system. The usefulness of the current practice of building a DSP system (or a simulation thereof) and then testing it is of questionable worth, partly because of the difficulty in selecting test cases. The number of tests associated with this type of verification increases linearly with the number of components (real or simulated) in the system. Expert system-based hardware verification and diagnosis is an especially attractive alternative to algorithmic techniques. This is because any piece of hardware is a well-defined environment, and expert systems describing hardware are easy to verify.[26] For instance, expert system techniques have been used successfully to analyze the signal behavior of MOS circuits.[27]

Currently, research is being done to investigate the possibility of solving the DSP circuit verification problem by using expert systems to develop designs which *cannot* be incorrect. While an appealing one, this approach has traditionally been avoided because of the difficulty associated with a large number of design alternatives. Expert system techniques, including methods for rapid searching and pattern matching, are ideally suited to this type of problem.

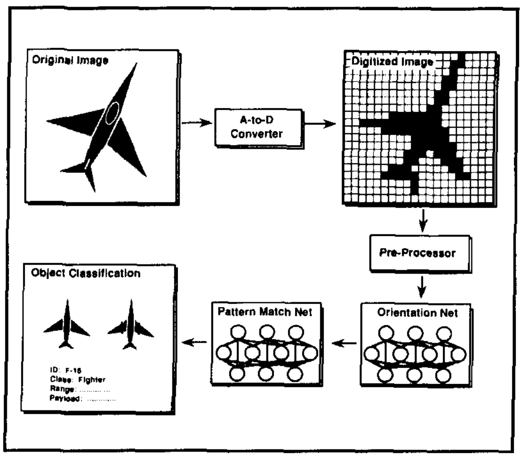

Figure 5. An example of how neural network technology can be used to provide practical image recognition capabilities. This military system, based on the TRW Mark IV Neural Network, can accurately and rapidly classify a large variety of aircraft.

Image recognition

One of the most difficult tasks in image analysis and recognition, and one in which AI techniques have been used with great success, is separating the objects of interest from the background noise and other extraneous signals.[28] Sophisticated digital pattern matching techniques (that is, converting image data arrays into LISP vectors for feature analysis) have been used when there is a priori knowledge of the properties of an object (for example, general shape, texture, color, or motion properties) which can be useful in detection.[29]

Although there has been considerable success using expert systems to minimize the search time in image recognition systems based on pattern matching,[30] the greatest promise in the domain image recognition lies in neural network technology. As I mentioned, neural networks can automatically identify and classify data (including video images), even in the presence of considerable noise. **Figure 5** is an example of a practical neural network-based image recognition system. This military system, based on a neural network with 2.5×10^5 nodes and 5×10^6 connections implemented in hardware, can classify aircraft with 95 percent accuracy.[12] As **Figure 5** shows, the system operates by first digitizing a video image of the aircraft to be classified. Once in digital form, the image is preprocessed into a form suitable for input to an orientation neural network. The orientation network performs a Fourier Transform on the image data, producing an output that's independent of the orientation and size of the original image. A second neural network, the pattern matching network, performs the actual image recognition and classification.

The future

The desire to find answers for DSP problems which are difficult to solve using conventional means will lead to solutions developed from a DSP perspective. Problems like real-time spectral power density estimation, which are complicated by a lack of data resulting from a lack of time,[31] could probably benefit from knowledge-based search strategies. Advances in AI research will also aid in the development of AI-DSP technologies. Work with silicrons (silicon-based neurons etched in the 3-D shape of neural cells) may lead to affordable hardware fast enough to handle high-speed DSP tasks on personal computers?[32] All in all, the future of coupled AI-DSP systems seems bright given the current interest in advancing both of these technologies. ■

REFERENCES

1. A. Barr and E. Feignbaum, *The Handbook of Artificial Intelligence*, HeuristicTec Press, Stanford, California, 1982.
2. B.P. Bergeron, NUIN, "Digital Signal Processing: The Fundamentals," *Ham Radio*, April 1990, page 24.
3. B.P. Bergeron, NUIN, "Digital Signal Processing: Working in the Frequency Domain," *Communications Quarterly*, Fall 1990, Page 40.
4. B.P. Bergeron, NUIN, "A.I. Applications in Radio Communications," *Ham Radio*, October 1989, page 30.
5. P.S. Sell, *Expert Systems—A Practical Introduction*, John Wiley & Sons, New York, 1985.
6. V. Barr, "Exploring Expert Systems," *Computer*, 1988, page 68.
7. W.D. Burnham and A.R. Hall, *Prolog Programming and Applications*, John Wiley & Sons, New York, 1985.
8. R. Crawford, "State Space: Minimal Search – Maximum Performance,", *Turbo Technix*, 1988, page 90.
9. A. Goldberg and D. Robson, *Smalltalk-80: The Language and Its Implementation*, Addison-Wesley, Reading, Massachusetts, 1983.
10. M. Suwa, A.C. Scott, and E.H. Shortliffe, "An Approach to Verifying Completeness and Consistency in a Rule-based Expert System," *AI Magazine*, 1982, page 16.
11. J.R. Giessman and R.D. Schultz, "Verification and Validation of Expert Systems," *AI Expert*, 1988, page 26.
12. R. Hecht-Nielsen, "Neurocomputing: Picking the Human Brain," *IEEE Spectrum*, March 1988, page 35.
13. C.C. Jorgensen and C. Matheus, "Catching Knowledge in Neural Nets," *AI Expert*, 1986, page 30.
14. B. Koski, "Constructing An Associative Memory," *Byte*, 1987, page 137.
15. P. Reece, "Perceptrons & Neural Nets," *AI Expert*, 1987, page 50.
16. R.J. Brown, "An Artificial Neural Network Experiment," *Dr. Dobb's Journal*, April 1987, page 16.
17. G. Hripcsak, "Problem-solving Using Neural Networks," *MD Computing*, 1988, page 25.
18. S. Haykin, *Introduction to Adaptive Filters*, Macmillan, New York, 1984.
19. W. Struszynski and G.F. Gott, "A Review and Comparison of Adaptive and DPSK systems for High-rate Data Transmission on HF," *Signal Processing Methods for Telephony*, 1969, page 74.
20. S.D. Stearns, "Fundamentals of Adaptive Signal Processing," *Advanced Topics in Signal Processing*, Lim and Oppenheim, Editors, Prentice-Hall, Englewood Cliffs, New Jersey, 1988.
21. D.H. Friedman, *Detection of Signals by Template Matching*, The John Hopkins Press, Baltimore, 1968.
22. S.A. Kassam, *Signal Detection in Non-Gaussian Noise*, Springer-Verlag, New York, 1988.
23. T. Ivall, "AI In Signal Processing," *Electronics and Wireless World*, 1989, page 570.
24. G.W. Garber and J. Liebowitz, "Expert Systems in Radio Spectrum Management," *Expert System Applications to Telecommunications*, Liebowitz, Editor, John Wiley & Sons, New York, 1988.
25. D.G. Bobrow, "Qualitative Reasoning About Physical Systems: An Introduction," *Qualitative Reasoning About Physical Systems*, Bobrow, Editor, MIT Press, Cambridge, Massachusetts, 1985.
26. H.G. Barrow, "VERIFY: A Program for Proving Correctness of Digital Hardware Design," *Qualitative Reasoning About Physical Systems*, Bobrow, Editor, MIT Press, Cambridge, Massacusetts, 1985.
27. B.C. Williams, "Qualitative Analysis of MOS Circuits," *Qualitative Reasoning About Physical Systems*, Bobrow, Editor, MIT Press, Cambridge, Massachusetts, 1985.
28.D.H. Ballard and C.M. Brown, *Computer Vision*, Prentice-Hall, Englewood Cliffs, California, 1982.
29. G. Banks, J.K. Vries, and S. McLinden, "Radiologic Automated Diagnosis (RAD)," *Proceedings of the Tenth Annual Symposium on Computer Applications in Medical Care*, 1988, page 228.
30. C. Levinthal and R.S. Schehr, "New Methods of Pattern Recognition for Three-dimensional Reconstruction and Display of Nerves and Molecules," *Proceedings of the Tenth Annual Symposium on Computer Applications in Medical Care*, 1988, page 225.
31. S. Kay, "Spectral Estimation," *Advanced Topics in Signal Processing*, Lim and Oppenheim, Editors, PrenticeHall, Englewood Cliffs, New Jersey, 1988.
32. J.K. Stevens, "Reverse Engineering the Brain," *Byte*, April 1985, page 287.

Hilton A. Turner, Jr., *KB8LS*
1513 Buick Lane
Kokomo, Indiana 46902

OPEN-WIRE TRANSMISSION LINES

Tools for design and analysis

Open-wire feedline has been popular with Amateurs for many years, and unlike coaxial cable, construction of balanced feedlines in the home workshop is both practical and economical. Most information on constructing open-wire line simply shows how to use familiar characteristic impedance formulas to find the correct wire spacing. But methods to determine velocity factor and losses have been lacking. Questions arise as to whether solid or stranded wire should be used, what wire diameter is needed, and what effect the size and spacing along the line of the insulated spacers have. Selections are often based on intuitive judgement because of a lack of information regarding these elements. However, these are questions that must be answered before the serious station operator begins construction and installation of this type of transmission line.

In this article, I will show how to calculate the physical dimensions for an open-wire transmission line, after choosing a specific characteristic impedance and acceptable attenuation loss. I will also show how to measure the actual characteristic impedance, attenuation losses, and velocity factor of the feedline by simply measuring the reflected impedance of the line.

Open wire assumptions and guidelines

To simplify the design equations and obtain predictable results, follow these rules (see **Figure 1**):

- The current flowing must travel on the outer surface of the conductors (the skin effect).
- Use solid copper wire, as stranded wire diameters can only be approximated. The solid wire diameter will be small compared with the wavelength, and both wires will have the same diameter.
- Make the spacing between conductors at least five times the wire diameter (reducing the chance of arcing and other proximity effects), yet small compared with the wavelength.
- Make sure the height of the line above ground is at least ten times the conductor spacing. This reduces stray capacitive effects.
- Make the length of the line long compared with the conductor spacing.
- Use low-loss material like polyethylene or Teflon™ for the insulating spacers. PVC,

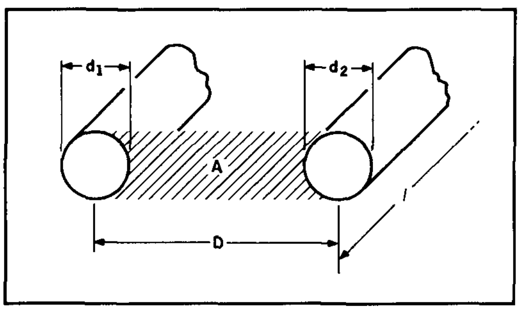

Figure 1. Open-wire transmission line conductor dimensions.
$d = d_1 = d_2$, where d is the conductor diameter (wire size).
D is the distance between conductor centers.
$\frac{D}{d}$ should be greater than five to prevent arcing and other proximity effects.
A is the air space between the conductors.
l is the unit length of the line.

acrylic, and ceramic are not recommended. The spacers should be fastened with nonmetallic low-loss materials such as plastic welders or cements. The spacers shouldn't occupy more than ten percent of the total air volume between the conductors to ensure minimum dielectric losses.

Design equations

The characteristic impedance (Z_0) is defined by:

$$Z_o = 120[\cosh^{-1}(D/d)] = 276[\log(2D/d)] \text{ ohms} \quad (1)$$

Where d is the diameter of each conductor and D is the distance between conductor centers. Because Z_0 and d are normally specified, **Equation 1** can be solved for D:

$$D = \frac{d[\log^{-1}(Z_0/276)]}{2} \quad (2)$$

Where D and d are in the same units. (Inches are used in all sample problems.) The attenuation loss (a) in general form is defined by:

$$a = \frac{r_s}{2(Z_o)} + \frac{g_p(Z_o)}{2} \quad (3)$$

$$\text{nepers per unit length}$$

Where r_s is the total opposition per unit length of the wires. This opposition is greater than the DC resistance of the wire because of the skin effect. The loss caused by the dielectric material is represented by g_p. Because the insulating spacers occupy no more than ten percent of the air volume between conductors, g_p is set to zero. The resulting equation:

$$a = \frac{r_s}{2(Z_o)} \quad (4)$$

is now used to derive a specific equation for the attenuation loss for open wire lines (see **Figure 2**).

$$r_s = \frac{8.30[\sqrt{(F)}]\ [10^{-6}]}{d/2} \text{ ohms} \quad (5)$$

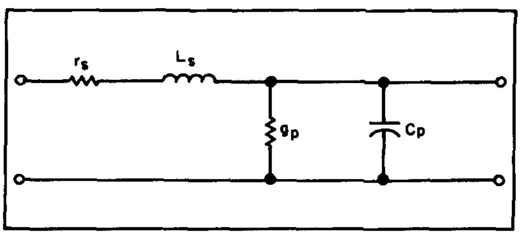

Figure 2. Lumped section of transmission line. For open-wire lines (g_p) ≈ 0.

Where F is the frequency in Hertz and d is in centimeters. Combining **Equations 4** and **5** yields:

$$a = \frac{8.655\ [\sqrt{(F)}]\ [10^{-6}]}{(d)\ (Z_o)} \text{ decibels per foot} \quad (6)$$

Where d has been converted from centimeters to inches. Examination of **Equation 6** reveals several important facts:

- Increasing the conductor size (d), reduces attenuation loss.
- Increasing the characteristic impedance (Z_0), reduces attenuation loss.
- The highest (worst case) attenuation loss occurs at the highest operating frequency.

The air volume (V_{air}) between the conductors without spacers is defined by:

$$V_{air} = [(d)(D) - (3.1416)(R^2)][l] \quad (7)$$

Where R is the radius of the conductors and l is the unit length of the line. Because the spacers must occupy no more than ten percent of V_{air}, the maximum spacer volume (V_{max}) is defined by:

$$V_{max} = (0.1)(l)[(d)(D) - (3.1416)(R^2)] \quad (8)$$

Using **Equations 1** through **8**, you can predict an open-wire line's physical dimensions based on a specified characteristic impedance and the attenuation loss for a given line length and cut-off frequency.

My first example deals with the design of an open-wire transmission line where the characteristic impedance is 400 ohms and the attenuation loss is no more than 0.2 dB for 100 feet of line at 30 MHz. We'll evaluate low-loss rectangular spacers 0.5 inch wide, 1.5 inches long, and 0.1 inch thick placed every 12 inches [l] in the line (see **Figure 3**).

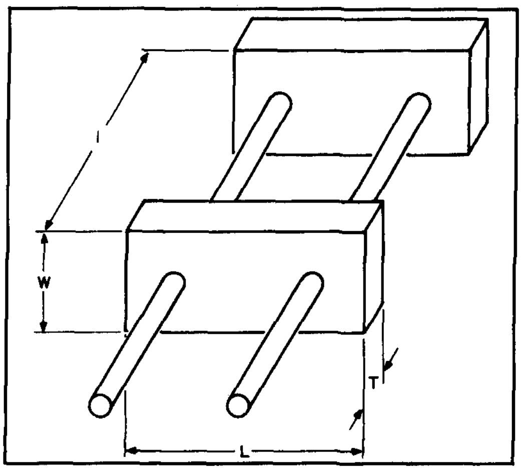

Figure 3. Typical open-wire line with rectangular spacers. Net spacer volume = {(W)(L)(T)} − 2(T)πr².

Gage (AWG) or (B&S)	Nominal Diameter inches	mm	Circular Mil Area	Weight pounds per M	Resistance at 68 °F ohms per M
10	0.1019	2.60	10380	31.43	0.9989
11	0.0907	2.30	8234	24.92	1.260
12	0.0808	2.05	6530	19.77	1.588
13	0.0720	1.83	5178	15.68	2.003
14	0.0641	1.63	4107	12.43	2.525
15	0.0571	1.45	3260	9.858	3.184
16	0.0508	1.29	2583	7.818	4.016
17	0.0453	1.15	2050	6.200	5.064
18	0.0403	1.02	1620	4.917	6.385
19	0.0359	0.912	1200	3.899	8.051
20	0.0320	0.813	1020	3.092	10.15
21	0.0285	0.724	812.1	2.452	12.80
22	0.0253	0.643	640.4	1.945	16.14
23	0.0226	0.574	511.5	1.542	20.36
24	0.0201	0.511	404.0	1.223	25.67
25	0.0179	0.455	320.4	0.9699	32.37
26	0.0159	0.404	253.0	0.7692	40.81

Table 1. Solid bare copper wire American Wire Gage. (Information from National Bureau of Standards Copper Wire Tables, Handbook 100.)

1. Select a wire size (d) from **Table 1** and calculate the spacing (D) between conductors.

(A) We'll evaluate no. 12 AWG solid copper wire; therefore, d equals 0.0808 inch.

(B) From **Equation 2**:

$$D = \frac{(0.0808)\log^{-1}[400/276]}{2} = 1.14 \text{ in.}$$

(C) D/d must be greater than five. If not, Z_o must be increased. (D/d) = (1.14)/(0.0808) = 14.11

2. Calculate the attenuation loss at 30 MHz:

(A) From **Equation 6**:

$$a = \frac{8.655\,[\sqrt{30{,}000{,}000}]\,[10^{-6}]}{(0.0808)\,(400)}$$
$$= 0.0015 \text{ dB per foot}$$

(B) For 100 feet of line, a = 0.15 dB. If a was greater than 0.2 dB for 100 feet of line, then d, or Z_o, or both would have to increase.

3. Check the net spacer volume to see that it doesn't exceed ten percent of the air volume (without spacers) between the conductors per unit line length:

(A) From **Equation 8**:

$$V_{max} = (0.1)(12)[(0.0808)(1.14) - (3.1416)(0.0404^2)] = 0.104 \text{ cubic inch}$$

(B) Net spacer volume (see **Figure 3**) = [(width)(length)(thickness) − (2)(thickness)(3.1416)(R^2)]
= [(0.5)(1.5)(0.1) − (2)(0.1)(3.1416)(0.0404^2)]
= 0.074 cubic inch

(C) The net spacer volume must be ≤ V_{max}: 0.074 ≤ 0.104

If this statement is not true, then the unit line length (distance between spacers) [l] must increase, the net volume of the spacer must be made smaller, or both. You now have enough preliminary information to build an open-wire line with a specified characteristic impedance and attenuation loss. Once the line is constructed, you need to measure the actual line parameters to verify your design.

As stated previously, the key parameters are the characteristic impedance and the attenuation loss. We'll now include the velocity of propagation.

There have been many articles written on how to measure each of the parameters. Normally, a different test equipment setup is needed for each parameter. But, it is possible to determine all three parameters using a single test configured to measure the reflected impedance of a sample section of the constructed line. In fact, this method will not only work for open-wire line, but for any two-conductor transmission line (parallel or coaxial).

The test setup in **Figure 4** shows the equipment required to measure the reflected impedance. This consists of the complex open-circuit impedance (Z_{OC}) and the complex short-circuit impedance (Z_{SC}). Z_{OC} and Z_{SC} are measured at one end of the line while the opposite end of the line is open circuited then short circuited, respectively. I recommend using commercial impedance bridges like General Radio 1606A, Hewlett Packard 4815, or Hewlett Packard 8405 with directional couplers because of their accuracy and wide reactance range. The null detector is only required for certain types of bridges, such as the General Radio 1606A, and can be any receiver with a signal strength indicator. Keep all connections as short as possible to reduce errors at higher frequencies. *Make the connection for the line from low inductance material like copper strap.*

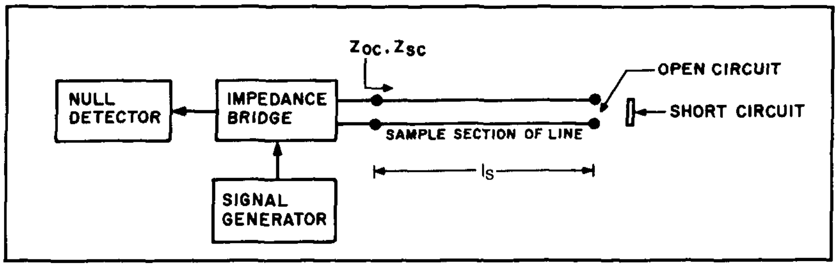

Figure 4. Test equipment required to measure the reflected impedance of a two-conductor transmission line.

Equations

In order to simplify the equations, keep the length of sample line (l_S) to be measured relatively short. As a general rule, l_S must be less than one quarter the free-space wavelength at the highest frequency of interest.

$$l_S < [246/\text{highest frequency (MHz)}]\ \text{feet} \quad (9)$$

After measuring both Z_{OC} and Z_{SC} at each frequency of interest, you can calculate the characteristic impedance (Z_o) from:

$$Z_o = \sqrt{(Z_{SC})(Z_{OC})}\ \text{in ohms} \quad (10)$$

The velocity of propagation (V_p) can be calculated from:

$$V_p = \frac{(4)(3.1416)(F)(l_S)}{[\{\arctan(B/A)\} + \{(K)(2)(3.1416)\}]\,C} \quad (11)$$

Where:

$$A + jB = \frac{1 + \sqrt{(Z_{SC})/(Z_{OC})}}{1 - \sqrt{(Z_{SC})/(Z_{OC})}}\ \text{in ohms} \quad (12)$$

F is the frequency in Hertz, C is the wave velocity in free space and equals 984,000,000 feet per second, and K is a quadrant correction factor. When finding the angle from the arctangent function using an electronic calculator, draw a quadrant diagram using the signs of A and B from **Equation 12**. If the angle is in the correct quadrant, K is set to equal zero. If the angle is in the wrong quadrant, K is set to move the angle to the correct quadrant. Convert the correct angle to radians from degrees after calculating the arctangent (B/A). One radian equals 57.296 degrees.

The attenuation loss can be calculated from:

$$a = \frac{8.69\,[\ln\sqrt{(A^2 + B^2)}]}{2\,l_S}\ \text{in dB per foot} \quad (13)$$

where:
(Ln) is the natural log or $\log_e$

Example

A 500-foot roll of transmission line has no markings or documentation. Determine the three key transmission parameters Z_o, V_p, and a at 5 and 10 MHz.

1. Choose a sample length of line to be measured.
From **Equation 9**:

$$l_S < 246/10 = 24.6\ \text{feet}$$

The line sample should be less than 24.6 feet. l_S is chosen arbitrarily to be 10.575 feet.

2. Next measure Z_{OC} and Z_{SC} of the sample line. The following results are obtained:

Frequency (MHz)	Z_{SC} (ohms)	Z_{OC} (ohms)
5	1.36+j31.80	0.54−j96.14
10	4.60+j95.00	0.70−j32.80

3. Calculate Z_o from **Equation 10**:

At 5 MHz,

$$Zo = \sqrt{(1.36+j31.80)\,(0.54-j96.14)} = 55.31-j1.03\ \text{ohms}$$

At 10 MHz,

$$Zo = \sqrt{(4.60+j95.00)(0.70-j32.80)} = 55.86-j0.76\ \text{ohms}$$

As you can see, except for minor measurement errors, Z_o is practically the same at both frequencies.

4. Calculate V_p. Solve **Equation 12** for A + jB, then solve **Equation 11** for V_p.

At 5 MHz:

$$(A+jB) = \frac{1 + \sqrt{(1.36+j31.80)/(0.54-j96.14)}}{1 - \sqrt{(1.36+j31.80)/(0.54-j96.14)}}$$
$$= 0.5133 + j0.8827$$

If you look at the diagram in **Figure 5**, you'll see that the angle resulting from the arctangent of B/A should be found in the first quadrant (between 0 and 90 degrees). The arctangent of 0.8827/0.5133 is 59.82 degrees, or 1.0441 radians; therefore, K is set to zero.

$$V_p = \frac{(4)(3.1416)(5\times10^6)(10.575)}{[\{arctan(0.8827/0.5133)\} + \{(0)(2)(3.1416)\}][984\times10^6]}$$
$$= 0.65 = 65\%$$

At 10 MHz:

$$(A+jB) = \frac{1 + \sqrt{(4.60+j95.00)/(0.70-j32.80)}}{1 - \sqrt{(4.60+j95.00)/(0.70-j32.80)}}$$
$$= -0.5024 + j0.9003$$

As you can see from the diagram in **Figure 6,** the angle resulting from the arctangent of B/A should fall in the second quadrant (between 90 and 180 degrees). However, the arctangent of 0.9003/−0.5024 (as computed) is −60.84 degrees or −1.062 radians, which is in the fourth quadrant (180 degrees out of position). K is set equal to 0.5 to obtain the correct angle.

$$V_p = \frac{(4)(3.1416)(10\times10^6)(10.575)}{[\{arctan(0.9003/-0.5024)\} + \{(0.5)(2)(3.1416)\}][984\times10^6]}$$
$$= 0.65 = 65\%$$

The velocity of propagation is the same at both frequencies.

5. Calculate the attenuation loss from **Equation 13.**

At 5 MHz:

$$a = \frac{8.69[Ln\{\sqrt{0.5133^2+0.8827^2}\}]}{(2)\ (10.575)}$$
$$= 0.0086 \text{ dB per foot}$$

Assuming the roll of transmission line is uniform, for 500 feet: a = (500) (0.0086) = 4.29 dB.

At 10 MHz:

$$a = \frac{8.69[Ln\{\sqrt{-0.5024^2+0.9003^2}\}]}{(2)\ (10.575)}$$
$$= 0.0125 \text{ dB per foot}$$

Again, assuming a uniform line, for 500 feet: $a = (500)(0.0125) = 6.27$ dB

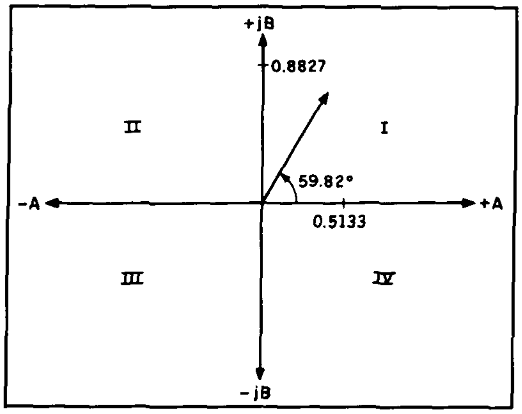

Figure 5. Quadrant diagram for 5 MHz. Because the arctan $\left(\frac{0.8827}{0.5133}\right)$ = 59.82 degrees is located in Quadrant I as defined by A+jB, no correction factor is needed. K is set to equal zero.

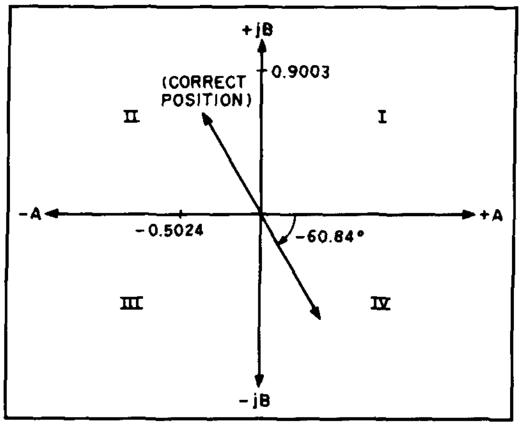

Figure 6. Quadrant diagram for 10 MHz. Because the arctan $\left(\frac{0.9003}{-0.5024}\right)$ = −60.84 is located in Quadrant IV and A+jB defines Quadrant II, a 180-degree correction factor is needed; therefore, K is set to equal 0.5.

As you can see, the attenuation loss increases as frequency increases.

Summary

You should now have the analytical tools to design open-wire transmission line with reasonable accuracy before constructing the line. You should also have the analytical tools to determine the three key transmission line parameters for any type of finished two-conductor transmission line. I hope these procedures will provide fresh insight to those interested in the subject of transmission lines. ■

BIBLIOGRAPHY

1. Albert P. Albrecht, L.J. Giacoletto, *Electronic Designer's Handbook*, Second Edition, McGraw-Hill, Section Eight.
2. Walther H. Buchsbaum, *Buchsbaum's Complete Handbook of Practical Electronic Reference Data*, Second Edition, Prentice-Hall, page 263.
3. *Reference Data for Radio Engineers*, First Edition (1943), Federal Radio and Telephone Corporation (ITT), page 116.
4. Stephen F. Adam, Hewlett-Packard, *Microwave Theory and Applications*, Prentice-Hall, Chapter 2.
5. Dennis Roddy, *Microwave Technology*, Prentice-Hall, Chapter 1.
6. Belden Wire and Cable, *Master Catalog 885*.
7. Brand-Rex, *Wire and Cable Engineering Guide*, publication WC-82.

By Norm Foot, *WA9HUV*
293 East Madison Avenue
Elmhurst, Illinois 60126

UPGRADE YOUR 1296-MHz CONVERTER

This 1152-MHz phase-locked oscillator is easy to build

It may seem surprising that, in this age of "store-bought" radio equipment, so many Amateurs and experimenters still build their own. Perhaps it's because catalog items like UHF transceivers usually carry hefty price tags. Even so, many Amateurs have neither the time nor the inclination to build their own equipment. However, there seems to be a hard-core group of experimenters who, like their predecessors from the very early days of radio, prefer the learning experience and satisfaction of constructing their own gear. I'm one of them.

Why the PLO?

I developed a phase-locked (PLO) oscillator to optimize the performance of my 1296-MHz converter by designing the local oscillator (LO) for very low phase noise. This minimizes the amount of phase noise superimposed on the relatively noise-free incoming signals. The critical area, where signal-to-noise degradation is most likely to occur, is the combination of mixer and LO.[1] Much depends on the mixer's efficiency, because mixer noise figure is equal to its insertion loss. Most experts agree that the double-balanced mixer (DBM) is best suited for VHF and UHF mixer service. However, the DBM requires somewhat higher local oscillator power to maintain good conversion efficiency.

While it's possible to achieve a mixer noise figure as low as 5.5 or 6 dB at UHF, this is seldom realized. Under some circumstances, it's desirable to insert 3-dB pads in

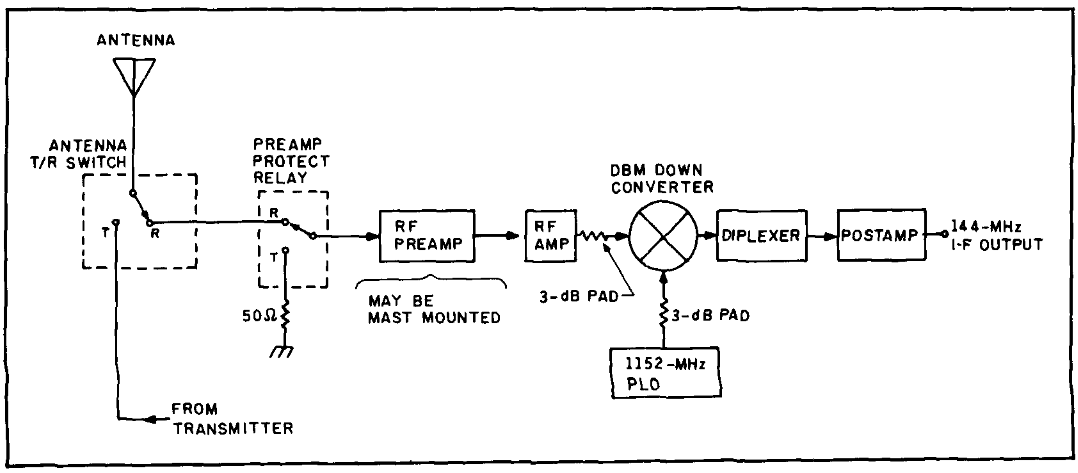

Figure 1. Typical 1296-MHz converter setup.

the LO and RF of DBM terminals. Doing so might degrade the mixer noise-figure, but *these pads are needed to minimize spurious* and intermodulation (IM) products.[2]

Figure 1 shows a typical 1296-MHz converter. The RF preamplifier should be mast-mounted close to the antenna feed point if your installation includes a long run of coaxial cable. I use a relatively low-noise RF amplifier between the preamplifier and the mixer. It has sufficient gain and a low enough noise figure to override losses associated with interconnecting cables within the station, thus retaining the low-noise characteristics of the preamplifier. The diplexer between the DBM and the IF post-amplifier provides a good termination for the mixer. It absorbs unwanted mixer products and is a *must* in terms of mixer efficiency. If you don't take these precautions, your potentially low-noise converter system may meet with disaster.

Background

I've been working on the UHF voltage-tuned oscillator (VTO) for this PLO for quite some time. Over the past ten years, I have built and tested various UHF LOs for my converters, including crystal-oscillator-multiplier strings. While the latter performed fairly well, I had to retune the chain of piston trimmers frequently, particularly those associated with the varactor-multiplier (output) stage. The PLO I described in the July/August 1986 issue of *Ham Radio* magazine[3] used digital dividers instead of frequency multipliers, which don't need piston trimmers for tuning. While the noise level of that PLO was very low, the overall circuit was more complex and larger than I desired. It was also difficult to adjust the 1152-MHz oscillator for proper operation. I wanted a simpler design.

I'd already built a multipurpose voltage-tuned UHF oscillator (VTO).[4] Used with a Plessy prescaler and a 6.0-MHz reference crystal oscillator, the VTO frequency could be tuned manually with a potentiometer and phase locked to various TV frequencies corresponding to the harmonics of the reference crystal. The circuit was similar in some respects to the one described here, but had a habit of drifting and falling out of lock under certain environmental conditions.

I came up with a simplified version of this circuit in 1981.[5] It used an inexpensive MV2201 tuning diode, an MRF-901 oscillator transistor, and an inexpensive prescaler. I could measure the oscillator frequency with a low-frequency counter by connecting the counter to the prescaler output. This oscillator wasn't equipped with a phase-locked loop. I used a potentiometer to achieve continuous tuning.

The unit performed well as the LO for a TV receiver, but it didn't have the long-term stability needed for CW or SSB reception. However, its short-term stability and low-noise characteristics were quite good. The circuit was similar in many respects to the one described in this article.

In the last ten years, I've made many important electrical and mechanical improvements. The new PLO is probably the most thoroughly tested unit I've ever built. It's also considerably easier to build than the earlier models. I retained the desirable features of my previous designs and added a relatively simple, yet effective, phase-locked loop (PLL). This PLL provides the stability and low-noise characteristics necessary for reception of CW and SSB at UHF.

Applications

The new PLO is intended primarily for use as a fixed LO for a down-converter operating in the 1245 to 1300-MHz Amateur band. The frequency of a reference crystal determines the portion of the band the converter will work. It's common practice to convert to 144 MHz. Tuning is done at this frequency, and narrow-band modes like CW and SSB are available. A double-conversion system, in which the 144-MHz IF is converted again to 28 MHz, is often used. In either case, you can then tune over a band of several hundred kHz, depending on the IF bandwidth.

Of course, there are other uses for this PLO. I use it to drive a power doubler[6] to provide +10 dBm for my 2304-MHz exciter. Low phase noise is very important when

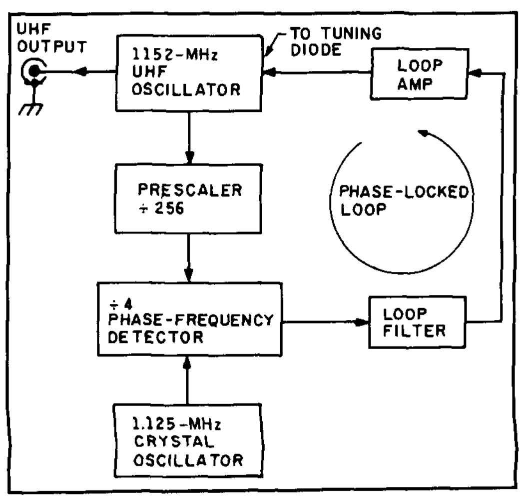

Figure 2. Block diagram, 1152-MHz PLO.

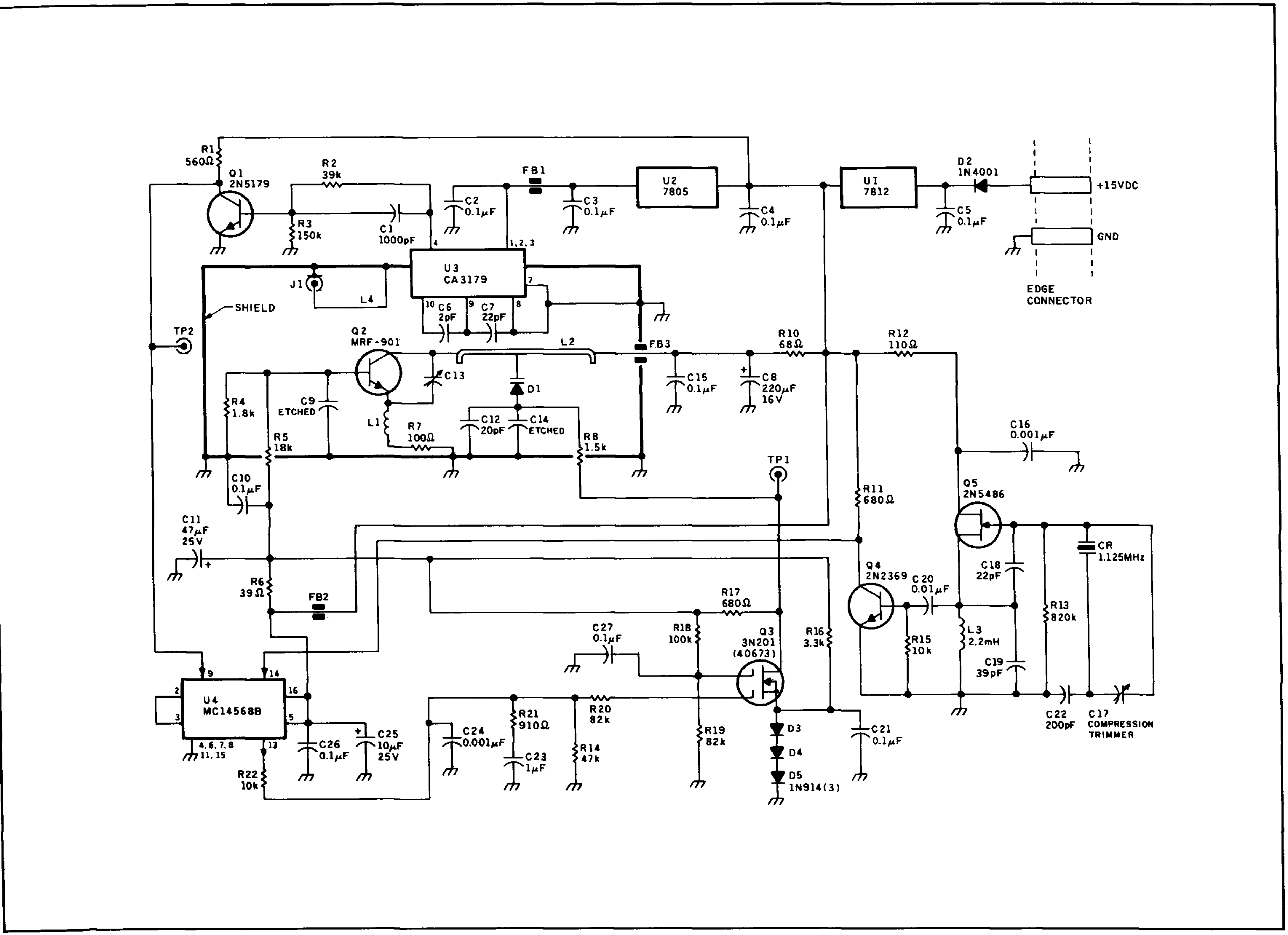

Figure 3. Circuit diagram, low-noise phase-locked oscillator.

driving a doubler, because the doubler multiplies phase-noise deviations.

The UHF PLO can also be used as a tripler for operation on the 3456-MHz band. Using a varactor multiplier, the fifth harmonic of 1152 MHz can put a signal on 5760 MHz.

Circuit description

The UHF PLO circuit is relatively simple. It consists of a self-excited UHF oscillator, a UHF prescaler, a reference crystal oscillator, and a phase-frequency detector. The UHF oscillator is equipped with a tuning diode driven from the output of the phase-frequency detector. I use no frequency multipliers, and 10 dBm of output power is available.

If you look at **Figure 2**, you'll see that phase lock is achieved at 1152 MHz using a 1.125-MHz crystal oscillator as a reference. This reference signal is fed to one input of the 14568 phase-frequency detector, and a 4.5-MHz signal from the prescaler output is fed to the other. The 4.5-MHz prescaler signal is divided by 4 inside the 14568, to match the reference frequency.

Before phase lock, the prescaler output-signal frequency is incorrect because the UHF oscillator is initially operating at the wrong frequency. In the process of phase locking, the 14568 generates a ramp of voltage for the tuning varactor. This tunes the oscillator toward 1152 MHz until the prescaler output frequency is exactly 4.5 MHz. These events leading to phase lock occur in a matter of milliseconds.

The reference crystal frequency is the desired LO operating frequency divided by 1024. In **Figure 2**, the phase-locked oscillator frequency is 144 MHz below 1296 MHz, or 1152 MHz. While this number scheme is most commonly used in 1245 to 1300-MHz converters, I've made provisions for operation at any frequency between about 1100 and 1200 MHz to accommodate other applications. A schematic diagram of the PLO signal source is shown in **Figure 3**.

Making the PC board

Recently, I read an article[7] where the author discouraged builders from making the type of double-sided pc boards which normally include plated-through holes. I've been making "one-shot" double-sided boards for many years, with excellent results. I use the "drafting tape and donut" method to prepare the board for etching. I add ground holes from the trace side of the board to the ground-plane at locations where DC or RF grounds are needed. Later, before I "stuff" the board with parts, I insert short lengths of no. 26 tinned-copper into each ground hole, bend them over, clip them short and solder them to each side of the board. I find this method works very well at frequencies of up to at least 4 GHz, where the ground-wire length is a small fraction of a wavelength. While this approach isn't necessary at HF, it's absolutely essential for circuits operating at VHF and above.

Once I've built a prototype board and corrected any mistakes, I make a 2:1 artwork on vinyl using 2:1-scale drafting tape, donuts, and precut "stick-ons" like DIP socket patterns. I then have the artwork photographically reduced to exactly 1:1 scale, as shown in **Figure 4A** (trace side) and **B** (ground plane). I then add the parts to a board made from this artwork and test it to verify the design. If you make a copy of this PLO, you can skip these steps and use etch-resist or presensitized board to make the printed circuit directly from the artwork of **Figure 4**. Or, you can order a board from Far Circuits (see parts suppliers section).

Preparing the pc board for assembly

If you plan to use the edge connector, make sure it plugs into the receptacle properly. You may have to trim it slightly to obtain a good fit. I used a double 15-pin edge connector with 0.156-inch contact spacing (available from Digi-Key or Mouser). Cut a slot for the key, if it includes one. You may connect the contacts mating the ground-plane side of the board to ground.

Drill out the two large right-hand pads with a no. 26 drill for mounting the voltage regulators with 6-32 screws. Also drill out the two crystal-socket holes at the lower right to fit the crystal holder you intend to use. I used an Augat™ holder, but a Johnson™ ceramic or other type of socket will work too. If the holder doesn't ground to the crystal case, use an L-shaped bracket to hold the crystal firmly in place and provide a good ground. *Do not* apply solder to the crystal pins or the case.

Ground holes

Before beginning the assembly, insert tinned-copper wire into each ground hole and solder on each side as I described. You'll be able to identify most of these holes by the large 1/8-inch diameter donuts.

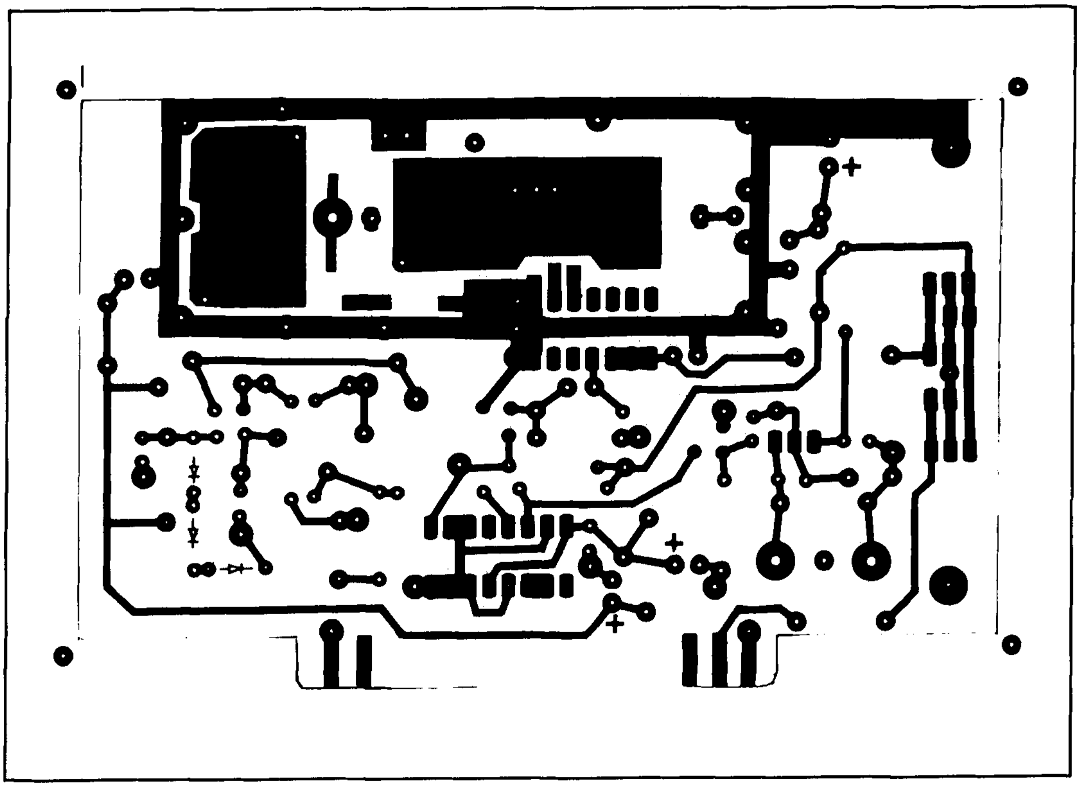

Figure 4A. PC board artwork, trace side.

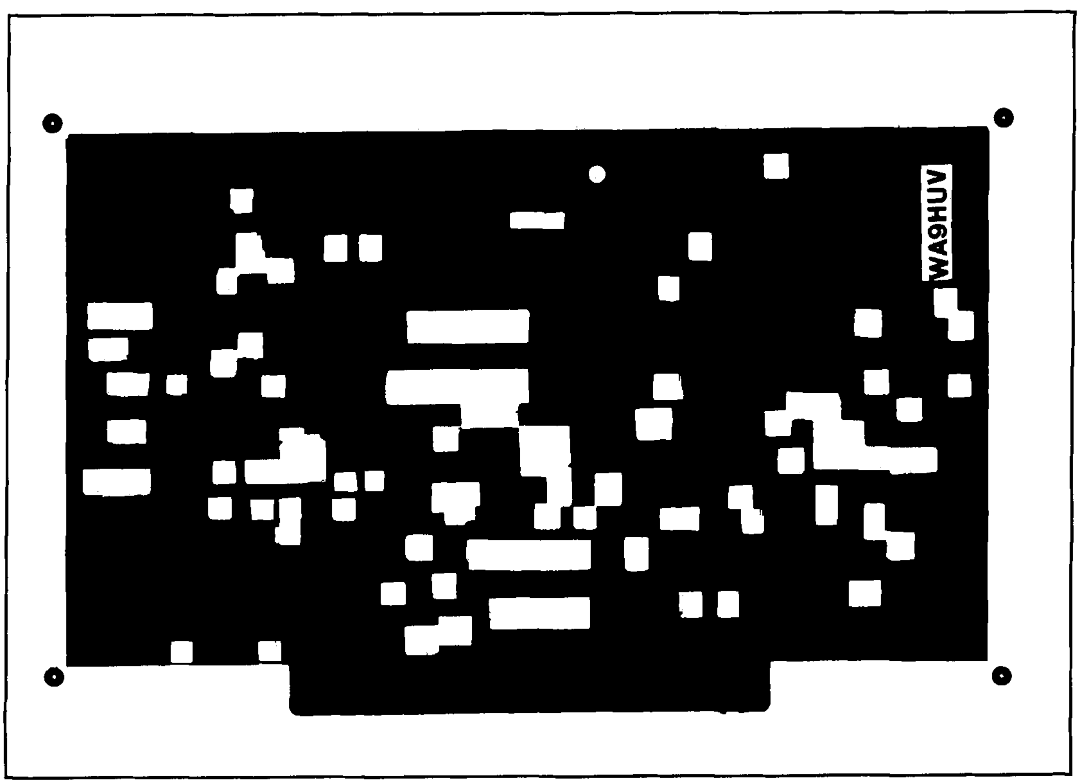

Figure 4B. PC board artwork, ground plane.

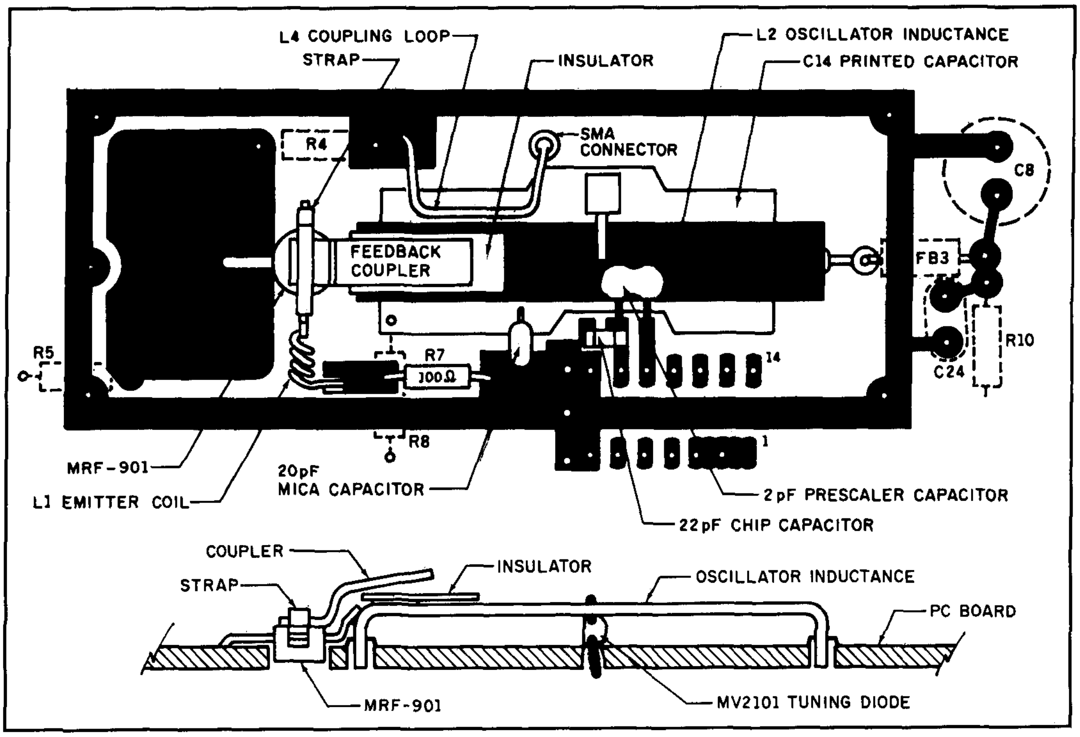

Figure 5. Plan and cross-sectional view of oscillator compartment showing locations of key components.

There are twelve ground holes around the periphery of the oscillator, one at the ground end of the coupling loop, and two to the left of prescaler pins 7 and 8. Ground the pad between the two voltage regulators. There are 13 other ground holes, or a total of 29.

UHF oscillator assembly

Figure 5 shows the layout and a cross-section of the oscillator, for use as an aid in assembly. First, cut out and form the metal parts shown in **Figure 6A** through **C**. Tin these parts with a soldering iron to make them easier to assemble.

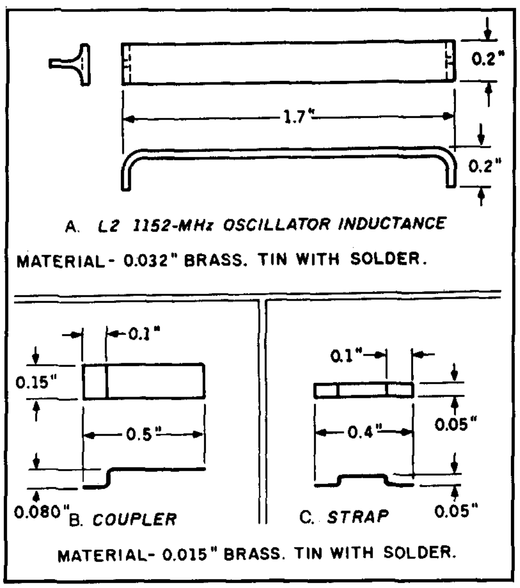

Figure 6. Metal parts used in oscillator assembly.

Mount and solder the oscillator inductance. Next, insert the MRF-901 into the hole provided, bend up the collector lead, clip it short, and solder it to the inductance. Use a scriber to hold the strap in place over the transistor while you solder it to the emitter leads.

Apply a pin-point of two-part, 5-minute epoxy cement on a 0.2 by 0.25 by 0.01-inch thick epoxy fiber glass insulator and attach it to the oscillator inductance, as shown in **Figure 5**.

After the cement has hardened, slide the coupler under the strap and solder it in place. Use the solder sparingly. Bend the coupler upward slightly, as shown.

Finally, insert the anode of the MV2101 tuning diode through one of the three holes in the printed-capacitor (C14) under the inductance. The hole you choose depends on the operating frequency range desired. Position the diode so the lead lengths are no greater than 1/16 inch, as illustrated in **Figure 7**.

The three holes in printed-capacitor C14 correspond to three overlapping operating ranges. The middle hole is for the range centered near 1152 MHz. The three ranges correspond approximately to those illustrated in **Figure 8**.

The emitter coil is made of four turns of no. 24 enamel copper wire wound using the shank of a 1/16-inch drill as a mandrel. Remove the coil from the bit and space the turns slightly. Surface mount the coil and a 1/8-watt, 100-ohm resistor in series from the emitter to ground. Insert all of the 1/4-watt resistors and capacitors into the board from the ground-plane side. You must add a miniature 20-pF mica capacitor with leads no longer than 1/16 inch between C14 and ground. Place this capacitor next to the prescaler **(Figure 5)**.

Solder a 22-pF chip capacitor between pins 8 and 9 of the CA3179 prescaler on the pads provided. Solder the 2-pF dipped mica capacitor, which serves as the RF coupling loop to the prescaler, between pins 9 and 10. The capacitor's location relative to L2 isn't critical, but don't couple it too tightly. To avoid an accidental short, include "spaghetti" on the leads.

The RF-output coupling loop consists of a 1-1/8 inch length of no. 18 enamel-coated copper wire. If you need a full 10 dBm of output power, couple the loop fairly close to L2. I find that relatively loose coupling provides 8 dBm output, which is adequate to drive most hot-carrier diodes.

Use an SMA coaxial fitting for the output connector. I salvaged a number of these rather expensive items for 50 cents apiece from surplus gear I found at a hamfest. Don't use a BNC connector here.

After you've mounted the oscillator parts, add an electrostatic enclosure. Form a length of 0.5-inch wide by 0.025-inch thick brass strip into a rectangle 3.1 inches long and 1.15 inches wide. You can find 12-inch lengths of this type of brass at most hobby shops. Now solder this brass "fence" to the outside edge of the rectangular trace around the oscillator, making sure the through-grounds are on the *inside* of the enclosure.

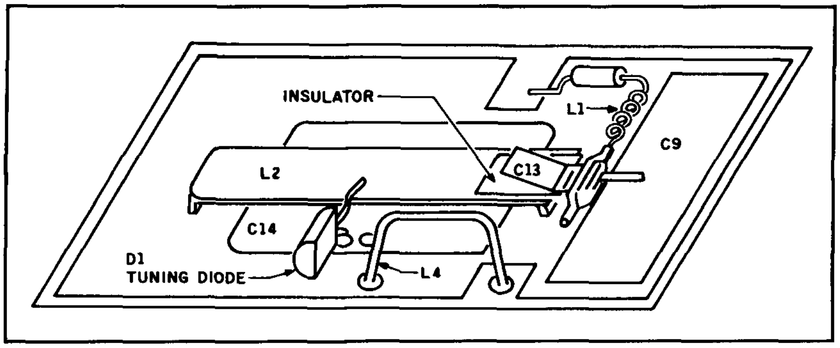

Figure 7. Isometric sketch showing parts mounting.

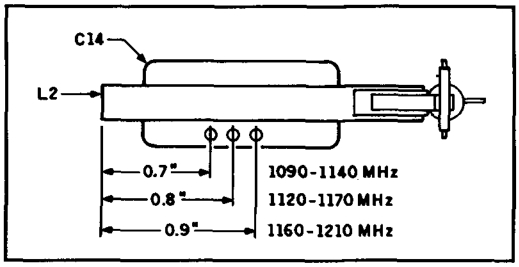

Figure 8. Varactor diode locations.

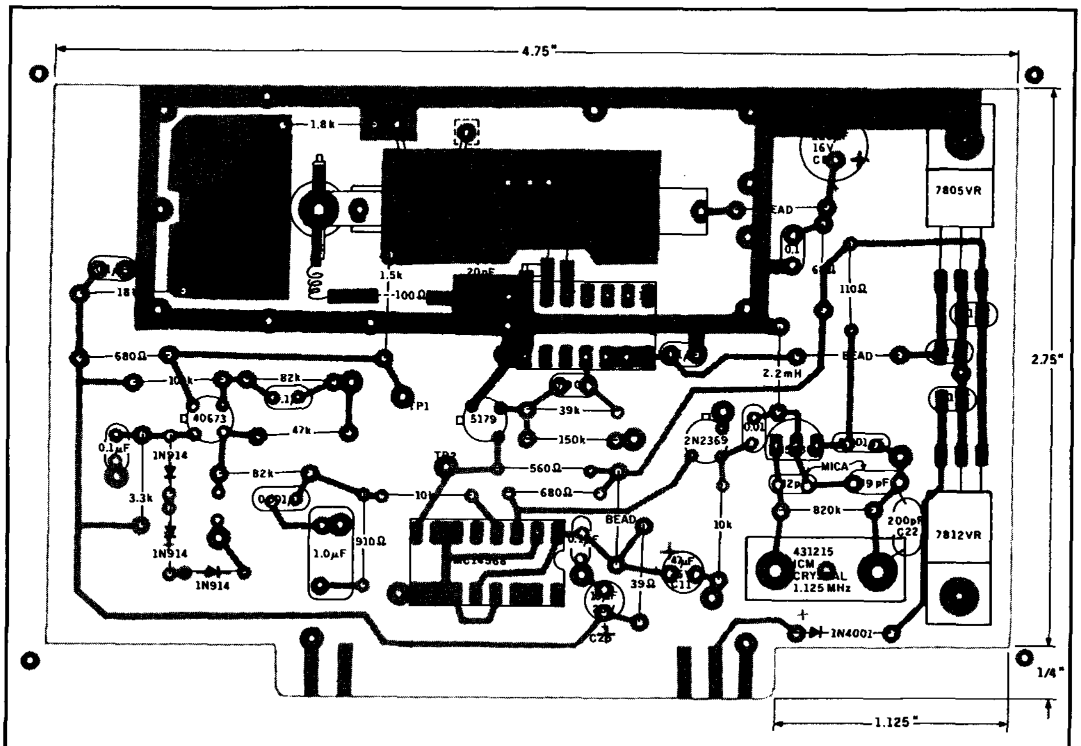

Figure 9. Phantom view showing parts through trace side of pc board.

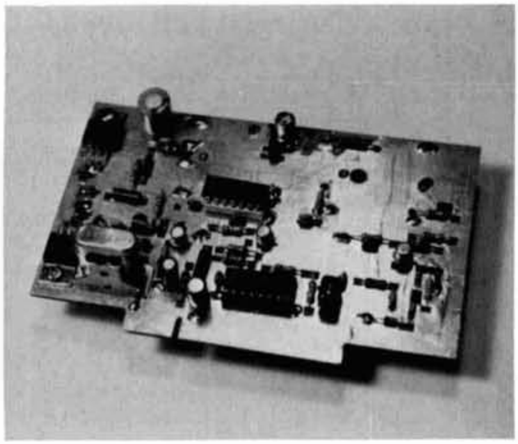

Photo A. Component side of oscillator pc board.

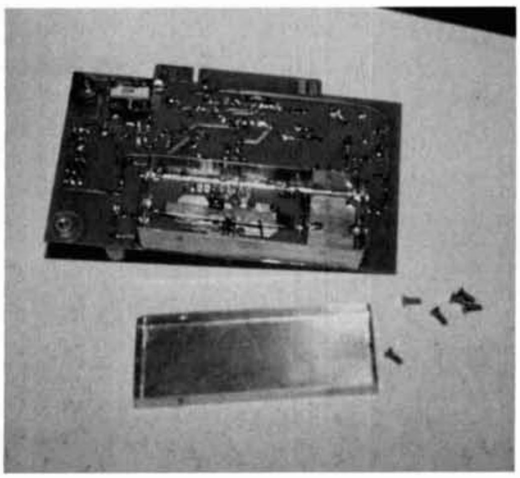

Photo B. Trace side of oscillator pc board, cover removed.

Close up the seam with solder. Add a tight-fitting cover made of 0.020-inch thick aluminum to prevent noise pickup from fluorescent lamps and other sources.

A good quality high-Q crystal is a must. I recommend an ICM crystal, part no. 431215. This number, together with the desired frequency, are all you need to identify the ICM crystal. (See the list of parts suppliers for ICM's address.)

There's nothing critical about the rest of the assembly. **Figure 9** shows parts placement as seen through the board from the trace side. **Photos A** and **B** show both sides of the completed project.

Checking performance

For 1152-MHz operation, the tuning diode control voltage measured between the test point (TP1) of the 3N201 drain and ground should be 6 to 7 volts DC. If the oscillator L-C circuit resonates either too high or too low, phase locking won't occur. The tuning-diode voltage will sit at about 11 volts DC if the frequency is too high, or at about 3.2 volts DC if it's too low. If the crystal is removed from its socket, the diode voltage will be about 11 volts DC.

To correct an out-of-lock condition, increase or decrease the capacitance of emitter-feedback capacitor C13 by bending it closer to, or away from, L2 while monitoring the voltage at TP-1. If the oscillator still won't lock, use the phase-lock tracking curve in **Figure 10** to determine if the L-C circuit frequency is too high or too low.

The curve of **Figure 10** shows the varactor tuning voltage as a function of the oscillator frequency for the phase-lock condition. I created this curve by substituting a signal generator for the reference crystal. As I varied the generator frequency, the UHF oscillator followed the variation. In this case, the tracking range was from 1115 to 1192 MHz. This corresponded to tuning the signal generator from 1.08887 to 1.16406 MHz. The oscillator wouldn't track beyond these points.

If the PLO doesn't appear to be operating properly after you've followed all the instructions given here, you might consider using the following technique. Remove the quartz crystal and solder a 3 or 4-foot long piece of RG-58 across the crystal socket, with braid on ground. Connect the other end to a signal generator. (Measurements Model 65B is ideal for this purpose.) Set the

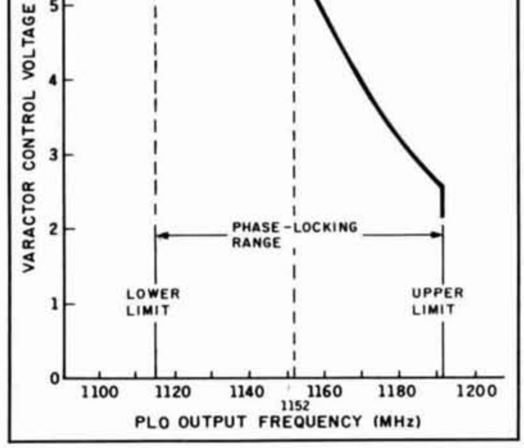

Figure 10. Phase lock tracking range.

output attenuator for 2 to 5 volts peak-to-peak across the crystal socket. Tune the signal generator in search of the tracking range. Multiply the upper and lower frequency limits by 1024 to find out if the oscillator's L-C circuit is tuned too high or too low. Monitor TP-1 to find these limits.

When the oscillator is operating properly, you'll observe a variation in the varactor-control voltage when you move your hand near the oscillator inductance, or when you remove or attach the cover. This variation of about 4 to 8 volts DC indicates that the loop is locked and is compensating for changes in oscillator capacitance. The tuning voltage should be approximately 6 volts DC with the cover attached.

Fine frequency adjustment

The ARCO compression trimmer (C17) shunted across the crystal is used for fine frequency adjustment. To make this adjustment, connect the RF output through a 10-dB pad to a UHF frequency counter and adjust C17 for the desired frequency. If you don't have a UHF counter, couple TP-2 to the input of an HF counter. The frequency at this point will be the UHF oscillator frequency divided by 256. For an 1152-MHz UHF oscillator frequency, this counter should read 4,500.000 kHz when adjusted with C17, bringing the output frequency within 1 kHz of 1152 MHz.

A few comments

You've heard it said "make changes and you're on your own." While this cautionary statement also applies to this project, you should have little or no difficulty getting this PLO to work if you follow the instructions carefully.

I recommend that you purchase your ICs with care. I bought a number of "bargain priced" CA3179s, only to discover they weren't up to full specs and wouldn't divide at 1152 MHz. To make sure you get your money's worth, purchase both the CA3179 and the 14568 from a reputable dealer. I bought my ICs from Schweber Electronics. They have stores in many cities.

On the air tests

The performance of my 1296-MHz converter has never been better. It outperforms all other systems I've used in the past 20 years or so. In fact, two-way SSB contacts are now routine over distances of 200 miles and more, summer and winter.

PARTS LIST

PART	DESCRIPTION/NOTES	SOURCE
C1	*51 pF disc, type 21 CB*	*Mouser*
C2	*0.1 µF monolithic, 50 volt*	*Mouser*
C3	*0.1 µF monolithic, 50 volt*	*Mouser*
C4	*0.1 µF monolithic, 50 volt*	*Mouser*
C5	*0.1 µF, monolithic*	*Mouser*
C6	*2 pF dip mica, prescaler coupling*	*Circuit Specialists*
C7	*22 pF chip*	*Mouser*
C8	*220 µF/16 volt electrolytic*	*Circuit Specialists*
C9	*Etched, base bypass*	
C10	*0.1 µF monolithic, 50 volt*	*Mouser*
C11	*47 µF/25 volt electrolytic*	*Digi-Key*
C12	*20 pF dipped mica*	*Circuit Specialists*
C13	*Variable coupling (see text)*	
C14	*Etched, tuning diode bypass*	
C15	*0.1 µF monolithic, 50 volt*	*Mouser*
C16	*0.001 µF monolithic*	*Mouser*
C17	*Arco 400 compression trim, frequency set*	*Circuit Specialists*
C18	*22 pF dip mica*	*Circuit Specialists*
C19	*39 pF dip mica*	*Circuit Specialists*
C20	*0.01 µF monolithic, 50 volt*	*Mouser*
C21	*0.1 µF monolithic*	*Mouser*
C22	*200 pF dip mica (surface mount)*	*Circuit Specialists*
C23	*1 µF stacked metalized film 50 volt, 5 percent Panosonic*	*Digi-Key*
C24	*0.001 µF monolithic*	*Mouser*
C25	*10 µF/25 volt electrolytic*	*Digi-Key*
C26	*0.1 µF monolithic, 50 volt*	*Mouser*
XTAL	*Reference crystal, 1.125 MHz*	*ICM*
D1	*MV2101 or MV2201, plastic tuning diode 6.8 pF at 4.0 volt DC*	*Circuit Specialists*
D2	*1N4001 silicon, protect diode*	*Circuit Specialists*
D3	*1N914 silicon, alternate: 1N4148*	*Circuit Specialists*
D4	*1N914 silicon, alternate: 1N4148*	*Circuit Specialists*
D5	*1N914 silicon, alternate: 1N4148*	*Circuit Specialists*
L1	*RFC, 4 turns no. 22 enamel copper (see text)*	
L2	*Strip line, UHF oscillator inductance (see text)*	
L3	*RFC Miller part no. 9250-225, 2.2 µH*	*Circuit Specialists*
L4	*Loop, output coupling (see text)*	
R1	*560 ohms, 1/4 watt, 5 percent resistor*	*Jameco*
R2	*39 k, 1/4 watt, 5 percent resistor*	*Jameco*
R3	*150 k, 1/4 watt, 5 percent resistor*	*Jameco*
R4	*1.8 k, 1/4 watt, 5 percent resistor*	*Jameco*
R5	*12 k, 1/4 watt, 5 percent resistor*	*Jameco*
R6	*39 ohms, 1/4 watt, 5 percent resistor*	*Jameco*
R7	*100 ohms, 1/8 watt, 5 percent resistor*	*Jameco*
R8	*1.5 k, 1/4 watt, 5 percent resistor*	*Jameco*
R9	*Deleted*	
R10	*68 ohms, 1/4 watt, 5 percent resistor*	*Jameco*
R11	*680 ohms, 1/4 watt, 5 percent resistor*	*Jameco*
R12	*110 ohms, 1/4 watt, 5 percent resistor*	*Jameco*
R13	*820 k, 1/4 watt, 5 percent resistor*	*Jameco*
R14	*47 k, 1/4 watt, 5 percent resistor*	*Jameco*
R15	*10 k, 1/4 watt, 5 percent resistor*	*Jameco*
R16	*3.3 k, 1/4 watt, 5 percent resistor*	*Jameco*
R17	*680 ohms, 1/4 watt, 5 percent resistor*	*Jameco*
R18	*100 k, 1/4 watt, 5 percent resistor*	*Jameco*
R19	*82 k, 1/4 watt, 5 percent resistor*	*Jameco*
R20	*82 k, 1/4 watt, 5 percent resistor*	*Jameco*
R21	*910 ohms 1/4 watt, 5 percent resistor*	*Jameco*
R22	*10 k, 1/4 watt, 5 percent resistor*	*Jameco*
Q1	*2N5179, bipolar switching transistor*	*Circuit Specialists*
Q2	*MRF-901, UHF oscillator bipolar transistor*	*Circuit Specialists*
Q3	*3N201, dual-gate CMOS (alternate: 40673 or 3N200)*	*Circuit Specialists*
Q4	*2N2369A, bipolar transistor*	*Circuit Specialists*
Q5	*2N5486, JFET transistor*	*Circuit Specialists*
U1	*7812, voltage regulator*	*Circuit Specialists*
U2	*7805, voltage regulator*	*Circuit Specialists*
U3	*CA3179, prescaler ÷ 256 (see text)*	*Motorola*
U4	*MC14568B, phase/frequency, detector/divider*	*Motorola*
FB1	*Ferrite molded bead, 0.138" D, 0.350" L, with pigtails*	*Fairite*
FB2	*Ferrite molded bead, 0.138" D, 0.350" L, with pigtails*	*Fairite*
FB3	*Ferrite molded bead, 0.138" D, 0.350" B, with pigtails*	*Fairite*
J1	*SMA jack, 142-0298-001 (E.F. Johnson)*	*Digi-Key*
PC Board		

I've built six of these PLOs. Two of them are under test in Indianapolis. I make two-way contacts on a regular basis with W9JIY, who also has one. The results have been gratifying. If you're interested in upgrading your homebrew 1296-MHz converter, this new and improved phase-locked local oscillator is for you. ■

REFERENCES

1. Gary A. Breed, Technical Editor, "Mixers: Making the Right Choice," *RF Design*, August 1986, page 24.
2. Joe Reisert, W1JR, "VHF/UHF World: VHF/UHF Receivers," *Ham Radio*, March 1984, page 43.
3. Norm Foot, WA9HUV, "Low Noise Phase-Locked UHF VCO," Parts 1 and 2, *Ham Radio*, July and August, 1986.
4. Norm Foot, WA9HUV, "Multipurpose Voltage-Tuned UHF Oscillator," *Ham Radio*, December, 1980, page 12.
5. Norm Foot, WA9HUV, "Simplifying the Multipurpose UHF Oscillator," *Ham Radio*, September 1981, page 26.
6. Norm Foot, WA9HUV, "UHF GaAsFET Doubler," *Ham Radio*, April 1989, page 65.
7. Dave Mascaro, WA3JUF, "Making Printed Circuit Boards," *Ham Radio*, January 1990, page 27.

Parts suppliers

Fred Reimers, N9ATW
Far Circuits
18N640 Field Court
Dundee, Illinois 60118*

Digi-Key
701 Brooks Avenue South
P.O. Box 677
Thief River Falls, Minnesota 56701-0677

Mouser Electronics, (West Coast)
11433 Woodside Avenue
Santee, California 92017

Mouser Electronics, (East Coast)
12 Emery Avenue
Randolph, New Jersey 07869

ICM
P.O. Box 26330
701 W. Sheridan
Oklahoma City, Oklahoma 73126-0330

Circuit Specialists, Inc.
P.O. Box 3047
Scottsdale, Arizona 85271-3047

*To purchase a pc board, send $9.50 plus $1.50 per order for shipping and handling.

James Melton, *KF5NL*
2747 Wentworth Drive
Grand Prairie, Texas 75052

CW CALLSIGN DECODER

No need to stick by the radio waiting for a call when you use this decoder/alarm system

When I'm in my garage fooling around with one thing or another, I listen in on one particular frequency for my Dad to call. I have two young children, so scheduling with him is almost impossible. Our hit-or-miss attempts at communications usually required that one or the other of us give a call on landline, to tell the other to get on the air! What we wanted was something that would alert us if either of us gave a radio call to the other – something that was useful within the Amateur Radio rules.

I needed a device that was active (listening) at all times, could selectively decode a signal meant for me, and give some kind of audible signal (like ringing a bell) so I didn't have to monitor the radio in person. I thought of using a commercially available DTMF decoder, but SSB reception doesn't have the frequency stability that DTMF requires – especially when using an inexpensive receiver, as I plan to do in the future. In the end, I came up with a CW decoder which doesn't require such strict frequency stability. It monitors a selected audio frequency, decodes a CW signal sent at 5, 10, or 20 wpm, and sets off an alarm when it decodes my callsign. Best of all, I can have it in service 100 percent of the time, and if band conditions are bad, I can turn off the speaker and still be monitoring the frequency.

Design goals

I wanted a design that anyone could build. The CW decoder doesn't require an

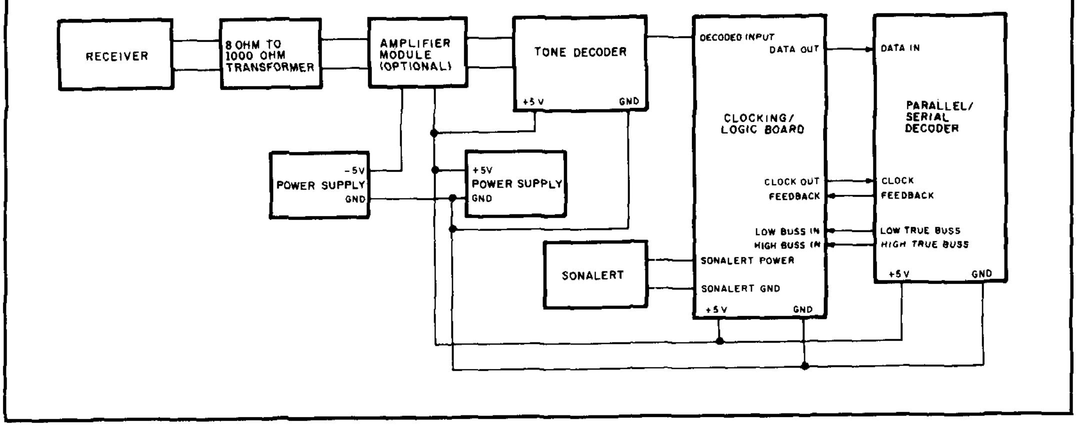

Figure 1. Interconnection diagram for the different modules of the CW Callsign Decoder.

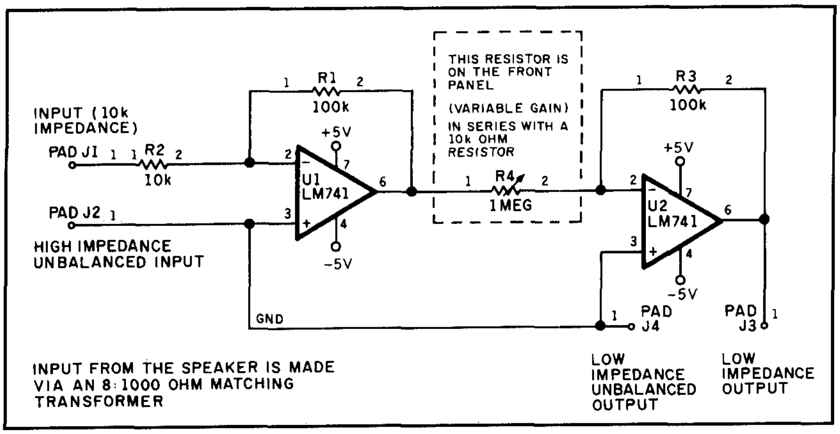

Figure 2. Input amplifier. This unit is optional, depending on your application.

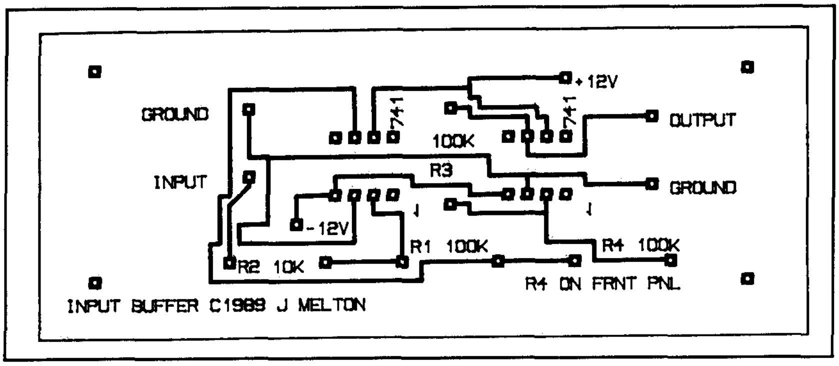

Figure 3. PC board layout for the input amplifier.

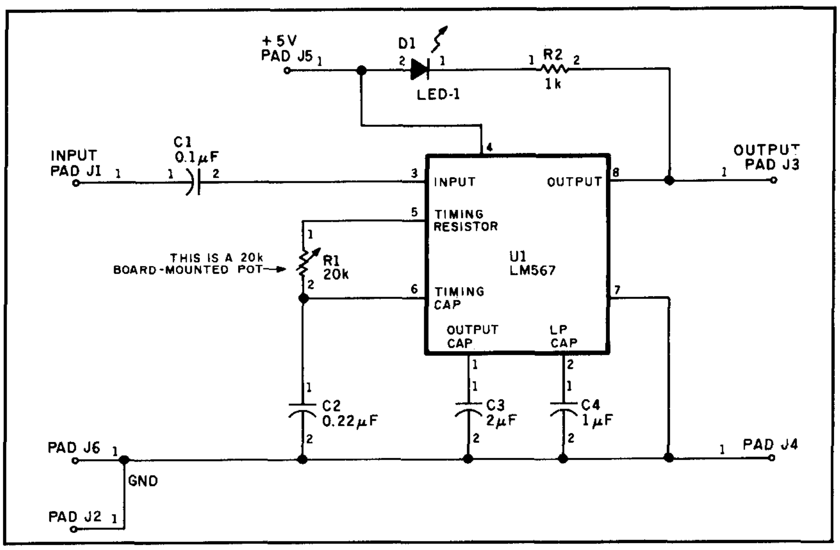

Figure 4. Tone decoder board.

EPROM (it's hard-wire programmed) or circuit boards. Circuit board layouts are provided for those who prefer this method and have the means to produce them, but this is a very low speed circuit which works fine if wire wrapped.

A quick note on the circuit board modules is in order. I made this project using separate modules for several reasons. First, because certain functions are universal to most projects, some of the boards are meant to be "universal" in their application. The input board, power supply, and tone decoder board all fit this description. Second, breaking the boards into modules made the circuit board layout many times easier, allowing me to design them faster, and making it easier to produce the finished project. Last, it's easier to mount several small boards in the space available than it is to put all the circuits on one big board and find a box big enough to hold it.

I eventually plan to put this decoder into a box with a 40-meter crystal controlled receiver, so I can leave it on all the time. Right now I take my radio down whenever I'm not there, or when a lightning storm threatens – a frequent occurrence in this part of Texas. If I'm using a cheaper receiver, I'll be more willing to let the receiver/decoder ride out the storm without powering down, and I'll be more likely to leave it in operation when I'm not actively hamming. It's crossed my mind that by leaving the decoder on all the time, I could easily let the output drive both the alarm and a relay that would energize a cassette recorder. This way I could record the callsign of the calling party (assuming it was someone other than my Dad) and give them a call back at a later time.

Circuit operation (Figure 1)

This device hooks into the audio line of your receiver, generally in parallel with the speaker, or instead of the speaker, if you have a dedicated receiver. It takes a 700 to 800-Hz tone from the audio and amplifies it before passing the signal on to a 567 tone decoder. The 567 tone decoder module converts the tone into a logic level signal that's passed to the clocking and decoding circuits. The clocking circuit is designed to pass clock pulses to the serial-to-parallel circuit as long as the signal is high, and one additional clock after the signal goes low. The clocking signal and the decoded tone signal are both passed on to the serial-to-parallel decoder board, where the logic is designed to signal when the incoming data matches a preset parallel output. When a match is found, the decoder drives an alarm for approximately 30 seconds.

Input board (Figures 2 and 3)

Audio from the receiver is tied to the input and ground pads of the input board via an 8:1000-ohm matching transformer. This board uses two general purpose op amps (741s) wired as voltage inverters and hooked in series. The feedback from R1 and R2 provides a *(10) voltage gain through U1, which is then fed to the second stage. The second stage uses a 10-k resistor in series with front-panel mounted R4 (1 meg) and R3 (100 k) to provide a voltage gain of *(0.1) through *(10). It also provides a low impedance output circuit. The combination of *(10) and *(0.1 through 10) gives a net voltage gain of 1 through 100. This allows operation with your receiver set at various volume levels. If you don't have enough gain, you can substitute a 1000-ohm resistor

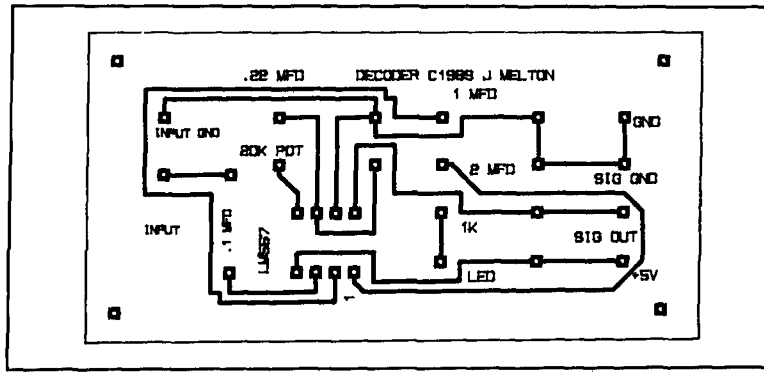

Figure 5. PC board layout for the tone decoder board.

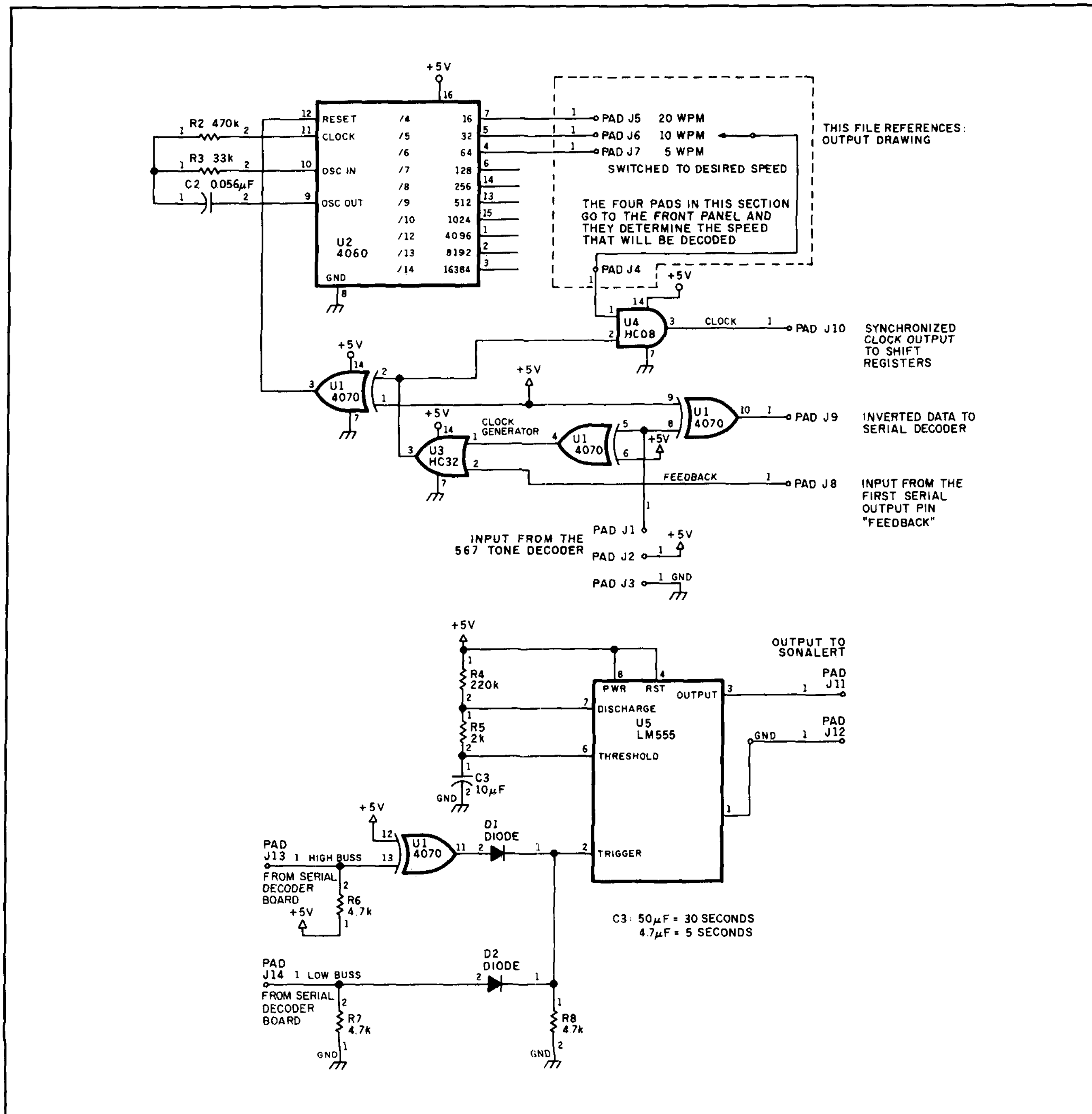

Figure 6. Logic board.

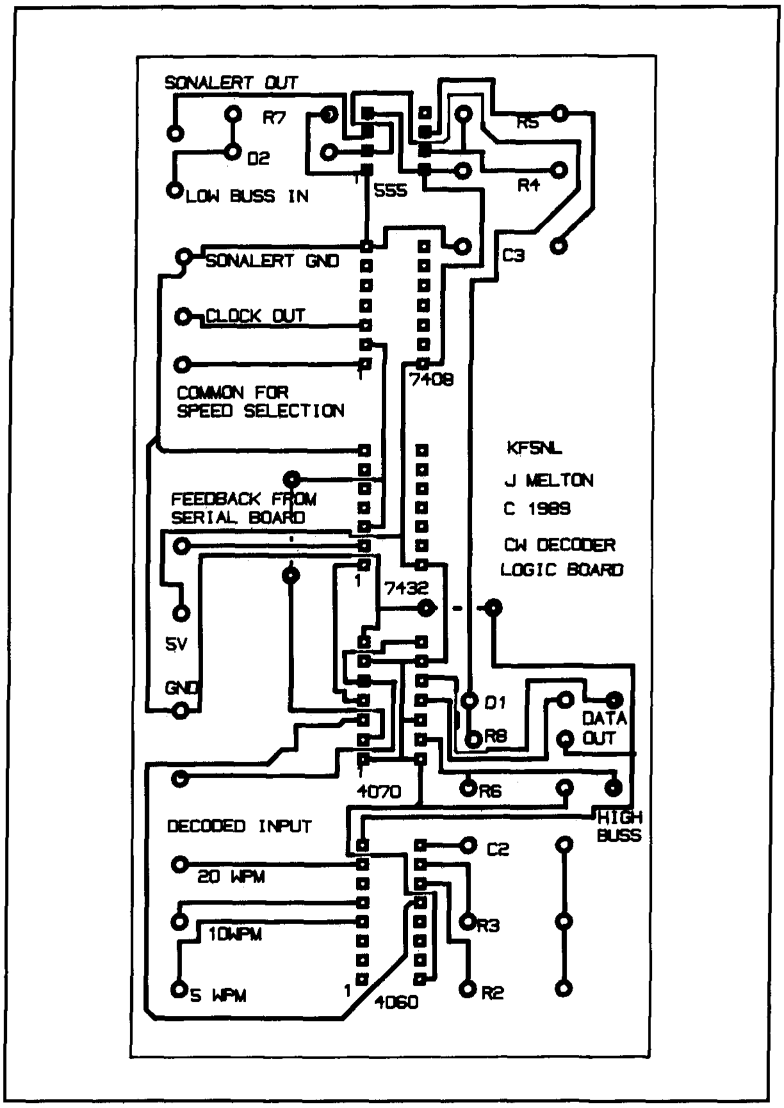

Figure 7. PC board layout for the logic board.

for R1. Doing so will give you a *(1) through *(1000) gain on this board. When you build this project, I suggest that you build the amplifier section last. I don't use the amplifier section on my decoder; but, if you need it, the board layout is included (see **Figure 3**). I suggest that you hook the input board in parallel to the speaker of your receiver so you still have audio. But if you desire silent operation, hook the input to your receiver using a headphone jack.

Tone decoder (Figures 4 and 5)

The tone decoder board is another "general purpose" board which is useful in many other projects. In this application, I use it as the tone decoder for the audio from my receiver. It's set to decode a signal from 700 to 800 Hz, which is where I like to listen to CW. If you prefer a different frequency, you can change it easily by using a pot for R1. In any case, the 567 (U1) will give you a reasonably wide detection band. The output of the 567 goes low whenever it receives a tone and then lights D1, an LED mounted on the front panel of the decoder, so you can tell when the box is decoding a signal. It's also useful for determining the correct volume level, because you want the input volume set so you can just barely detect the normal noise level (LED barely flashing).

Main logic board (Figures 6 and 7)

The main logic board consists of three separate functions. First, the clocking section derives a clock for the serial-to-parallel converter. Second, it accepts two inputs from the serial-to-parallel board and drives an alarm (the "Sonalert") based on the condition of these two lines. Third, it accepts the output from the tone decoder and inverts it with a gate from U1 before sending it to the CW decoder.

I'd like to discuss the clocking in greater detail. You're looking for a clock to the serial board if the output from the tone decoder is active (low) or if the last bit clocked into the serial board was high. U2, a 4060, is driven by an internal oscillator whose frequency is set by R2, R3, and C2 so that it's at approximately the "dit-space" data rate. The oscillator is held in reset until data is received from the 567 decoder board. When the 4060 is released (from incoming data), the first rising edge of the output occurs in the middle of the incoming data. This gives you some margin for error in the sending speed and quality. During a "dash," the incoming data line is held low (and inverted for the CW decoder) and the 4060 (U2) is allowed to clock in three high pulses to the serial board. After each valid "bit" of data, the 4060 is allowed to clock in one more bit – the low bit which follows. In some cases there will only be one low bit following a data bit; in most cases there will be more than one. In any case, only one bit is allowed into the serial-to-parallel decoder.

The first three outputs of the 4060 provide clocks for 20, 10, and 5 wpm. Should you desire a different set of speed ranges, you can change C2, R2, and R3 on the main logic board to suit the speed ranges you desire. The speed you use depends on the noise level and the skill of the transmitting station. (Some allowance is made for slightly sloppy sending, but if you're using a straight key, you'll have to send very good copy to be received correctly). I don't recommend going faster than 20 wpm, and 5 wpm is as slow as is necessary to decode all but the noisiest of signals. The clock

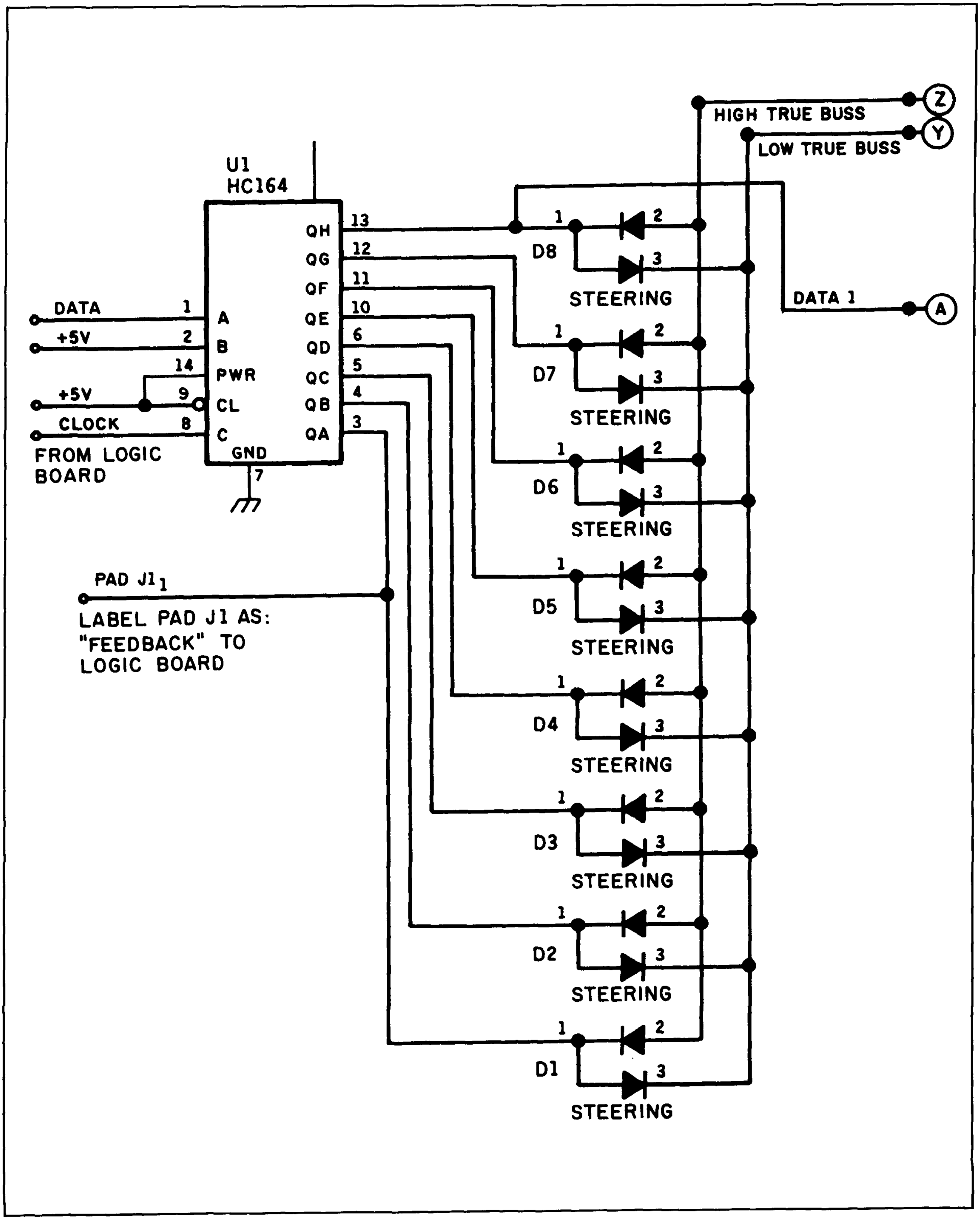

Figure 8. Serial-to-parallel decoder board. You "hard wire" program your callsign on this board.

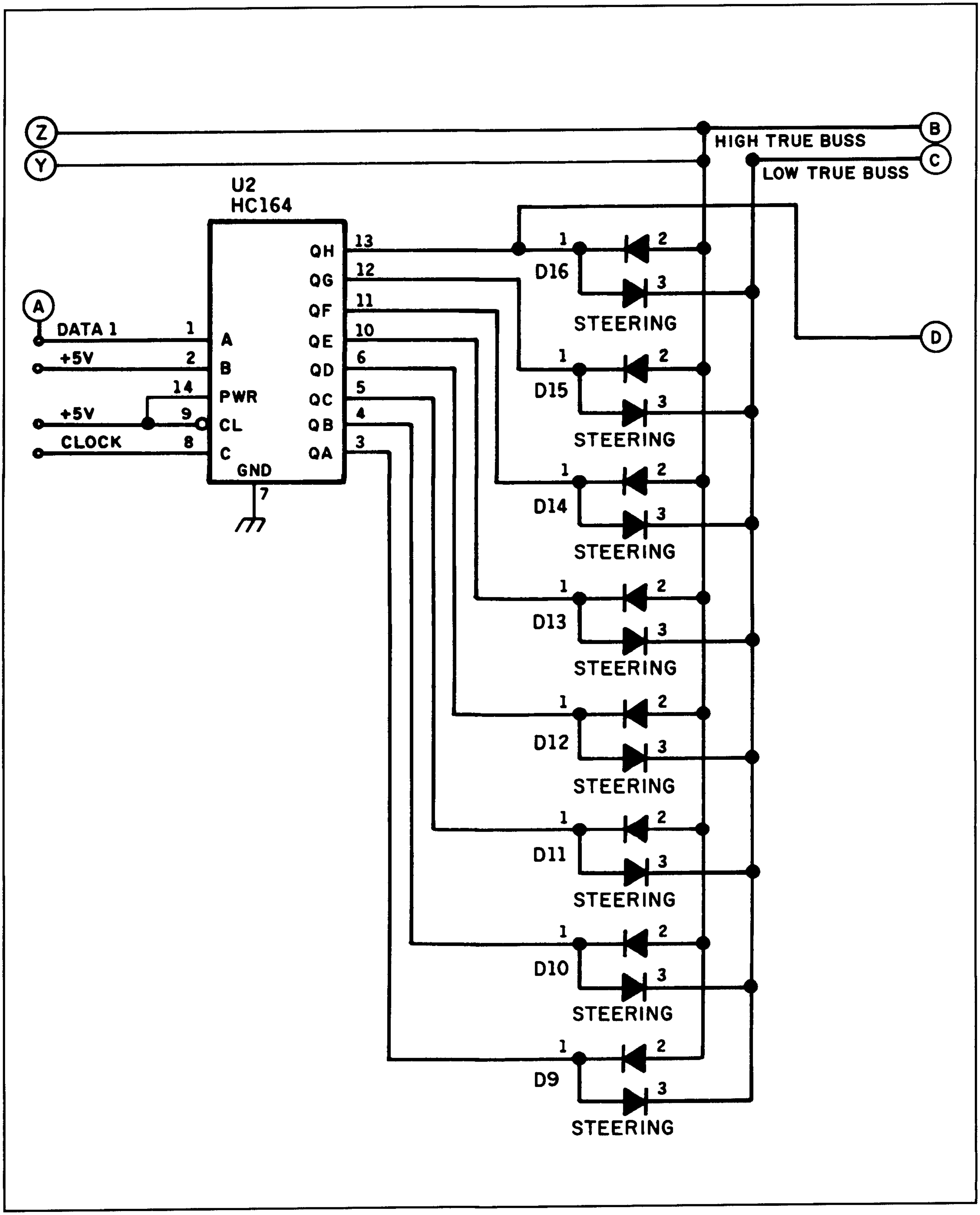

Z
Y
B
C
HIGH TRUE BUSS
LOW TRUE BUSS
U2
HC164
A
DATA 1
+5V
+5V
CLOCK
A
B
PWR
CL
C
GND
QH
QG
QF
QE
QD
QC
QB
QA
D
D16
D15
D14
D13
D12
D11
D10
D9
STEERING

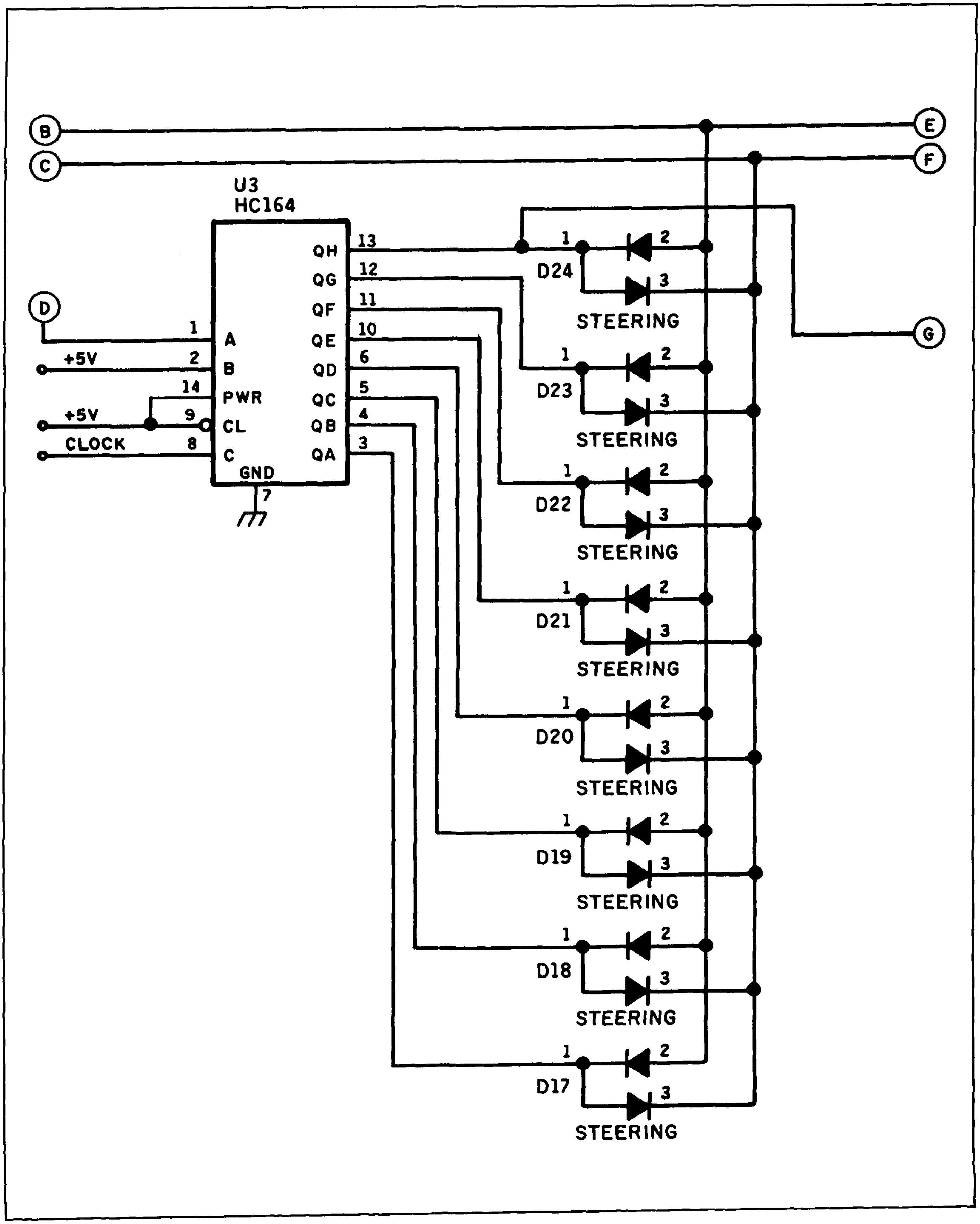

B
C
E
F
G
D
U3
HC164
QH
QG
QF
QE
QD
QC
QB
QA
13
12
11
10
6
5
4
3
1
A
+5V
2
B
14
PWR
+5V
9
CL
CLOCK
8
C
GND
7
D24
D23
D22
D21
D20
D19
D18
D17
STEERING

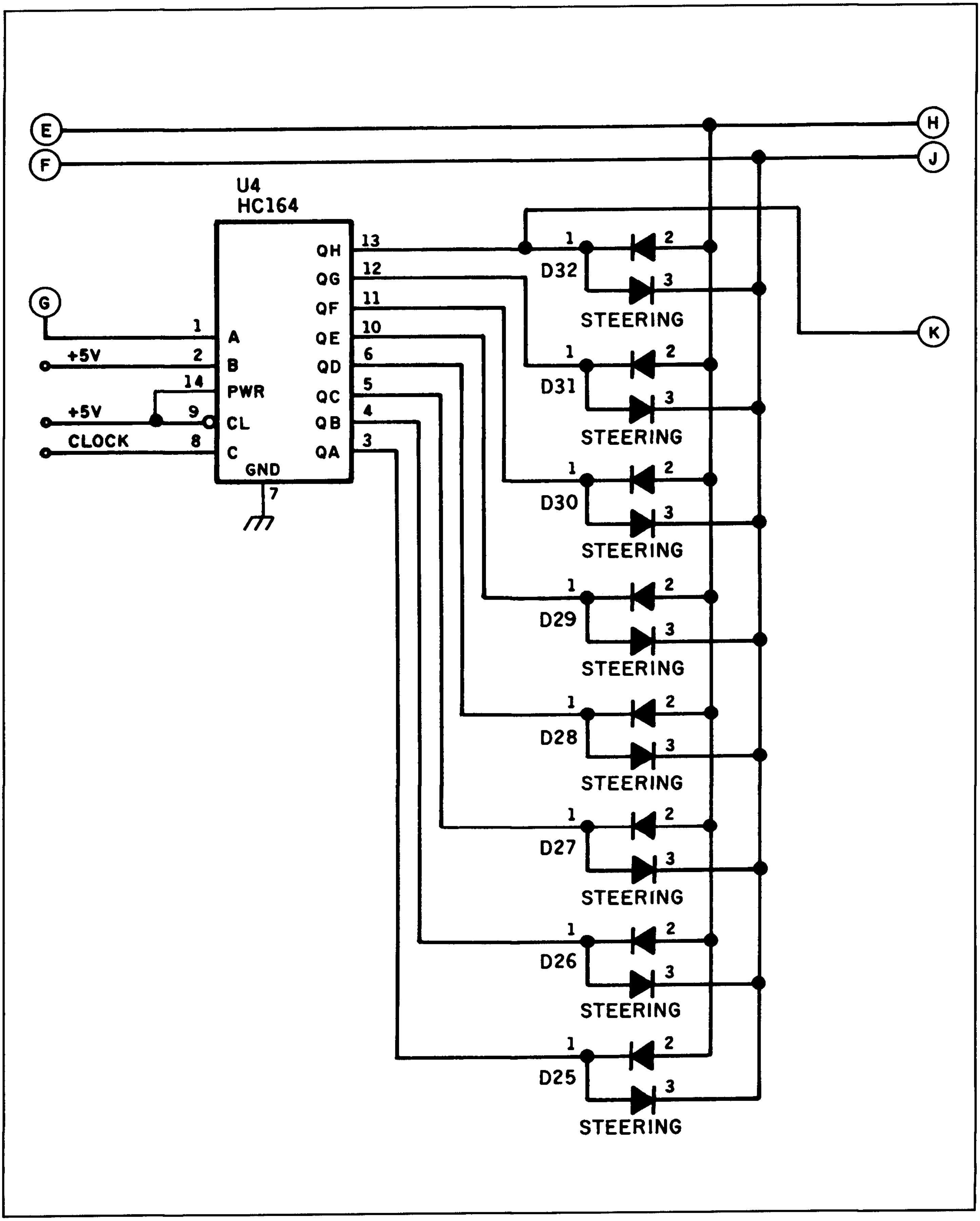
E
F
H
J
G
K
U4
HC164
A
B
PWR
CL
C
GND
QH
QG
QF
QE
QD
QC
QB
QA
+5V
+5V
CLOCK
D32
D31
D30
D29
D28
D27
D26
D25
STEERING

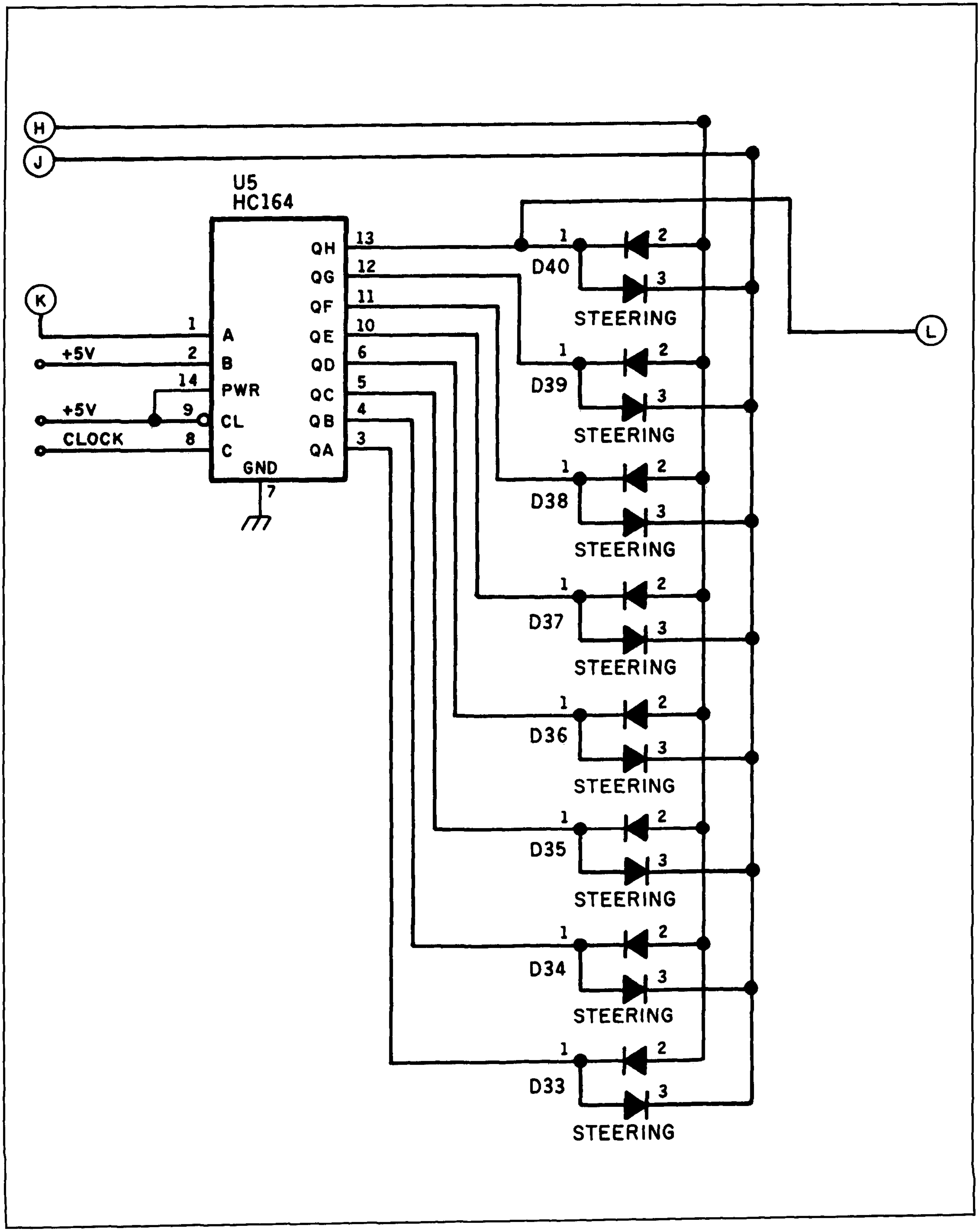
H
J
K
L
U5
HC164
A
B
PWR
CL
C
GND
QH
QG
QF
QE
QD
QC
QB
QA
1
2
14
9
8
7
13
12
11
10
6
5
4
3
+5V
+5V
CLOCK
D40
D39
D38
D37
D36
D35
D34
D33
STEERING

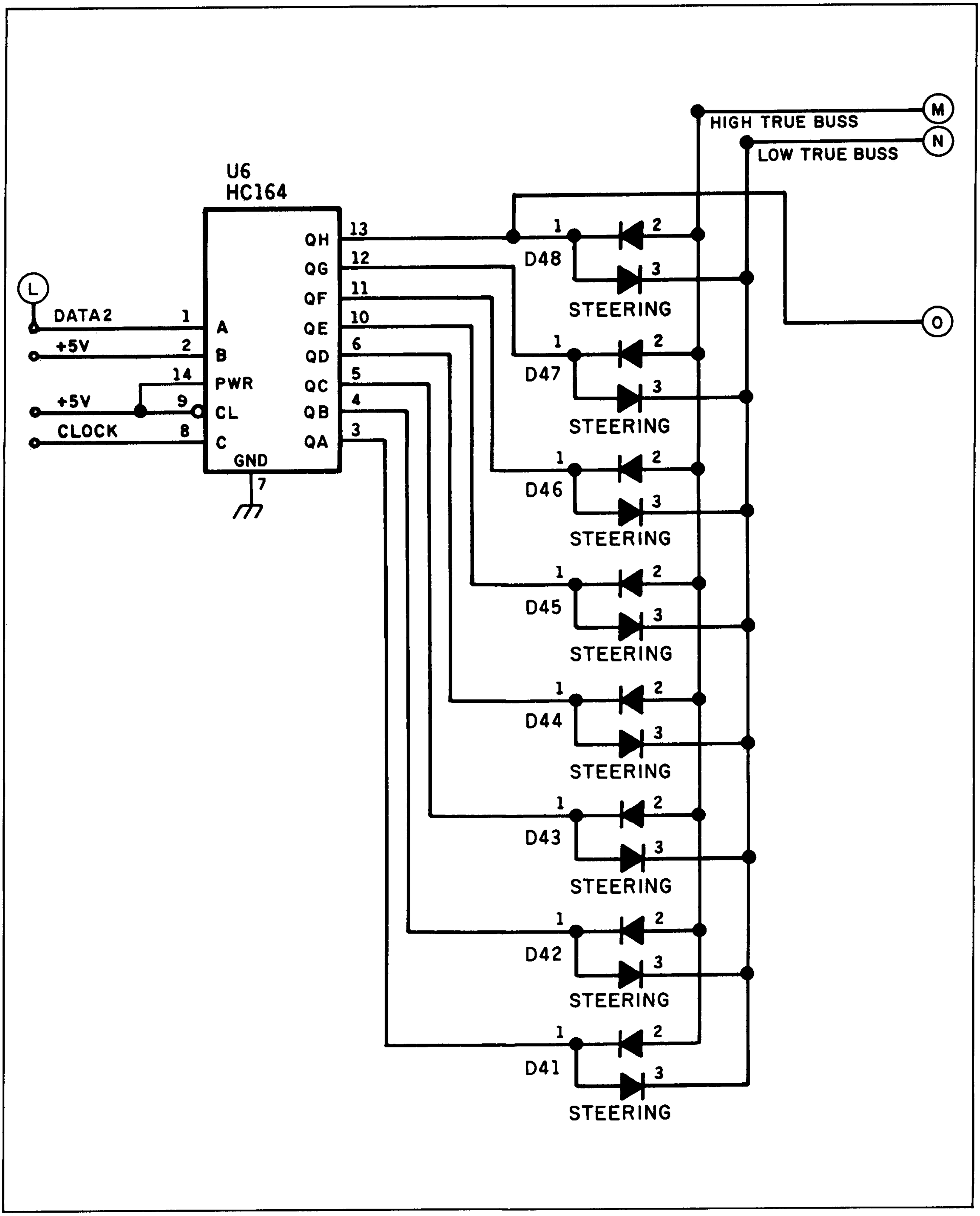
U6
HC164
QH
QG
QF
QE
QD
QC
QB
QA
A
B
PWR
CL
C
GND
13
12
11
10
6
5
4
3
1
2
14
9
8
7
L
DATA2
+5V
+5V
CLOCK
HIGH TRUE BUSS
LOW TRUE BUSS
M
N
O
D48
D47
D46
D45
D44
D43
D42
D41
STEERING
STEERING
STEERING
STEERING
STEERING
STEERING
STEERING
STEERING

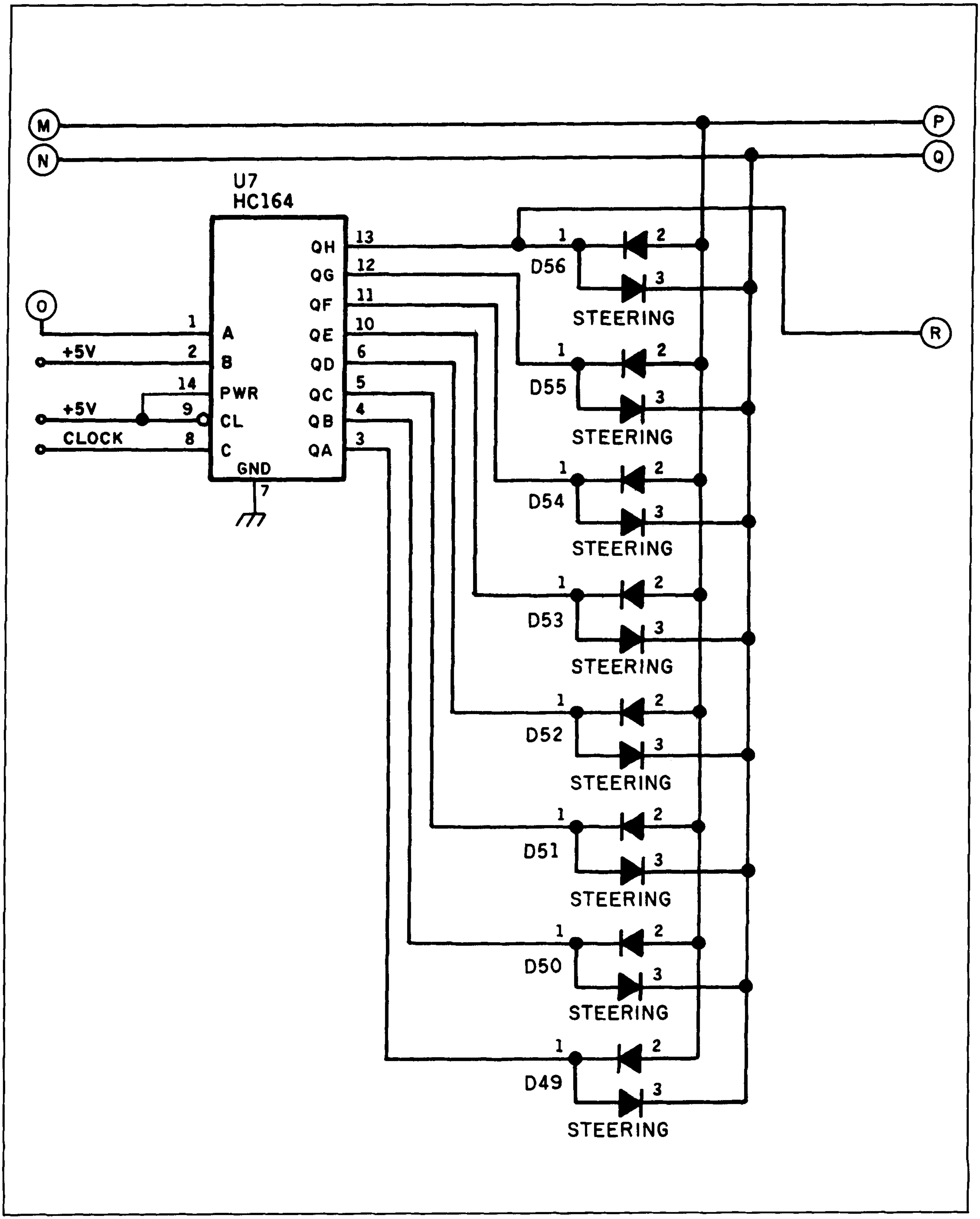
M
N
P
Q
R
O
U7
HC164
QH
QG
QF
QE
QD
QC
QB
QA
A
B
PWR
CL
C
GND
+5V
+5V
CLOCK
1
2
14
9
8
7
13
12
11
10
6
5
4
3
D56
D55
D54
D53
D52
D51
D50
D49
STEERING

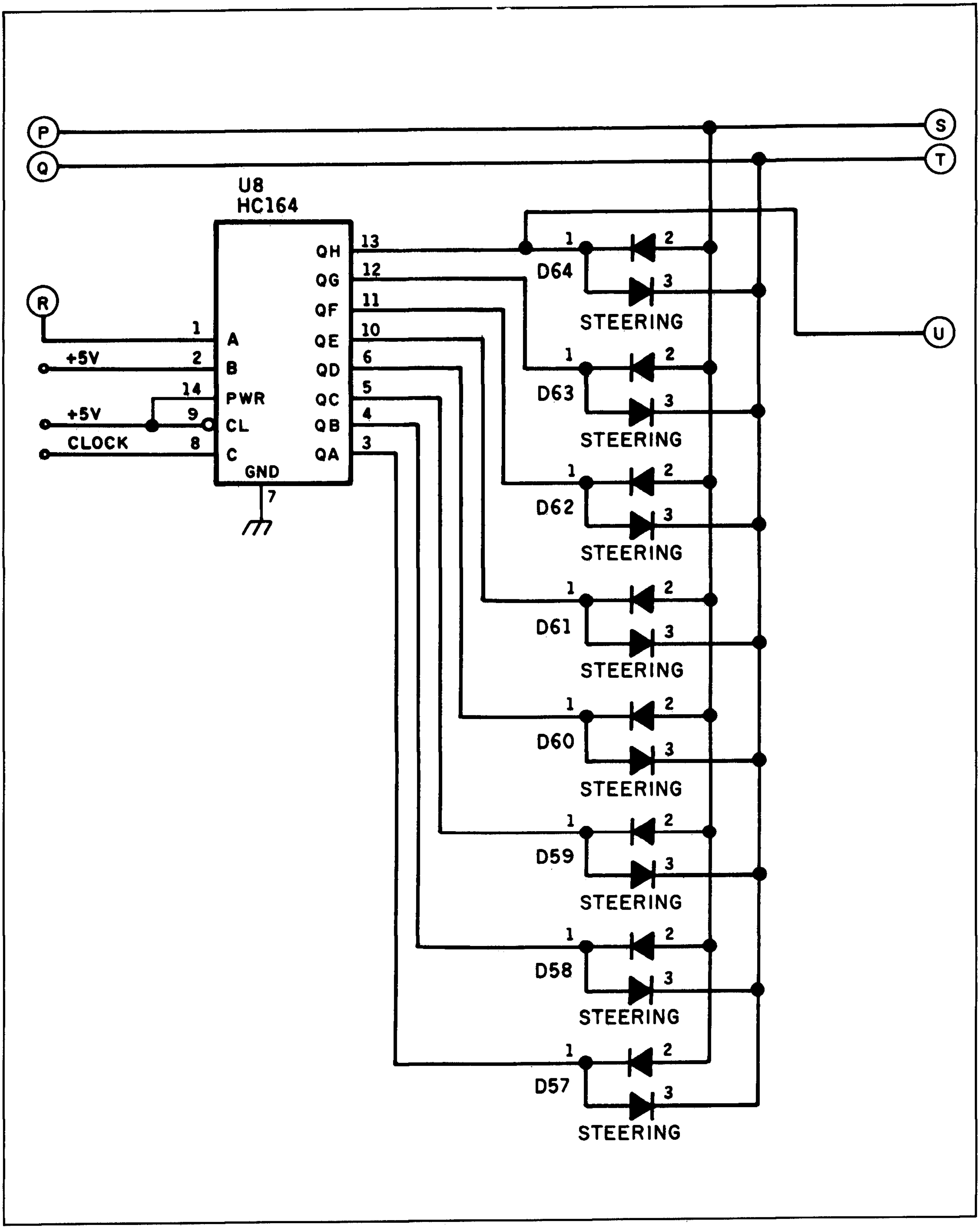
P
Q
S
T
U
R
U8
HC164
QH
QG
QF
QE
QD
QC
QB
QA
A
B
PWR
CL
C
GND
+5V
+5V
CLOCK
D64
D63
D62
D61
D60
D59
D58
D57
STEERING

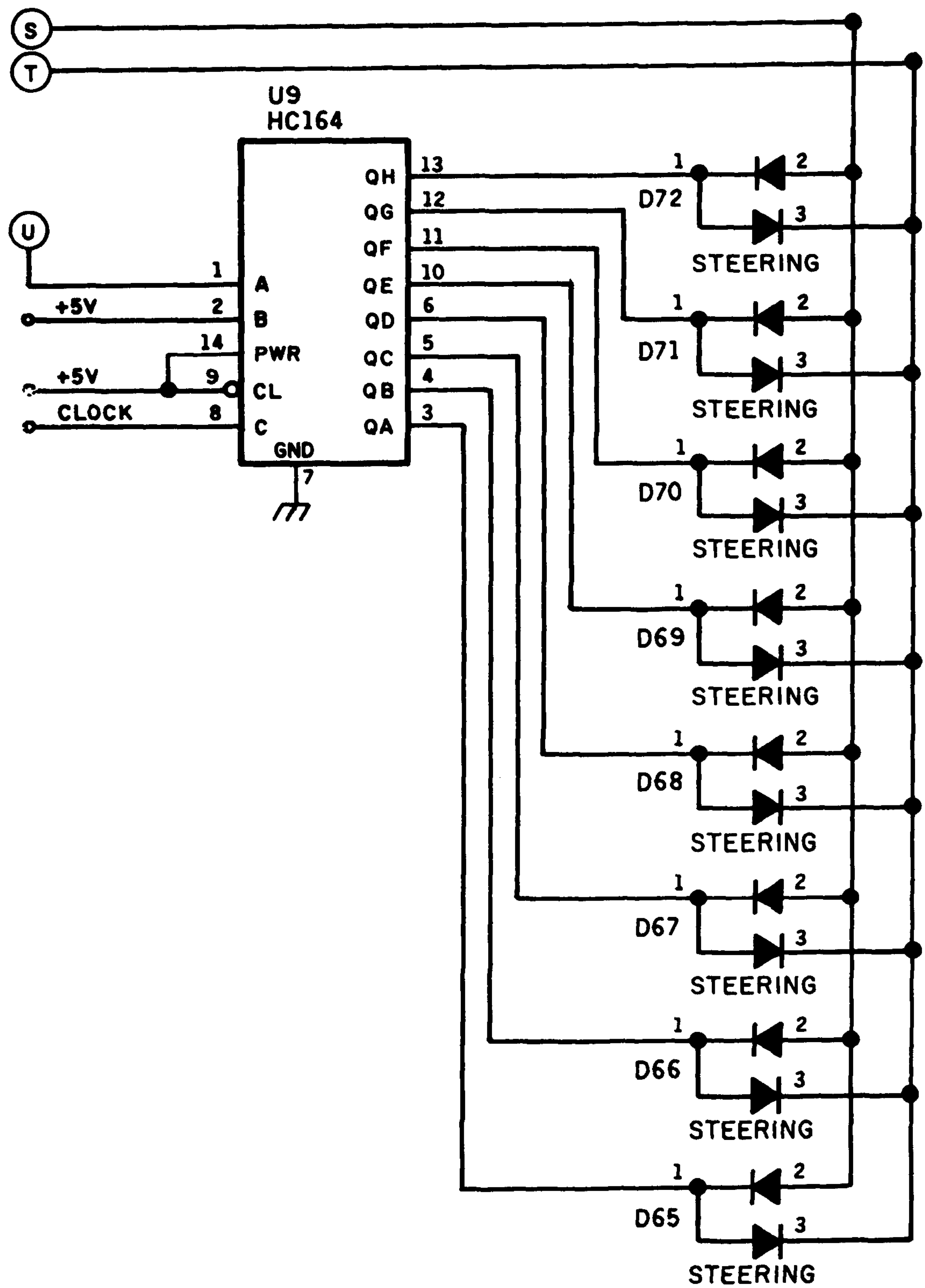
S
T
U9
HC164
U
A
B
PWR
CL
C
GND
QH
QG
QF
QE
QD
QC
QB
QA
+5V
+5V
CLOCK
1
2
14
9
8
7
13
12
11
10
6
5
4
3
D72
D71
D70
D69
D68
D67
D66
D65
STEERING

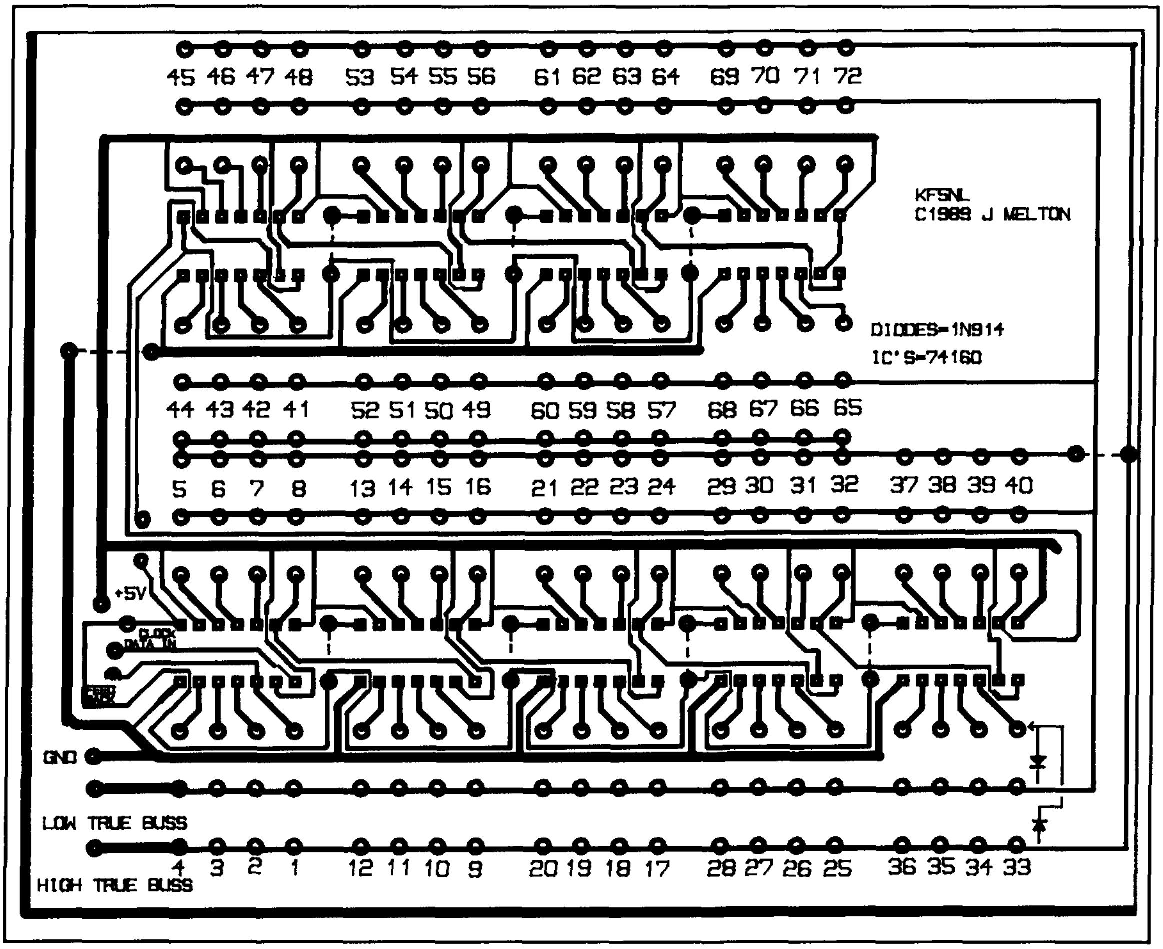

Figure 9. PC board layout for the serial-to-parallel decoder board.

board decodes the output from the serial-to-parallel board by sending a low pulse to the 555 (U5) whenever the high bus is high and the low bus is low via the logic in U1, a quad exclusive OR gate. The low pulse triggers the 555 timer. This provides a 30-second output used to drive an alarm which notifies you when your callsign has been decoded.

CW decoder (Figures 8 and 9)

On the CW decoder board, the serial data stream is converted to a parallel format. The incoming serial data is sent to U1 (a serial-to-parallel converter) and an appropriate clock is presented to U1-U9 on the CW decoder board. U1's last parallel data bit is tied to the data in of U2, U2's last bit is tied to U3, and so on down to U9. The common clock causes the incoming data stream to run from U1 through U9 and the output of these ICs is presented to the steering diodes as a 72-bit wide parallel word. Only one steering diode of the pair shown is used for each bit position. If the word presented to the array is the one you have programmed into the diodes, then the high bus will be released to go high and the low bus will be allowed to go low, pulling the trigger input of U8 on the clock board low and setting the 555 to drive an alarm.

Programming the decoder

Programming the diode array involves a little paperwork. The clocking circuit drives the serial-to-parallel chips at the selected data rate for the "dits" of the message. It relies on the 1:3:1 ratio of dits:dahs:spaces to decode the callsign. The logic board eliminates spaces between letters, and *any spaces that are received are treated as if they were just one bit long.* This is an important point to remember when programming. When you are preparing to program this card, do not put in more than **one diode per space**. The logic board allows you to use only one bit for a space, no matter how long it lasts.

I'll use my callsign, KF5NL, as a design example. Write KF5NL down on a piece of paper and then break the letters down into dits, spaces, and dahs directly underneath.

```
"HLHLHHHLHLHLHHHLHLHLHLHLHLHLHHHLHLHLHHHLHLHHH"
          111111111122222222223333333333444444
1234567890123456789012345678901234567890123456789012345
```

Figure 10. Diode placement pattern.

Write in three hyphens for a dash, a single space for **any** space (again, regardless of whether it would really be one or three "normal" clock periods), and one hyphen for every dit. "K" would be "--- - ---", "F" would be "- - --- -", "5" would be "- - - - -", and so on. Now take all these components of the letters and string them together, allowing only one space between letters:

K F 5 N L
"--- - --- - - --- - - - - - - - - - --- - - --- - -"

This pattern corresponds to the arrangement of diodes on the CW Decoder, with the exception that diode position "1" on the board represents the last data bit because that's the direction in which you are clocking. The dashes represent diodes that should be connected to the high bus; the spaces represent diodes that should be connected to the low bus. My callsign, then, would be:

"HHHLHLHHHLHLHLHHHLHLHLHLHLHLHHHLHLHLHHHLHLH"

On the decoder board, the diodes are labeled from the first clocked position towards the last, and the first diode will contain the **latest** or **last** data bit. In other words, the **last** valid bit is in the position marked "**first.**" This means that the pattern above should be programmed in reverse order. Starting with the diode labelled "1" on the board, you'd put in the diodes as shown in **Figure 10.**

The other diode positions should be left blank. Any chips (74164s) that aren't used on the decoder board can be left off the decoder.

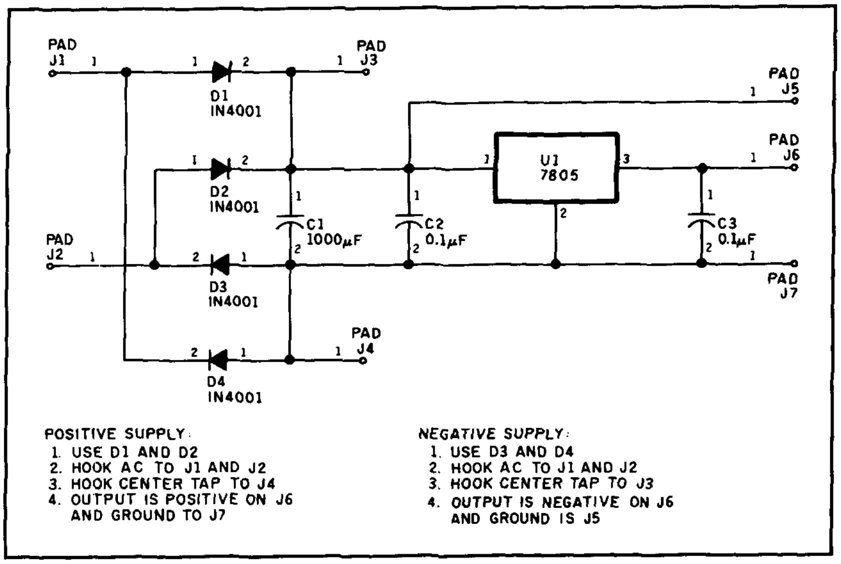

Figure 11. Power supplies. Two of these are required to run the decoder — one positive, one negative.

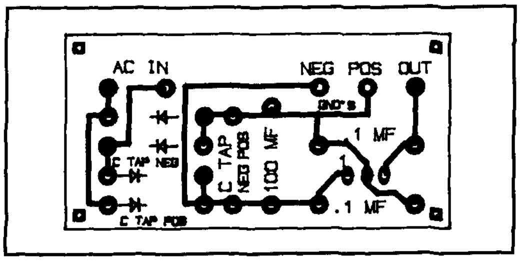

Figure 12. PC board layout for the power supply.

Power supply (Figures 11 and 12)

The power supply for this project may be the most generally useful of any of the multi-use boards. Not all projects require a tone decoder or an amplifier stage, but all do require some type of power supply. This circuit board is designed so that it can be used with positive or negative three-terminal regulators of the 78xx/79xx variety. It provides full-wave rectification for both center tap and regular transformers. If you need a split supply, like the one required by the decoder, you can use two of these boards with a center tap transformer and get full-wave rectification on both the positive and negative supplies.

Tuning the CW decoder

The 567 tone decoder board is the only board that requires any tuning. To set the center frequency of the decoded signal, measure the frequency on pin 5 of the 567 and adjust R1 until you read the frequency you desire. I like to decode 800 Hz because that's the center frequency of the narrow filter on my HF rig.

Alternatively, if you don't have a frequency counter, you can set your 567 center frequency by injecting a signal of the proper frequency (800 Hz in my case) into the tone decoder and adjusting the pot until the LED glows. This technique would be useful if you didn't know the precise center frequency of your receiver because you can adjust the 567 using a live signal off the air, and you don't have to know the frequency.

Conclusion

I hope that your CW decoder gives you as much satisfaction as mine gives me. I know you've heard this many times, but you won't appreciate how much fun it is to use a piece of equipment until you're using something you built yourself. Getting this project built "in my mind" was very simple. But the things I learned on the way to the completion of an actual working model are easily as valuable as the equipment itself. I want to thank two people who were instrumental in helping me complete this project, Jim Melton, WR5B, (the **goading** light) and Ken Thomas, WB5DDN, (the guru's guru). ■

PARTS LIST

AMPLIFIER	
R1,R3	*100-k, 1/8-watt, 10-percent resistor*
R2	*10-k, 1/8-watt, 10-percent resistor*
R4	*1-meg panel mounted pot in series with 10-k, 1/8-watt 10-percent resistor*
U1,U2	*LM741 op amp*
TONE DECODER BOARD	
R1	*20-k, 20-turn potentiometer*
R2	*100-ohm, 1/4-watt, 10-percent resistor*
C1,C4	*0.1-μF, 25-volt ceramic capacitor*
C2	*0.22-μF, 25-volt ceramic capacitor*
C3	*0.2-μF, 25-volt ceramic capacitor*
D1	*Red light-emitting diode*
U1	*LM567 tone decoder chip*
CLOCKING/LOGIC BOARD	
R6-R8	*4.7-k, 1/8-watt, 10-percent resistor*
R2	*470-k, 1/8-watt, 10-percent resistor*
R3	*33-k, 1/8-watt, 10-percent resistor*
R4	*220-k, 1/8-watt, 10-percent resistor*
R5	*2-k, 1/8-watt, 10-percent resistor*
C2	*0.056-μF, 25-volt ceramic capacitor*
C3	*50-μF (30-second alarm) or 4.7-μF (5-second alarm), 25-volt electrolytic capacitor*
D1,D2	*1N4001 general purpose diodes*
U1	*4070 quad XOR gate*
U2	*4060 oscillator/counter*
U3	*74HC32 quad OR gate*
U4	*74HC08 quad AND gate*
U5	*LM555 timer chip*
Misc	*single pole, three-position rotary switch*
SERIAL-TO-PARALLEL CONVERTER	
D1-D72	*Steering (programming) diodes 1N914 (see text)*
U1-U9	*74HC164 serial-to-parallel shift registers*
POWER SUPPLIES	
D1-D4	*1N4001 diodes (see text)*
C1	*100 to 470-μF, 50-volt electrolytic capacitors (see text)*
C2,C3	*0.1-μF, 25-volt ceramic disc capacitors*
U1	*7805 or 7905 T0220 voltage regulator*

By Bob Atkins, *KA1GT*
103 Division Avenue
Millington, New Jersey 07946

RADIO PROPAGATION BY TROPOSPHERIC SCATTERING

A reliable propagation mode for working VHF/UHF/microwave DX

The nature of radio frequency propagation changes considerably as we move from HF, through VHF/UHF, to the microwave bands. At HF frequencies, propagation is mainly via ground wave or reflection and scattering from layers in the ionosphere. As frequency increases into the VHF and UHF region, other modes like E skip, troposcatter, meteor scatter, auroral reflection, EME transequatorial (TE) propagation, and various forms of ducting come into play. At microwave frequencies, the main propagation modes are line-of-sight, ducting, and tropospheric scatter. W1JR covered the basics of many of these propagation modes in the July and August 1986 "VHF/UHF World," columns in *Ham Radio*, and I refer readers to those columns for a good overview of the subject. In this article, I'd like to take a closer look at tropospheric scatter – the most reliable propagation mode for working VHF/UHF/microwave DX.

Propagation modes

Line-of-sight operation will, in general, give the strongest signals for a given path length, but line-of-sight paths are limited in both number and length. Ducting, the trapping of signals in a waveguide-like duct formed by atmospheric layers of different refractive index, can propagate VHF/UHF/microwave signals with very little loss over long distances. Unfortunately, ducting is rare and relatively unpredictable, and it's difficult to calculate the magnitude, length, and frequency characteristics of a duct in advance. Propagation by E skip, auroral, and trans-equatorial modes is also unpredictable and limited in frequency and duration. Communication via meteor scatter is possible on a fairly reliable basis on the lower VHF bands, but communication time is limited to very brief intervals. EME provides the ultimate in DX, but requires special antenna systems (high gain and the ability to elevate and track the moon) and high power levels. Communication is only possible when the moon is visible to both stations. Of all the possible propagation modes, only tropospheric scatter (troposcatter) provides a reliable and predictable mode of operation for working DX on the VHF/UHF/microwave bands on a day-in, day-out basis using moderate equipment. In fact, troposcatter circuits are often used commercially when over-the-horizon communication is desired and the use of repeaters isn't possible.

A nice feature of troposcatter propagation is that it's possible to make reasonably accurate estimates of path loss. Such estimates can be instructive from a number of viewpoints. Because the calculation is based on parameters like antenna height, local topography, and station separation it can, for example, predict what effect increased antenna height will have on signal strength.

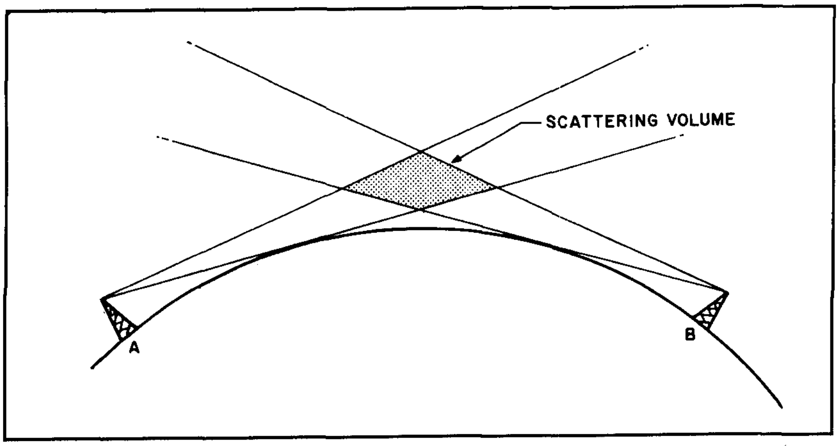

Figure 1. Though the antennas at A and B cannot "see" each other directly, they can both "see" a common region labeled the "scattering volume."

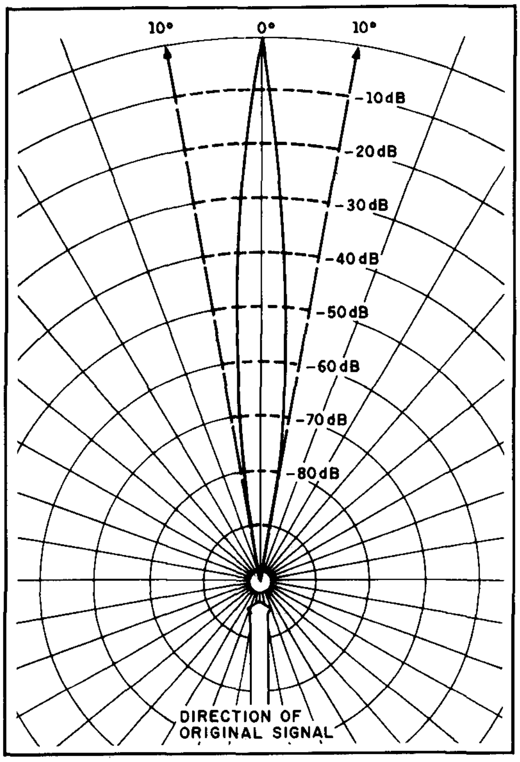

Figure 2. Relative scattering intensity as a function of scattering angle.

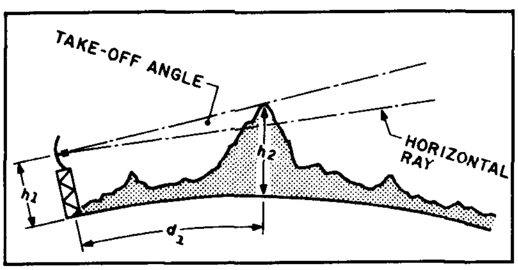

Figure 3. Definition of take-off angle.
Take-off angle =

$$\left(\frac{h_2 - h_1}{d_1} - \frac{d_1}{2R}\right) * \frac{180}{\pi}$$

where h_2, h_1, d_1, and R are the same as in *Figure 4*.

In combination with receiver and transmitter parameters, troposcatter propagation can indicate what kind of a VHF talk-back station would be needed for liaison on a DX microwave record attempt, and what the likelihood is of working a given microwave DX path.

The basic mechanism of tropospheric scatter is shown in **Figure 1**. The antennas of the two stations at the ends of the path cannot "see" each other, but they can each "see" a common volume of the atmosphere, labeled in the figure as the "scattering volume." Signals from one station are scattered by atmospheric inhomogeneities in this region, and some of the scattering is in the direction of the second station. The region of the atmosphere involved is called the troposphere and it extends from the ground up to a height of about 15 km. It's the region in which all weather phenomena occurs, airplanes fly, and is the region in which the "air" is found. Although this region looks clear and uniform to the eye, it really contains a lot of turbulence and stratification. Anyone who has had a bumpy ride in an aircraft has felt this first hand, just as anyone who has seen a star twinkle has directly observed the optical effects of atmospheric turbulence.

One characteristic of tropospheric scattering is that it occurs mainly in the original direction of the signal, as shown in **Figure 2**. As the scattering angle increases, the magnitude of the scattering falls off very rapidly (around 10 dB per degree), so the process is only useful where the scattering angle is limited to a few degrees. Two major factors are involved in determining the scattering angle between two stations. The first is the distance between the stations and the second is the "take-off angle" at the two stations. Take-off angle is defined as shown in **Figure 3**; that is, it's the angle between a horizontal ray from the antenna and a ray from the antenna to the radio horizon. Take-off angle has a strong influence on path loss. For a given path, a 1-degree increase in take-off angle will result in a decrease of around 10 dB (depending on the scattering model) in the received signal strength. If the take-off angles are large, then not only will the scattering angle be large, but the scattering volume will extend to high altitude, where the atmosphere is thinner and the scattering is therefore diminished.

Models for calculating path loss on troposcatter links

There have been many models developed to calculate the path loss on a troposcatter link, including those of ITT[1] NBS[2] CCIR[3] Collins[4] Yeh[5] and Rider[6] A review of these models (except for ITT) was made by Larsen[7] who found that the Collins model performed best, followed by Yeh, CCIR, and NBS, though all were capable of yielding good results. On paths ranging from 275 to 994 km at frequencies from 77 MHz to 3.7 GHz, path losses were often predicted to within a few dB. The ITT model has been shown to be very accurate on many paths[8] Rider's model was found to be inferior to the others. The NBS model is very complex and really requires a computer program to be practical. The CCIR method is a slightly simplified version of the NBS model, and the Collins and ITT models rely on the use of graphs which cover only a limited parameter range. This leaves Yeh's model as the best alternative for a simple computational method to determine tropospheric scatter path loss.

Yeh breaks down path loss into four basic components:

- Free space path loss
- Scattering loss
- A loss factor dependent on the refractive index of the air
- Aperture-to-medium coupling loss, which is a function of the scattering angle and the antenna beam widths used.

Taking these in turn:

Free space path loss

The free space path loss (in dB) between isotropic antennas can be calculated from first principles. Without going into details of the derivation, it can be shown to be given by the expression:

$$10\log_{10}(4\pi d/\lambda)^2$$

Where d is the distance and λ is the wavelength (in the same units).

When this is rearranged and stated in customary units, it can be expressed as the well-known relationship:

$$L_{fs} = 32.5 + 20\log_{10}(d) + 20\log_{10}(f)$$

Where d is the (great circle) distance in km and f is the frequency in MHz.

Scattering loss

Yeh determined the scattering loss empirically based on two sets of experimental observations. The first was that scattering loss was proportional both to frequency and to the scattering angle (10 dB per degree). The second was that the scatter loss at a 1-degree scattering angle (about a 90-mile path) was 57 dB at 400 MHz. These observations may be combined to yield the relationship:

$$L_S = 57 + 10(\theta - 1) + 10\log_{10}(f/400)$$

This can be simplified to:

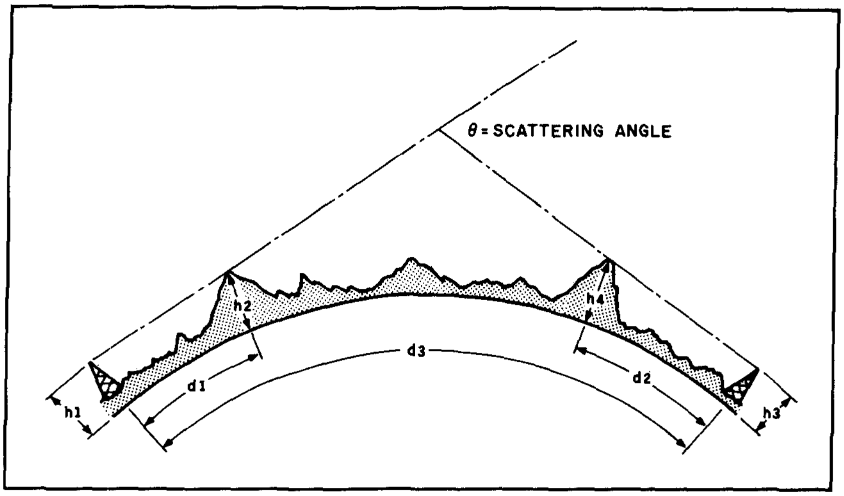

Figure 4. Geometry of a troposcatter path.

$$\theta = \frac{d_3}{R} + \frac{h_2 - h_1}{d_1} - \frac{d_1}{2R} + \frac{h_4 - h_3}{d_2} - \frac{d_2}{2R}$$

Multiply θ (radians) by $\frac{180}{\pi}$ to convert to degrees. Distances d_1, d_2, and d_3 are great circle distances. Yeh defines R as the 4/3 earth radius = 8475 km. *Note*: All distances and heights must be in the *same* units. h_1 and h_3 are the antenna heights above sea level. h_2 and h_4 are obstruction heights above sea level.

$$L_S = 21 + 10(\theta) + 10\log_{10}(f)$$

Where θ is the scattering angle as defined in **Figure 4** and f is the frequency in MHz.

The determination of θ depends on knowing the local topography around the stations at each end of the troposcatter link. It's important to determine the "take-off angle" for each station. To do so, you must know the height of the antenna and the height and location of the geographic feature which determines the local radio horizon in the direction of the distant station. You can determine this by using the path profile plotting techniques described in the appendix to this article.

Variation in the value of the radio index of refraction

The third factor is dependent on the radio refractive index of the air. This rests on a number of variables, the most important of which are air temperature and humidity. The surface refractivity, N_S, is the refractive index expressed in millionths above unity. For example, if the refractive index is its nominal value of 1.000310, the value of N_S = 310. The value and range of variability of N_S is a function of geographical location and season. It's highest in the summer in tropical coastal regions, and lowest in the winter in the mountains.

Because N_S is dependent on atmospheric pressure, it follows that it's also a function of altitude. To avoid confusion when reporting surface refractivity values from different sites at different altitudes, it's common to give values of surface refractivity corrected to sea level — often designated as N_0. For example, in Denver, at an altitude of approximately 1.6 km above sea level, a typical value of N_0 might be given as 300. The actual surface refractivity will be lower and can be approximated by the formula:

$$N_s = N_0 e^{-0.1057h}$$

Where h is the elevation above sea level in km.

For Denver, with h = 1.6 and N_0 = 300, the surface refractivity, N_s, would be 253. Though Yeh doesn't discuss how to define N_s (or calculate it from N_0) for situations in which the surface refractivities at two sites are different, it's reasonable to take the average of two values.

Values of N_0 in the United States can range from a low of around 260 in the Rocky Mountain region in the winter to over 380 along the coast of the Gulf of Mexico in the summer. Typical values for the Midwest and eastern regions of the U.S. are around 310 in the winter and 350 in the summer. A method of estimating N_s from barometric pressure, temperature, and humidity data is given in **References 8** and **9**.

The importance of the radio refractive index lies in the fact that a higher value of N_s causes radio waves to bend back towards the earth to a greater extent. More accurately, it's the change in refractive index with height which results in this effect which can be likened to the bending of light rays passing through a graded index lens. Thus radio waves don't travel in a straight line when passing through the atmosphere, but tend to bend back slightly towards the earth. An alternative way of looking at the same phenomenon is to regard the radio waves as traveling in straight lines above an earth whose radius is larger than the true radius. This gives rise to the well-known 4/3 earth radius approximation which predicts that, under average conditions, the radio horizon is at a distance 4/3 greater than the optical horizon (or more accurately, the geometric horizon, because light rays are also bent slightly).

The variation in loss as a function of N_s is approximated by Yeh as:

$$L_n = 0.2(N_s - 310)\ (dB)$$

Aperture-to-medium coupling loss

The last loss factor is the aperture-to-medium coupling loss. It has been observed experimentally that, on long haul troposcatter paths, signal strength doesn't increase as much as would be predicted when antenna gains are increased. The effect is only observed for very high gain antennas, when the antenna beam width is decreased to a value close to that of the scattering angle. The mechanism of this loss is complex and not well understood. It's derived from the way in which the antennas couple with the scattering process and may be associated with phase incoherence resulting from scattering by multiple random atmospheric inhomogeneities. Yeh based his estimate of aperture-to-medium coupling loss on the results of a number of experimental studies, rather than a theoretical model. In his original paper, a graphical determination is presented which may be approximated by the relationship:

$$L_{amc} = 2.5 + 1.8(\theta/\alpha) - 0.063(\theta/\alpha)^2$$

Where:

α = square root ($\sqrt{bw_1 bw_2}$)

bw_1 = the beam width of antenna 1 (degrees)

bw_2 = the beam width of antenna 2 (degrees)

θ = the scattering angle (degrees)

A couple of points are worth noting here. Yeh suggests that there may be some error when aperature-to-medium loss is extrapolated outside the region of experimental data, which ranges from values of θ/α of about 0.5 to 4. Extrapolating to very small values (as would often be the case using Amateur antennas of modest gain) gives a minimum value of 2.5 dB, whereas other studies show much smaller coupling loss when θ/α is small. There are a number of other empirical relationships for determining the magnitude of this loss. The value used in the CCIR method[3] is given by:

$$L_{CCIR} = 0.07e^{(0.055\,(G_1 + G_2))}$$

Where G_1 and G_2 are the gains (in dB) of the two antennas.

As you can see, this relationship doesn't involve the scattering angle at all. Thus, it's evident that determination of aperture-to-medium coupling loss isn't an exact science! Luckily it's of small importance, typically only a few dB, with the types of antennas Amateurs are likely to be using. For consistency with the rest of Yeh's method, his estimation of coupling loss should probably be used here.

Adding all four of the preceding loss factors together, you come up with an expression for the total loss of a troposcatter path:

$$\begin{aligned} L &= L_{fs} + L_s + L_{amc} + L_n \\ &= 32.5 + 20\log_{10}(d) + 20\log_{10}(f) + 21 \\ &\quad + 10(\theta) + 10\log_{10}(f) + 0.2(N_s - 310) \\ &\quad + 2.5 + 1.8(\theta/\alpha) - 0.063(\theta/\alpha)^2 \end{aligned}$$

Which reduces to:

$$L = 56 + 20\log_{10}(d) + 30\log_{10}(f) + 0.2(N_s - 310) + 10(\theta) + 1.8(\theta/\alpha) - 0.063(\theta/\alpha)^2$$

When the mean yearly value of N_s is used, the loss predicted by this expression is the all-year median (or most probable) path loss. A discussion of the statistical probability of the signal differing from this level would fill many more pages, so I won't go into that now. For a *very* rough rule of thumb for overland paths of 100 to 300 km in a climatic region similar to that of the continental United States, path loss will be 10 dB higher or lower than the median about 10 percent of the time and 20 dB higher or lower than the median about 1 percent of the time. Fluctuations in path loss tend to decrease as path length increases over 300 km or drops below 100 km. On average, signals will be stronger in the summer than in the winter. They will also be stronger in the early morning and late evening, when the air is turbulent due to heating and cooling, than in mid-afternoon, when the air is well mixed and stable.

Now that you have a way to calculate troposcatter loss, it's obviously of interest to ask how accurate the estimate will be. Larson[7] looked at sixteen paths ranging from 275 to 994 km at frequencies from 77 MHz to 3.67 GHz, with measured path losses ranging from 163 to 257 dB. He found that Yeh's method gave a mean error (independent of sign) of 5.9 dB. When the sign of the error was taken into account, the mean error (sum of errors/number of examples) was −3.0 dB; that is, there was a slight tendency to underestimate the path loss. The mean error of the other methods of estimating path loss referred to earlier were within a few dB of those of Yeh. This might not be surprising at first, but the methods have significant differences. For example, the Collins method has no term dependent on N_S, which has a significant effect on the loss predicted by Yeh. On the other hand, both the NBS and CCIR methods contain a climate correction factor not used in any of the others! Using Yeh's method, Gannaway[10] estimates the troposcatter loss of a particular 110 km path at 10.368 GHz to be 232 dB. Averaging careful measurements over a period of months, he found an experimental path loss of 235 dB, a difference of only 3 dB.

Although Yeh doesn't discuss frequency limits in his paper, the method, as described here, is probably restricted to a range from about 50 MHz to 10 GHz. Below 50 MHz, the dominant mode of DX propagation may not be troposcatter, because ionospheric reflection starts to come into play. Above 10 GHz, absorption of RF energy by oxygen and water vapor can make a significant contribution to path loss. If these losses are added to the calculated troposcatter loss, then total path loss predictions can be made at frequencies above 10 GHz. It may be noted that even below 10 GHz, atmospheric attenuation will be a small factor on long paths. For example, over 500 km, an additional loss of about 5 dB over the troposcatter loss can be expected at 10 GHz.[11]

Assuming the accuracy of troposcatter prediction is quite good, it's interesting to calculate the potential communication range between two reasonably equipped stations (see **Reference 12**). As an example, take two stations with a capability of 100 watts output on 432 MHz, each using a single 18-dBi gain Yagi with a receiver noise figure of 1 dB and having 1-dB line loss on both transmit and receive. If both stations have an unobstructed view of the horizon (take-off angle of zero degrees), they should be able to communicate on CW over a range of 650 km. This is considerably greater than most station operators would guess, and suggests the unrealized potential of many stations.

One question which often comes up in discussions about troposcatter paths is should the antennas be elevated above the horizon in order to better illuminate the scattering volume? The answer is almost always no; the antennas should point at the horizon. Many studies have shown that when using very high gain, narrow beam width (< 1 degree) antennas, elevation even by a fraction of a degree results in signal loss. This is because elevation of the antennas increases the scattering angle. A 1-degree elevation at each end results in a 2-degree increase in scattering angle and a consequent increase of 20 dB in troposcatter path loss. The effect is significant when the antenna's beam width is of the same order as the angle of elevation. In this case, the gain in the direction of the horizon will drop drastically and so there will be little contribution to troposcatter from low altitude, low angle scattering. On the other hand, if antennas with a relatively large beam width (low gain) are elevated slightly, their gain in the direction of the horizon will drop only slightly. In this case, they will still illuminate the same low angle scattering volume with only slightly less signal than they did when they were pointed directly at the horizon, thus signals will not decrease much. However, after saying all this, there are infrequent occasions on which elevation

```
'program to calculate troposcatter path loss by YEH's method
start:
cls
'first input the required path parameters
input "Enter height of antenna at station #1 (in m a.s.l.)       : ";h1
input "Enter height of radio horizon at station #1 (in m a.s.l.) : ";h2
input "Enter distance to radio horizon from station #1 (in km)   : ";d1
print
input "Enter height of antenna at station #2 (in m a.s.l.)       : ";h3
input "Enter height of radio horizon at station #2 (in m a.s.l.) : ";h4
input "Enter distance to radio horizon from station #2 (in km)   : ";d2
print
input"Enter the distance between station #1 and station#2 (in km): ";d3
print
input"Enter the antenna gain at station #1  (in dB) : ";g1
input"Enter the antenna gain at station #2  (in dB) : ";g2
print
input"Enter the radio index of refraction (Ns)      : ";ns
print
input"Enter frequency of operation (in MHz)         : ";f
'convert heights from meters to kilometers
h1=h1/1000 : h2=h2/1000 : h3=h3/1000 :h4=h4/1000
'YEH's method uses a 4/3 earth radius model where R=8475 km
r=8475
'calculate take off angle at station #1 (in degrees)
toa1=(((h2-h1)/d1)-(d1/(2*r)))*57.29578
'calculate take off angle at station #2 (in degrees)
toa2=(((h4-h3)/d2)-(d2/(2*r)))*57.29578
'calculate total scattering angle
tsa=(d3/r)*57.29578 + toa1 + toa2
'estimate antenna beamwidth from gain (assume equal E and H plane beamwidths)
bw1=sqr(27000/(10^(g1/10)))
bw2=sqr(27000/(10^(g2/10)))
'estimate aperture-to-medium coupling loss
lamc=2.5 + 1.8*(tsa/sqr(bw1*bw2)) - 0.063*(tsa/sqr(bw1*bw2))^2
'estimate effect of radio refractive index on loss
ln=0.2 * (ns - 310)
'calculate total path loss
tpl=56 + 20*log(d3)/2.303 + 30*log(f)/2.303 + 10*tsa + ln + lamc
'print results
print
print"*****************************************************************"
print
print"Take off angle at station #1 = ";
print using "###.##";toa1;
print " degrees"
print"Take off angle at station #2 = ";
print using "###.##";toa2;
print " degrees"
print "Total path loss = ";
print using "####.#";tpl;
print " dB"
input"Run program again (y/n) : ";ip$
if ip$="y" then goto start
```

Listing 1. This program calculates troposcatter loss by Yeh's method. It is compatible with QuickBASIC®, TURBO BASIC®, and PowerBASIC®, but will need line numbers and REM statements to run under GW-BASIC®.

of the antennas does lead to an increase in signal strength. This may be due to a rare circumstance when elevation of the antennas results in illumination of a high altitude, very intense scattering region of the atmosphere, such as a thunderstorm cell. In fact it has been observed that during rainstorms, microwave signals can be received by "rain scatter" with the antenna at one end of a troposcatter link pointing vertically upwards! The moral here is that when no signals can be detected with antennas pointing at the horizon (assuming beam headings and frequencies are known to be correct), it can't hurt to try elevating the antennas by a few degrees — but don't expect it to do much good very often.

As I mentioned earlier, calculation of troposcatter loss can be used to estimate the effects of an increase in antenna height, assuming that the antenna is clear of all local obstructions (trees, buildings, etc.). For example, consider two stations 200 km apart, each with antennas on 15 meter (ca. 50 feet) towers and separated by a level plain (sounds like Kansas!). On 1296 MHz, the troposcatter path loss between these stations would be about 206.5 dB. If one station doubled the height of its tower to 30 meters, the path loss would fall to 206 dB. This is only a difference of 0.5 dB (this difference is independent of frequency), and would probably be negated by the extra feed line loss required to reach the antenna. This shows that if your antenna is in the clear, and you have a very low level horizon, there's no real advantage to be gained by increasing antenna height. This is a situation where the more cost effective solution to better signals is to increase the antenna gain.

However, let's look at a different situation where one of the stations I've described has a 30-meter (100 foot) high hill at a distance of 1 km, instead of an unobstructed horizon. If this station uses the same 15-meter high antenna, the path loss will be 216.9 dB. If the antenna is raised to 30 meters, this loss drops to 208.1 dB. In this situation, the increase in signal is 8.8 dB — a considerable improvement. Because this increase in signal would be realized on all the microwave (and VHF/UHF) bands, the cost-effective solution to increased signal strength in this case would be to increase the antenna height, as eight times as many antennas on each band would be required to equal the effect of a 15-meter increase in antenna height.

Another use for this type of calculation is in estimating the equipment needed to work a given path. For example, take the path between Cadillac Mountain in Maine (466 meters asl, the highest point on the Eastern seaboard) and the tip of Cape Cod in Massachusetts (sea level) — a distance of about 300 km. Yeh's method of troposcatter prediction indicates a path loss at 10.368 MHz of around 244 dB for this path (the other methods mentioned earlier are several dB more optimistic). Using the standard relationships between path loss and equipment parameters (see **Reference 12**), it can be calculated that on 10 GHz, this path should be just workable (+1.5 dB S/N) under flat conditions using CW with a 100-mW transmitter, a 3-dB noise figure receiver, and a 3-foot dish. This setup is typical of the narrow-band equipment used by many Amateurs on this band. Calculations indicate that a 144-MHz SSB talk-back link (+14 dB S/N) can be established for this path with 10-watt transmitters and 10-dBi gain antennas (4-element Yagis).

Conclusion

In this article, I have tried not only to present a method for estimating troposcatter loss, but also to provide some physical understanding of the processes involved. The procedures outlined here, can be used as a basis for the selection of an optimum VHF/UHF/microwave site, or can give a quantitative estimate of the benefits to be gained by increasing antenna height. An analysis of troposcatter loss combined with equipment path loss capabilities may reveal the unrealized potential of many stations.

SERIAL NUMBER = 10001

TROPOSPHERIC SCATTERING LOSS CALCULATION—KA1GT

STATION PARAMETERS	STATION #1	STATION #2
Antenna height (m asl)	125	240
Obstruction height (m asl)	150	275
Distance to obstruction (km)	3	4.6
Transmitter power (watts)	100	50
Transmitter line loss (dB)	1.2	0.8
Receiver noise figure (dB)	1.65	2.15
Receiver line loss (dB)	1.2	0.8
Antenna gain (dBi)	23.4	20.7
Antenna noise temperature (K)	300	300
Receiver band width (Hz)	2700	2700
Receive system sensitivity (dBW)	−190.1	−187.3
Frequency (MHz)	1296	
Distance between stations (km)	256	
N_o value of refractive index (~310)	310	

Scattering angle = 2.61
TOA #1 = 0.47 obstruction limited
TOA #2 = 0.42 obstruction limited

	YEH	ITT	COLLINS
Path loss =	225.6	221.8	221.6
S/N ratio at station 1 =	1.4	5.3	5.4
S/N ratio at station 2 =	4.0	7.8	7.9

RECALCULATE ? (y/n) ?

Table 1. Example of a troposcatter link calculation.

Notes

A PowerBASIC® listing (compatible with PowerBASIC® and QuickBASIC®) of a simple troposcatter path loss calculator program is given in **Listing 1**. You must add line numbers if you wish to use GW BASIC. This program, together with a compiled version of a much more complex program, can be obtained from the author. The second program calculates troposcatter loss by several different methods (including those of Yeh, ITT, and Collins – and maybe others by the time this appears!) and also calculates received signal-to-noise levels based on transmitter, receiver, and antenna parameters. A sample output screen is shown **Figure 5**. Parameters are changed easily by moving the cursor and entering new values. For a copy of these programs on an IBM compaticle disk, plus program notes, send $10 (or $5 and a preformatted disk) to me at the address at the beginning of the article. Please state the disk size and density you require (360 K, 5¼ inch is the default).

For more information

Readers who want to learn more, might like to consult the references listed at the end of this article. **Reference 2** probably gives the most extensive treatment of tropospheric path loss available, though much of the text is quite mathematical.

Some of the first seven references may be hard to find, even in college libraries. I can recommend the book listed in **Reference 8**, which includes brief reviews of some of the other references and much more very useful information. **Reference 10** is an excellent treatment of Yeh's method of calculating troposcatter loss and includes a number of graphs and examples. It's recommended reading, if you can obtain a copy.

Appendix

Path plotting and determination of take-off angles

One of the important parameters used in calculating troposcatter path loss is the take-off angle at the stations at each end of the path. This depends on the topography (that is, the height of the land) between the two stations, and is frequently dependent on the local terrain at each end of the path. In order to determine the height of geographical features between the stations, a topographic graph is required. A series of such maps covering the entire United States is published by the US Geological Survey (USGS). The largest scale maps cover an area of about 7 × 9 miles at a scale of 1:24000 (or about 2.5″ = 1 mile). These are useful for locating your station exactly and determining the elevation of the local terrain. A number of other scale maps are

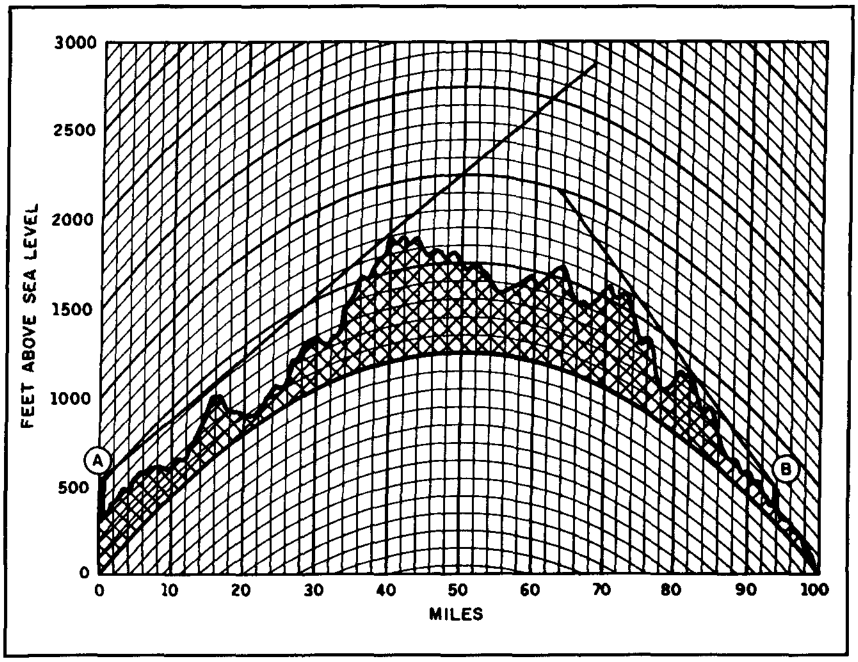

Figure 5. Path profile. In this example, the antenna at A is at a height of 500 feet above sea level (asl). There is a hill 16 miles away peaking at 350 feet above sea level, which is probably the visual horizon as seen from the antenna. However, the radio horizon is formed by the 700-foot hill situated 40 miles away. The antenna at B, 94 miles away from A, is at 200 feet asl. Its radio horizon is formed by a 400-foot hill at a distance of 12 miles.
***Note*: If the horizontal scale is divided (or multiplied) by a factor "x", then the vertical scale must be divided (or multiplied) by x^2. For example, if the horizontal axis is rescaled to read from 0 to 50 miles, the vertical axis will read from 0 to 750 feet.**

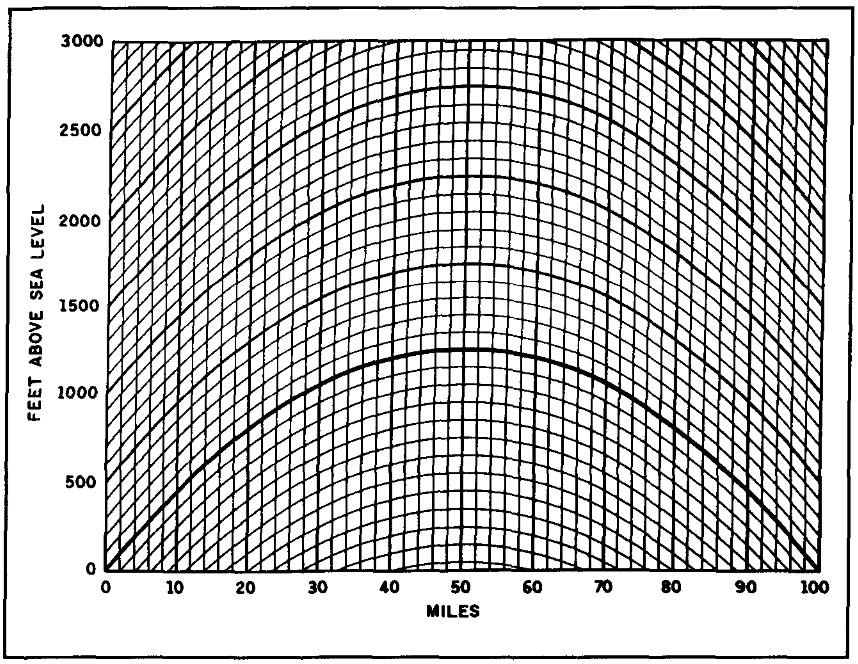

Figure 6. This path profile plotting paper is drawn for a value of $N_s \approx 300$; i.e., 4/3 earth radius scale. If each horizontal division represents 2 miles, then each vertical division represents 100 feet. The axes may be rescaled as described in *Figure 5*.

available, including the 1:25000 (about 1" = 4 miles) series, each of which cover an area the size of the state of Connecticut (about 100 × 70 miles). Check in the "Map—Dealers" section of the yellow pages in your local phone book for map suppliers. These maps are also often stocked by good bookstores and some outdoor sports stores. Alternatively, you can contact the USGS directly at the US Geological Survey, Distribution Branch, Box 25268, Federal Center, Denver, Colorado 80225.

Once you have the map, draw a line from your QTH in the direction of the other station. Then make a list of the height of the land and the distance from your station at intervals along this line. Pay particular attention to locating places where the height peaks. Next, determine which of the peaks along the line constitutes your local radio horizon. Once you've found that, it's easy to calculate your take-off angle.

There are two ways to find which feature determines your local radio horizon. One way is to calculate the take-off angle (using the formula given in **Figure 3**) which each feature along the line would produce. The feature giving the largest take-off angle determines your local radio horizon and thus gives the take-off angle for use in the troposcatter calculation.

The second method is to plot land versus distance on special parabolic graph paper. A straight line on such paper represents the path of radio waves, so the feature which determines the local radio horizon can be found as shown in **Figure 5**. The height and distance of this feature can then be used to calculate the take-off angle. As an aside, plotting the full path between two stations on parabolic graph paper can show whether a path is obstructed or line-of-sight. Parabolic graph paper is quite difficult to find. You can copy the example shown in **Figure 6**, or if you have a computer and access to a HPGL (Hewlett-Packard Graphics Language) compatible plotter, the BASIC program in **Listing 2** will generate a similar plot. The advantage of plotting your own graph paper is that it can be generated for the radio index of refraction (N_S) which exists in your region at any particular time. The example in **Figure 6** is drawn assuming average conditions (that is, $N_S = 300$, $k = 1.33$, 8475 km effective earth radius). More details can be found in **Reference 9**. ■

REFERENCES

1. H. Smith, *ITT Federal Laboratory Technical Memorandum*, June 1963, pages 63-175, and R.E. Grey, *ITT Federal Laboratory Technical Memorandum*, October 24, 1961.
2. P.L. Rice, A.C. Longley, K.A. Norton, and A.P Barsis, *NBS Technical Note 101*, May 1965 (revised January 1967).
3. *CCIR Documents of the XIth Plenary Assembly*, Oslo, 1966, pages 143-167.

```
'PROGRAM TO GENERATE PARABOLIC GRAPH PAPER ON
'A PLOTTER USING HPGL COMMANDS

input"Enter Ns (radio index of refraction - e.g 300 is typical) : ";ns
'calculate k
k=1/(1-0.04665*exp(0.005577*ns))

open "com1: 9600,s,7,1,RS,CS,DS,CD5000" as #1

print #1, "SP 1;"
print #1, "VS 10;"
print #1, "IP; SC -50,50,0,3000;"
print #1, "iw 250,279,10250,7479;"
print #1, "PU -50,0;"
for x=0 to 3000 step 100
  print #1,"PA-50,";x;",PD "
  for d=-50 to +50 step 1
    h=x + (2*50^2)/(3*k) - (2*d^2)/(3*k)
    print #1, d;",";h;" "
  next d
print #1,";"
print #1,"PU ;"
next x

'plot grid
print #1, "SP 2;"

for x=-50 to 50 step 2
  print #1, "PA ";x;",0,PD,";x;"3000,PU,"
next x
print #1,";"

for y=0 to 3000 step 3000
  print #1, "PA -50,";y;"PD,50,";y;"PU,"
next y
print #1,";"

print #1, "PA -8,200;"
print #1, "LBNs =";ns;"   k =";k;" "+chr$(3)

end
```

Listing 2. This program generates parabolic graph paper for plotting on a plotter which uses HPGL (Hewlett-Packard Graphics Language); eg., HP ColorPro. The program assumes the plotter is set for 9600-baud operation, space parity, 7 data bits and 1 stop bit, and uses hardware handshaking. It is written in PowerBASIC® (compatible with TURBO BASIC® and QuickBASIC®). Use with GW-BASIC will require the addition of line numbers and REM statements.

4. *Instruction Manual for Tropospheric Scatter — Principles and Applications*, USAEPG-SIG 960-67, U.S. Army Electronic Proving Ground, Fort Huachuca, Arizona, March 1960.
5. L.P. Yeh, "Simple Methods for Designing Troposcatter Circuits," *IRE Transactions on Communications Systems*, September 1960, pages 193-198.
6. C.C. Rider, *Marconi Review*, 3rd quarter 1962, pages 203-210.
7. R.A. Larsen, *IEE London Tropospheric Wave Propagation Conference*, 1968.
8. P.F. Panter, *Communications Systems Design*, McGraw-Hill.
9. Dennis Haarsager, N7DH, *The ARRL UHF/Microwave Experimenter's Handbook*, pages 3-37.
10. Julian Gannaway, G3YGF, "Tropospheric Scatter Propagation," *Radio Communications*, August 1981. Also reprinted in *QST*, November 1983, pages 43-48.
11. Roger Freeman, *Telecommunications Transmission Handbook*, John Wiley & Sons.
12. Bob Atkins, KA1GT, "Estimating Microwave System Performance," *QST*, December 1980, page 74.

Editor's Note:

The booklet "Transmitting Antennas and Ground Systems for 1750 Meters," by Michael Mideke, mentioned in Max Carter's article "Super Narrowband Techniques Equalize Power Inequity on 1750 Meters" in the Fall 1990 issue, is no longer available. The author has no plans to reprint the booklet at this time.

ADVERTISER'S INDEX

Repeat Performance.

FT-990

HF All-Mode Transceiver

In the battle of the base stations, the FT-990 all mode HF transceiver is the clear winner. Designed on the remarkable performance, ease of operation and the features of the FT-1000. The FT-990 is an extraordinary achievement, compare the advantages yourself. Feel the silky smooth tuning, hear the dual digital SCF (Switch Capacitance Filter) provide unsurpassed reception quality never before obtained. Be heard with the CPU controlled RF FSP (RF Frequency-Shifted Speech Processor) for the extra pile-up "PUNCH." See the lightweight and compact FT-990 with built-in AC switching power supply. The FT-990 is a true champion HF rig without compromise. Leave it only to Yaesu to offer powerhouse performance that leaves the rest far behind.

Features and Options:

- Dual VFO's With Direct Digital Synthesis (DDS): Two Ten-Bit DDS Plus Three Eight-Bit DDS.
- High Dynamic Range: 108dB. RF circuit design with quad FET first mixer similar to the FT-1000 as only Yaesu's unsurpassed tradition can provide.
- CW 500Hz Crystal Filter (included)
- Dual Digital SCF Filter and IF Shift, IF Notch: Superior interference reduction.
- Automatic mode-dependent AGC Selection
- Full and Semi Break-In CW Operation: With built-in iambic memory keyer with BFO offset and CW spot. Key jacks on both front and rear panels.
- 6 Function Multimeter
- Adjustable RF Power Output with internal heatsink and whisper-quiet temperature switched squirrel cage blower.
- Adjustable Level Noise Blanker: For a wide variety of noises and woodpecker.
- CPU controlled RF FSP (RF Frequency-Shifted Speech Processor): For better intelligibility and pile-up "PUNCH" for competitive situations.
- High Speed Automatic Antenna Tuner: With 39 Memories.
- 50 Memories: Independent ATU and mode/IF Filter Memory.
- Multimode Selection on Packet/RTTY
- Front Panel Rx Antenna Selection: Allows Quick Switching.
- Digital Voice Storage (DVS-2): Option provides instant playback of 16-second receive memory, plus two 8-second or 4-second "CQ Contest" messages on transmit.
- Built in Switching AC Power Supply: Reliable performance with significantly reduced size and weight.
- Band Stacking VFO System: Each VFO register memorizes your most recent operating frequency, mode, bandwidth, and clarifier information for instant return to your favorite frequency and mode.
- Accessories/Options: TCXO-2 (Temperature Compensated Crystal Oscillator), XF-10.9M-202-01 (2nd IF SSB Narrow 2.0kHz), XF-445C-251-01 (3rd IF CW Narrow 250Hz), SP-6 (External Speaker), MD-1C8 (Desk Microphone), YH-77ST (Headphones), LL-5 (Phone Patch Module).

The Best of the Best

YAESU

Performance without compromise.[SM]